MINERALOGY AND PETROLOGY OF AN OLIVINE DIABASE SILL COMPLEX AND ASSOCIATED UNUSUALLY POTASSIC GRANOPHYRES, SIERRA ANCHA, CENTRAL ARIZONA

Thesis by

Douglas Smith

In Partial Fulfillment of the Requirements

For the Degree of

Doctor of Philosophy

California Institute of Technology

Pasadena, California

1969

(Submitted August 30, 1968)

PLATE 1

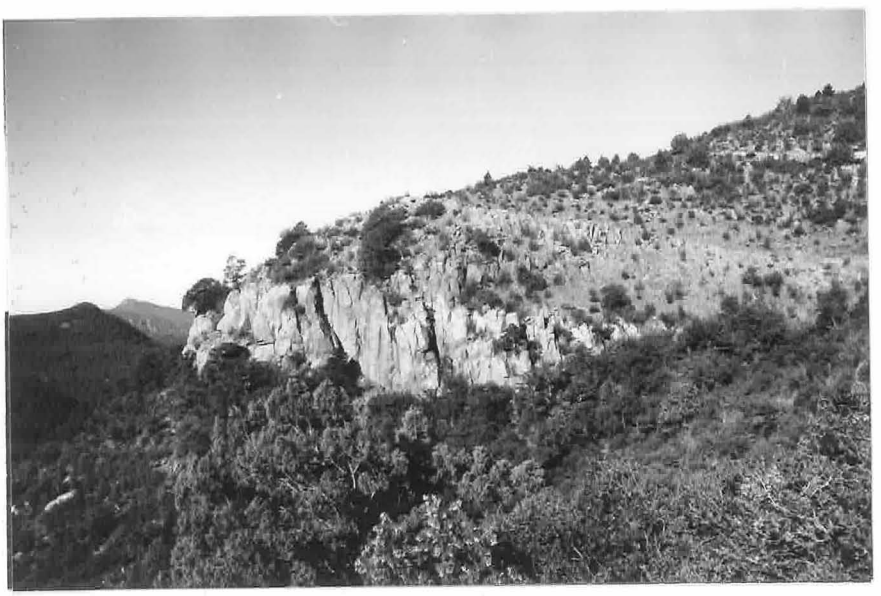

Potassic hornblende granophyre and pyroxene granophyre form these bold cliffs north of Reynolds Creek at the roof of the Sierra Ancha sill complex. Olivine diabase and feldspathic olivine-rich diabase underlie the slopes below the granophyre mass. The sharp upper contact of the granophyre with the potassic rocks of the Dripping Spring Quartzite is visible in the photograph; the contact dips gently into the hill. The association of such impressive masses of granophyre with an olivine diabase intrusive is one of the problems which provoked this study. (Photograph-L.T. Silver.)

ACKNOWLEDGMENTS

Dr. Leon T. Silver, my thesis advisor, first suggested that the Sierra Ancha sill complex would be an appropriate subject for this study. His aid and advice were of value throughout the periods of research and thesis preparation.

Dr. Andrew Shride of the U.S. Geological Survey generously shared some results from his unpublished geological mapping in the McFadden Peak quadrangle with the author and also provided other useful information on the characteristics of diabase intrusions in central Arizona.

The writer is indebted to Dr. Arden Albee for discussions on several aspects of this work. Arthur Chodos instructed the author in microprobe techniques and was responsible for keeping the microprobe in excellent operating condition throughout the period of research. Dr. A.E. Bence and Dr. Albee kept the author informed of their progress in the preparation of their system for the conversion of microprobe data to element proportions and permitted him to use the system before publication.

My wife, Jean, cheerfully spent innumerable hours typing and preparing thesis material and was a constant source of encouragement.

During part of this research the author was supported by graduate fellowships from the National Science Foundation and the Kennecott Copper Corporation.

Research funds were provided principally by National Science Foundation grant GA-287. Several facilities and some support were derived from U.S.A.E.C. contract AT(04-3)-427.

ABSTRACT

The Precambrian Sierra Ancha sill complex, 700 to 800 feet thick, was intruded into flat-lying sedimentary rocks of the Apache Group in central Arizona. The bulk of the complex consists of a central layer of feldspathic olivine-rich diabase and upper and lower layers of olivine diabase. Diabasic rocks present in relatively minor quantity in the upper part of the complex include diabase pegmatite, albite diabase, and quartz diabase. Potassic granophyres locally form lenses up to two hundred feet thick near and at the roof of the complex. The intrusion was studied in the field and in the laboratory to determine the origins of the rock types and the conditions under which they formed. Extensive electron microprobe studies of mineral compositions and zoning are presented together with nineteen new whole rock chemical analyses.

The Sierra Ancha olivine diabase has a high-alumina olivine basalt composition. Olivine diabase and olivine-rich diabase display a differentiation pattern characterized by moderate iron enrichment. Diabase pegmatite is relatively enriched in alkalis.

The principle primary minerals in feldspathic olivine-rich diabase and olivine diabase include: plagioclase (An_{72}-An_{16}); augite ($Wo_{43}En_{44}Fs_{13}$ to $Wo_{40}En_{38}Fs_{22}$); olivine (Fo_{74}-Fo_{54}); orthopyroxene (En_{77}-En_{44}); magnetite$_{ss}$ ($Mgt_{66}Usp_{34}$-$Mgt_{89}Usp_{11}$); and ilmenite$_{ss}$ ($Ilm_{86}Hem_{14}$-$Ilm_{96}Hem_{4}$). All of the orthopyroxene is primary. Fe-Mg fractionations between mafic mineral pairs increase with iron enrichment and declining crystallization temperatures. Ilmenite which formed by reaction-exsolution from magnetite was found to be consistently different in composition from primary ilmenite.

The late-crystallizing diabase pegmatites contain an assemblage including iron-rich chlorite together with calcic pyroxene; from textural evidence the two phases appear primary. The calcic pyroxene has a compositional range from $Wo_{49}En_{28}Fs_{23}$ to $Wo_{49}En_{14}Fs_{37}$; its compositions define an iron-enriched trend in the pyroxene quadrilateral more calcic (i.e., closer to the diopside-hedenburgite join) than other iron-enriched igneous pyroxene trends described in the literature.

Most diabasic rocks in the sill display some deuteric alteration. The mineral assemblage seemingly stable in the most-altered rocks includes albite (An_{2-0}), prehnite, calcic pyroxene (salite), chlorite, sphene, and apatite. Albite diabase contains this assemblage and apparently formed by recrystallization of normal diabase under deuteric conditions. The alteration assemblages are similar to those found in spilites. They provide an important example of the development of a spilitic assemblage by autometamorphism.

The massive granophyres at and near the top of the sill appear to be igneous. The larger lenses occur at local high points in the roof of the complex near discordant contacts. The granophyres consist primarily of alkali feldspar with subordinate calcic pyroxene, iron-rich hornblende, biotite, and quartz and minor plagioclase and other phases. They have no relict sedimentary textural features, and they contain miarolitic cavities and rotated and displaced sedimentary rock inclusions. Locally, they occur as masses truncating overlying strata and as dikes in the overlying sedimentary rocks. Some of the dikes have apparent chilled contacts against the sedimentary rocks, suggesting that they were emplaced largely as melts.

The granophyres formed as a result of the interaction of diabase magma with stratified rocks of the overlying Dripping Spring Quartzite. The massive granophyres are generally similar in composition to the overlying sedimentary rocks; both rock types have very unusual and distinctive high potassium contents. Contact metamorphism by the diabase has produced layered metasedimentary rocks with granophyric textures and mineral assemblages comparable to those in some massive granophyres. Consistent compositional differences between granophyres and sedimentary rocks may have been caused by metasomatic processes or by mixing of diabase magma with the sedimentary rock material which constitutes most of the granophyres.

The interaction of diabase and sedimentary rocks may have occurred because magma in the upper part of the intrusion absorbed water from the overlying sedimentary rocks and solidified after magma in the central part of the intrusive. If this happened, the sedimentary rocks over the sill might have been melted to form the granophyres. No chilled facies of diabase occurs at the sill roof where granophyres are present. Compositional trends in mineral series indicate that the diabase magma in the upper part of the sill solidified towards the roof in at least one locality.

Normal processes of magmatic differentiation produced feldspathic olivine-rich diabase, olivine diabase, and diabase pegmatite in the Sierra Ancha complex. The processes which produced the granophyres include recrystallization and fusion of rocks overlying the intrusion. The Sierra Ancha granophyres offer a superb opportunity to study these processes and others which may have produced many of the granitic rocks in the crust of the earth.

Photographic materials on pages ii, 25, 27, 40, 43, 50, 55, 68, 72, 76, 78, 97, 155, 156, 209, 210, 219, 224, 229, 230, and 237 are essential and will not reproduce clearly on Xerox copies. Photographic copies should be ordered.

TABLE OF CONTENTS

TITLE	PAGE
INTRODUCTION	1
Previous Work on the Sierra Ancha Complex	2
Topography and Accessibility	4
Distribution of Outcrops	5
Procedures of Investigation	6
Thesis outline	6
INTRUSIVE ENVIRONMENT OF THE DIABASE	8
Form of the Intrusion	8
Stratigraphic Section	11
Depth of Intrusion	14
The Potassium Phenomenon	15
Outline of the problem	15
Previous work on the potassium problem	18
Petrography and chemistry of the potassium-rich rocks	20
Origin of the potassium-rich rocks	28
Stratigraphic implications	31
THE DIABASIC ROCKS	32
Feldspathic Olivine-rich Diabase	38
Mineralogy of the layer	39
Contacts of the olivine-rich layer	42
Origin of the feldspathic olivine-rich layer	45
Olivine Diabase	48
Least-altered olivine diabase	49
Typical olivine diabase	51
Intensely-altered diabase	52
Albite Diabase	56
Chilled Facies of the Diabase Magma	59
Coarse-grained Diabasic Rocks	62
Segregations and Lenses	62
Diabase Pegmatite	64
Feldspar in diabase pegmatite	66
Pyroxenes	70
Chlorite	73
Iron-titanium oxides and sphene	75
Other pegmatite minerals	79

TITLE	PAGE
Summary of pegmatite mineral sequence	79
Inhomogeneity of diabase pegmatite and sampling procedure	80
Similar differentiates in other mafic intrusives	81
Quartz Diabase	82
Distribution of quartz diabase	82
Mineralogy and petrography of the quartz diabase	84
Origin of the quartz diabase	85
MINERALOGY OF THE DIABASIC ROCKS	87
Pyroxenes	88
Calcium-rich pyroxene	88
Pigeonite	100
Orthopyroxene	101
Pyroxene trends in relation to those in other intrusions	106
Olivine	110
Application of Partition Data Between Pyroxenes and Olivine	113
Fe-Mg partition between olivine and orthopyroxene	116
Fe-Mg partition between augite and olivine	124
Fe-Mg partition between augite and orthopyroxene	124
Partition of Ni between olivine and augite	128
Summary of Principal Observations and Conclusions on Pyroxenes and Olivine	130
Feldspars	133
Plagioclase in olivine-rich and olivine diabase	133
Alkali feldspar-plagioclase relationship in rock Ad163c	136
Feldspars in diabase pegmatite and deuterically-altered rocks	138
Feldspar in quartz diabase	139
Iron-titanium Oxides	140
Introduction	140
Analytical procedures for Fe-Ti oxides	142
Petrography of coexisting ilmenite$_{ss}$ and magnetite$_{ss}$	146
Analytical data	147
Compositions of magnetite$_{ss}$	151
Compositions of ilmenite$_{ss}$	154
Compositional criteria for distinguishing primary and exsolved ilmenite$_{ss}$	158

TITLE	PAGE
Temperatures and oxygen fugacities	160
Minor element partitions between oxides	163
Compositional trends in primary ilmenite ss	168
Summary of Fe-Ti oxide data	175
WHOLE ROCK CHEMISTRY OF THE SIERRA ANCHA DIABASES	177
Composition of the Undifferentiated Magma	177
Crystallization Temperatures Deduced from Experimental Melting Studies	182
Whole Rock Differentiation Trends	185
Relation of Bulk Rock Trends to Mineral Trends	192
PROCESSES OF DIABASE DIFFERENTIATION	197
DEUTERIC ALTERATION, ALBITE DIABASE, DIABASE PEGMATITE, AND THE SPILITE PROBLEM	200
Spilitic Assemblages Formed by Deuteric Alteration ...	200
Spilitic Assemblages in Diabase Pegmatites	202
Temperatures of Formation of the Spilitic Minerals	203
Implications of the Spilitic Mineral Assemblages Developed in the Diabase	204
GRANOPHYRES	205
Introduction	205
Previous studies of the granophyric rocks	206
Outline of the discussion of the granophyres	207
Mineralogy and Textures of Layered Metasedimentary Rocks	208
Recrystallization of rocks in the upper member of the Dripping Spring Quartzite	208
Metamorphism of the Mescal Limestone	213
Summary of metamorphic effects in the obviously metasedimentary rocks	214
Igneous-Looking Crystalline Rocks	215
Types of granophyric rocks	218
Structural Settings of the Granophyres	220
Distribution of the Granophyric Rock Types	221
Internal Features of the Granophyre Lenses	223
Contacts of the Granophyre Lenses	226
Inclusions and Dikes in the Diabase	232

TITLE	PAGE
Inclusions in diabase	232
Dikes of granophyre within diabase	233
Mineralogy of the Granophyric Rocks	233
Feldspars	233
Feldspars in the different rock types	238
The feldspars as geothermometers	238
Quartz	241
Pyroxene	241
Hornblende	245
Biotite	248
Oxides and sulfides	249
Other minerals in granophyric rocks	250
Compositions of the Granophyric Rocks	251
Compositional gradients in granophyre lenses	252
Comparison of granophyre, sedimentary rock, and diabase compositions	256
Source of the Granophyres	264
Chemical Interactions between Diabase and Sedimentary Rocks	267
Physical mixing between diabase and sedimentary rocks	267
Metasomatic movement of material between diabase and granophyre	269
Possible low temperature alkali metasomatism of the granophyres	271
Possible metasomatic effects in layered metasedimentary rocks	273
Possible metasomatism of recrystallized sedimentary rocks by diabase in the Karroo province	274
The Granophyres as Melts	275
Rheomorphism, mobilization, and fusion	275
Melting temperatures deduced from bulk rock compositions	277
Melting of Wall Rocks and the Cooling History of the Diabase Sill	279
The role of water	279
Cooling history of the sill and wall rock temperatures	281
Possible Reasons for Localization of the Granophyres ...	288

TITLE	PAGE
PETROLOGIC IMPLICATIONS OF THE SIERRA ANCHA GRANOPHYRES	290
APPENDIX	295
Analytical Procedures and Accuracy of Results	295
Wet chemical analyses	295
X-ray fluorescence analyses for potassium	297
Trace element emission spectographic analyses	298
Procedures for microprobe analyses	298
Precision and accuracy of microprobe analyses	300
Calculation procedures for rock norms	304
BIBLIOGRAPHY	305

LIST OF TABLES

TABLE	TITLE	PAGE
1	Chemical Analyses, Dripping Spring Quartzite	16
2	Potassium Analyses, Dripping Spring Quartzite	17
3	Average Alkali Contents of Selected Rock Types	17
4	Potassium Analyses of Sedimentary and Metasedimentary Rocks	21
5	Analyses of Diabasic Rocks	35
6	Analyses of Diabasic Rocks	37
7	Analyses of Diabase at Chilled Contacts	60
8	Analyses of Chlorite in Diabase Pegmatite	74
9	Augite Analyses	89
10	Augite, Bleached Pyroxene, and Calcic Pyroxene Analyses	96
11	Orthopyroxene Analyses	102
12	Olivine Analyses	111
13	Compositions of Contacting Olivine and Orthopyroxene	117
14	Minor Elements in Olivine and Orthopyroxene	123
15	Compositions of Contacting Olivine and Augite	125
16	Compositions of Contacting Orthopyroxene and Augite	126
17	Plagioclase Compositions in Diabase	134
18	Analyses of Ilmenite-hematite Standards	145
19	Compositions of Iron-titanium Oxides in Diabase	148
20	Compositions of Iron-titanium Oxides in Diabase	149
21	Compositions of Ilmenite in Granophyre	150
22	Temperatures and Oxygen Fugacities Calculated from Oxide Pairs	161

TABLE	TITLE	PAGE
23	Comparison of Ilmenite and Rock Compositions	173
24	Comparison of Diabase and Basalt Compositions	178
25	Summary of Selected Parameters Related to Differentiation of the Diabase	193
26	Analyses of Granophyres	216
27	Compositions of Alkali Feldspar in Granophyre	235
28	Analyses of Pyroxene and Chlorite in Granophyre	242
29	Analyses of a Zoned Amphibole Crystal in Granophyre	246
30	Average Compositions, Dripping Spring Quartzite	257
31	Comparison of Diabase, Granophyre, and Sedimentary Rock Compositions	259
32	Calculated Solidification Times for the Sill	282
33	Chemical Analyses of Duplicate Standards	296
34	Count Ratios for Pairs of Microprobe Standards	301
35	Comparison of Microprobe Analyses of Standard Clinopyroxenes with Analyses in the Literature	303
36	Analyses of Standard Feldspars	303

LIST OF FIGURES

FIGURE	TITLE	PAGE
1	Idealized stratigraphic section of the upper member of the Dripping Spring Quartzite	13
2	Schematic cross section through the Sierra Ancha sill complex	33
3	Schematic drawing showing sample localities in and near the Reynolds Creek diabase section	34
4	Schematic portrayal of feldspar textures in diabase pegmatite	67
5	Representative compositions of primary calcic pyroxenes plotted in the pyroxene quadrilateral	90
6	Range of augite compositions present in a thin section of one rock	91
7	Al and Ti variations in augite and primary calcic pyroxene	93
8	Compositions of pyroxene in a single polished thin section of diabase pegmatite	99
9	Orthopyroxene analyses plotted in part of the pyroxene quadrilateral	103
10	Compositions of primary pyroxenes in diabasic rocks plotted in the pyroxene quadrilateral	107
11	Ranges of values of the Fe/(Fe + Mg) ratio in pyroxene and olivine in selected rocks	115
12	Schematic drawing of olivine-orthopyroxene relationships	117
13	Fe/(Fe + Mg) ratios of points a few tens of microns apart across the boundaries of contacting olivine and orthopyroxene grains compared with ratios determined experimentally	120
14	Ni fractionation between olivine and augite in feldspathic olivine-rich diabase compared with the observed fractionations in mineral pairs from a Hawaiian lava lake	129

FIGURE	TITLE	PAGE
15	Plagioclase compositions in olivine diabase and feldspathic olivine-rich diabase	135
16	One micron microprobe traverse for Fe, Ti, and Al in an inhomogeneous magnetite grain	152
17	Microprobe traverses for Fe, Al, and Ti across parts of magnetite grains	153
18	Results of a microprobe traverse across one boundary of an ilmenite lamella within a magnetite grain	159
19	Experimental iron-titanium oxide relationships determined by Lindsley (1963)	161
20	Distribution of Mn and Mg between coexisting ilmenite and magnetite grains in volcanic rocks	166
21	Mg and Mn variations in a zoned ilmenite crystal	169
22	Variations in Ti, Fe, Mg, and Mn shown by a microprobe traverse across an ilmenite blade	170
23	Relationship between Mg and Mn variations in a bladed crystal of ilmenite	171
24	Sierra Ancha olivine diabase compositions compared with compositions of different types of basalts	180
25	AFM diagram for Sierra Ancha diabasic rocks	186
26	Silica variation diagram for diabasic rocks	188
27	Na_2O-K_2O-CaO diagram for Sierra Ancha diabasic rocks	190
28	Sample locations in a section through the upper part of the sill complex near Workman Creek, together with mineral compositional data for some of the diabase samples	195
29	Alkali feldspar solvus determined by Orville (1963)	235
30	Compositions of coexisting clear alkali feldspar and plagioclase in two granophyre samples	239

FIGURE	TITLE	PAGE
31	Representative compositions of pyroxenes in granophyres and metasedimentary rocks plotted in the pyroxene quadrilateral	243
32	Sections through granophyre	253
33	Sections through granophyre	254
34	Comparison of granophyre and sedimentary rock compositions on a silica variation diagram	258
35	Compositions of sedimentary rocks, granophyres, and diabasic rocks plotted on an AFM diagram	260
36	Compositions of sedimentary rocks, granophyres, and diabasic rocks plotted on an Na_2O-K_2O-CaO diagram	261
37	Compositions of possible intermediate rocks plotted on AFM and Na_2O-K_2O-CaO diagrams	263
38	Normative compositions of granophyres plotted on a projection of the liquidus surface of the system Ab-Or-SiO_2-H_2O at one kilobar pressure	278
39	Temperature gradients in sedimentary rocks at the sill roof for two simple models	285

LIST OF PLATES

PLATE	TITLE	PAGE
1	Granophyre bluff north of Reynolds Creek	ii
2	Location of McFadden Peak quadrangle, together with the distribution of diabase in central Arizona	3
3	Geologic map of the southwest part of McFadden Peak quadrangle	9
4	Geologic map, Reynolds-Workman Creeks area	pocket
5	Geologic map, Grantham Peak area	pocket
6	Photomicrograph, K-rich sedimentary rock	25
7	Photomicrographs, K-rich sedimentary rock	27
8	Photomicrographs, feldspathic olivine-rich diabase	40
9	Diabasic rocks	43
10	Photomicrographs, olivine diabase	50
11	Photomicrographs, albite diabase and altered diabase	55
12	Photomicrographs, feldspar in diabase pegmatite	68
13	Photomicrographs, diabase pegmatite	72
14	Photomicrographs, ilmenite-chlorite-sphene aggregates	76
15	Photomicrographs, skeletal ilmenite crystals	78
16	Photomicrographs, partly-reacted augite in diabase pegmatite	97
17	Photomicrographs, ilmenite-magnetite intergrowths	155
18	Photomicrographs, ilmenite-magnetite intergrowths	156
19	Photomicrographs, recrystallized sedimentary rocks	209

PLATE	TITLE	PAGE
20	Photomicrographs, recrystallized sedimentary rocks	210
21	Photomicrographs, aplitic pyroxene granophyre and hornblende granophyre	219
22	Aplite and granophyre	224
23	Discordant granophyre-sedimentary rock relationships	229
24	Photomicrographs, aplite-sedimentary rock contact and granophyric intergrowth	230
25	Photomicrographs, turbid feldspar in granophyre	237

INTRODUCTION

Understanding the chemical and physical changes which occur in a crystallizing body of basaltic magma is one of the classic problems of igneous petrology. The unique parental role assigned to basaltic magmas and the variety and importance of their differentiates make the problem especially interesting. In particular, understanding the relationship between genetically related basaltic and granitic rocks is important both for the light it sheds on the origins of differentiated rock suites and also for its bearing on problems as fundamental as the origin of continents. This thesis was undertaken in an effort to characterize the mineral and chemical changes taking place during formation of a differentiated basaltic intrusive and associated granitic rocks and to relate the changes to variations in physical and chemical parameters.

Classical methods of field, petrographic, and petrologic investigation were combined in this investigation with extensive use of the electron microprobe in analyzing minerals. Accurate mineral compositions can be determined more easily with the microprobe than was previously possible. Moreover, a detailed knowledge of mineral zoning and compositional relationships unobtainable by any other means can be obtained with the microprobe. The microprobe was used to characterize accurately major and minor element compositional trends in important mineral groups.

A flat-lying Precambrian olivine diabase sill complex in the Sierra Ancha of central Arizona was chosen for the study. A combination of features make it an excellent subject for an investigation of processes of igneous differentiation. The complex contains a variety of genetically related mafic rocks, including feldspathic olivine-rich

diabase, olivine diabase, and diabase pegmatite. The complex also contains spectacular occurrences of granophyric syenites and granites. Though the complex is Precambrian, no later igneous or metamorphic events have noticeably affected it or the surrounding sedimentary rocks. The rugged topography of the Sierra Ancha provides for generally good exposures. The geology of the McFadden Peak quadrangle, which contains the sill, has been mapped recently (A. Shride, in press), and the geological setting of the sill is well-defined.

The Sierra Ancha diabase sill complex is one of many similar bodies intruded into flat-lying sedimentary rocks of the Precambrian Apache Group in central Arizona. The regional distribution of diabase in central Arizona and the location of the quadrangle containing the sill complex studied are shown together in Plate 2, adapted from Shride (1967). The diabase intrusions are Precambrian; Silver (1960) dated zircons from granophyric rocks formed by the diabase sill studied here and assigned them a probable age of 1200 million years or greater. Diabase sills exposed in the Grand Canyon 150 miles north of the Sierra Ancha have been dated by Silver (personal communication) and found to be the same age. The Sierra Ancha diabase thus represents part of a regional Precambrian intrusive event and may be part of a very large event.

Previous Work on the Sierra Ancha Complex

The first studies of the Sierra Ancha diabase were made in conjunction with studies of uranium and asbestos deposits in rocks overlying the sill. Williams (1957) and Neuerburg and Granger (1960) have published chemical and petrographic data on the diabase

PLATE 2

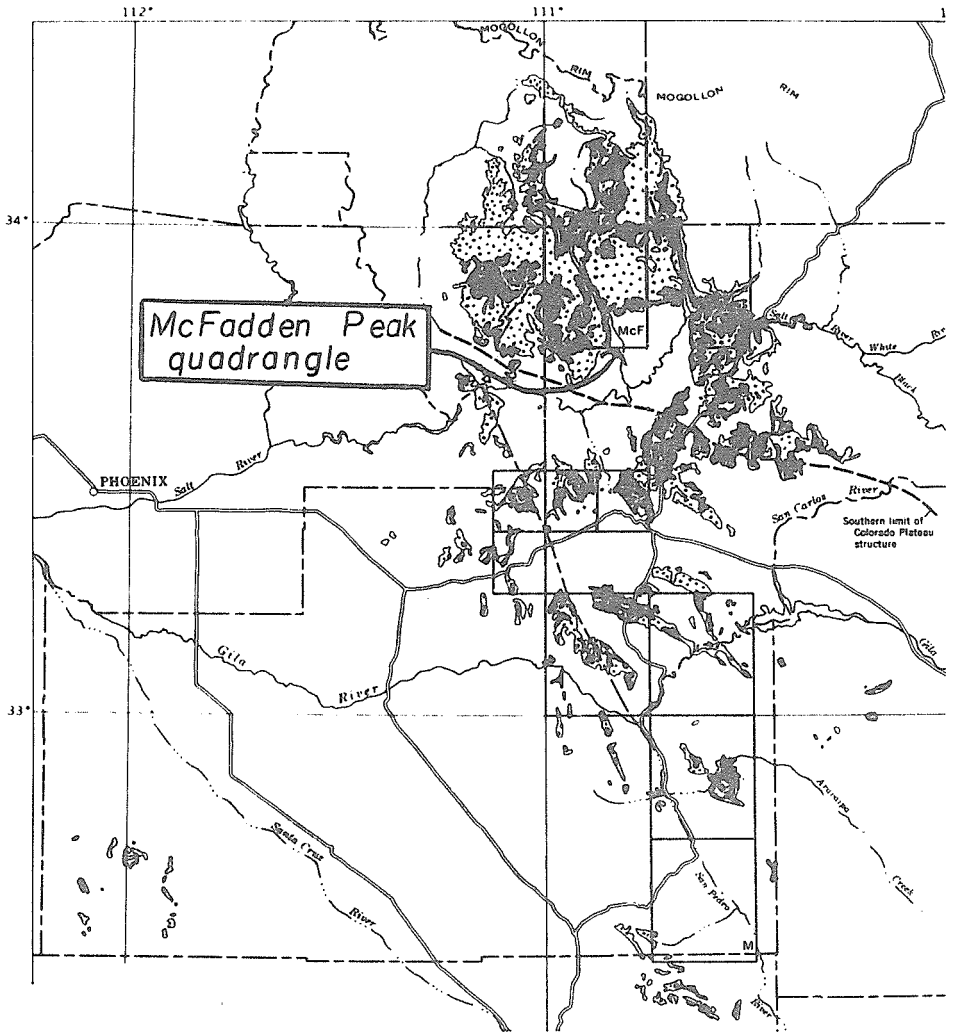

Diabase

Younger Precambrian sedimentary rocks

Adapted from Shride (1967)

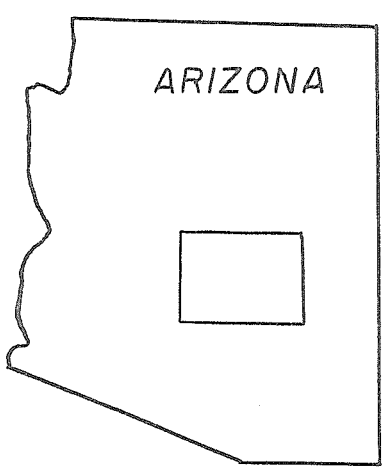

0 miles 50

Location of McFadden Peak quadrangle, together with the distribution of diabase and younger Precambrian rock in central Arizona.

and its differentiates as part of their investigations of the uranium deposits. Cherukupalli (1959) wrote an unpublished masters thesis at Columbia University on the petrography of rocks collected from the sill. Shride (1967) discussed the general structure and petrography of all the diabase intrusives in the region in a recent publication on the younger Precambrian rocks. Shride has mapped the McFadden Peak quadrangle, and his unpublished geologic map of the quadrangle was used extensively in preparing this work. This thesis is designed to complement his broader, less specific investigations.

Topography and Accessibility

The Sierra Ancha lies in a transition zone between two great physiographic provinces, the Colorado Plateau Province to the northeast and the Basin and Range Province to the southwest. Structurally, the range is most like the Plateau Province. The Sierra Ancha is characterized by resistant flat-lying sedimentary rocks and less-resistant diabase sills dissected into a range of high mesas cut by rugged canyons. Narrow north-trending structural zones of faulting and folding locally interrupt the flat-lying strata.

The area studied lies at the southern edge of the range on the north slope of the Salt River drainage. The main access road, an improved gravel road connecting Globe and Young, runs from north to south through the western part of the area (Plate 3). Most of the road lies on diabase. To the east of the road the diabase is capped by high-standing mesas of flat-lying sedimentary rocks. These mesas are cut by canyons of the four main creeks in the area -- Reynolds, Workman, Parker, and Pocket Creeks. Most

of the granophyre masses studied crop out on steep slopes at and near the roof of the sill complex in these canyons. Pocket Creek cuts completely through the sill complex, and Reynolds and Workman Creeks deeply dissect it. Rough but useable roads lie along these creeks.

Altitudes in the area range from 4500 to 7500 feet. North-facing slopes, canyons, and high mesas bear yellow pine or juniper forests; south-facing slopes and lower elevations have a locally thick cover of chaparral and cactus. The creeks in the larger canyons flow all year. In winter the higher elevations receive considerable snow. Summer days are hot, but nights are pleasantly cool.

A few ranchers and highway maintenance workers are the only permanent occupants of the range. Loggers periodically devastate small areas. Deer and small game are abundant.

Distribution of Outcrops

Outcrops of diabase are generally good along streams and are locally good elsewhere. However, diabase is one of the least resistant rock types in the area. In some places it is covered by soil, and in other places it is covered by debris from more resistant overlying rocks. The granitic and syenitic rocks are massively resistant and are generally well-exposed. The mesa-forming sedimentary rocks crop out in bold cliffs, and locally debris from these cliffs covers both granophyre and diabase on the sides of the canyons.

Procedures of Investigation

The problems were attacked with an integrated program of field and laboratory studies. About thirty field days spread over a period of two and one-half years were spent studying, sampling, and mapping rock types in the sill complex. Most of this time was spent in studying the distribution of leucocratic rocks near the sill roof. U. S. Agricultural Service air photos (scale 1:15, 000) were used as a map base. The area north of Reynolds Creek was studied in greatest detail, but the areas near Workman Creek and Grantham Peak were also carefully examined. These areas are shown in Plate 3. Geologic maps made of critical areas are reproduced in Plates 4 and 5.

Over two hundred and fifty thin sections of sill rocks were examined. Extensive electron microprobe studies of mineral compositions were made on polished thin sections of representative rocks; analytical procedures are described in an appendix. Selected whole rock samples of diabase and granophyre were prepared and sent to the Japan Analytical Chemistry Research Institute for wet chemical analysis. Other samples were prepared for potassium and trace element determinations at Caltech. Problems of analytical accuracy and precision are discussed in an appendix.

Thesis outline

The size, shape, and outcrop area of the sill complex and the nature of the sedimentary rocks around it are discussed in the first section to provide a framework for the more detailed investigations to follow. Because the sedimentary rocks have interacted

with diabase to produce the leucocratic rocks at the roof of the complex, the chemistry of the sedimentary rocks is important and is treated in the first section.

The diabasic rocks forming the bulk of the complex are discussed next. First, the distribution, petrography, and general mode of origin of the important types of diabasic rocks are described. Next, the compositions of pyroxenes, olivines, feldspars, and iron-titanium oxides, their compositional trends, and the partitions of elements between them are discussed. The mineralogic studies provide information on the changing physical conditions during crystallization of the magma as well as on the path of differentiation. Later, the bulk rock chemistry of the diabasic rocks is described, and bulk rock trends are related to mineral trends. The differentiation processes which formed the various rock types are discussed briefly. Albite-calcic pyroxene-chlorite assemblages were formed in altered diabase and diabase pegmatite. The relationships between these assemblages and spilite assemblages are also discussed.

The unusual potassium-rich granitic and syenitic rocks near the roof of the sill complex are treated in the following sections. The distribution, mineralogy, and chemistry of these rocks are described. They are products of the interaction of the diabase with the sedimentary country rocks. The processes which may have formed these rocks are discussed, and their relevance to problems of the origins of granitic rocks are considered.

INTRUSIVE ENVIRONMENT OF THE DIABASE

Form of the Intrusion

The diabase sill complex studied was intruded into flat-lying Precambrian sedimentary rocks, as were most of the other diabase bodies in central Arizona. Shride (1967, pp. 53-55) has noted that some characteristic features of the Arizona diabase intrusives are: (1) most of the diabase is in tabular, concordant bodies, but all sills are locally discordant; (2) many sills "... change horizon by high-angle abrupt steps up or down across the host strata," while others have contacts that cut across the host strata at low angles; (3) "many sills end abruptly with chilled contacts against high-angle faults." All these features can be seen in the diabase body studied for this thesis.

The diabase intrusive and surrounding sedimentary rocks are shown in a geologic map of a small area in the southwestern portion of the McFadden Peak quadrangle (Plate 3). The flat-topped mountains and major drainages which are the important geographic features lie in a north-south belt through the center of the area. From north to south these features are: McFadden Peak, Reynolds Creek, Workman Creek, Parker Creek, Grantham Peak, and Pocket Creek.

Exposures of diabase which can be definitely related to this particular sill complex are restricted to an area of about 10 to 12 miles, the heart of which is shown in Plate 3. The region to the west of the area shown has not been mapped in detail, but work published by E. D. Wilson on the Gila County geologic map shows that exposures of this particular diabase body are continuous for only a few miles to the west. Detailed mapping by Shride summarized on the Gila County map shows that just to the northeast of the map area the diabase

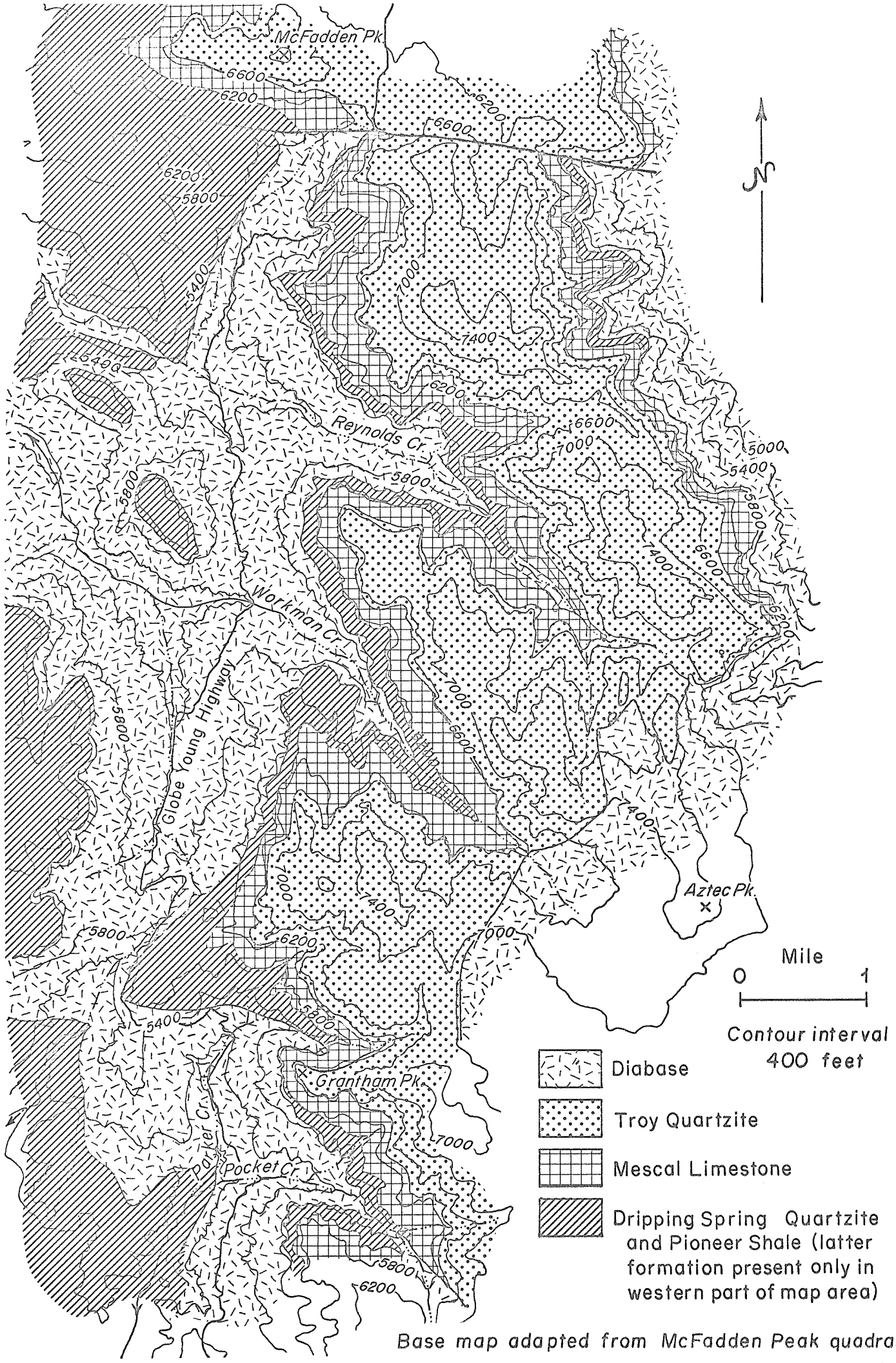

Base map adapted from McFadden Peak quadrangle

The geology is taken from a contribution of Andrew F. Shride to the Geologic Map of Gila County, Arizona (Arizona Bureau of Mines) and has been adapted according to suggestions by Shride. Minor changes, chiefly in the Reynolds Creek area, have been made by the author.

PLATE 3: Geology of the southwestern part of the McFadden Peak quadrangle.

terminates at a pre-diabase structural belt exposed along Cherry Creek; to the east the diabase abruptly cuts up section and forms a flat-lying body below Aztec Peak. Exposures of diabase are limited several miles south of the map area by the southern boundary of the mountain range. It is probable that the original extent of the intrusive body was far greater than the 10 by 12 mile area of fairly continuous exposure remaining.

The upper and lower contacts of the diabase with its sedimentary host rocks are generally concordant. The lower contact is exposed with certainly only near Pocket Creek in the southern part of the map area. Here the sill complex is 700 to 800 feet thick. It is at least 700 feet thick locally near Reynolds Creek in the northern part of the area. The upper contact of the sill is exposed over the entire length of the area. Near and north of Grantham Peak the upper contact is markedly discordant; it is slightly discordant near Reynolds Creek. Both these places are of particular interest because large masses of granitic and syenitic rocks are exposed near the upper contact there. Detailed maps of the two localities are shown in Plates 4 and 5.

The diabase has steeply dipping discordant contacts with the sedimentary country rocks in the portions of the map area north of Reynolds Creek and near Parker Creek. The east-west trending contact just south of McFadden Peak may be a fault caused simply by inflation of the sedimentary section with the diabase and may have occurred at the time of intrusion, as suggested by Shride (1967, p. 68). The diabase might or might not continue at a lower elevation north of this fault. The north-trending high-angle contacts may be related to a north-trending belt of faulting and folding which extends through the west-central part of the map area; Shride (1967, p. 66)

has traced this belt for twenty miles and believes it was caused by pre-diabase deformation. Just to the west of the high-angle contact south of McFadden Peak, the sedimentary rocks dip steeply to the east, and some beds very near the contact are overturned; a few hundred feet west of the contact the beds are approximately horizontal. The intense folding at the contact may reflect drag along a pre-diabase fault zone. Shride (1967, p. 66) has noted that such zones have commonly been intruded by diabase dikes that may have been the principle feeder conduits for the sills.

In summary, the general tabular nature of the sill complex is evident from its relatively flat, concordant upper contact. The sill complex crops out only within a ten by twelve mile area, but its original extent may have been much greater. However, the diabase intrusive cannot be considered as a simple tabular body of indefinite lateral extent. The complex has steep, discordant boundary contacts in the northern part of the map area (Plate 3) and along Cherry Creek to the east of the area. Its upper contact, though generally conformable and flat-lying, locally cuts the overlying strata. The intrusion is connected by a dike to the thick sill below Aztec Peak at the eastern edge of the map area. Both of the diabase bodies may have been fed by magma from dikes in the immediate vicinity, perhaps along one or both of the north-trending structural zones along the western part of the map area and along Cherry Creek.

Stratigraphic Section

Flat-lying sedimentary rocks of the Precambrian Apache Group and overlying Troy Quartzite are the important host rocks for diabase in this part of the Sierra Ancha. Shride (1967) has

divided the Apache Group into three formations: the Pioneer Shale, the Dripping Spring Quartzite, and the Mescal Limestone. The following general descriptions are taken from his work. The Apache Group is unconformable upon a basement complex of deformed, commonly schistose metamorphic rocks and intrusive salic plutons. The Pioneer Shale, the basal formation of the Apache Group, consists of a basal unit of conglomerate, a unit of tuffaceous mudstone, and an upper unit of arkose and tuffaceous mudstone. The Dripping Spring Quartzite rests with possible disconformity on the Pioneer Shale: it consists of a thin, basal member of conglomerate, a middle member of arkose and quartzite, and an upper member of highly feldspathic, fine-grained "siltstone" with arkose interbeds. The Mescal Limestone, which rests with erosional disconformity on the Dripping Spring Quartzite, consists of a lower member of cherty dolomite with a basal breccia, a central member of massive stromatolitic dolomite, and an upper member of argillite. It contains several basalt flows. The Troy Quartzite, which lies with slight regional unconformity on the Mescal, consists of quartzite, sandstone, and arkose. Approximate thicknesses in the Sierra Ancha for the Pioneer, Dripping Spring, Mescal, and Troy strata are 300, 600, 400, and 1200 feet, respectively.

The top of the main diabase sill in the area studied lies within the upper member of the Dripping Spring Quartzite everywhere except south of Parker Creek, where it locally contacts the Mescal Limestone. Granger and Raup (1964) have published detailed descriptions of the stratigraphy of the Dripping Spring Quartzite, and their terminology for units in the upper member is used here. Figure 1, based on the work of Granger and Raup (1964), shows an

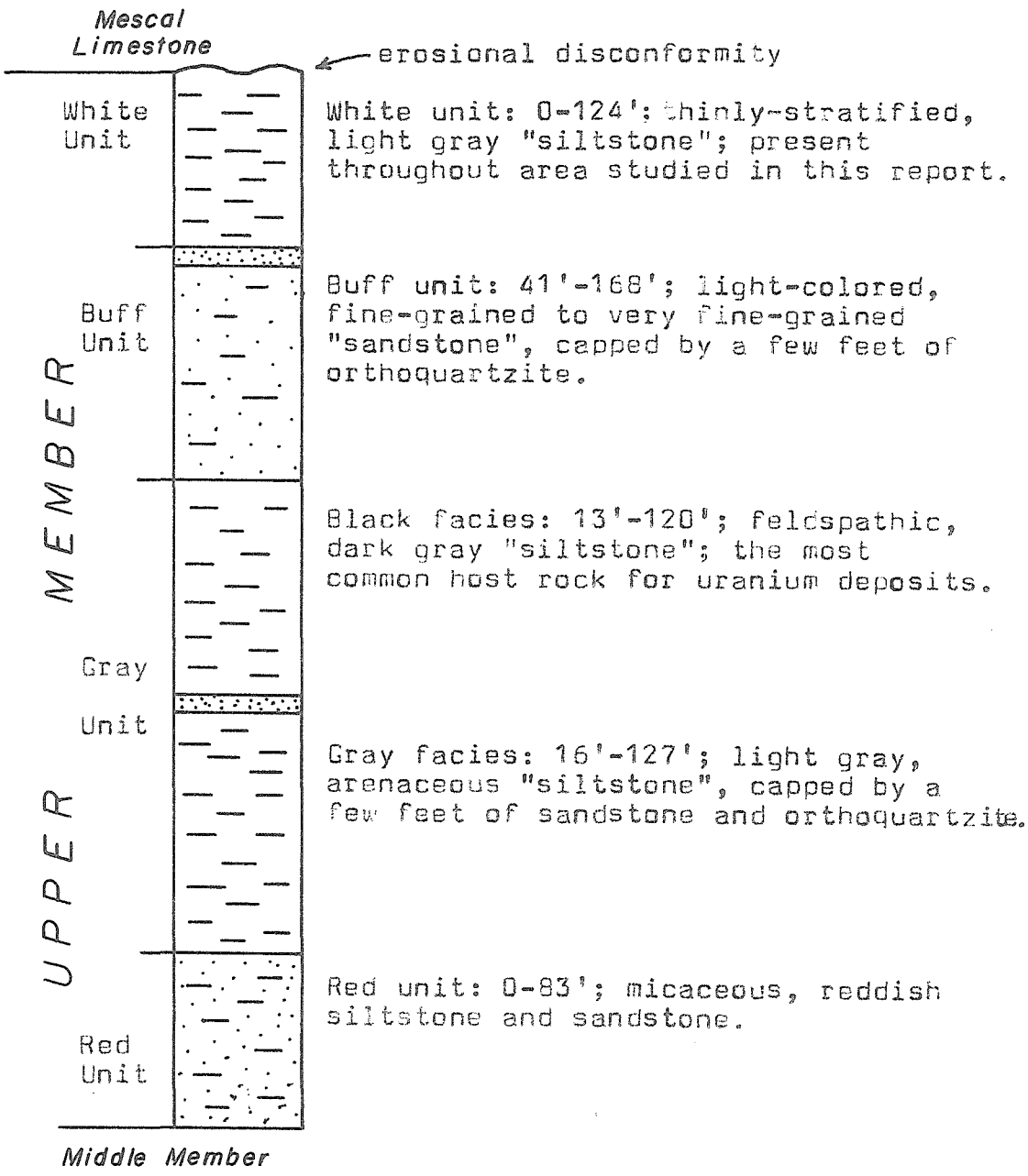

Figure 1. Idealized stratigraphic section of the upper member of the Dripping Spring Quartzite. Adapted from Granger and Raup (1964, Figure 4).

idealized stratigraphic section of the member. Though the upper contact of the diabase sill studied is not everywhere in precisely the same stratigraphic position, generally it lies near the top of the gray unit of the upper member.

Depth of Intrusion

An estimate of the depth of intrusion can be obtained by consideration of sedimentary thicknesses and of the age of the diabase. A minimum depth of intrusion for diabase in the Dripping Spring Quartzite is the combined thicknesses of the overlying Mescal Limestone and Troy Quartzite, about 1600 feet using Shride's (1967) measurements. The Troy Quartzite is the youngest Precambrian sedimentary rock exposed in central Arizona. As noted by Shride (1967), diabase intrusive into the upper part of the Troy is petrographically similar to stratigraphically lower intrusives, suggesting that at the time of diabase intrusion the Troy had a substantial sedimentary rock cover.

The sections of younger Precambrian rock exposed in Arizona are not thick, and it is unlikely that the diabase was intruded at great depth. The thickest known section of younger Precambrian sedimentary rocks exposed in Arizona is in the Grand Canyon about 150 miles north of the Sierra Ancha. It has a maximum thickness of about 12,000 feet (Wilson, 1962, p. 9). Diabase sills of the same age as the Sierra Ancha intrusives were emplaced in strata in the lower part of the section. The 12,000 foot thickness is one guide to the maximum amount of overburden which might have existed at the time of diabase intrusion in the Sierra Ancha. It corresponds to a lithostatic pressure of near a kilobar.

The Potassium Phenomenon

Rocks in the upper member of the Dripping Spring Quartzite intruded by the Sierra Ancha diabase are extremely potassium-rich and have highly unusual compositions for sedimentary rocks. Since alkalic, fluid differentiates were a product of magmatic processes in the sill, an important question is posed. Did the diabase intrude highly potassic sedimentary rocks and by interaction with them produce potassic granophyric rocks, or did magmatic differentiation of the diabase produce potassium-rich end products which in part crystallized as granophyric rocks and in part potassium-metasomatized the sedimentary rocks? Arguments relevant to the question come from studies of the granophyres, of the differentiation trend of the diabase, and of the sedimentary rocks themselves. These last arguments suggest that the sedimentary rocks were potassium-rich before diabase intrusion.

Outline of the problem

There are very few analyzed igneous or sedimentary rocks with compositions like those of rocks from the upper member of the Dripping Spring Quartzite. Complete chemical analyses of rocks from the unit are presented in Table 1, together with the theoretical composition of potassium feldspar. Analyses for potassium only are presented in Tables 2 and 4. Many of the rocks analyzed contain over 10% K_2O; there is very little Na_2O in the wet-chemically analyzed samples. Average alkali contents of some common rock types are given in Table 3 for comparison. A few leucite-bearing igneous rocks and rare trachytes have K_2O contents approaching or

TABLE 1

Complete Chemical Analyses, Upper Member, Dripping Spring Quartzite

	1a	1b	1c	1d	2a	2b	3	4	5	
SiO_2	56.48	64.65	66.64	61.70	59.4	57.9	74.75	66.73	64.76	SiO_2
TiO_2	1.21	0.63	0.74	0.95	0.86	0.86	0.52			TiO_2
Al_2O_3	15.12	13.93	14.31	15.64	14.7	14.8	11.56	12.78	18.32	Al_2O_3
Fe_2O_3	1.12	1.09	0.00	0.97	3.7	0.5	0.46	2.92		Fe_2O_3
FeO	5.48	3.41	2.27	3.42	0.35	6.8	0.14	1.26		FeO
MgO	0.83	0.49	0.52	1.14	1.0	1.8	0.53	0.54		MgO
CaO	1.97	0.53	0.81	2.49	1.8	0.4	0.50	0.61		CaO
Na_2O	0.73	0.20	0.87	0.41	0.18	0.17	0.13	0.43		Na_2O
K_2O	13.40	12.31	12.49	11.98	12.4	11.7	9.60	10.54	16.92	K_2O
P_2O_5	0.09	0.04	0.13	0.07	0.11	0.08	0.07	0.10		P_2O_5
MnO	0.08	0.01	0.00	0.03	0.02	0.05	0.01	0.07		MnO
H_2O^+	1.71	0.68	0.78	0.22	0.77	2.0	0.72	1.13		H_2O^+
H_2O^-	0.10	0.13	0.03	0.16			0.65	0.59		H_2O^-
CO_2	0.00	0.00	0.00	nil	2.5	.51				CO_2
S	2.69	1.89		1.45	2.7	2.7	0	0.93		S
	101.01	99.99	99.59	100.63	100.49	100.27	99.64	98.63	100	

1a,b,c,d — Williams (1957, Table 2). Samples are probably from the gray unit and are "...unaffected or only very slightly affected by the diabase" (Williams, 1957, p.58).

2a,b — Granger and Raup (1964, Table 4). Black facies, gray unit.

3* — Rock Ad125h, white unit. An apparently unrecrystallized rock from north of Reynolds Creek.

4* — Rock Ad125r, black facies, gray unit. A recrystallized rock from north of Reynolds Creek.

5 — $KAlSi_3O_8$, theoretical composition.

*Analyst: Asari.

TABLE 2

Potassium Analyses of Samples of the Black Facies of the Upper Member of the Dripping Spring Quartzite from Granger and Raup (1959, Table 3)

Sample	1	2	3	4	5	6
K_2O (weight percent)	14.6	12.2	11.6	12.2	10.5	12.6

1,2,3 McFadden Peak quadrangle

4 Just south of McFadden Peak quadrangle

5,6 Bluehouse Mountain quadrangle (about 20 miles east of the area shown in Plate 3.)

TABLE 3

Average Alkali Contents of Selected Rock Types

	K_2O	Na_2O
calc-alkali granite[1]	5.46	3.08
calc-alkali syenite[1]	6.53	3.92
calc-alkali trachyte[1]	7.38	3.85
shale[2]	3.24	1.30
arkose[3]	4.99	1.84

1. Nockolds, 1954

2. Clark, 1924, quoted in Pettijohn, p.344.

3. Pettijohn, 1957, p.324.

exceeding 10%; even if common, these rocks would be unlikely source rocks for the Dripping Spring Quartzite because they lack quartz. Highly unusual orthoclase-quartz dike rocks with nine to thirteen weight percent K_2O from South Dakota, which were described by Noble (1948), have analyses remarkably like some of those of rocks from the formation. However, no similar intrusive rocks or flows have been recognized in central Arizona. The most common Precambrian igneous rocks in the Sierra Ancha region are quartz monzonite and granodiorite with subordinate rhyolite and mafic rocks. These rocks are most unlikely to have been sources of highly potassic sedimentary debris. Shales are commonly said to undergo a potassium enrichment process in the sea water, but Pettijohn (1957, p. 369) indicates that only about one shale in twenty has greater than 5% K_2O. A very few high-potassium shales have been described, as will be discussed later.

Previous work on the potassium problem

The upper member of the Dripping Spring Quartzite has been the subject of considerable attention in the past because it locally contains disseminated uranium deposits. Early in the search for uranium, geologists realized that the upper member of the formation was abnormally radioactive, and that the radioactivity could in large part be attributed to the high potassium content of the unit. The uranium deposits and host rocks were studied in detail by Williams (1957), Granger and Raup (1959), and Neuerburg and Granger (1960), all of whom presented chemical data demonstrating the high potassium content of the gray unit of the upper member. Granger and Raup (1964) presented minor

additional data on potassium within the gray unit in their detailed stratigraphic discussion. Shride (1967) also described the stratigraphy of the formation. Only Granger and Raup (1959, 1964) have discussed possible reasons for the anomalous potassium contents of the sedimentary rocks. Although they concluded that the potassium was pre-diabase, their arguments are not entirely convincing.

Williams (1957) thought the fine-grained rocks in the upper member of the Dripping Spring Quartzite to be potassium-rich tuffs. He noted that some of the rocks contained angular quartz fragments scattered through a finer-grained matrix, and he interpreted the fragments as being altered volcanic shards. Four wet chemical analyses reported by him (Table 1) all come from rocks associated with uranium deposits. Though he believed the analyses represented sedimentary rocks little affected by the diabase, he also believed that the uranium deposits in them were formed by hydrothermal activity related to the intrusion. The possibility that the hydrothermal activity also influenced the analyzed rocks in other ways must be considered. As noted above, exceedingly few tuffaceous rocks have compositions like rocks in the upper Dripping Spring Quartzite; it is highly unlikely that they are unaltered tuffs.

Granger and Raup (1959), Neuerberg and Granger (1960), and Granger and Raup (1964) have reported complete and partial analyses of the black facies of the gray unit of the upper member. Wet chemical analyses from their works are in Table 1; potassium determinations are in Table 2. They do not discuss the position of the diabase with respect to the positions of most of their analyzed samples. With the possible exception of one sample difficult to locate, cross-references between the three papers demonstrate that their analyzed samples come from uranium deposits, or the

immediate vicinity of deposits, or from near the diabase. Neuerburg and Granger (1960) argue that the diabase was the source of the disseminated uranium in the ore deposits in the Dripping Spring Quartzite. If uranium was introduced into the section, potassium might also have been. Neuerburg and Granger (1960, p. 766) reported semiquantitative analyses of Hakatai Shale in the Unkar group and of argillite from the upper member of the Mescal Limestone with greater than 10% potassium. Perhaps it is significant that they report both specimens were slightly recrystallized by nearby diabase intrusions.

Though Shride (1967) writes that outcrops of diabase are coextensive with outcrops of the Apache Group in Arizona, Granger and Raup (1964) describe complete sections of the Dripping Spring Quartzite that are not intruded by diabase. They do not indicate that the lithology of the upper member in locations free from diabase differs systematically in any way from the lithology at locations intruded by diabase except for local contact effects.

Granger and Raup (1964, p. 38) concluded that the feldspar in the black facies of the upper member "...formed diagenetically as an authigenic potassic alteration of detrital clay minerals." They based their conclusion on x-ray diffractometer studies which showed the feldspar to be monoclinic and very low in sodium, facts suggesting a low-temperature origin for the mineral.

Petrography and chemistry of the potassium-rich rocks

Petrographic and chemical studies of sedimentary rocks in the Dripping Spring Quartzite were undertaken in this work to clarify the origin of the potassium-rich rocks and to help in understanding

TABLE 4

Potassium Analyses of Sedimentary and Metasedimentary Rocks

	Sample	K_2O[1] (%)	Stratigraphic Position	Comments
1.	Ad250b	12.3	Near base of upper member	Mica-rich spots suggest incipient metamorphism.
2.	Ad252b	9.6	White unit	No metamorphic effects visible.
3.	Ad260a	14.3	Black facies	No metamorphic effects visible; uranium prospect nearby. See Plate 6.
4.	Ad262a	7.3	White unit	Spots of chlorite(?) suggest incipient metamorphism.
5.	Ad262c	4.9	White unit	No metamorphic effects visible.
6.	Ad125h	9.8	Buff unit	Chlorite spots suggest incipient metamorphism.
7.	Ad125r	10.7	Black facies	Largely recrystallized; just above sill.
8.	Ad91a	11.9	Upper member	Recrystallized; just above thick granophyre layer.
9.	Ad141a	12.9	Upper member	Recrystallized; just above thin granophyre layer.
10.	Ad82	9.2	Upper member	Inclusion in thick granophyre layer.
11.	Ad152e	12.9	Black facies	Contains a coarsely-recrystallized granitic layer.
12.	Ar-Co-Dsq #F12	6.2	Middle member	Slight recrystallization of quartz? Arkose from Little Dragoon Mountains.
13.	Ar-Co-Dsq #F21	8.3	Middle member	Slight recrystallization of quartz? Arkose from Little Dragoon Mountains.
14.	Ar-Gi-Apt #1b	11.4	Pioneer Shale	No metamorphic effects visible. An altered tuff from 6 miles west of Young.
15.	Ar-Gc Hsh#1	6.0	Hakatai Shale	No metamorphic effects visible; a siltstone from the Grand Canyon.
16.	Ar-Gc Hsh#2	3.8	Hakatai Shale	No metamorphic effects visible; a shale from the Grand Canyon.

[1] K_2O determinations for all samples, except 6 and 7, by x-ray fluorescence by E. Bingham. See appendix. Samples 6 and 7 were wet-chemically analyzed by Asari.

TABLE 4 (continued)

Sample Descriptions and Localities

1. Above saddle one mile SW of McFadden Peak; no diabase in section. (see Plate 3). A pinkish-gray, red-brown weathering siltstone composed of detrital quartz, dusty-brown feldspar, and minor muscovite with very fine-grained matrix material (45% of rock). A few secondary micaceous spots are present.

2. Same location as #1. A very fine-grained, light gray, featureless rock composed of angular silt-sized quartz and feldspar grains (10%) distributed through a very fine-grained matrix (90%). Styolites common.

3. SE quarter, Section 1, T5N, R13E, north of North Fork of Parker Creek; diabase in middle member here. A laminated siltstone consisting of black, very fine-grained layers and of gray layers with silt-sized, angular quartz and dusty-brown feldspar grains in a very fine-grained matrix. Styolites common. An x-ray diffractometer scan showed that the black layers consist of microcline with minor quartz. Photomicrograph in Plate 6.

4. Same location as #3. A light gray, very fine-grained, buff-weathering rock consisting of quartz grains up to 0.03 mm in diameter and a few spots of chlorite(?) in a very fine-grained matrix. Styolites common.

5. Same location as #3. A dense, light gray, flinty rock with (5%) angular grains of quartz or feldspar 0.01 to 0.03 mm in diameter in a (95%) very fine-grained matrix. An x-ray diffractometer scan showed the rock to consist primarily of quartz with subordinate microcline.

6. Section 7, T6N, R14E, north of Reynolds Creek; about 70 feet above diabase. A brown-weathering, flesh-colored rock with a few 0.1-0.5 mm quartz grains in a very fine-grained, slightly silty matrix. A few chlorite(?) spots are present. Photomicrographs in Plate 7.

7. Same location as #6; a few feet above diabase. A fine-grained, dark gray, recrystallized siltstone: 70% feldspar, 20% quartz, 5% sulfides, 4% biotite, 2% sphene. Bedding is still well preserved.

8. SW quarter, section 6, T6N, R14E; just above "granophyre" at top of sill. A light gray, fine-grained, equigranular, recrystallized rock, average grain size 0.1 mm: 75% feldspar, 15% diopside, 7% sulfides, 2% quartz, 1% biotite.

TABLE 4 (continued)

9. Section 17, T6N, R14E; just above thin "granophyre" layer at top of sill. A medium-gray, fine-grained, recrystallized rock, relict bedding prominent: 85% K feldspar, 6% augite, 4% sulfides, 3% quartz, 1% biotite, traces of albite and sphene.

10. Section 18, T6N, R14E, north of Reynolds Creek; inclusion near base of thick granophyre lens. Fine-grained, light gray, recrystallized rock, average grain size near 0.2 mm: 90% feldspar, 6% quartz, 2% sphene, 1% augite, trace of albite, opaques.

11. Section 19, T6N, R14E, north of Workman Creek; 10 feet over fill. Dark gray, laminated metasiltstone cut by a coarser-grained syenite-like lens: 80% feldspar, 6% opaques, 5% quartz, 4% biotite, 3% augite, 1% sphene.

12. NW¼ Section 21, T15S, R22E, Dragoon quadrangle, Cochise County. Dark red, fine-grained arkose with green, chloritized slate chips. A 0.01 mm matrix makes of 1/5 of 2/3 of the arkose layers.

13. Same location as #12. Dark red, very fine-grained arkose consisting of 0.1 mm grains of quartz and dusty-brown feldspar with a minor amount of fine-grained matrix.

14. 34°05.4'N, 111°03.9'W, Diamond Butte quadrangle, Gila County. The rock, a red-brown "argillite", consists of silt-sized grains of quartz (10%) and dusty-brown feldspar (60%) with wisps of opaques (10%) and a very fine-grained matrix (20%). Some thin sections show relict shard structures like those described by Gastil (1954).

15. About ½ mile due south of suspension bridge, South Kaibab Trail, Bright Angel quadrangle. A brick-red, very fine-grained sandstone with pea-sized bleached spots. The rock consists of subangular grains of quartz, feldspar, and altered feldspar in a carbonate matrix.

16. Same location as #15. A dark red "argillite" with pea-sized bleached spots. Itconsists of silt-sized quartz grains (5%) distributed in a very fine-grained matrix (95%).

Samples 12 through 16 collected by L.T. Silver.

the origin of the granophyric rocks over the diabase. Samples of the formation close to and far from diabase were chosen to be analyzed for potassium by x-ray fluorescence. Two rocks were chosen for complete wet chemical analysis. In addition, two samples of Hakatai Shale and one of tuff from the Pioneer Shale were chosen for potassium analyses. Analytical results, locations, and descriptions of the specimens analyzed for potassium are in Table 4. Complete wet chemical analyses of two specimens are in Table 1.

The analytic results show that the potassium contents of rocks in the Dripping Spring Quartzite are apparently not spatially related to intrusions of diabase. Apparently unaffected rocks collected some distance from diabase, such as Ad252b and Ad260a, show the same high potassium contents as recrystallized rocks adjacent to sills, such as Ad91a and Ad125r. Only rocks from the gray unit had been analyzed previously; results here show that rocks in the white unit, buff unit, and middle member also have high K_2O contents. The analyses of rocks from the middle member in the Little Dragoon Mountains, 130 miles south of Reynolds Creek, considerably extend the known outcrop area of Dripping Spring Quartzite with abnormal potassium content. Tuffaceous rocks from the Pioneer Shale at least in part have high potassium contents, as shown by the analysis of rock Ar-Gi-Apt #1b with 11.4% K_2O. One of the two samples of Hakatai Shale from the Grand Canyon has 6% K_2O, a somewhat high value.

All unrecrystallized high-potassium rocks from the upper member of the Dripping Spring Quartzite contain large amounts of very fine-grained material, dusty-brown in thin section and with an average grain size much less than 0.01 mm. X-ray diffractometer

PLATE 6

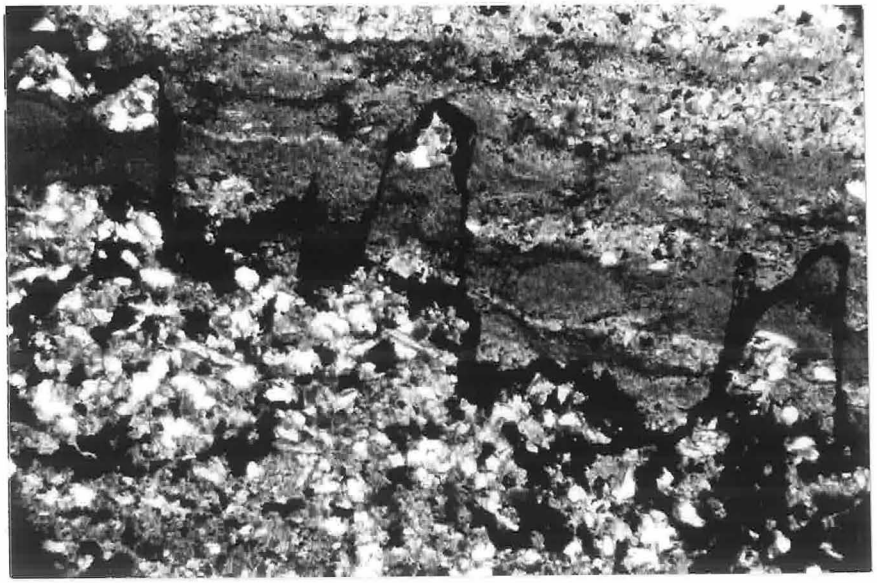

Rock Ad260a. 2x3 mm. Relatively coarse-grained, quartz-rich lamella and styolite in a fine-grained rock from the black facies of the upper member of the Dripping Spring Quartzite. Clear grains are quartz. Black material along styolite is probably pyrite and graphite. This rock contains 14.3% K_2O. (Table 4).

studies of the fine-grained material from rocks Ad260a and Ad262c confirm the conclusion of Granger and Raup (1964) that the material is almost entirely microcline and quartz. In rock Ad260a from the black facies, it is chiefly microcline. The extremely fine grain size of much of the feldspar in the upper member is additional evidence that the mineral formed by authigenic process. A detrital origin for such fine-grained potassium feldspar is unlikely because it would be readily altered to clays during sedimentary transport. Its fine grain size also indicates that it probably formed under low-temperature conditions, an unlikely situation if the rocks were extensively metasomatized by the diabase; such fine-grained material should readily recrystallize during high-temperature metasomatism.

There is some evidence that rocks in the upper member of the formation might be in part altered, water-laid ash tuffs. Positive evidence for a tuffaceous origin, such as the presence of shards, was not observed. However, most potassic rocks in the upper member contain angular fragments of quartz and, less commonly, of feldspar in lamellae or distributed through a very fine-grained matrix. The angular fragments have not been transported far and might well be shattered fragments of phenocrysts. Rocks such as Ad125h are most likely to represent altered ash falls, as they contain a small population of 0.1-0.5 mm angular quartz grains distributed randomly in a matrix with an average grain size less than 0.01 mm. A few of the large quartz grains have embayed margins suggestive of resorption in a magma, as seen in photomicrographs in Plate 7. Ripple marks and mudcracks in the upper member described by Granger and Raup (1964) indicate a shallow

PLATE 7

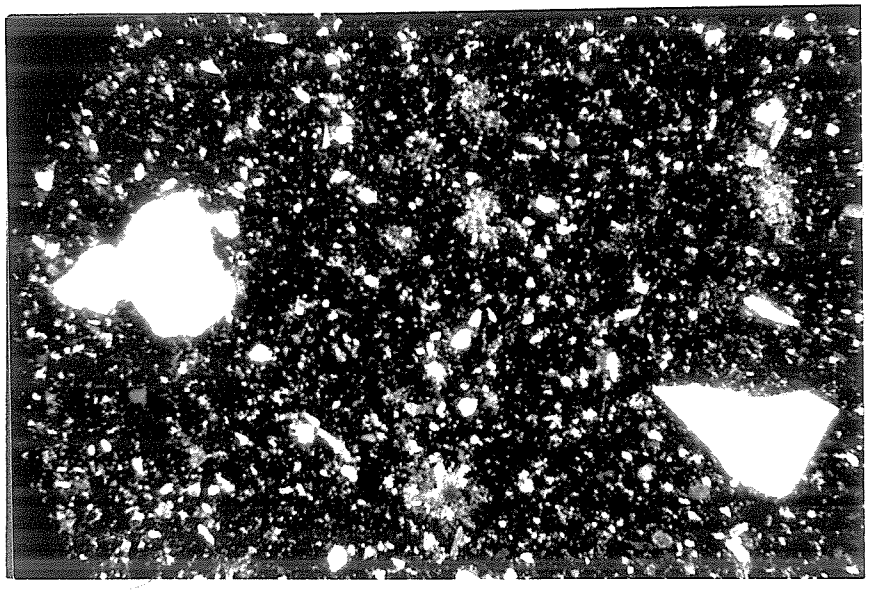

Rock Ad125h. 2x3 mm. Crossed nicols. The two large grains are quartz. Note the embayed outline of one grain, the angular outline of the other. This rock contains 9.8% K_2O.

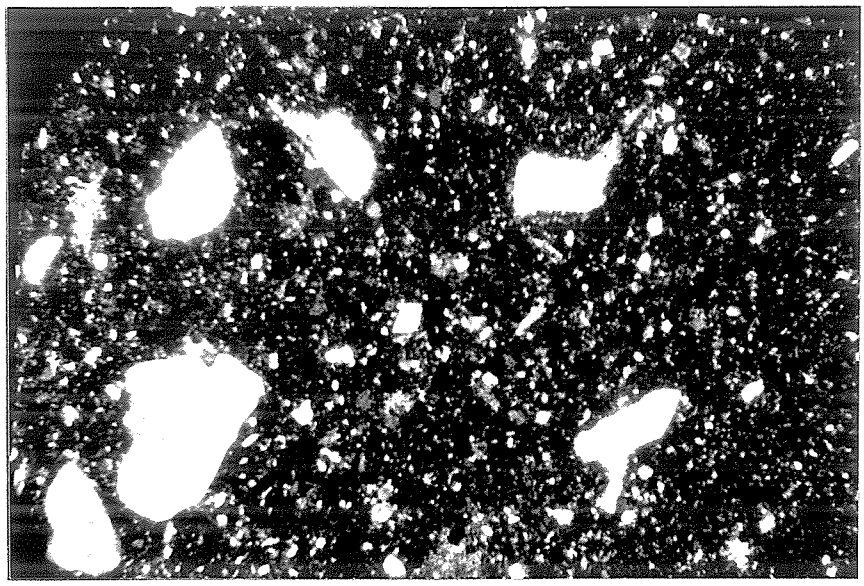

Rock Ad125h. 2x3 mm. Crossed nicols. The large grains are quartz. Grain shapes suggest that the rock may be an altered ashfall containing fragments of quartz phenocrysts.

water and mud flat depositional environment, consistent with the presence of tuffaceous rocks.

The analyzed specimen of Pioneer Shale with 11.4% K_2O was collected from a thin layer with definite relict shard structures similar to the ones in Pioneer Shale described by Gastil (1954). It is proof that some high K rocks in the Apache Group do represent tuffs.

Origin of the potassium-rich rocks

The lack of evidence of potassium contribution by the diabase and the fine-grained, pure nature of the K feldspar make attractive the hypothesis that the widespread potash-rich rocks were formed by diagenetic feldspathization of fine-grained, partly tuffaceous rocks of more normal composition. Other occurrences of authigenic feldspar in high-potash sedimentary rocks somewhat similar to the occurrences here have been described. Certain characteristics of the overlying Mescal Limestone suggest a favorable environment for the feldspathization of the upper Dripping Spring Quartzite.

Feldspathized beds of volcanic ash described by Weiss (1954) have compositions much like parts of the upper member; he reports an analysis with 13.25% K_2O and 0.17% Na_2O. The ash beds, only a few inches thick, occur in the Ordovician Galena and Dubuque Formations in Minnesota. Fossils in the beds are locally replaced by feldspar, clearly indicating a post-depositional origin for the mineral. The fine-grained fraction of the Ordovician Glenwood Shale in Minnesota has 10.85% K_2O (Gruner and Thiel, 1937) and is similar to the fine-grained material in the upper

Dripping Spring Quartzite. Gruner and Thiel concluded that the fine-grained fraction consisted largely of authigenic feldspar.

Environments in which authigenic potassium feldspar has been formed recently offer clues to the conditions which may have created the high-potash rocks in the Apache Group. Authigenic potassium feldspar is a common diagenetic mineral associated with zeolites in altered clays and tuffs (Sheppard and Gude (1964), Hay and Moila (1963), Hay (1966)). Assemblages containing authigenic alkali feldspar are particularly common in sediments in saline, alkaline nonmarine environments (Hay, 1966, p. 1). In the basin of Searles Lake, authigenic K feldspar forms as much as 50% of tuffaceous beds and 20% of non-tuffaceous clays (Hay and Moila, 1963, p. 323); sediments with 50% authigenic K feldspar have 8.5% K_2O. Hay and Moila (1963, p. 327) quote figures indicating that Searles Lake brines have a K/(K+Na) ratio of about 1/10. Orville (1963, p. 201) determined that the K/(K+Na) ratio in vapor in equilibrium with two feldspars decreases with falling temperature from 0.26 at 670°C to 0.16 at 400°C; extrapolation of the trend indicates that in the low-temperature Searles Lake brines Na feldspar might be unstable relative to K feldspar.

Hay (1966, p. 2) notes that "...alkalic feldspars may possibly be stable relative to zeolites in quartz-bearing sedimentary rocks under most conditions of sedimentary burial." He describes instances where K-poor analcime has reacted toform nearly pure K feldspar, the potassium probably being derived from aqueous solutions. Hay (1966, p. 99) also states: "Nonmarine tuffs of rhyolite, dacite, and trachyte composition are commonly transformed to beds of nearly pure authigenic K feldspar."

Characteristics of the lower member of the overlying Mescal Limestone suggest that the Dripping Spring Quartzite was thoroughly soaked in highly saline waters which may have created an environment like those most favorable for the production of authigenic K feldspar in recent clays and tuffs. The lower member of the Mescal is cherty dolomite lying with erosional disconformity on the Dripping Spring. Shride (1967) has described the member in considerable detail. He writes (p. 27): "Abundant halite molds and small scale sedimentary structures indicate that much of the dolomite was deposited in very shallow highly saline waters... molds of halite are ubiquitous in individual beds...the lower part of the Mescal probably accumulated in a broad uniformly shallow quiet body of water, such as a lagoon or other almost landlocked setting." The lower member contains an extensive breccia unit, interpreted by Shride as formed when abundant evaporite salts were leached from unconsolidated sediments.

Perhaps authigenic K feldspar was formed together with zeolites in brine-soaked rocks at least in part of tuffaceous origin in the upper member of the Dripping Spring Quartzite at the time of deposition of the Mescal Limestone. With the passage of time zeolites may have been leached away and replaced by additional K feldspar, as has happened in recent tuffs studied by Hay (1966, p. 98). Styolites are abundant in all fine-grained rocks in the upper member. Granger and Raup (1964, p. 52) describe a rock from the K-rich black facies containing thirty styolites in an inch-thick layer; they observe that some sections of the upper member must be considerably thinner now than at the time of deposition. The styolites may have developed as the rocks were leached, enriched in

authigenic K feldspar, and depleted in other constituents. Much of the potassium in the upper member may have come from a interstitial brine.

Stratigraphic implications

Certainly the most singular feature of the upper member of the Dripping Spring Quartzite is the presence of rocks unusually high in potassium. If the K feldspar content of the rocks was an original depositional feature, then it might be an important aid in correlating the formation with other Precambrian rocks in the southwest. If, as suggested here, the high potassium content of the rocks is due to potassium gain during diagenesis, the potassium content would not be such a useful correlation feature. It would not uniquely characterize stratigraphic horizons. However, if only tuffaceous rocks are heavily feldspathized, high K contents might enable rocks to be identified as tuffs. They might also characterize rocks which underwent diagenesis in similar physical and chemical environments.

THE DIABASIC ROCKS

Most of the igneous rocks in the Sierra Ancha sill complex can be readily separated into two groups on the basis of any of a number of criteria, such as location in the sill, petrography, mineralogy, and chemistry. The first group consists of rocks of obvious diabasic affinities, while the second group consists of granitic and syenitic rocks with characteristics in part derived from pre-existing sedimentary rocks. Since only the rocks with diabasic affinities can be considered to form a normal igneous differentiation series, these rocks will be described together and the granophyric rocks will be discussed in a following section.

The important diabasic rock types in the sill--feldspathic olivine-rich diabase, normal olivine diabase and diabase pegmatite--are located in a schematic cross section in Figure 2. Chemical analyses, modes and norms of these and other diabasic rock types are listed in Table 5. In the following section the occurrences and petrography of the diabasic rock types are described in the following order: feldspathic olivine-rich diabase, normal diabase, albite diabase, chilled marginal diabase, pegmatitic diabase, and quartz diabase.

The cross section in Figure 2 is schematic because the base of the sill is not exposed in the Reynolds and Workman Creek sections studied most extensively here. A complete section of the sill along Pocket Creek described by Williams (1957) lacks granophyric rocks but is otherwise much like the schematic section. The actual section exposed in Reynolds Creek and the locations of some analyzed samples are shown in Figure 3.

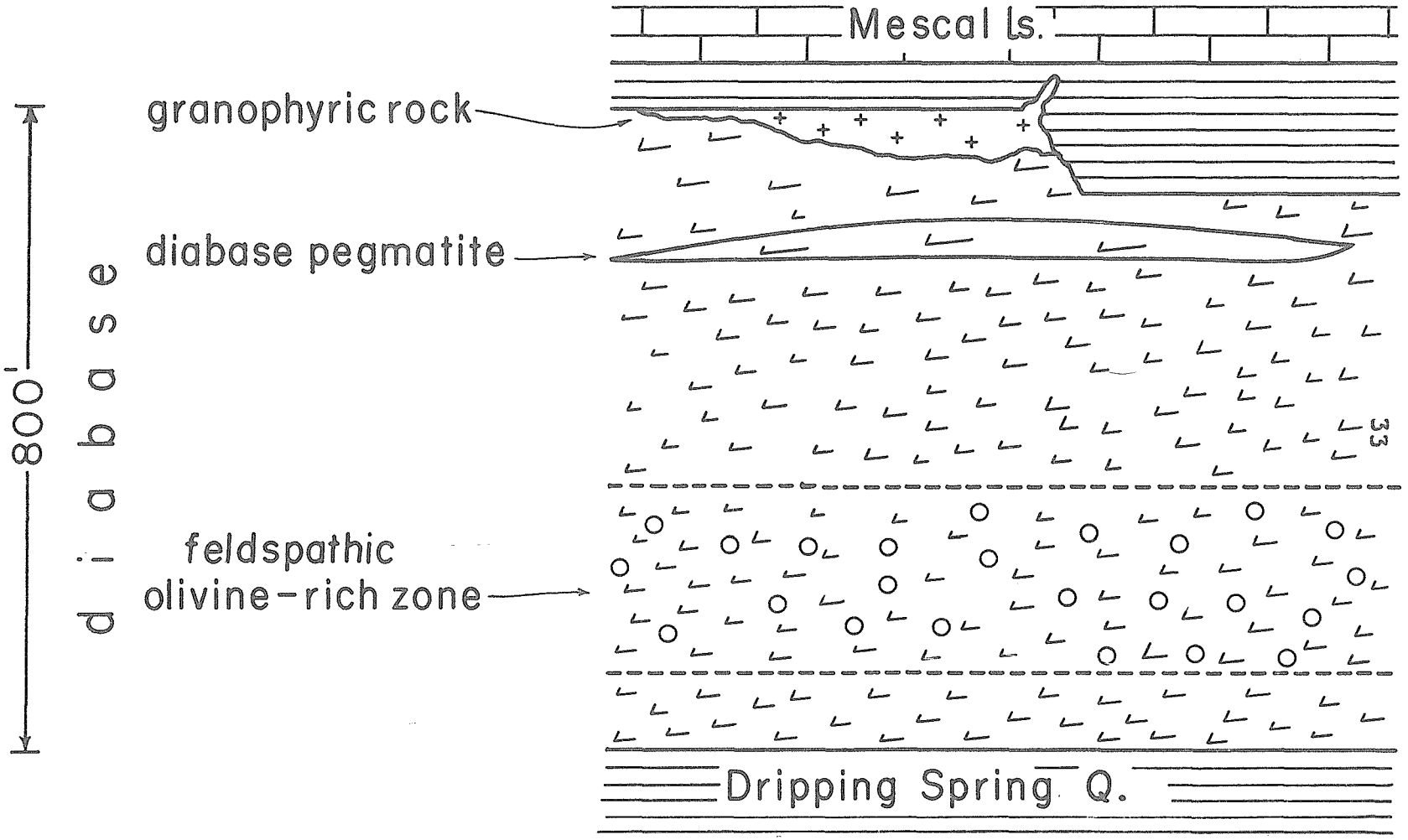

Figure 2. Schematic cross section through the Sierra Ancha sill complex.

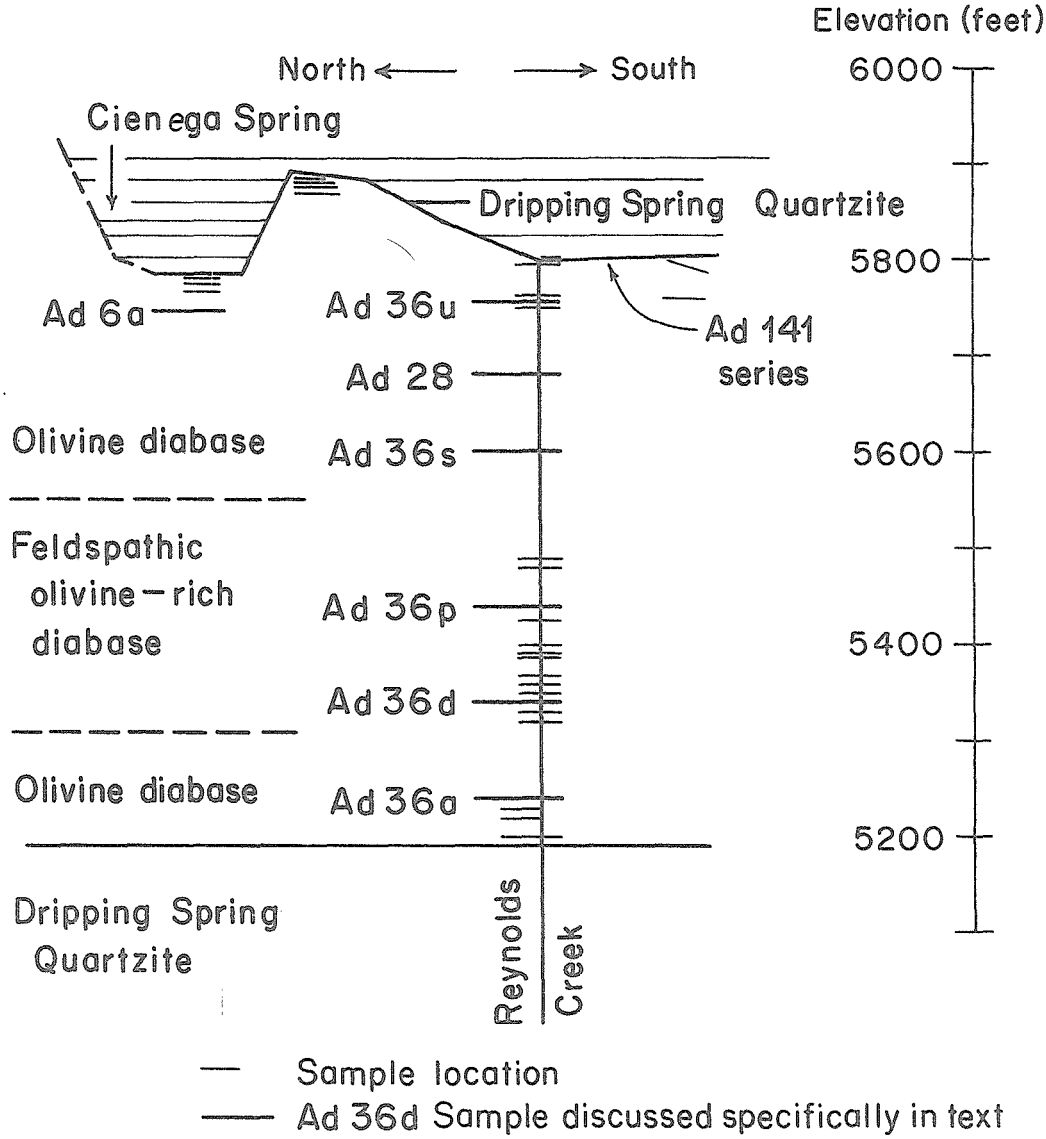

Figure 3. Schematic drawing showing sample localities in and near the Reynolds Creek diabase section.

TABLE 5

Analyses of Diabasic Rocks

Wet Chemical Analyses*	1 Ad36d feldspathic olivine-rich diabase	2 Ad36s olivine diabase	3 Ad163e olivine diabase	4 Ad163f coarse-grained segregation	5 Ad98b1 diabase pegmatite	6 Ad98b2 diabase pegmatite	7 Ad28 diabase pegmatite	8 Ad141d albite diabase	9 Ad286e quartz diabase
SiO_2	46.22	45.47	47.04	47.13	48.66	51.05	52.98[1]	51.40	52.90
TiO_2	0.63	3.24	2.02	5.64	3.31	2.47	2.70	3.74	2.89
Al_2O_3	21.33	17.02	16.96	13.86	14.86	15.87	14.45	13.13	13.57
Fe_2O_3	1.61	2.34	3.22	3.80	3.04	3.61	1.94	2.36	3.35
FeO	6.37	8.02	7.46	8.25	7.81	5.14	5.50	3.96	7.96
MnO	0.09	0.15	0.15	0.22	0.21	0.15	0.18	0.15	0.21
MgO	9.65	8.03	6.72	4.24	4.38	3.15	3.24	5.44	3.10
CaO	10.04	10.25	9.25	8.20	10.19	9.00	9.30	12.00	5.13
Na_2O	2.64	2.66	3.04	3.57	4.48	5.11	5.18	4.78	4.10
K_2O	0.36	0.64	1.30	2.01	0.82	1.55	1.86	0.26	3.35
H_2O^+	1.21	1.64	2.18	2.11	2.11	2.40	1.56	2.07	1.97
H_2O^-	0.46	0.49	0.57	0.68	0.55	0.67	0.46	0.75	0.96
P_2O_5	0.07	0.24	0.31	0.59	0.19	0.16	1.24	0.65	0.76
S	0.04	0.12	0.11	0.11	0.08	0.06	0.16	0.17	0.00
Total	100.72	100.31	100.33	100.41	100.69	100.41	100.75	100.86	100.25
Approximate Modes									
Quartz	–	–	–	–	–	–	–	–	3
Plagioclase	65	45	35	5	30(?)	35(?)	30(?)	50	40(?)
An content	(71-60)	(67-52)	(59-35)	(48-2)	–	(1-0)	(2-0)	(1)	
Alkali feldspar	–	–	–	25(?)	5(?)	10(?)	10(?)	–	
Augite & Calcic Pyroxene	4	30	20	30	15	25	30	35	15
Hypersthene	trace	trace	3	–	–	–	–	–	–
Fe/(Fe+Mg)	(.23-.26)	(.33-.35)	(.34-.56)	–	–	–	–	–	–
Olivine	25	10	6	–	–	–	–	–	–
Fe/(Fe+Mg)	(.26-.30)	(.31-.36)	(.43)	–	–	–	–	–	–
Opaques	3	4	3	5	7	4	6	2	4
Sphene	–	–	–	–	3	1	4	6	–
Biotite	1	2	3	–	–	–	–	–	5
Apatite	–	trace	trace	1	3	3	4	1	1
Amphibole	–	5	10	7	15	10	trace	–	20
Chlorite	1			3	8	3	4	2	–
Feldspar alteration products	trace	5	20	25(?)	15(?)	10(?)	10(?)	5(?)	15(?)
Weight % Norm**									
Quartz	–	–	–	–	–	–	–	–	1.95
Nepheline	.87	–	–	–	3.89	3.95	1.29	0.46	–
Albite	20.95	22.93	26.36	30.95	31.50	37.13	42.02	40.40	35.65
Anorthite	45.72	33.22	29.50	16.24	18.38	16.22	10.82	13.88	8.97
Orthoclase	2.15	3.85	7.87	12.17	4.94	9.41	11.13	1.57	20.34
Diopside	3.30	13.64	12.48	17.13	25.99	22.27	22.42	29.80	9.97
Hypersthene	–	1.36	1.07	4.38	–	–	–	–	10.67
Olivine	23.20	14.45	13.02	0.87	3.78	–	1.02	–	–
Magnetite	2.36	3.46	4.78	5.64	4.50	5.38	2.85	1.84	4.99
Ilmenite	1.21	6.27	3.93	10.97	6.41	4.82	5.19	7.24	5.64
Pyrite	0.08	0.23	0.21	0.21	0.15	0.12	0.30	0.32	–
Apatite	0.17	0.58	0.75	1.43	0.46	0.44	2.97	1.57	1.85
Others	–	–	–	–	–	0.26	–	2.90	–
Total	99.99	99.98	99.99	100.00	99.99	99.99	100.02	99.99	100.04
Fe/(Fe+Mg) in normative silicates	0.23	0.22	0.26	0.17	0.32	0.20	0.28	0.00	0.42

* analyst: Tadashi Asari

** see appendix for calculation method

[1] average of two duplicate analyses.

TABLE 5 (Continued)

Spectographic Analyses* (ppm)

	1 Ad36d	2 Ad36s	3 Ad163e	4 Ad163f	5 Ad98b1	6 Ad98b2	7 Ad28	8 Ad141d	9 Ad286c
Ba	90	160	270	460	130	230	220	31	570
Co	54	44	41	26	15	15	20	19	28
Cr	92	340	240	45	3	n.d.	n.d.	12	n.d.
Cu	12	38	45	29	22	13	22	15	17
Ga	12	14	12	13	16	20	17	13	15
Mn	870	1100	1200	2200	1700	1300	1650	1100	2300
Ni	180	150	120	39	n.d.	n.d.	n.d.	42	n.d.
Sc	n.d.	33	29	44	23	<20	38	43	40
Sr	440	340	200	160	150	77	170	76	130
V	84	200	190	200	110	160	140	270	110
Y	n.d.	<20	34	74	120	130	140	110	100
Yb	n.d.	3	3	7	8	9	8	7	5
Zr	20	70	100	210	200	300	350	280	230

*Analyst: E. Bingham
n.d. not detected

1. Ad36d Feldspathic olivine-rich diabase. Reynolds Creek, elevation 5360'.

2. Ad36s Olivine diabase. Reynolds Creek, elevation 5600'.

3. Ad163e Olivine diabase. Steep ravine, north side of Workman Creek, NE quarter Section 30, T6N, R14E.

4. Ad163f Coarse-grained segregation. Several feet from Ad163e.

5. Ad98b1 Diabase pegmatite. A few feet above Ad163e.

6. Ad98b2 Diabase pegmatite. Same hand specimen as Ad98b1.

7. Ad28 Diabase pegmatite. Reynolds Creek, elevation 5680'.

8. Ad141d Albite diabase. South bank of Reynolds Creek, 12 feet below contact.

9. Ad286c Quartz diabase. North slope of Grantham Peak, NW quarter Section 7, T5N, R14E.

Sample locations shown on Plates 4 and 5 .

TABLE 6

Analyses of Diabasic Rocks from Pocket Creek
Williams, 1957, Appendix I

	1	2	3	4
SiO_2	47.11	45.94	47.24	52.34
TiO_2	0.69	2.30	2.14	3.15
Al_2O_3	20.28	17.50	15.95	13.34
Fe_2O_3	1.14	3.41	2.48	1.14
FeO	7.33	9.46	9.25	6.83
MnO	0.09	0.23	0.23	0.23
MgO	9.17	6.62	8.03	4.68
CaO	9.67	8.60	9.92	8.92
Na_2O	3.09	2.79	2.81	5.04
K_2O	0.29	0.87	0.81	0.92
H_2O^+	1.46	2.07	1.15	2.38
H_2O^-	0.03	0.02	0.06	0.27
P_2O_5	0.12	0.44	0.26	0.65
S	-	-	-	-
	100.47	100.25	100.33	99.89

1. Feldspathic olivine-rich diabase

2. Olivine diabase below olivine-rich layer

3. Olivine diabase above olivine-rich layer

4. Diabase pegmatite

Feldspathic Olivine-rich Diabase

Feldspathic olivine-rich diabase is the most mafic rock type in the sill; a chemical analysis, mode, and norm of a representative specimen from Reynolds Creek, Ad36d, are given in Table 5. A chemical analysis reported by Williams (1957, #738) of a sample of the same rock type from Pocket Creek is listed in Table 6. The most distinctive feature of this diabase is that it contains about 25% modal olivine. Because some of the rock consists almost entirely of olivine and plagioclase, it might be termed troctolite. Though its mineral compositions lie on trends defined by minerals from other rocks in the sill, feldspathic olivine-rich diabase contains more magnesian pyroxene and olivine and more calcic plagioclase than other rock types. The pyroxenes and iron-titanium oxides in it contain higher trace element percentages than those from other rock types, suggesting higher temperatures of formation. All evidence indicates that the olivine-rich diabase contains the earliest crystallization products of the Sierra Ancha diabase magma.

The rock type occurs in a layer about 240 feet thick slightly below the center of the exposed sill section in Reynolds Creek. The layer is of similar thickness and crops out about the same distance below the sill roof in Workman Creek. In the 700-foot-thick Pocket Creek section, Williams (1957) found olivine-rich diabase from 190 to 440 feet above the base of the sill. Olivine-rich diabase is more resistant than other mafic rocks in the sill, and it is generally well-exposed. The layer is expressed topographically as a resistant bench which can be observed in many places east of the Globe-Young road between the sampled localities. Since the diabase both below and

above the layer contains more iron-enriched minerals which crystallized at lower temperatures, the position of the layer is somewhat unusual.

Mineralogy of the layer

Plagioclase (An_{71}-An_{59}) and olivine (Fo_{75}-Fo_{70}) form the bulk of all rocks in the layer, and in some specimens the modal percentages of the two minerals together total over 90 percent. The layer is homogeneous except for occasional coarser-grained segregations rich in augite and plagioclase and containing little or no olivine. Even when modal mineral percentages cannot be estimated accurately, feldspathic olivine-rich diabase can be distinguished in the field from olivine diabase because generally the former has a distinctly smaller average grain size.

Plagioclase in the olivine-rich diabase occurs in tabular crystals parallel to (010) with an average maximum diameter of 1 mm; larger crystals up to 5 mm in maximum diameter occur sparsely in all samples. These larger crystals stand out conspicuously on weathered surfaces. Most crystals have either albite or albite-Carlsbad twinning and are commonly normally zoned, though some have several zoning reversals. In most rocks in the layer a rough orientation of plagioclase can be observed, many of the tabular crystals being subparallel to the horizontal sill roof and layer boundaries. This orientation might have been caused either by crystal rotation during movement of a crystal-liquid mush or by settling and packing of tabular crystals into their present sites.

Olivine occurs in two readily distinguishable textural habits. Most olivine crystals in all samples are anhedral, equant, and from

PLATE 8

Rock Ad36b. 2x3 mm. Crossed nicols. Feldspathic olivine-rich diabase. Note alignment of plagioclase laths.

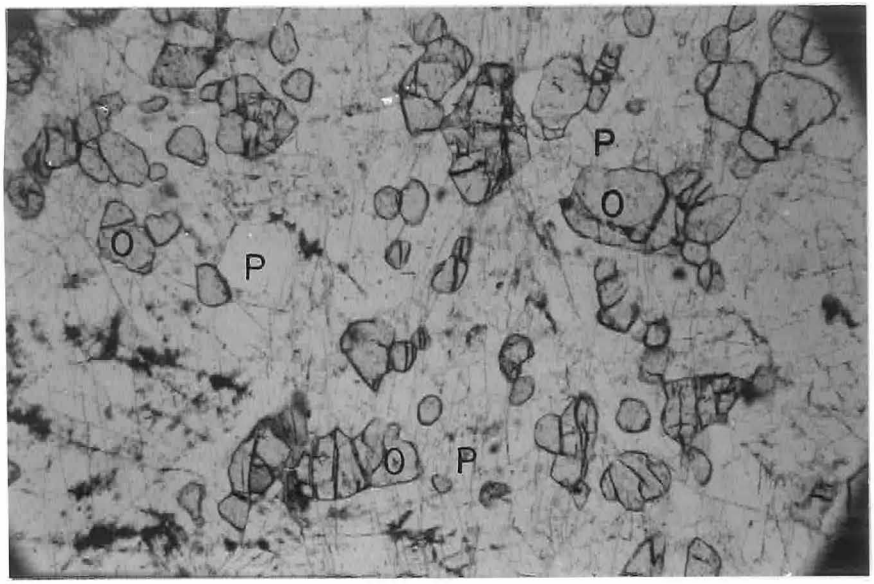

Rock Ad36b. 2x3 mm. Feldspathic olivine-rich diabase. Note equant olivine crystals. (O, Olivine; P, Plagioclase.)

0.05 to 0.4 mm in diameter. All rocks contain some larger olivine crystals with irregular shapes; some of these are poikilitic, and a few are strikingly interstitial to plagioclase.* No systematic differences in composition between the larger and smaller crystals were found either with the microscope or with the microprobe. In rocks consisting almost entirely of olivine and plagioclase with very little augite, relatively few large olivine crystals occur. In rocks with more abundant augite, large olivine crystals are more abundant.

Augite comprises from 3% to 15% of rocks in the layer. In general, rocks in the lower part of the layer contain less augite than those in the upper part. The augite, tan in thin section, occurs in ophitic crystals, some of which are crystallographically continuous for thin section distances as great as 16 mm. Its crystal form clearly shows that calcic pyroxene was not a cumulate mineral.

Ilmenite$_{ss}$, magnetite$_{ss}$, orthopyroxene, and biotite are the remaining primary phases in the layer. Ilmenite$_{ss}$ and magnetite$_{ss}$ together make up two to five percent of rocks in the layer. Ilmenite$_{ss}$ occurs in striking, interstitial crystals, while magnetite$_{ss}$ occurs in more equant grains. Orthopyroxene, present only in trace amounts, is most commonly found in small grains at the rims of olivine crystals. Biotite, also present in very small quantity, generally occurs partially rimming opaque grains.

Though feldspathic olivine-rich diabase is the least-altered rock in the sill complex, most specimens contain several percent of chlorite and other sheet structure minerals replacing olivine. In addition, many olivine crystals contain inconspicuous, tiny opaque

*The intergrowths of interstitial olivine with plagioclase would be called "ophitic" if the mafic phase were augite.

grains concentrated along curving fractures, probably the result of high-temperature oxidizing deuteric alteration (Haggerty and Baker, 1967). Most rocks contain a few partially-sericitized plagioclase grains.

Contacts of the olivine-rich layer

The lower contact of the feldspathic olivine-rich diabase layer was seen in only one locality, at an elevation of about 4860' in a small drainage entering Pocket Creek from the north. Here the rock type is in contact with a facies of diabase with an average grain size at least three times greater. The contact is knife-edge sharp, not gradational (Plate 9). Locally in the rock above the contact are scarce pockets, one to three inches in diameter, of a coarser-grained rock more like that below; these may be small segregations. Neither rock type shows any sign of chilling at the contact, and obvious dikes of one type in the other were not observed in the limited exposure. Though the contact is approximately horizontal, it has local relief of one to two feet, and there are angular projections of the olivine-rich diabase into the coarser rock below. No conclusive evidence was observed, but the coarser facies appeared to have been intruded beneath overlying rock which had solidified to rigidity. However, the absence of chilling at the contact indicates that the time interval between the intrusive pulses was small.

The feldspathic olivine-rich diabase over the contact displays the oriented plagioclase crystals characteristic of the unit. In addition, in thin section a few specimens from near the contact show zones of shearing in roughly horizontal planes.

PLATE 9

Typical weathered surface of olivine diabase. Nodular surface reflects presence of large ophitic augite crystals.

Sharp lower contact between darker-colored, finer-grained feldspathic olivine-rich diabase (above) and lighter-colored, coarser-grained olivine diabase (below). Exposure is in a small drainage on the north side of Pocket Creek.

The coarse-grained facies for a few feet below the contact is also characterized by oriented plagioclase crystals. It has 20 to 25 modal percent olivine, about as much as the overlying feldspathic olivine-rich diabase. However, the olivine occurs in large, interstitial crystals and groups of large crystals rather than in the small, equant crystals characteristic of the overlying rock. A sample from twenty feet below the contact contains less olivine (15-20 modal percent), and two rocks from about one hundred and forty feet below the contact (elevation of about 4720') contain 10-15 modal percent olivine[1], a value closer to that in olivine diabase above the feldspathic olivine-rich layer.

An irregularly shaped plate of sedimentary rock is exposed along the Globe-Young road between Pocket and Parker Creeks at the elevation of the lower contact of the fine-grained feldspathic olivine-rich diabase. The beds in the plate are nearly horizontal and include perhaps 50 to 100 feet of section, possibly representing both Dripping Spring and Mescal. The upper and lower contacts of the plate were not exposed. The southern-most exposures are terminated at a vertical contact with chilled diabase. The chilled facies is extensively altered, and accurate modal estimates could not be made; however, the diabase was obviously olivine-rich. Similar plates of sedimentary rock have been described by Shride (1967, pp. 53-55) in his general discussion of the geometry and form of diabase intrusions in southern Arizona; he concluded that the plates "...can be considered everywhere as proof of multiple intrusions."

1. These rocks contain 3-5% orthopyroxene in aggregates replacing olivine(?); the orthopyroxene occurrences are different from those observed in the Reynolds Creek and Workman Creek rocks studied.

The upper contact of the layer was not observed. Exposures in Reynolds Creek bracket the contact only within about one hundred feet of section. However, the contact can be more accurately located because of the topographic expression of the more resistant olivine-rich rock. Cherukupalli (1959, p. 19) states that the upper contact of the zone is gradational in Pocket Creek.

Origin of the feldspathic olivine-rich layer

The feldspathic olivine-rich diabase layer may have formed from a magma containing abundant suspended olivine and plagioclase crystals intruded at or near the bottom of a sheet of olivine diabase magma. In another pulse of magma, olivine diabase was intruded beneath the layer. Alternative hypotheses for the formation of the layer include: (1) segregation of early-crystallized olivine and plagioclase into the center of the sill by flow differentiation; (2) multiple intrusion with central intrusion of a liquid of troctolitic composition; and (3) gravity accumulation of crystals at the bottom of a cooling, initially homogeneous intrusion followed by an intrusion of diabase beneath the layer. Though detailed field mapping is necessary to firmly establish how the layer originated, textural, chemical, and contact features of the layer make these three hypotheses less probable than the first one mentioned.

It is unlikely that the composition of feldspathic olivine-rich diabase represents an original liquid composition because the analyzed sample (Ad36d, Table 5) contains 21.3% Al_2O_3, a value considerably higher even than that of most high-alumina basalts. It is more probable that the rock contains plagioclase and olivine crystals accumulated from a larger body of magma.

Textures in the layer support the contention that the feldspathic olivine-rich diabase is a cumulate rock, the term as used simply implying accumulation of early-formed crystals from a larger body of liquid. As mentioned earlier, the orientation of plagioclase laths is due either to flow of a crystal mush or to settling of the laths. The relationship of olivine and augite in the olivine-rich rocks provides more subtle evidence for a cumulate origin. Augite makes up from three to fifteen percent of feldspathic olivine-rich diabase and is more abundant near the top of the layer. Cumulate rocks contain two types of minerals -- those which in part are cumulate crystals and those which crystallized from the magma about the collected crystals (Wager, Brown, and Wadsworth, 1960). The amount of intercumulate magma present reflects the abundance and packing of the cumulate phases. Since the crystal form of augite clearly shows it was not a cumulate phase, the abundance of augite is a guide to the relative proportions of cumulate crystals and intercumulate magma in different parts of the layer. Rocks containing little augite primarily contain the small textural types of olivine, suggesting that the 0.05 to 0.4 mm olivine crystals are in large part cumulate crystals. Rocks containing more augite contain relatively more large olivine crystals, suggesting that the large olivine crystals owe their size to post-cumulus growth. The fact that some of the large crystals are interstitial supports the conclusion that they grew late in the crystallization history of the rock. Surprisingly, post-cumulate crystallization of olivine seems to have resulted in effective growth of only a few crystals rather than a general enlargement of the many cumulate olivine crystals present.

Formation of the layer by flow differentiation (Bhattacharji, 1967) does not seem probable for several reasons. First, the sharp contact between facies of quite different grain size near Pocket Creek and the plate of sedimentary rock near the contact to the north make multiple intrusion seem likely. Second, the layer persists in the Reynolds Creek area where the sill is bounded by abrupt structural boundaries on the north and west; it is questionable whether flow differentiation would operate in such a situation. Finally, if the magma were so fluid that olivine and plagioclase were concentrated into a central layer by flow, it would be surprising if they did not settle to the bottom of the sill when flow ceased.

Though possible, it is unlikely that the feldspathic olivine-rich diabase represents a simple gravity cumulate in place. Gravity cumulates in place are commonly characterized by phase layering, that is, by layers enriched in certain minerals relative to others. The layering is formed because of different crystallization temperatures and settling velocities of cumulate minerals. The densities of olivine and plagioclase are quite different*, and it would be surprising if the two minerals were not locally separated in the accumulation of a layer the thickness of the Sierra Ancha olivine-rich sheet. Though small layers particularly rich in either olivine or plagioclase were looked for carefully, none was found.

The most likely explanation remaining for the origin of the feldspathic olivine-rich layer is that it represents a separate intrusive pulse of magma containing abundant suspended olivine and plagioclase crystals. The diabase beneath it was emplaced separately, as indicated by the sharp lower contact and by the plate of sedimentary rock

*Densities of $Forsterite_{70}$ and $Anorthite_{70}$ are about 3.5 and 2.7, respectively.

located presumably at the contact. Since the upper contact of the layer was not seen, it is not certain whether the layer was emplaced before or after the diabase above it. Emplacement of the olivine-rich rock near the bottom of a still-molten upper layer is quite possible. Drever and Johnston (1967) have suggested that separate emplacement of olivine-rich rocks in the central portions of diabase sills is a common process. A sill intrusive into the Pioneer Shale in the Sierra Ancha described by Gastil (1950, p. 119) also has a central olivine-rich zone.

All the problems connected with the distribution of diabase rock types in the Sierra Ancha sill will not be resolved without detailed mapping over a wide area. For instance, the origin of the coarse-grained olivine-rich rock immediately below the feldspathic olivine-rich layer near Pocket Creek remains enigmatic. The case seems strong for multiple intrusion in the sill. However, mineral and bulk rock compositional trends provide evidence that all the diabasic rocks are genetically related and originated from a common magma source.

Olivine Diabase

Olivine diabase, the typical rock of the sill, is represented in Table 5 by the analyses, modes, and norms of samples Ad36s and Ad163e and by analyses 2 and 3 in Table 6. The diabase is dark gray in hand specimen and has an average grain size of several millimeters. Primary minerals in the rock are plagioclase, augite, olivine, $ilmenite_{ss}$, $magnetite_{ss}$, and minor hypersthene and biotite.

Olivine diabase throughout the sill contains deuteric minerals and in many rocks these minerals are major constituents. "Deuteric" is used here in the sense intended by Sederholm (1929, p. 870). He defined deuteric processes as: "...those that have taken place in direct continuation of the consolidation of the magma of the rock itself." Sederholm further stated: "...minerals should be designated as deuteric only when a replacement of definite primary minerals belonging to the same magmatic cycle has occurred." Deuteric processes were of considerable importance in the crystallization history of the Sierra Ancha sill complex. The results of these processes will be described here, while the processes themselves will be discussed in a subsequent section.

Least-altered olivine diabase

The olivine diabase with the least deuteric alteration is near the center of the sill above the relatively fresh feldspathic olivine-rich diabase. The analyzed specimen Ad36s (Table 5) is an example of this least-altered olivine diabase; photomicrographs of the rock are shown in Plate 10. The compositions of the primary phases in this rock and others are described in the sections on the individual mineral groups. Plagioclase occurs in laths averaging 1.5 mm in length, with albite or albite-Carlsbad twinning. Most crystals contain dark-colored, very fine-grained aggregates of alteration minerals, presumably clays, concentrated along fractures. Augite, tan in thin section, occurs in spectacular ophitic crystals with a maximum diameter of 30 mm. Augite crystals are more resistant to weathering than feldspar and stand out on weathered surfaces, giving some outcrops a knobby appearance (Plate 9). The augite contains no

PLATE 10

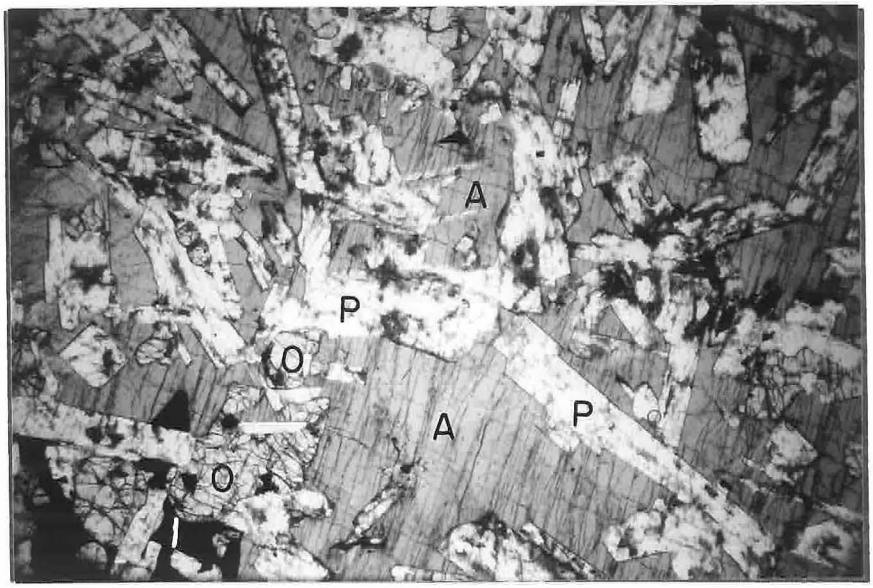

Rock Ad36s. 6x9 mm. Olivine diabase. (A, Augite; O, Olivine; P, Plagioclase; I, Ilmenite). Augite in photomicrograph represents parts of only two crystals.

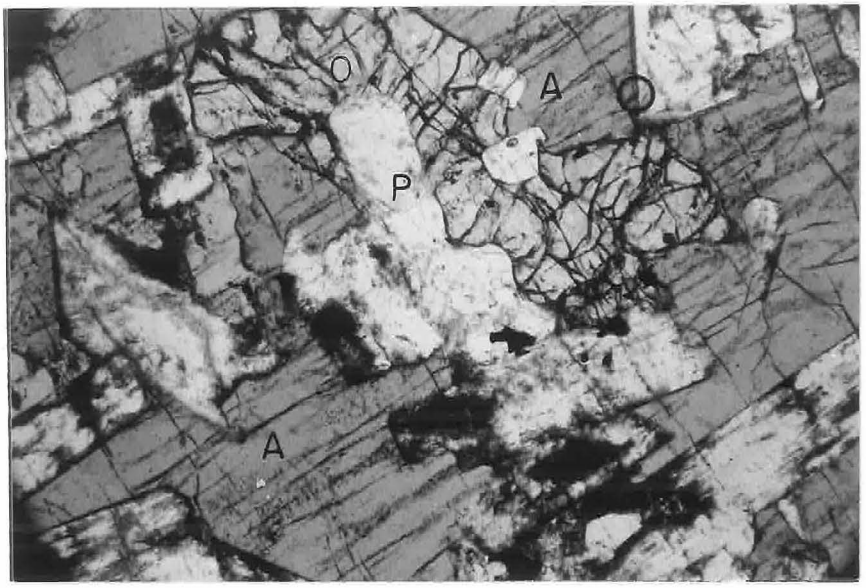

Rock Ad36s. 2x3 mm. Augite is optically continuous. Note shape of olivine crystal. Black, dusty plagioclase alteration is typical.

identifiable pyroxene exsolution lamellae. Olivine occurs in anhedral grains averaging about 1 mm in diameter; though some grains are equant, others are irregular in shape and poikilitic or interstitial. Both augite and olivine contain tiny, unidentified inclusions concentrated along sparsely-distributed, curving planes. While augite is almost unaltered, many olivine grains show marginal alteration and a few have been completely replaced by felty aggregates of white mica and chlorite. At least two types of low-birefringent chlorite replace olivine -- one type pleochroic in shades of green and one type colorless. A few olivine grains have been replaced by pale brown felty material with moderate birefringence and parallel orientation, probably some form of iddingsite. Hypersthene occurs as tiny grains commonly bordering olivine crystals; it appears to be primary. Opaque grains are interstitial to the silicates. Biotite most commonly occurs rimming opaque grains. A little fibrous amphibole occurs with other alteration products.

Typical olivine diabase

The intensity of alteration is greater both in the diabase below the olivine-rich layer and in that higher in the sill than Ad36s. The analyzed sample Ad163e is typical of most of the diabase above and below the central layer. Its chemical analysis (Table 5) and mineral compositions indicate it crystallized from a more differentiated, iron-enriched magma than Ad36s. Primary mineral assemblages (Table 5) are the same in the two samples. Ad163e contains more hypersthene; the calcium-poor pyroxene occurs not only as grains marginal to olivine grains but also as independent

crystals. Grain sizes and shapes are about the same as in rock Ad36s; plagioclase laths average about 2 mm in length. About two-fifths of the plagioclase is replaced by fine-grained, dark alteration products. About half the olivine has been replaced by felty aggregates of green to pale brown sheet-structure silicates with moderate birefringence. Though most of the augite is fresh and tan in thin section, some of it is bleached and contains many small inclusions of opaques and amphibole or biotite. This type of pyroxene alteration occurs throughout the sill, and the chemical and physical changes involved are discussed in the section on pyroxene mineralogy. Amphibole, in part sodic as indicated by its deep blue-green pleochroism and small 2V, apparently has replaced orthopyroxene and perhaps augite. Two types of biotite are present. The most common variety, pleochroic from dark brown to golden brown to red-brown, occurs as rims on opaque grains and as separate crystals. The less common variety occurs in small crystals pleochroic from green to brown.

Intensely-altered diabase

Intensely-altered diabase occurs in the upper part of the sill. Sections of the upper part of the sill containing little or no granophyre and capped by diabase chilled against overlying Dripping Spring Quartzite were studied in Reynolds Creek and in the drainage leading from near Cienega Spring into Reynolds Creek. In the upper fifty or so feet of these sections the diabase below the chilled marginal facies is slightly coarser-grained and lighter-colored

than lower in the sill. The lighter color is due to the milky-white color of altered plagioclase. The alteration assemblages in these rocks are particularly interesting, as they are similar to the assemblages in the late, pegmatitic differentiates in the sill complex.

Most of the plagioclase in the rocks has been replaced by aggregates of clay and white mica. Prehnite has been formed in the centers of some feldspar grains. No feldspar grains are fresh; the best-preserved have the dusty, speckled alteration and pericline-albite twinning characteristic of almost pure Na feldspar in the pegmatites, suggesting that most of the feldspar left is albite. Olivine is absent. Most rocks contain about one percent apatite in acicular prisms. The most altered specimens contain one to two percent of sphene, probably in part formed from titanium released during the pyroxene alteration. Some specimens contain calcite, apparently filling vugs(?). Polished section examination and microprobe work shows that magnetite$_{ss}$ was unstable and was partially replaced by chlorite and unidentified minerals. Ilmenite$_{ss}$ was apparently unaffected by the alteration, although some grains of it are rimmed by sphene.

The most complex and interesting alteration processes are those which affected augite. The rocks contain remnants of primary, tan, ophitic augite. Some of the ophitic augite has recrystallized to colorless calcic pyroxene studded with tiny inclusions of opaques, biotite and amphibole. The colorless pyroxene is crystallographically continuous with the primary tan augite, the color change taking place at a sharp front. This colorless pyroxene itself has locally been replaced by chlorite and aggregates of

amphibole. Chlorite*, the most common alteration product, in one rock was intermixed with and apparently partly replaced by biotite. The most common amphibole is pleochroic light to dark green. Other secondary minerals, such as tremolite, sodic amphibole, white mica, sphene(?) and other varieties of chlorite are also present in replacement aggregates. Some of these minerals might be replacements of olivine. In the most intensely-altered rock, some primary augite has been replaced by aggregates of secondary pyroxene crystals and chlorite (Plate 11). Most of this pyroxene is colorless in thin section, though some is pale green. Many grains have numerous twin lamellae. It appears to coexist with chlorite and to be one of the alteration products of primary augite. In the most intensely-altered diabase this late deuteric pyroxene is the most abundant mafic alteration product and chlorite is second in abundance. In these rocks amphibole is not an important alteration product. Probe studies of the composition of the late deuteric pyroxene are reported in the section on pyroxenes.

In summary, deuteric alteration of diabase has resulted in the following mineralogic changes. Calcic plagioclase and olivine were the first minerals to be altered; the former was replaced by clays, white mica, prehnite and albite, while the latter was replaced by a variety of sheet-structure minerals. Primary titaniferous augite was first bleached colorless and then replaced by chlorite and hornblende and perhaps by white mica, biotite, and other sheet silicates. In some intensely altered rocks a colorless

*The chlorite is pleochroic from light brown to green. It is optically negative, apparently uniaxial, and has a low birefringence and an anomalous blue extinction color.

PLATE 11

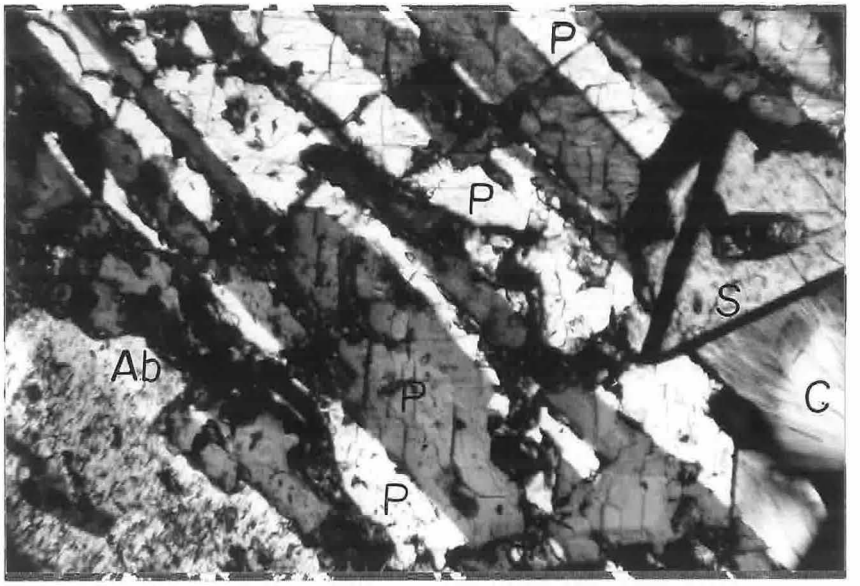

Rock Ad141d. 0.4x0.6 mm. Crossed nicols. Albite diabase. A single calcic pyroxene crystal (P) with twin lamellae, euhedral sphene (S), albite (Ab), and chlorite (C).

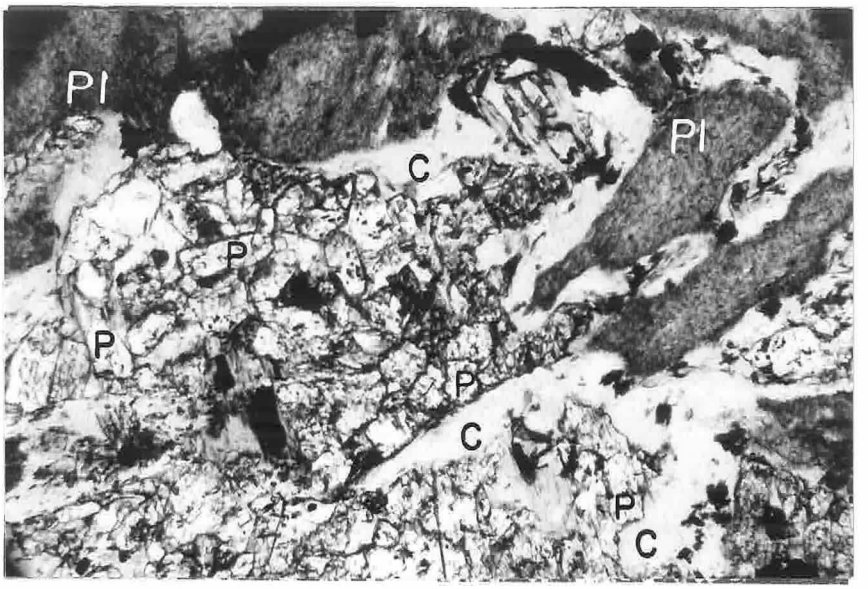

Rock Ad36u. 2x3 mm. Aggregate of deuteric calcic pyroxene (P) and chlorite (C) pseudomorphic after augite surrounded by altered plagioclase (Pl).

pyroxene and chlorite were the stable(?) alteration products of the original augite. Magnetite$_{ss}$ was replaced by chlorite and unidentified minerals. Ilmenite$_{ss}$ was apparently unaltered. Sphene was formed. The assemblage in the diabase seemingly stable under conditions of intense deuteric alteration was: colorless calcic pyroxene, chlorite, albite, prehnite, sphene, ilmenite(?), apatite, clays and white mica, and minor amphibole and calcite.

Albite Diabase

Locally, along the banks of Reynolds Creek, a few feet of "granitic" rock have formed at the contact and chilled diabase is absent. A diabase sample collected four feet below the "granitic" rock was found to be albite diabase; the exposed section containing the sample is shown in Figure 33. In hand specimen the rock appears to be typical altered diabase, medium gray in color and with an average grain size of one to two millimeters. In thin section the rock appears relatively unaltered but has a mineral assemblage like that developed elsewhere by intense deuteric alteration.

An analysis, mode, and norm of rock Ad141d are given in Table 5. Plagioclase occurs in anhedral grains with albite, albite-Carlsbad, and, in a few instances, albite-pericline twinning. All the grains contain numerous specks of clay minerals(?) and tiny pockets of chlorite scattered through them, and a few contain larger flakes of clay(?); prehnite inclusions were seen in several grains. The plagioclase is only slightly zoned, and microprobe results show the bulk of it to be almost pure albite ($Ab_{99}An_1$). Colorless calcic pyroxene occurs in anhedral grains which commonly have multiple twinning (Plate 11). Microprobe results show the major element

pyroxene composition to vary between $Ca_{49}Mg_{39}Fe_{12}$ and $Ca_{47}Mg_{33}Fe_{20}$. Ilmenite(?) occurs in small anhedral grains rimmed by sphene. Most sphene grains are anhedral, but a few are euhedral. Chlorite, pleochroic in pale shades of brown and green, is in some instances intergrown with pyroxene and in others not associated with it. Small prisms of apatite make up the remainder of the rock.

Rock Ad141d is simple in mineralogy and composition, and experimental studies in the system albite-diopside help to understand its origin. Both the mode and norm of the rock contain about 85 percent plagioclase plus calcic pyroxene (Table 5). In the mode the plagioclase is almost pure albite and the pyroxene is magnesium-rich salite. In the norm the plagioclase is calcic oligoclase while the pyroxene is pure diopside.* The system albite-diopside has been studied by Schairer and Yoder (1960). They found that the system was not binary, the plagioclase crystallizing being slightly calcic (estimated to be about An_{25} by Yoder and Tilley, 1962, p. 395). Plagioclase and diposide coexist on the liquidus at a composition of $albite_{91}diopside_{9}$ and at a temperature of about 1130°C. The system is completely crystalline at temperatures near 1030°C. The albite and pyroxene in rock Ad141d apparently formed with chlorite, a mineral unstable above about 650°C. at water pressures of less than a kilobar (Yoder, 1967, and Turnock, 1960). It seems unlikely that water pressure of no more than a kilobar (an estimate of the probable maximum load pressure) and the presence of minor constituents could lower the melting temperature of the rock to a value within

*The presence of aluminous chlorite, prehnite, and clays(?) in the mode may contribute to the more calcic normative plagioclase.

the chlorite stability field. It seems more probable that the mineral assemblage in albite diabase formed by the complete recrystallization of an earlier mineral assemblage which crystallized from a diabase melt.

Diabase similar to Ad141d is common for twenty to thirty feet below the granophyre lenses on the ridge north of Reynolds Creek. It contains the same basic mineral assemblage as sample Ad141d. Pyroxene occurs in colorless to pale green, anhedral or subophitic grains, rather than in the large tan ophitic crystals common in more normal diabase. However, unlike in rock Ad141d, in many cases albite crystals in these rocks have cores rich in clay minerals. In some cases the cores of albite grains contain prehnite.

The mineral assemblage -- albite, calcic pyroxene, sphene (and ilmenite), chlorite, and apatite -- is very similar to that developed as a deuteric alteration product of diabase lower in the sill. This similarity, together with the fact that clay(?) specks are included throughout the albite, also suggests that rock Ad141d might be a product of the recrystallization pre-existing diabase. The albite diabase probably represents the most intense expression of the deuteric alteration seen in other diabasic rocks. The mineral assemblage in the albite diabase is that of a spilite. The significance of the spilite mineral assemblage and the nature and causes of the deuteric alteration will be explored in a subsequent section.

The albite diabase may have undergone slight metasomatic changes during recrystallization. Rock Ad141d contains less K_2O and has a higher Na/K ratio than any other diabasic rock analyzed. It also contains more CaO and less Al_2O_3 than the rest of the analyzed suite.

Chilled Facies of the Diabase Magma

Fine-grained diabase, a chilled marginal facies, is present at the floor of the sill and at the sill roof where granophyre does not occur. Three chemical analyses of marginal diabase in the Sierra Ancha sill, two reported by Williams (1957, p. 92) and one by Neuerburg and Granger (1960, Table 5), are given in Table 7. If the marginal diabase were unaltered, the analyses would represent the actual composition of diabase magma. Unfortunately the marginal diabase invariably seems to have been altered.

Two fine-grained diabase samples were collected from within three feet and four feet of the chilled upper contact of the sill in the Reynolds Creek drainage area. In both samples the average grain size is less than 0.5 mm, though one of the rocks contains a few altered plagioclase phenocrysts up to 3 mm long. Olivine and augite occur in anhedral, equant to subophitic grains. At least half the olivine, augite and plagioclase grains have been replaced by sheet-structure minerals, amphibole, and clays. Both rocks contain about 8 percent each of biotite and opaques. The biotite, pleochroic from dark brown to red-brown to golden brown, occurs in poikilitic crystals up to 4 mm in maximum diameter. Most opaques occur in anhedral grains about 0.2 mm in diameter, while a few have rod-like forms and comprise skeletal crystals. Most of the biotite and opaques seem secondary. A sample of chilled diabase from a smaller intrusion of diabase higher in Reynolds Creek was collected from within a few inches of overlying Mescal Limestone. Though fresher than the two samples described above, the rock is similar in petrography and also contains poikilitic biotite.

TABLE 7

Analyses of Diabase at Chilled Contacts

	1	2	3
SiO_2	43.71	47.54	47.76
TiO_2	3.76	2.85	3.00
Al_2O_3	15.12	11.11	18.62
Fe_2O_3	2.10	6.38	0.71
FeO	12.07	11.17	10.21
MnO	0.36	0.26	0.30
MgO	6.14	6.59	4.81
CaO	6.75	7.70	6.37
Na_2O	1.99	2.96	3.52
K_2O	4.42	1.21	2.08
H_2O^+	2.05	2.50	2.00
H_2O^-	0.07	0.06	0.14
P_2O_5	1.13	0.37	0.39
S	0.11		nil
BaO	0.05		
CO_2	0.01	0.00	nil
F	0.13		
	99.86	100.70	99.91

1. Lower contact; exact location unspecified, possibly Asbestos Point(?). (Neuerburg and Granger, 1960, Table 5.)

2. Lower contact at Pocket Creek. (Williams, 1957, p.92.)

3. Upper contact at Workman Creek. (Williams, 1957, p.92.)

One sample was collected from within a few inches of the lower contact of the sill at Pocket Creek. The rock is almost completely altered. It has an average grain size of 0.5 mm or less, though plagioclase laths one millimeter or longer are not uncommon. Plagioclase has been replaced almost completely by clays and white mica. Amphibole, chlorite, and minor biotite are the only ferromagnesian minerals present, all olivine and augite having been replaced. The rock contains about 5 percent opaque minerals, many of which have rod-like shapes and form skeletal crystals; these opaques seem secondary.

The petrography of the analyzed specimens is not well-established. Williams (1957, p. 107) mentions that the analyzed specimen of the lower contact at Pocket Creek (Table 7, #2) contains "...plagioclase phenocrysts, pyroxene, and magnetite." Cherukupalli (1959, p. 18) mentions that the specimen contains abundant biotite. The specimen from the upper contact (Table 7, #3) is described as containing "...phenocrysts of long plagioclase laths...small but abundant pyroxene, biotite, hornblende, magnetite" (Williams, 1957, p. 108). Neuerburg and Granger (1960, p. 773) state that the marginal diabase has abundant alteration minerals "...such as biotite, sericite, magnetite, and chlorite...". They do not further describe their analyzed sample.

In view of the pervasive alteration of rocks at the contacts of the sill, it is unlikely that any of the analyses of chilled diabase represent the composition of the original diabase magma. Williams (1957, p. 67) suggests that the analyzed sample from the lower chilled contact at Pocket Creek (Table 7, #2) is "...most representative of the early magma." However, the analysis is significantly higher in potassium and iron and lower in aluminum than analyses of more

typical and less-altered diabasic rocks in the sill (Tables 5 and 6). The high iron value is quite unusual for a basaltic rock. It is likely that the high potassium and iron values in the analyses in Table 7 reflect the presence of secondary biotite and opaques in the marginal rocks. The alteration of chilled diabase was probably accompanied by enrichment in potassium and iron. Since diabase chilled against Mescal Limestone contains poikilitic biotite, the source of the potassium was probably the diabase rather than the sedimentary rocks. Walker (1957, p. 11) remarks that chilled phases of basaltic sills in the Palisadan and Karoo provinces commonly contain poikilitic biotite. Potassium enrichment of the chilled facies is perhaps a typical phenomenon in diabase sills.

Coarse-grained Diabasic Rocks

Coarse-grained diabasic segregations and dikes are common in the Sierra Ancha sill complex. Similar rocks have been called "pegmatoids" in some of the literature. The coarse-grained rocks occur in two manners in the complex -- as small lenses and segregations and as large tabular lenses and dikes. Since the rock in the larger bodies generally differs from that in the smaller bodies in appearance and mineral proportions, the two types will be described separately. For convenience of reference, the term "diabase pegmatite" will be used only in referring to the rock type forming the large tabular lenses and dikes.

Segregations and Lenses

Small segregations and lenses coarser-grained and more leucocratic than the surrounding diabase occur throughout the sill.

Most of the segregations are only a few inches to a foot in maximum diameter, and the lenses are most commonly only a few inches thick. However, one lens almost eight feet thick is exposed in Reynolds Creek near the center of the sill.

The most abundant mineral in these relatively coarse-grained rocks is plagioclase. It is generally heavily altered to clays and white mica and, less commonly, to prehnite. In contrast to the situation in the large pegmatite bodies, alkali feldspar and alkalic rims on plagioclase are inconspicuous or lacking. The plagioclase laths reach a maximum length of about 10 mm. Ophitic crystals of primary augite and interstitial crystals of ilmenite(?) are spotted throughout the plagioclase-rich rocks. The augite is commonly bleached and locally altered to hornblende, chlorite, and tremolite. In at least one rock deuteric, multiply-twinned calcic pyroxene was formed as an alteration product of primary augite. However, primary calcic pyroxene of the type found in the large bodies of diabase pegmatite does not occur in these smaller segregations. A remnant of olivine was observed in one specimen, but olivine and pseudomorphs after it are rare in these rocks. Several percent of sphene and apatite are commonly present.

A few of the small, coarse-grained bodies have some mineralogical characteristics approaching those of the diabase pegmatites. For instance, many of the plagioclase laths in these transitional segregations have dusty rims of alkali feldspar. Rock Ad163f, represented by an analysis, mode and norm in Table 5, is such a transitional rock.

Counterparts of the small, coarse-grained segregations and lenses are found in many other diabase sills, as discussed in the review by Walker (1953). As in the cases discussed by Walker, the

small segregations contain later differentiates than normal diabase and earlier differentiates than large sheets of pegmatite.

Diabase Pegmatite

Tabular lenses and dikes of diabase pegmatite are common near the sill roof. These pegmatites are coarse-grained and gaudy, mottled with patches of pink-rimmed feldspar crystals and large black augite crystals. The pegmatites are more resistant to weathering than olivine diabase, and their distinctive lithology makes them easy to recognize. Analyses, modes, and norms of three samples of diabase pegmatite (Ad98b1, Ad98b2, and Ad28) are in Table 5.

The most common occurrence of the pegmatites is in flat-lying tabular lenses cropping out within one hundred feet of the sill roof. The width of the lenses varies from three to fifteen feet. Generally the lateral extent of the lenses cannot be determined because of a paucity of outcrops, but near Workman Creek one large lens was traced for over one thousand feet. The tabular lenses were observed in the Pocket Creek, Workman Creek, and Reynolds Creek areas and north of Reynolds Creek.

Pegmatite similar in appearance but with a slightly different mineralogy occurs in masses just below the sill roof associated with the granophyre bodies exposed on the ridge north of Reynolds Creek. The shapes of these masses were difficult to determine because of a scarcity of outcrops, but in one locality the pegmatite appears to occur in a dike cutting steeply down into the diabase below. The pegmatites were not observed cutting the sedimentary rocks, and they seem to be restricted to the sill complex.

The mineralogy and compositions of the diabase pegmatites are particularly interesting, as these rocks may be the latest uncontaminated differentiates of the Sierra Ancha diabase magma. The alkali enrichment in the rocks and the iron enrichment in their pyroxenes show that the pegmatites represent later differentiates than the other quartz-free diabasic rocks, as will be discussed in subsequent sections. The field occurrence, petrography, and compositions of the pegmatites provide strong evidence that most of them are uncontaminated differentiates. Their similarities to other bodies of diabase pegmatite described in the literature reinforce the interpretation that they are simple differentiates and not hybrid products.

The strongest field argument that most of these pegmatites are uncontaminated differentiates is simply that most bodies are not located near the overlying sedimentary rocks. The pegmatites occur at distances as great as 100 feet below the sill roof and do not contain xenoliths. One tabular sheet of pegmatite, twelve feet thick, extends laterally for at least one thousand feet near Workman Creek; it is at least sixty feet below the sill roof and is bounded by normal, apparently uncontaminated diabase. The uniform mineralogy of the sheet, taken in conjunction with its lateral extent and position in the sill, makes a hybrid origin seem unlikely. Shride (1967, pp. 59-60) suggests other factors, such as the abundance of pegmatites in sites favorable for volatile concentration, which make a pegmatite origin by contamination doubtful.

The petrography of pegmatites is complex. Augite and calcic plagioclase crystallized early from the pegmatitic magma. These minerals reacted at lower temperatures. Calcic pyroxene, alkali feldspar, apatite, sphene, and chlorite were stable minerals in the

late stages of crystallization. No quartz formed in the pegmatites except when they were intruded against and presumably reacted with the roof rocks. The compositions of the minerals are described in detail in the sections on the individual mineral groups. The petrography, to be described here, is consistent with the hypothesis that the rocks formed from an uncontaminated magma.

Feldspar in diabase pegmatite

Feldspar in diabase pegmatite occurs in stout laths generally from three to fifteen millimeters long, though some rocks contain laths as long as thirty millimeters. In hand specimen many laths have gray centers and pink rims; where the rims are abundant, they give the rock a pink color. The gray centers of many of the laths contain anhedral grains of prehnite* surrounded by albite. Some lath centers contain flakes of clay minerals as well as prehnite and albite, and some laths contain only clays and albite. The albite is in all cases lightly dusted with specks of unidentified minerals, probably clays; some albite laths contain very small inclusions of chlorite. While the centers of the albite grains generally have only albite or albite-Carlsbad twinning, the margins commonly have cross-hatched albite-pericline twinning. In most specimens most laths have definite rims composed of fine patch intergrowths of albite and K feldspar.

*Prehnite was first identified by its optical characteristics -- moderate relief, second-order birefringence, positive 2V of 60-70 degrees. The identification was confirmed in rock Ad28 by x-ray diffractometer and microprobe studies. An x-ray diffractometer chart of material picked from the cores of feldspar laths showed a good reflection at d = 3.08, a strong reflection for prehnite but not one for albite or epidote. Electron microprobe studies showed that the mineral contains 26.8 percent CaO, a value typical for prehnite.

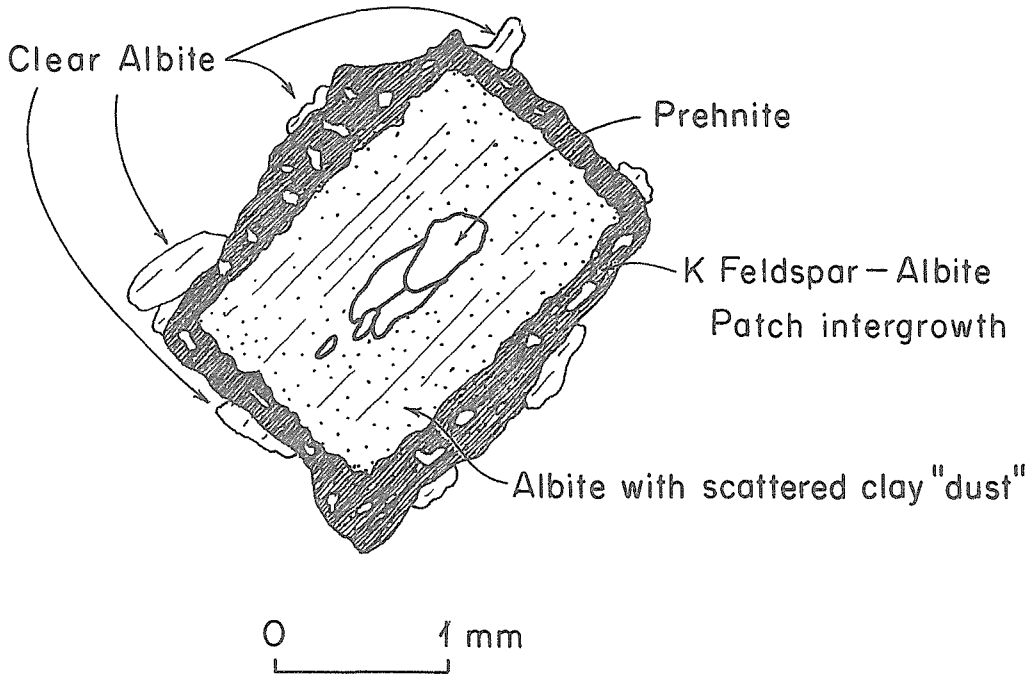

Figure 4. Schematic portrayal of feldspar textures in diabase pegmatite.

PLATE 12

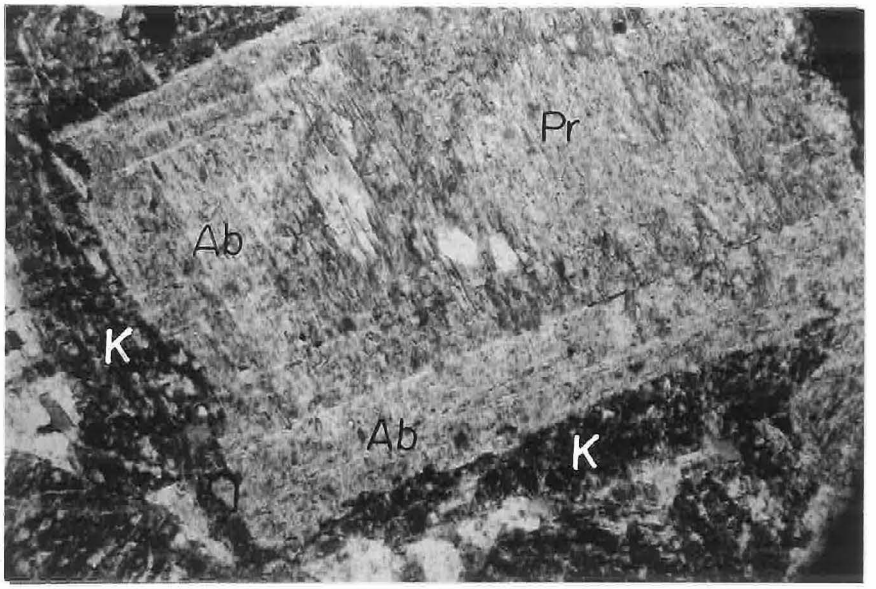

Rock Ad28. 2x3 mm. Shows typical feldspar texture in diabase pegmatite. (Pr) prehnite; (Ab) albite; (K) potassium feldspar-rich rim.

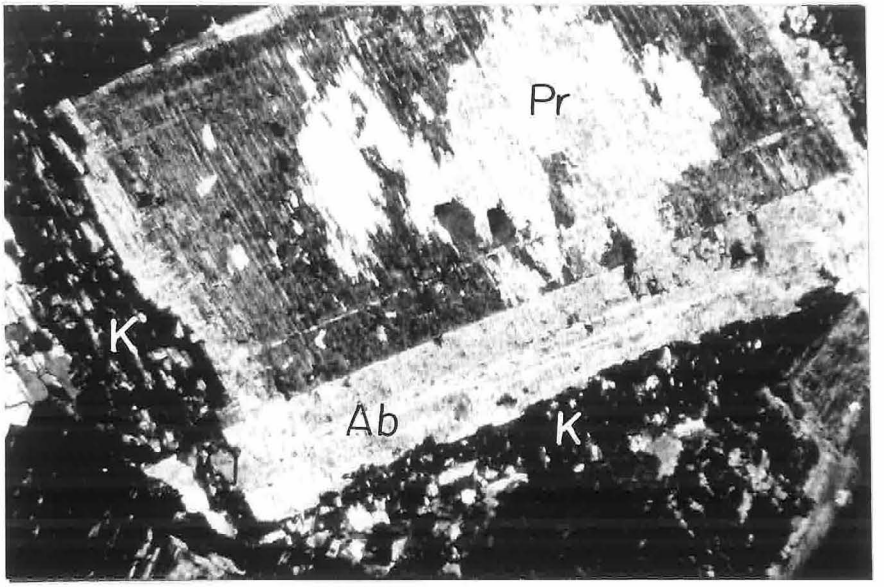

Rock Ad28. Same field of view as above. Crossed nicols. Note patches of albite in K feldspar-rich rim.

The K feldspar is commonly so intensely dusted with specks of clays(?) as to appear almost black in thin section. The albite, less intensely dusted, has albite-pericline twinning, and it is in optical continuity with albite in the interiors of the laths. Clear albite, the only clear feldspar in the rocks, occurs in interstices between the feldspar laths with apatite, chlorite, calcic pyroxene, and sphene. The clear albite is commonly in optical continuity with albite in the rims and centers of adjoining feldspar laths. Photomicrographs of a typical feldspar grain are in Plate 12, and a schematic drawing illustrating the feldspar textures is shown in Figure 4. All pegmatite samples examined contain the typical feldspar textures, though certain features are better developed in some rocks than in others. For instance, rims rich in K feldspar are well-developed in some rocks and scarce in others. Prehnite is common in some rocks and rare in others. In one specimen prehnite forms independent clusters of crystals as well as occurring in the center of feldspar laths.

Compositions of the feldspars were investigated optically and with the microprobe. The optical properties of albite in the pegmatites indicate it is very sodic. Electron microprobe studies were made on the feldspar in the analyzed specimens Ad28 and Ad98b. The most calcic albite measured had the composition $Ab_{97.5}An_{2.2}Or_{0.3}$, and albite as pure as $Ab_{99.7}An_{0.2}Or_{0.1}$ was found. Some of the albite spots analyzed have less potassium than the Amelia albite standard. K feldspar spots studied with the microprobe had essentially no calcium and generally contained less than 2 percent albite molecule.

The feldspar-rimming relations and the purity of the feldspar end-members in the diabase pegmatite cannot be attributed to any plausible sequence of direct crystallization. The textures and

compositions can be explained by a sequence of feldspar crystallization followed by reaction with a late fluid phase in the pegmatites. That the first feldspar to crystallize in the pegmatites was calcic plagioclase is suggested by the presence of prehnite in the centers of many of the albite laths. Even albite laths without central concentrations of clay or prehnite are dusted with tiny clay(?) inclusions. The hypothesis that all the albite cores were formed deuterically from more calcic plagioclase is supported by the ubiquitous inclusions. The K feldspar-albite rims probably formed by the unmixing of an alkali feldspar rim. The presence of unaltered clear albite outside and adjacent to the rims weighs against any explanation based on replacement of the margins of albite grains by K feldspar. The patch intergrowth of nearly pure K feldspar and albite in the rims suggests almost complete unmixing at a relatively low temperature. A plausible explanation for the development of the observed feldspar relations can be separated into magmatic and deuteric stages. In the magmatic stage calcic plagioclase initially crystallized, and, as the melt became more alkalic, it was rimmed by alkali feldspar. In the deuteric stage the anorthite component of plagioclase reacted to albite, prehnite, and clays. The alkali feldspar rims unmixed to albite and K feldspar.

Pyroxenes

Partly altered ophitic crystals of primary augite, averaging ten to fifteen millimeters in maximum diameter, are present in all samples of diabase pegmatite. These large crystals of primary augite, tan in thin section, display all the types of alteration described for deuterically-altered augite in normal diabase. Small

equant pyroxene crystals, pale green in thin section, occur in interstices of feldspar laths. These crystals appear to be primary and to have crystallized after the augite. This late primary pyroxene occurs in all samples studied except those from Pocket Creek. The crystals of late pyroxene are euhedral to anhedral, rarely subophitic, and some have multiple twinning. They are smaller than the early augite crystals; maximum diameters rarely exceed three millimeters and are generally less than one millimeter. While the early augite has a normal calcium and moderate titanium and aluminum content, the late calcic pyroxene is exceptionally calcic and contains little aluminum and practically no titanium. It is more enriched in iron than the early augite. The compositional differences are described in detail in the section on pyroxenes.

Though the late calcic pyroxene is unaltered, alteration of the early augite is commonly extensive. One of the striking features of the alteration is its variability. While some crystals of augite are almost untouched, nearby crystals may be completely replaced. In the least intense cases of alteration, augite, initially tan in thin section, has been bleached and spotted with inclusions of opaques and amphibole; the bleached augite commonly occurs near grain boundaries and is optically continuous with unaltered augite. Near grain boundaries the bleached augite itself may be iron-enriched and tinted green and similar in composition to the late calcic pyroxene, as discussed in the section on pyroxene mineralogy. Some augite crystals have been completely replaced by aggregates of tremolite, hornblende, and, more rarely, by chlorite. Other augite crystals have been replaced by masses of a very fine-grained, fibrous amphibole, brown in thin section. In a few rocks

PLATE 13

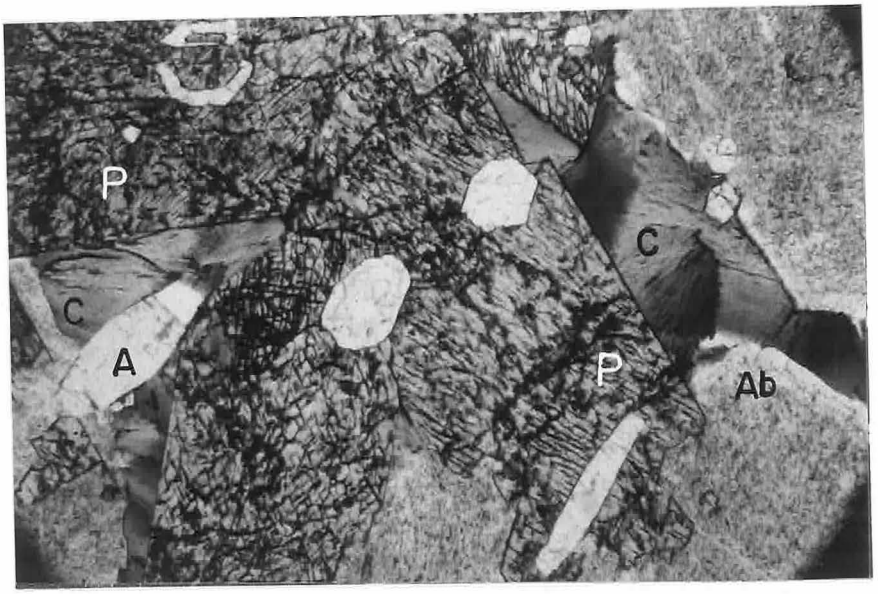

Rock Ad98b. 2x3 mm. Diabase pegmatite. Albite (Ab), calcic pyroxene (P), primary chlorite (C), and apatite (A). Note skeletal apatite at top left.

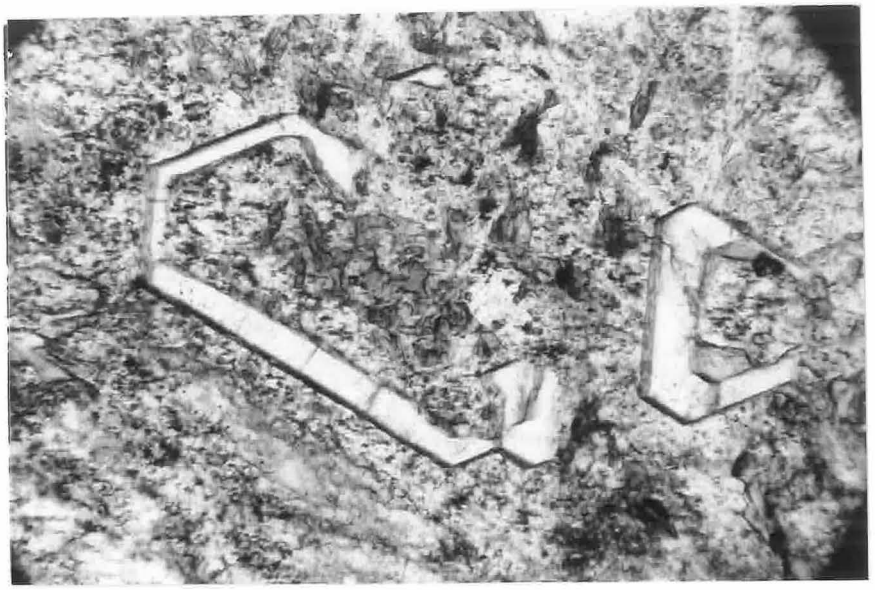

Rock Ad98b. 0.5x0.75 mm. Skeletal apatite within albite. Note specks of clay and flakes of chlorite within the albite.

augite has been replaced by aggregates of deuteric, colorless calcic pyroxene crystals with multiple twinning.

Chlorite

Chlorite is present in three textural settings in the diabase pegmatites. It occurs: (1) with tremolite in aggregates replacing augite; (2) in intricate intergrowths with ilmenite and sphene; and (3) in fan-shaped crystals associated with calcic pyroxene, apatite, sphene and clear albite in pockets interstitial to large feldspar laths. The chlorite in this last association appears primary (Plate 13). The chlorite "fans" give no indication that they have replaced or interacted with calcic pyroxene or any of the other late-crystallizing minerals associated with them. The "fans" are generally 0.1 to 0.3 mm in maximum diameter, are pleochroic from green to pale tan, and have radiating extinction. The crystals are uniaxial negative, have no abnormal interference colors, and have a birefringence in the range 0.01 to 0.015. The optical properties are consistent with those described by Albee (1962) for Fe-rich chlorite. Two microprobe analyses of chlorite in one interstitial pocket in a diabase pegmatite sample from Workman Creek are presented in Table 8. The high Fe/(Fe +Mg) ratios (0.82 and 0.78) of the two analyses support the hypothesis that the chlorites crystallized from a residual magmatic liquid.

Very few primary igneous chlorites have been described. Significantly, one of the best-documented occurrences is in the New Zealand spilites described by Battey (1956). An analysis of spilitic chlorite reported by Battey is presented in Table 8 for comparative purposes.

TABLE 8

Microprobe Analyses of Apparently Primary Chlorite in a Sierra Ancha Diabase Pegmatite together with an Analysis of Chlorite from a New Zealand Spilite

Chlorite Compositions

	Diabase Pegmatite Ad98b(A3)	Diabase Pegmatite Ad98b(A15)	New Zealand Spilite
	1	2	3
SiO_2	24.5	24.7	27.11
TiO_2	n.d.	n.d.	0.35
Al_2O_3	17.1	16.9	17.42
Fe_2O_3			2.91
FeO			30.98
Fe as FeO	41.6	40.0	
MnO	0.22	0.23	
MgO	5.2	6.4	9.75
CaO	0.04	0.06	0.21
Na_2O	0.01	0.34	
K_2O	n.d.	n.d.	
H_2O^+	n.a.	n.a.	11.07
H_2O^-	n.a.	n.a.	0.51
	(88.7)	(88.6)	100.31

1,2 Microprobe analyses

3 Battey, (1956, Table 2)

n.a. not analyzed
n.d. not detected

Iron-titanium oxides and sphene

Ilmenite and sphene are common minerals in the diabase pegmatites. Sphene but not ilmenite commonly occurs in interstitial pockets with other late-crystallizing phases such as apatite and calcic pyroxene. Moreover, sphene commonly rims and replaces ilmenite, while the reverse relationship is never seen. Sphene, therefore, is the titanium-rich phase stable in the final igneous assemblage.

Both ilmenite and sphene occur in striking skeletal crystals and in geometric intergrowths of multiple crystals in the diabase pegmatites. Examples of the intergrown and skeletal crystals are shown in photomicrographs in Plates 14 and 15. It is difficult to describe adequately the intricacy and variety of the patterned intergrowths present. Plates of ilmenite in skeletal crystals in some cases form roughly-defined triangular nets and in other cases form parallel arrays in thin section. Ilmenite plates are in many cases rimmed by and in some cases replaced by sphene. Commonly interstices between plates are filled by aggregates of chlorite or similar sheet-structure minerals. In some cases the ilmenite-sphene-chlorite aggregates seem to be pseudomorphic after pre-existing minerals. These aggregates are commonly found in altered and replaced augite crystals, but they are not observed in unaltered augite crystals. In some instances alkali feldspar, apatite, calcic pyroxene and other minerals occur between oriented ilmenite plates. Ilmenite also occurs in larger anhedral grains and in sets of smaller, roughly-oriented, elongate anhedral grains. Sphene also occurs in primary euhedral grains and in primary skeletal crystals with orthohombic symmetry.

PLATE 14

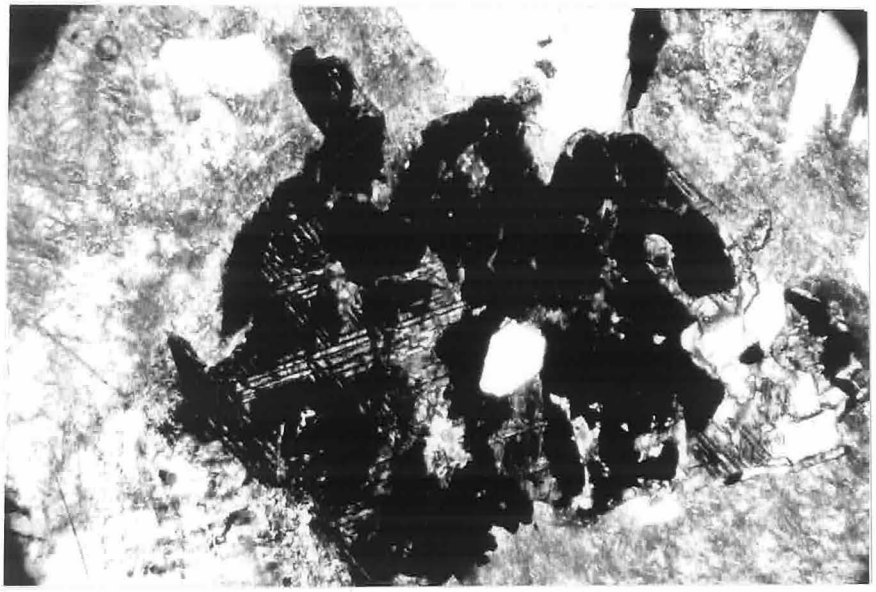

Rock Ad11. 2x3 mm. Diabase pegmatite. Ilmenite and chlorite(?); possibly a magnetite pseudomorph.

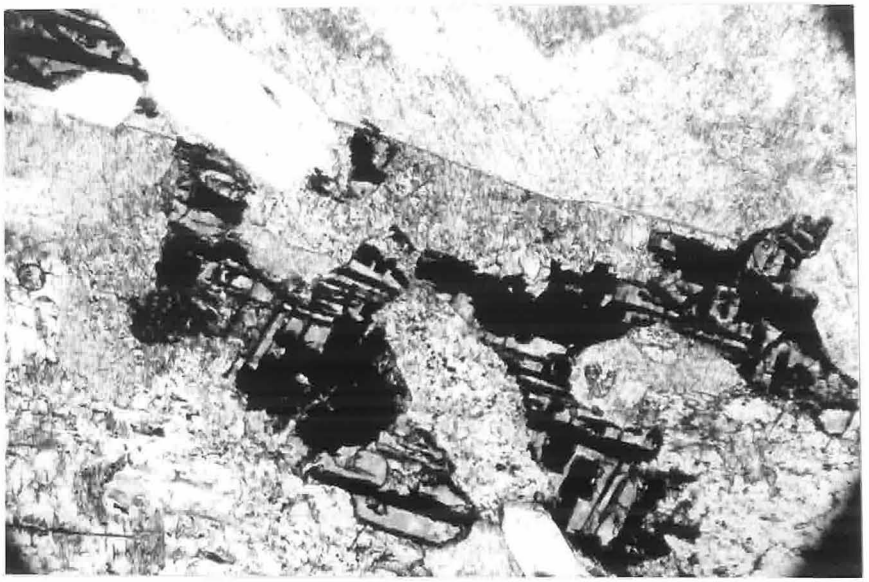

Rock Ad28. 2x3 mm. Diabase pegmatite. Aggregates of ilmenite, chlorite, and sphene in a bleached pyroxene crystal.

Some of the ilmenite-sphene-chlorite intergrowths may be pseudomorphic after original magnetite$_{ss}$ crystals. In a discussion of the opaque minerals in Keweenawan lavas, Cornwall (1951a, p. 55) described magnetite-ilmenite intergrowths in which "...the magnetite is partly to completely replaced by chlorite and sphene..." The ilmenite in such an intergrowth would be in plates oriented parallel to the (111) planes of the original magnetite host. Lindsley (1960, pp. 126-132) discussed in detail the origin of skeletal ilmenite crystals in pegmatitic lenses in a series of basalt flows. He found that the ilmenite plates were oriented in octahedral planes and that they included magnetite in some cases. He concluded that the skeletal ilmenite crystals present were initially "exsolved" from crystals of magnetite$_{ss}$ and that the magnetite$_{ss}$ was subsequently resorbed by the silicate melt.

Such an explanation is probably true for some of the skeletal ilmenite crystals in the diabase pegmatite. It is almost certainly not appropriate for others. The triangular nets of ilmenite plates appear to lie in octahedral planes in some instances and in hexagonal planes in others; the angles formed by intersecting octahedral planes (109.4° and 70.6°) are similar to those for hexagonal planes (120° and 60°), and the two cases cannot be distinguished readily in randomly oriented thin sections. In favor of the Lindsley explanation is the fact that in deuterically-altered diabase magnetite was partly replaced by chlorite and unidentified minerals while ilmenite was unaltered. The following observations weigh against this explanation for many of the skeletal crystals. The crystals are particularly common in replaced augite grains; the explanation here would require a complicated history -- alteration of augite, growth of magnetite, "exsolution" of ilmenite, and replacement of magnetite. Formation of ilmenite from iron and

PLATE 15

Rock Ad286c. 2x3 mm. Quartz diabase. Note oriented rods of ilmenite in calcic pyroxene and altered plagioclase.

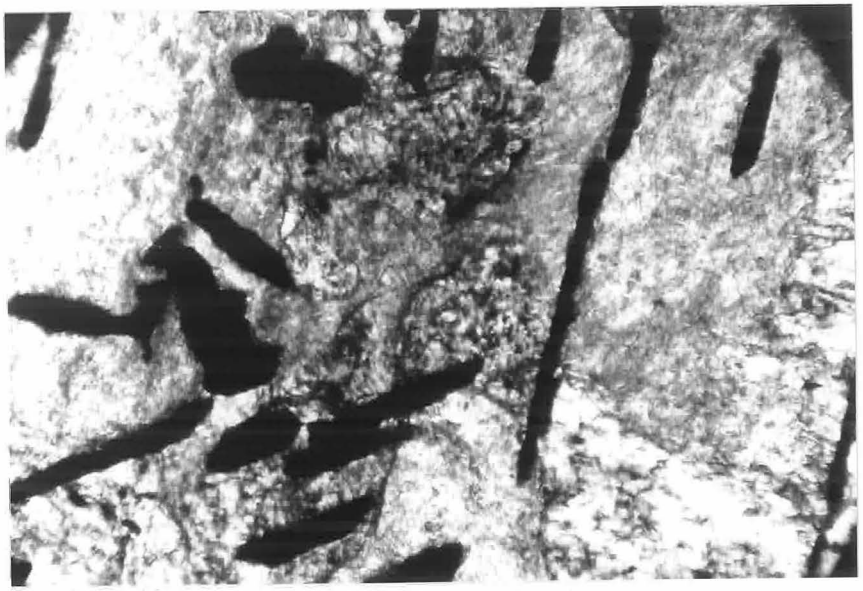

Rock Ad140b. 0.5x0.75 mm. Diabase pegmatite. Note skeletal ilmenite crystals.

titanium released during augite alteration seems more plausible. Some skeletal ilmenite crystals are apparently crystallographically but not physically continuous for many millimeters and actually contain little ilmenite within their borders. These crystals probably are primary. Electron microprobe studies indicate some skeletal crystals are zoned in Mn and Mg in the same manner as crystals of undoubted primary origin. In a review of the petrology of diabase pegmatites, Walker (1953, p. 46) remarks that their iron ores commonly have platey and skeletal crystal forms. Many of the skeletal crystals of ilmenite in the Sierra Ancha diabase pegmatites are probably primary; the chlorite, apatite, feldspar and calcic pyroxene between the skeletal plates are probably also primary. The sphene is probably in part primary and in part formed by reaction of ilmenite with residual melt.

Other pegmatite minerals

Apatite is more abundant in diabase pegmatite than in normal olivine diabase. It occurs in elongate prisms up to 3 mm in length. Many of the apatite prisms are skeletal and are intergrown with albite, calcic pyroxene, chlorite and other late phases (Plate 13). Traces of apparently primary epidote and amphibole occur in some rocks.

Summary of pegmatite mineral sequence

In summary, the minerals in the Sierra Ancha diabase pegmatites can be divided into three groups -- early primary minerals, deuteric minerals, and late primary minerals. Augite, tan in thin section, is the only certain early primary mineral pre-

served, though perhaps ilmenite$_{ss}$ should be classed as an early primary mineral. Calcic plagioclase was an early primary mineral, and magnetite$_{ss}$ may have been one as well, though neither mineral is preserved. Textural evidence suggests alkali feldspar may have been an early primary phase. These minerals all reacted with the remaining magma. Deuteric minerals which replace the early primary minerals include albite, prehnite, clays(?), amphibole, chlorite, calcic pyroxene, and sphene. In the deuteric stage alkali feldspar unmixed to albite and K feldspar. Late primary minerals of importance were iron-enriched calcic pyroxene and chlorite, apatite, and sphene. The assemblage of minerals stable in the late history of the pegmatites includes both deuteric and late primary phases. The important phases in this final assemblage are: calcic pyroxene, chlorite, albite, K feldspar, prehnite, sphene and apatite. This assemblage is similar to the assemblages in albite diabase and in normal diabase which underwent intense deuteric alteration.

Inhomogeneity of diabase pegmatite and sampling procedure

Diabase pegmatite is notably inhomogeneous on the scale of hand specimens and thin sections. The blotchy appearance of outcrops mentioned earlier is due to concentrations both of albite and of pink K feldspar-albite rims. The concentrations are in a few cases as much as a foot in diameter. Different thin sections from the same hand specimen commonly differ in proportions of early primary, deuteric, and late primary minerals. For this reason, estimated modes of the analyzed specimens of pegmatite (Table 5) must be regarded as rough approximations.

The analyzed samples of diabase pegmatite (Table 5) were prepared so as to take into account the inhomogeneity of the pegmatites. For sample Ad28 a split for analysis was taken from about 650 grams of powdered rock, so the analysis of Ad28 should be a fair representation of the bulk composition of the rock. The analyzed samples Ad98b1 and Ad98b2 were prepared from two different 30 gram samples from the same hand specimen; Ad98b2 contained a higher proportion of late primary minerals than Ad98b1 and thus should be more representative of the late fluids in the rock. The bulk composition of rock Ad98b should lie between the two analyzed samples.

Similar differentiates in other mafic intrusives

Dikes and lenses of coarse-grained rock are commonly found among differentiates of diabase sills (Walker, 1953 and 1957). However, calcic plagioclase, augite, iron ore, micropegmatite, and abundant hornblende are characteristic minerals in pegmatites in sills crystallized from saturated or oversaturated magmas. Though mineral assemblages like that in the Sierra Ancha diabase pegmatites are not common, other examples have been described, and the deuteric alteration so well developed in these pegmatites is seen poorly developed in many sills. The pegmatitic facies in the thick Keweenawan flows described by Cornwall (1951, p. 163) has many similarities to the Sierra Ancha diabase pegmatite. In the Keweenawan pegmatites, augite, ilmenite, magnetite, chlorite, and apatite are interstitial to laths of albite-oligoclase; secondary prehnite is common. Albitic pegmatites in a Triassic sill of tholeiitic diabase described by Shannon (1926) also have a similar

mineralogy, though they contain quartz; in particular, Shannon described augite-diopside relationships much like the augite-calcic pyroxene relationships in the Sierra Ancha sill. Bowen (1933, p. 114) wrote that albitization characteristically occurs in gabbroic magmas with a high concentration of "hyperfusibles." Walker (1953, p. 46) noted that late stage albitization is common in diabase pegmatites; he also noted (1957, p. 11) that quartz-albite-diopside veins commonly occur in tholeiitic sills and may be "ultimate magmatic residues."

The other described occurrences show that the mineralogy of the Sierra Ancha pegmatites is not unique. It is the extensive development of the mineralogy which is striking. As noted earlier, the late stage assemblages in the pegmatites, in albite diabase, and in deuterically altered diabase are similar to one another and to spilite mineral assemblages. The implications of the similarities will be discussed in a later section.

Quartz Diabase

Diabase characterized by the presence of quartz and apparently primary hornblende and with alkali feldspar rims on cores of altered plagioclase occurs locally in the sill complex. It is generally coarser-grained, lighter-colored, and more resistant to weathering than typical diabase. An analysis, mode, and norm of a specimen of quartz diabase are given in Table 5.

Distribution of quartz diabase

In the Reynolds Creek and Workman Creek areas, quartz diabase is restricted to locations below granophyric rocks. Though

the upper contact of the dark-colored diabase can generally be defined within an inch or so in these locations, the diabase is not chilled against the overlying light-colored granophyric rocks. Instead, a coarse-grained and locally almost pegmatitic facies of diabase is developed for a few feet down into the sill below the contact. The coarse-grained facies contains quartz in most but not all localities. It grades down into diabase with less quartz, which in turn grades into diabase with extensive deuteric alterations, or, in a few cases, into albite diabase. Less-altered diabase is found lower in the sill. Complete profiles through the quartz-bearing and altered zones were studied in Reynolds and Workman Creeks (Figures 28 and 33). Outcrops of the quartz-bearing diabase are commonly blotchy, light patches rich in pink alkali feldspar being scattered throughout darker rock. The zone of quartz diabase is in some cases only a few feet thick, and in no instance was it found more than a few tens of feet below the granophyres.

On the north and northwest slopes of Grantham Peak south of Parker Creek, an exceptional mass of quartz diabase developed. The analyzed specimen, Ad286c, came from this mass. The quartz diabase is associated with a thick lense of granophyre in a structural trap, a local high point in the sill roof. It contains scattered xenoliths of probable sedimentary origin, which are described in the discussion of the granophyres. Petrographically, it is very similar to the quartz diabase in the thin zones near Reynolds and Workman Creeks.

Mineralogy and petrography of the quartz diabase

Quartz, the diagnostic mineral, seldom exceeds around five modal percent of the rocks. It occurs in micrographic intergrowths with alkali feldspar rims and in anhedral grains associated with shreds of a dark brown biotite(?).

Alkali feldspar and apparently primary hornblende are more wide-spread than quartz, and they occur without it in the lower parts of several zones which separate more normal diabase from overlying granophyric rocks. The alkali feldspar occurs as rims around cores of plagioclase altered to clays. Some of the alkali feldspar rims are clear while others are dusty with specks of clay(?). Most have unmixed to patch intergrowths of K and Na feldspar. Hornblende occurs both as apparently primary crystals and as single crystals and aggregates of crystals replacing pyroxene. The primary-appearing crystals are anhedral and are commonly pleochroic from light to dark brown to greenish-brown. Some single crystals are zoned from colorless centers to brown rims to green margins. Other hornblende crystals include relict centers of pyroxene.

Fresh pyroxene is present in some quartz-bearing diabase, and it is a major constituent of some specimens. The pyroxene, colorless or tan in thin section, occurs in some instances in ophitic crystals and in others in equant anhedral grains. It is primary, not deuteric.

Ilmenite and apatite are common accessory minerals in these rocks. Zircon commonly occurs in trace amounts, and secondary biotite is developed in some samples. For the most part, sphene and chlorite are absent. Ilmenite occurs most abundantly in tabular plates. Characteristically, in these rocks the plates are in

sets with parallel orientation of most individuals within a set, suggesting the presence of large skeletal crystals (Plate 15). These crystals in extreme cases have maximum diameters as great as fifty millimeters. The plates commonly occur in replaced augite crystals, suggesting that the skeletal ilmenite crystals in part grew in the solid state. In some instances aggregates of ilmenite grains apparently formed pseudomorphs after a preexisting mineral, perhaps magnetite. Zircon commonly occurs in intricate skeletal crystals. Many of the zircon crystals occur in aggregates of hornblende replacing augite, again suggesting skeletal crystal growth in the solid state.

Origin of the quartz diabase

The field relations of quartz diabase to the overlying rock types are important. As discussed later, several lines of evidence indicate that the leucocratic granophyres are derived in part from the sedimentary country rocks. Since in the Workman and Reynolds Creek areas quartz diabase occurs in a thin zone underneath granophyres, and since it is not chilled but rather is coarser-grained at the granophyre contacts, contamination may have been a factor in producing the quartz-bearing rock. Contamination could have occurred either by assimilation of xenoliths or by vapor phase transfer, as miarolitic cavities in the granophyres indicate that a vapor phase was present in them. It is noteworthy that where diabase is separated from the overlying rock by a chill zone, quartz-bearing diabase was not found. The Grantham Peak mass of quartz diabase contains xenoliths of probable sedimentary origin; these xenoliths are obvious possible sources of contamination.

The composition and norm of the sample of quartz diabase resemble those of a monzonite. Diabase richer in quartz and alkali feldspar than the analyzed rock occurs in small quantities in the sill complex, and, had more samples been analyzed, syenitic and quartz syenitic compositions might have been found. Rocks of such compositions have been shown in some cases to be differentiates of uncontaminated basaltic magmas. However, quartz diabase in the Sierra Ancha sill occurs where contamination by sedimentary country rocks is suspect. The diabase pegmatites which occur where contamination is unlikely to have taken place do not contain quartz. These quartz-free pegmatites may represent the uncontaminated differentiates of the parent magma of the diabasic rocks. Quartz diabase may represent a contaminated differentiate.

MINERALOGY OF THE DIABASIC ROCKS

Extensive electron microprobe investigations were made of compositions of pyroxenes, olivines, feldspars, and iron-titanium oxides in typical rocks in the sill complex. A principle aim of the investigations was to determine how compositions of the major minerals varied throughout the sill and, by comparison with experimental data and data on other natural occurrences, to determine as far as possible variations of temperature and other intensive variables during crystallization of the diabase magma. Another important aim was to determine quantitatively the extent of compositional variations within single mineral grains and in one mineral within single rocks, a difficult and sometimes impossible task before the advent of the electron microprobe. Information on these variations in turn yields information on how closely chemical equilibrium was attained as the magma crystallized and on differentiation trends.

Innumerable microprobe analyses have been made of the important and variable elements in the principal mineral groups, and analyses of all major elements have been calculated for mineral points with representative compositions. A simple tabulation of analytical results would be exceedingly lengthy, so representative data have been presented in graphs and figures and results have been summarized in the text. Typical analyses for each mineral group have been presented in tables. The analytical procedures, the precision and accuracy of the data, and the method of data reduction are discussed in the appendix.

Pyroxenes

Pyroxenes form the most informative and interesting mineral group in the Sierra Ancha sill complex. Calcic pyroxenes have rather complex compositions that are sensitive to changes in their environments during crystallization. They are present in almost all rocks in the sill complex, and compositional variations in pyroxenes can be traced from one rock type to another. Pyroxenes in other basic igneous rock complexes have been studied in detail, and comparisons of pyroxene variations in the Sierra Ancha complex with those in other igneous bodies yield information on relative physical and chemical conditions during crystallization.

Calcium-rich pyroxene

Augite is the only abundant primary pyroxene in the samples of feldspathic olivine-rich diabase and olivine diabase studied in detail. The augite is tan in thin section and has a moderate positive $2V(45^{o}-50^{o})$ and slight optic axis dispersion ($r > v$). The crystals are ophitic and, in some cases, poikilitic. Most crystals have no exsolution lamellae of any sort. A few locally are faintly streaky in plane light, perhaps due to the presence of fine exsolution lamellae of a calcium-poor pyroxene. A few crystals locally contain clusters of small, oriented spindle-shaped inclusions which commonly appear opaque; perhaps these are exsolved ilmenite needles.

Augite compositions in the Sierra Ancha sill complex are similar to those in many other basic intrusions. Representative microprobe analyses of augite are in Table 9. Major element variations in the augites are similar to those in other differentiated

TABLE 9

Representative Augite Analyses

	1	2	3	4	5
SiO_2	50.3	50.8	50.3	50.1	49.9
TiO_2	1.1	1.2	1.1	0.84	1.1
Al_2O_3	2.5	2.0	1.8	1.5	1.8
Fe as FeO	7.9	9.5	11.2	12.9	13.5
MnO	0.20	0.25	0.33	0.43	0.41
MgO	15.8	15.6	15.1	13.6	13.3
CaO	21.6	20.5	19.4	19.0	19.5
Na_2O	n.a.	n.a.	0.39	0.29	0.33
K_2O	n.a.	n.a.	n.d.	n.d.	n.d.
Cr_2O_3	0.02	n.a.	n.a.	n.a.	n.a.
	99.4	99.8	99.6	98.6	99.8

1. $Wo_{43.4}En_{44.0}Fs_{12.6}$ From an analyzed sample of feldspathic olivine-rich diabase, Reynolds Creek Ad36d(B3)

2. $Wo_{41.1}En_{43.5}Fs_{15.0}$ From olivine diabase near Workman Creek Ad163g(B3)

3. $Wo_{39.3}En_{42.5}Fs_{18.2}$ From an analyzed sample of olivine diabase, near Workman Creek Ad163e(A3)

4. $Wo_{39.4}En_{39.0}Fs_{21.5}$ From an analyzed sample of diabase pegmatite, Reynolds Creek Ad28(A1)

5. $Wo_{39.8}En_{38.0}Fs_{22.2}$ From quartz diabase, near Workman Creek Ad163a(B2)

n.a. not analyzed
n.d. not detected

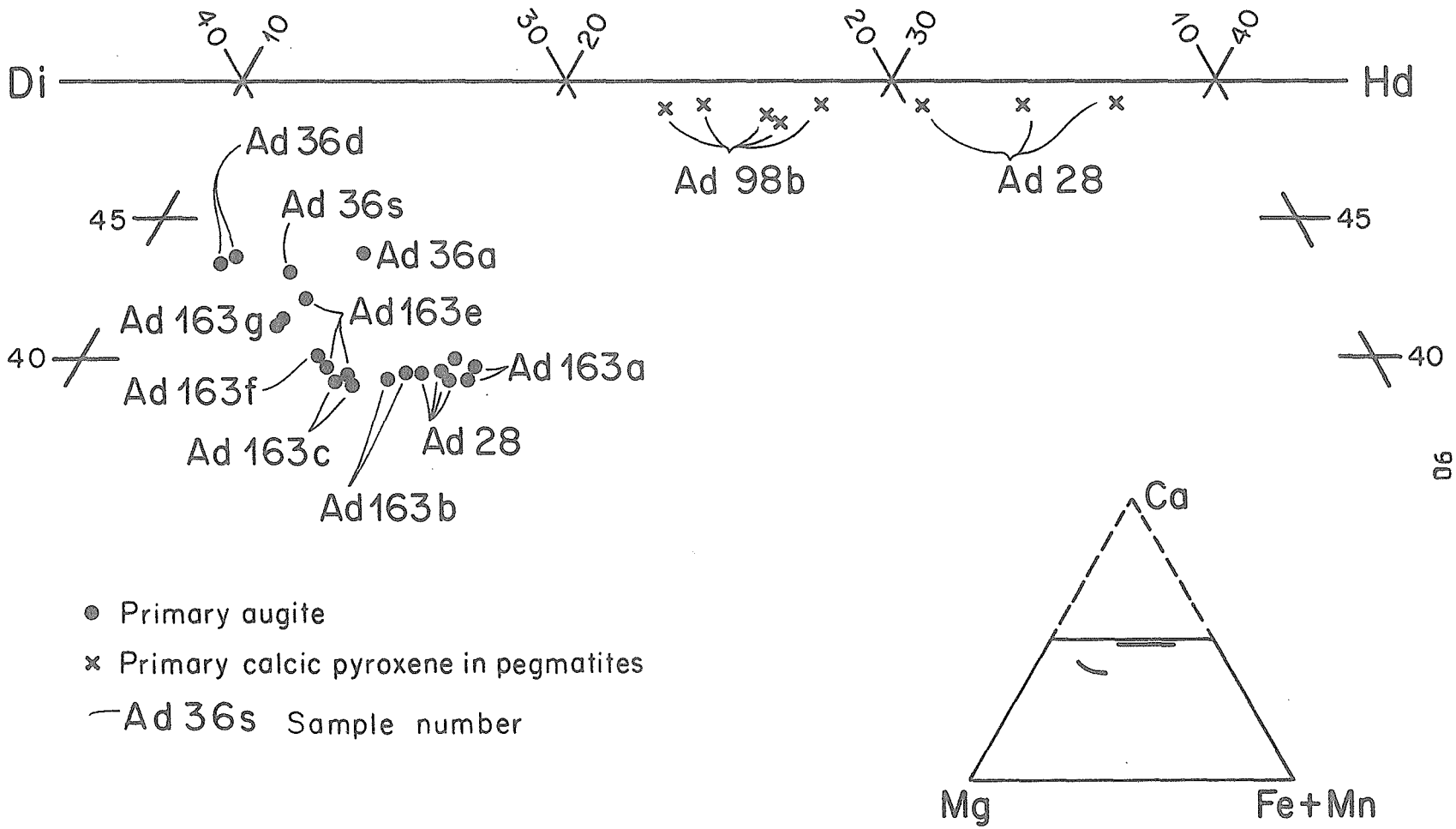

Figure 5. Representative compositions of primary calcic pyroxenes plotted in the pyroxene quadrilateral.

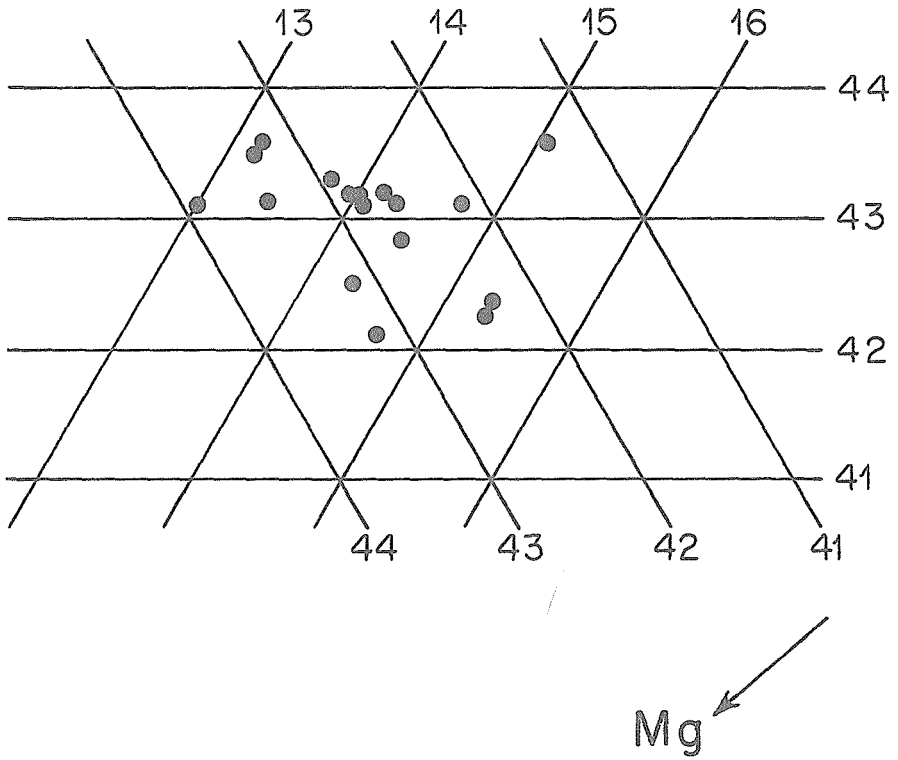

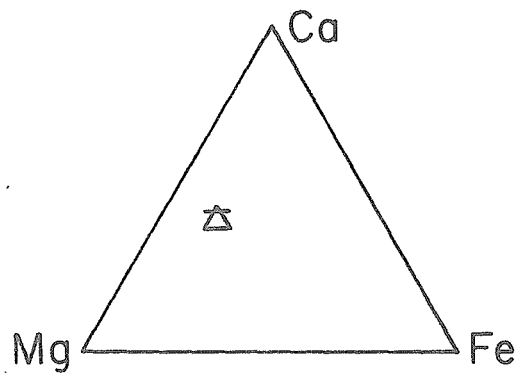

Figure 6. Range of augite compositions present in a thin section of one rock, analyzed olivine diabase specimen Ad36s, computed from microprobe analyses for Ca, Fe, and Mg.

intrusives, and they can be best displayed in the familiar pyroxene quadrilateral. Typical augite compositions from a series of rocks are plotted in a portion of the quadrilateral in Figure 5. The compositions form a rough trend in the quadrilateral. Augite in quartz diabase (Ad163a) and in diabase pegmatite (Ad28) define the iron-rich end of the trend. Augite in feldspathic olivine-rich diabase (Ad36d) defines the magnesium-rich end.

The large, ophitic augite crystals show surprisingly little major element compositional zoning, and the total compositional variation of unaltered augite within one rock is small compared to the variation within the sill. The major element compositional variation within augite in one thin section is shown in the plot (Figure 6) of points calculated from a selection of partial analyses (CaO, MgO, and FeO only) from the analyzed specimen Ad36s. Though the spread of points is due in part to problems of analytical precision, it closely reflects real compositional variations. Extremities of intricate, ophitic crystals are generally slightly enriched in iron compared to central portions. The range of Fe/(Fe + Mg) ratios in augite in eight rocks is shown in Figure 11.

Previous work on compositional variations in augite in intrusives of basaltic composition, most notably in the Skaergaard intrusion (Brown and Vincent (1963), and others), has shown that the degree of iron enrichment in augite can be correlated with the degree of differentiation of the magma from which the augite crystallized. In any one intrusion, augite crystallizing at lower temperatures from more-differentiated magma contains more of the ferrosilite molecule than that crystallizing at higher temperatures from less-differentiated magma. In some subsequent discussions the degree of iron enrichment in unaltered augite will be

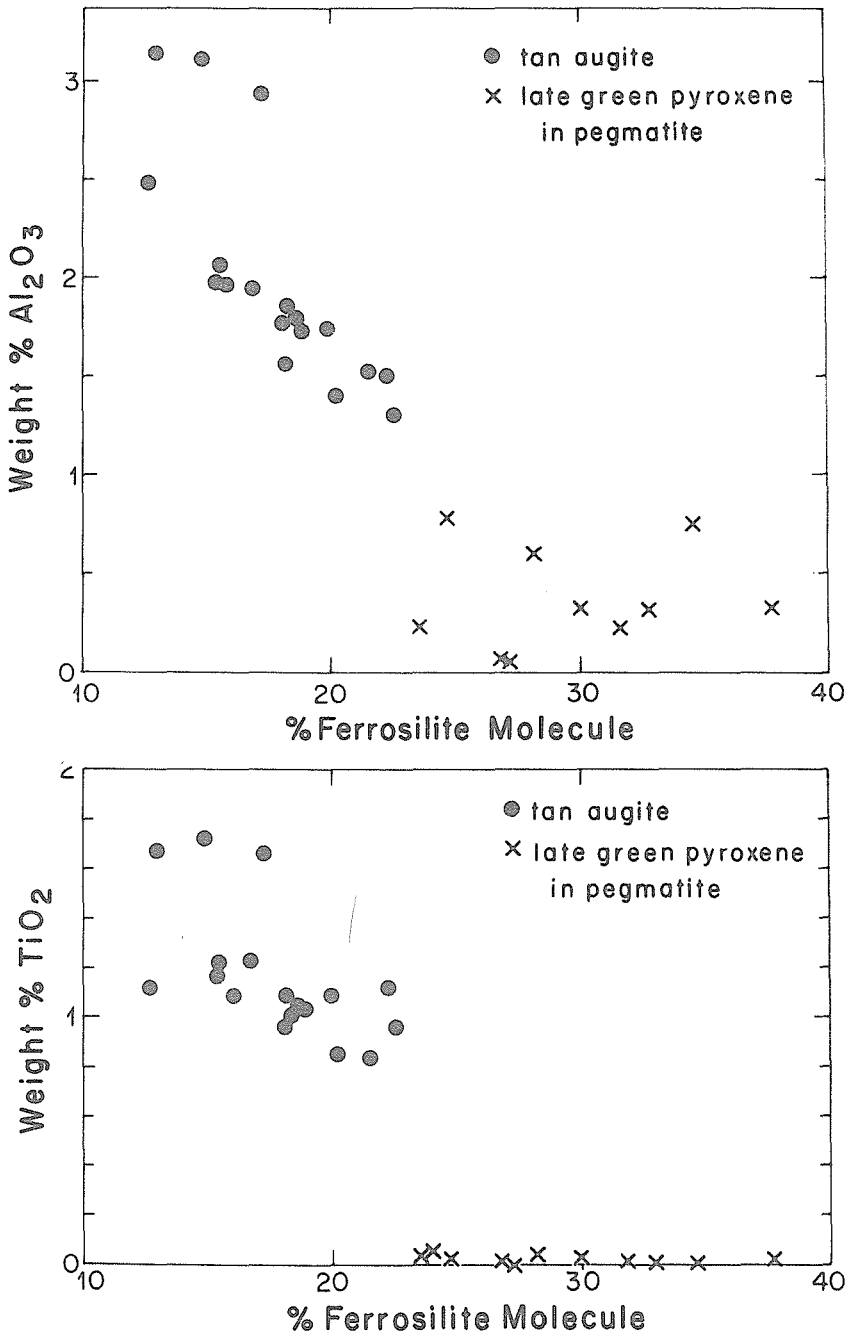

Figure 7. Al and Ti variations in augite and primary calcic pyroxene.

used as a differentiation index and guide to relative temperatures of crystallization of rocks in the Sierra Ancha sill complex. The index is consistent with other mineral trends and with the available whole rock chemical data.

The aluminum and titanium contents of the augite lie in the upper parts of the ranges of values of these elements commonly found in augite in tholeiitic rocks; augite in rocks of alkalic basalt composition commonly contains considerably more aluminum and titanium (Kushiro, 1960). Both elements vary with iron enrichment in augite; aluminum decreases markedly, while titanium shows a slight decrease (Figure 7). Verhoogen (1962) suggested that the amounts of aluminum and titanium in augite are strongly controlled by the entropy-of-mixing effect and that consequently the amounts should decrease with falling temperature. The trends observed in the Sierra Ancha augites support his conclusions. A few point analyses have unusually high values of both aluminum and titanium but have aluminum/titanium ratios similar to those of most other analyzed points (Figure 7). One possibility is that these analyses represent original crystal nuclei which grew rapidly from a super-saturated magma rather than in equilibrium.

In contrast to the behaviour of titanium and aluminum, manganese in augite increases with increasing ferrosilite content. The ratio of manganese to iron also increases from about 0.025 in the least iron-rich augite to about 0.03 in the most iron-rich augite.

In the discussion of the petrography of the rocks it was noted that throughout the sill augite locally had reacted with deuteric solutions and was bleached. Important features of the reaction are: the boundary between primary augite, tan in thin section, and

bleached pyroxene occurs at a sharp front; bleached pyroxene is optically continuous with tan augite but has a higher 2V; it is studded with numerous small inclusions of ilmenite(?) and amphibole and/or biotite. Photomicrographs of partly reacted augite are shown in Plate 16. Deer, Howie, and Zussman (1963, v. 2, p. 131) note that augite commonly undergoes such a reaction. Microprobe analyses of bleached and unbleached pyroxene (Table 10) show that bleached pyroxene is higher in calcium and considerably lower in aluminum and titanium than primary augite. Analyses 6 and 7 (Table 10) come from bleached and unbleached pyroxene points less than 0.2 mm apart in the same crystal (Plate 16).

The deuteric, multiply-twinned calcic pyroxene occurring in aggregates with chlorite replacing augite is even more calcic than the bleached pyroxene. Partial microprobe analyses of pyroxene in a replacement aggregate with chlorite from a rock (Ad36u) in the upper part of the sill in Reynolds Creek show compositions near $Wo_{49}En_{46}Fs_4$. The associated chlorite is more iron-rich, having a Fe/Mg ration near 2/3. Grains of multiply-twinned colorless pyroxene in the analyzed specimen of albite diabase, Ad141d, have a range of calcic compositions, typical values being $Wo_{49}En_{39}Fs_{12}$ and $Wo_{50}En_{35}Fs_{15}$; the most iron-rich composition found was $Wo_{47}En_{33}Fs_{20}$. Adjacent twin lamellae in pyroxene grains showed no compositional differences.

The most unusual pyroxene in the sill is the late, primary calcic pyroxene which crystallized in diabase pegmatite lenses with chlorite, sphene, and apatite. The pyroxene generally occurs in small equant crystals which are pale green in thin section (Plate 13) and have positive 2V's of 55^{o} to 60^{o}. Some crystals have multiple twinning.

TABLE 10

Augite, Bleached Pyroxene, and Calcic Pyroxene Analyses

	6	7	8	9	10	11
SiO_2	50.3	51.2	51.9	49.9	50.1	50.6
TiO_2	0.81	0.14	0.06	0.05	0.03	0.05
Al_2O_3	1.4	0.61	0.20	0.23	0.33	0.23
Fe as FeO	13.1	11.3	14.3	19.2	22.3	14.6
MnO	n.a.	0.44	0.62	0.27	0.29	0.20
MgO	13.5	13.4	10.7	6.7	4.6	9.8
CaO	19.1	21.4	22.1	23.6	23.2	24.1
Na_2O	n.a.	n.a.	n.a.	n.a.	0.29	0.17
K_2O	n.a.	n.a.	n.a.	n.a.	n.d.	n.d.
Cr_2O_3	n.a.	n.a.	n.a.	n.a.	n.a.	n.a.
	98.2	98.4	99.9	100.0	101.1	99.8

6. $Wo_{39.6}En_{39.1}Fs_{21.3}$ Unaltered augite, analyzed diabase pegmatite from Reynolds Creek Ad28(A7)

7. $Wo_{43.5}En_{37.8}Fs_{18.7}$ Bleached pyroxene, in the same crystal as the point represented by analysis 6 Ad28(B1)

8. $Wo_{45.4}En_{30.7}Fs_{23.9}$ Bleached pyroxene enriched in iron, nearer the margin of the same crystal as above Ad28(C3)

9. $Wo_{48.9}En_{19.4}Fs_{31.6}$ Primary calcic pyroxene, same pegmatite hand specimen Ad28(D1)

10. $Wo_{49.1}En_{13.5}Fs_{37.4}$ Most iron-rich primary calcic pyroxene, same pegmatite hand specimen Ad28(E4)

11. $Wo_{48.9}En_{27.7}Fs_{23.5}$ Least iron-rich primary calcic pyroxene, diabase pegmatite in Workman Creek Ad98b(A12)

n.a. not analyzed
n.d. not detected

PLATE 16

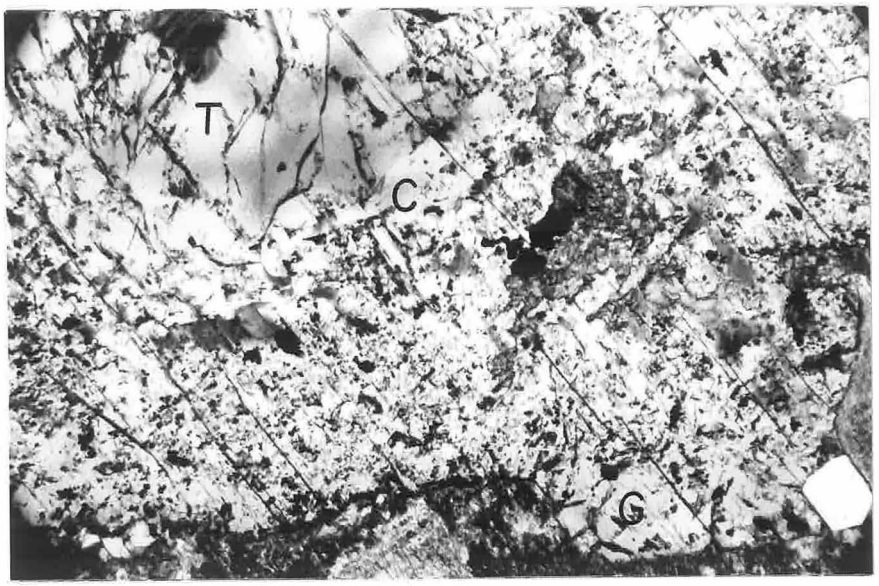

Rock Ad28. 2x3 mm. Part of a single, altered augite crystal. Tan unaltered augite (T); Colorless bleached pyroxene (C); Greenish, iron-enriched pyroxene (G). For microprobe analyses on this crystal see Figure 8 and Table 10.

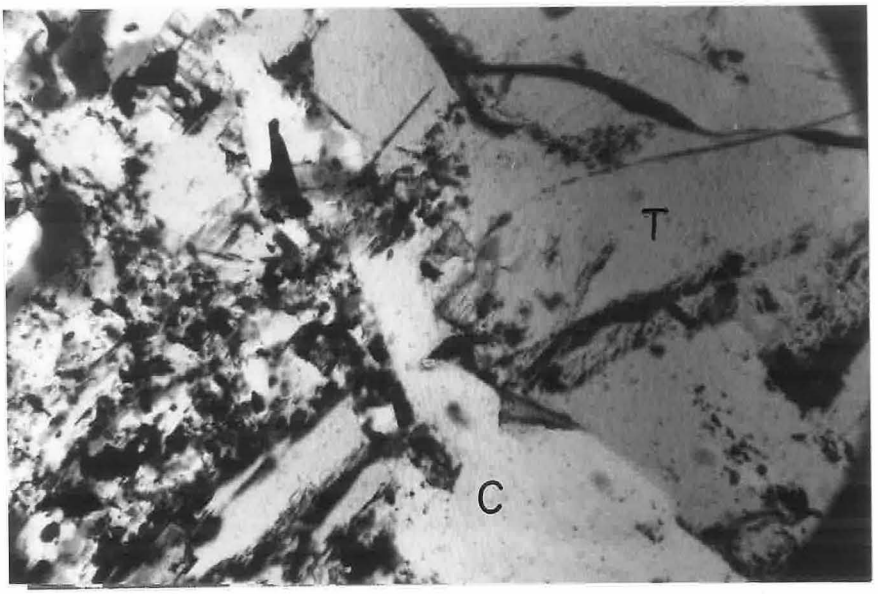

Rock Ad28. 0.5x0.75 mm. Close-up of the sharp contact between tan augite (T) and bleached pyroxene (C) shown above. See Table 10.

The compositions of these late primary pyroxenes form an iron-enriched trend more calcic than any other described in the literature. Analyses 9, 10, and 11 (Table 10) give the compositions of three points on calcic pyroxene grains. These and other complete analyses of primary calcic pyroxene from two analyzed pegmatite samples (Ad28 and Ad98) are plotted in a portion of the pyroxene quadrilateral in Figure 5. The crystals are irregularly zoned; the maximum zoning observed in a single crystal corresponds to a variation of about 4 percent ferrosilite. A total range of about 6 percent ferrosilite was found in primary calcic pyroxene in each of the two pegmatite samples, the grains studied being richer in iron in sample Ad28 than in sample Ad98b. The pyroxenes contain little aluminum and almost no titanium; these elements do not vary in any systematic way with iron enrichment (Figure 7). The low aluminum and titanium contents are probably a reflection of the low temperature of crystallization of the primary calcic pyroxene; the aluminum present in the residual magma during calcic pyroxene crystallization went into chlorite and possibly into feldspar, while the titanium went into sphene. Manganese in late calcic pyroxene also does not vary systematically with iron enrichment and is generally lower with respect to iron than in augite. In many occurrences of alkalic diabase described in the literature, pyroxenes enriched in iron are also enriched in sodium; here, the late calcic pyroxenes contain low, variable sodium contents much like those in early augites (compare analyses 10 and 11, Table 10, with analyses 3, 4, and 5, Table 9).

Since augite, bleached augite, and primary calcic pyroxene occur together in diabase pegmatite, the total range of pyroxene composition in any specimen of pegmatite is surprisingly large

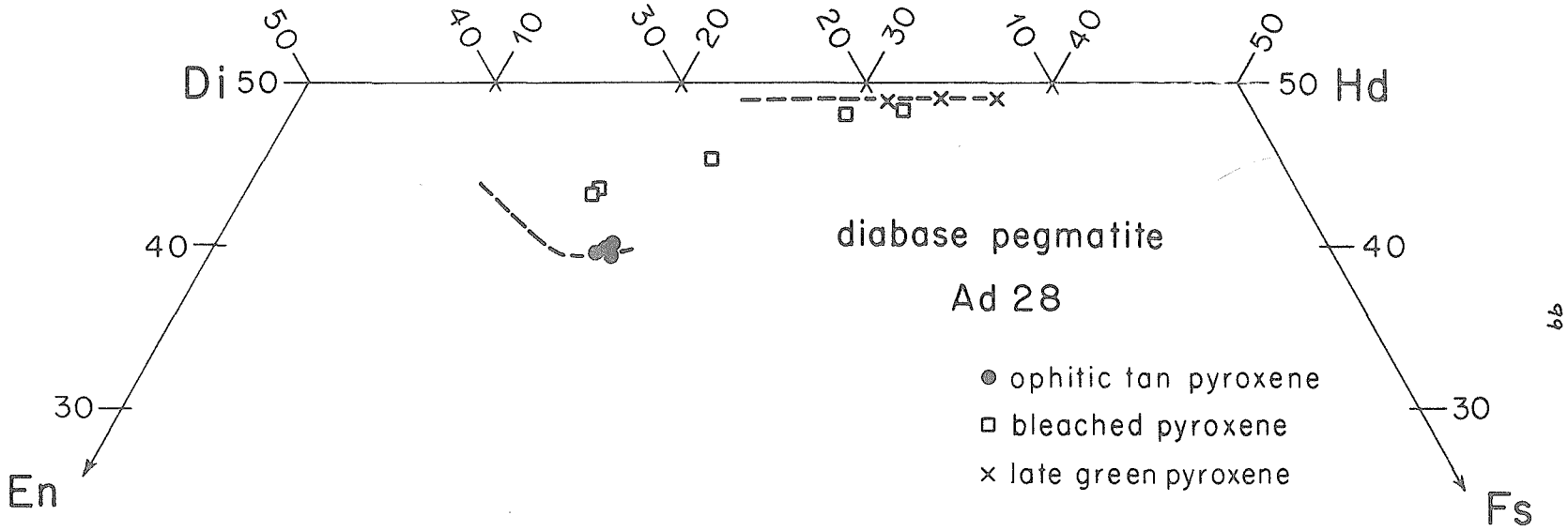

Figure 8. Compositions of pyroxene in a single polished thin section plotted in part of the pyroxene quadrilateral. All of the analyses of tan pyroxene and bleached pyroxene were made on spots on the portion of the single crystal shown in a photomicrograph in Plate 16.

(Figure 8 and Table 10). All of the analyses of augite and bleached augite plotted in Figure 8 were made on the portion of the large, ophitic crystal shown in the photomicrograph in Plate 16. The analyses of primary calcic pyroxene were made on much smaller crystals in the same polished thin section. The primary augite crystal apparently reacted with the residual liquid until the composition of the rim of the crystal closely approached the composition of the primary calcic pyroxene crystallizing from the liquid.

Pigeonite

Pigeonite did not crystallize in the Workman Creek or Reynolds Creek sections of the sill or in any of the granophyric rocks. The hypersthene in the diabasic rocks is primary, not an inversion product of pigeonite. Likewise, pigeonite did not crystallize in the Pocket Creek section of the sill studied by Williams (1957). However, two samples collected from a thick olivine diabase dike exposed in Pocket Creek above the roof of the sill complex contain large, ophitic hypersthene crystals with numerous lamallae and blebs of exsolved calcic pyroxene. Many of the crystals are intergrown with augite. These hypersthene crystals are thought to have been pigeonite originally. This occurrence of hypersthene is completely different from any occurrence observed within the sill complex. It is not described further here, but the interesting textural relationships observed merit further study and some exploratory microprobe work.

Orthopyroxene

Primary orthorhombic pyroxene occurs in all samples of feldspathic olivine-rich diabase and olivine diabase studied, except those which have undergone particularly intense deuteric alteration. It was not recognized in diabase pegmatite, albite diabase, or granophyre. There are no suggestions that any of the orthopyroxene formed by inversion from pigeonite. No lamellae of more calcium-rich pyroxene were detected either optically or with the microprobe in the calcium-poor pyroxene.

Only trace amounts of orthopyroxene (less than one-half percent) are found in feldspathic olivine-rich diabase. In these rocks it occurs at the margins of olivine crystals in anhedral grains with maximum diameters of 0.1 to 0.2 mm. In normal olivine diabase orthopyroxene occurs both as small, anhedral grains at the margins of olivine crystals and as independent, anhedral to euhedral crystals less than 1 mm in maximum diameter. It is more abundant in the more iron-rich rocks, and the amount present is as much as four or five modal percent in a few specimens.

The compositional range of orthopyroxene in the sill extends from bronzite ($En_{77}Fs_{23}$) to ferrohypersthene ($En_{44}Fs_{56}$). Analyses of points on orthopyroxene grains with typical compositions are in Table 11. Points representing all the complete analyses and some of the partial analyses are plotted in a portion of the pyroxene quadrilateral in Figure 9. The ranges of orthopyroxene composition in six rocks in the sill are shown in Figure 11.

All orthopyroxene crystals studied were at least slightly zoned in Fe and Mg, and most of the more iron-rich crystals were strongly zoned. Major element zoning follows typical patterns. In

TABLE 11

Representative Orthopyroxene Analyses

	1	2	3	4	5	6	7
SiO_2	52.6	53.0	49.6	51.0	51.1	50.9	49.9
TiO_2	0.34	0.06	0.08	0.34	0.12	0.08	0.05
Al_2O_3	0.55	0.09	0.45	0.49	0.70	0.04	0.06
Fe as FeO	21.6	23.2	33.5	25.1	25.7	31.6	33.2
MnO	0.55	0.62	0.65	0.60	0.75	0.78	0.92
MgO	23.4	23.3	14.9	20.1	20.2	16.3	15.1
CaO	1.28	0.33	0.54	1.5	0.72	0.76	0.69
Na_2O	n.a.	0.01	0.01	0.04	n.a.	n.a.	n.a.
K_2O	n.a.	n.d.	n.d.	n.d.	n.a.	n.a.	n.a.
Cr_2O_3	n.a.	n.a.	n.a.	n.a.	n.a.	n.a.	n.a.
	100.3	100.6	99.7	99.2	99.3	100.4	99.8

1. $Wo_{2.5}En_{63.6}Fs_{33.8}$ Analyzed point near the margin away from olivine in a small crystal contacting olivine Ad163g(B9)

2. $Wo_{0.6}En_{63.1}Fs_{36.2}$ Analyzed point near olivine in a small crystal contacting olivine Ad163e(B6)

3. $Wo_{1.1}En_{43.2}Fs_{55.7}$ Analyzed point near the outer margin away from olivine in the same crystal as Analysis 2 Ad163e(B8)

4. $Wo_{3.1}En_{56.4}Fs_{40.5}$ Representative analyzed point in an independent, interstitial orthopyroxene crystal, same rock as Analyses 2 and 3 Ad163e(C9)

5. $Wo_{1.4}En_{56.7}Fs_{41.8}$ Analyzed point at the center of an independent crystal Ad36a(G4)

6. $Wo_{1.6}En_{46.6}Fs_{51.9}$ Analyzed point, intermediate position, same crystal as Analysis 4 Ad36a(G3)

7. $Wo_{1.4}En_{43.5}Fs_{55.1}$ Analyzed point near the margin of the same crystal as Analysis 4 Ad36a(G10)

n.a. not analyzed
n.d. not detected

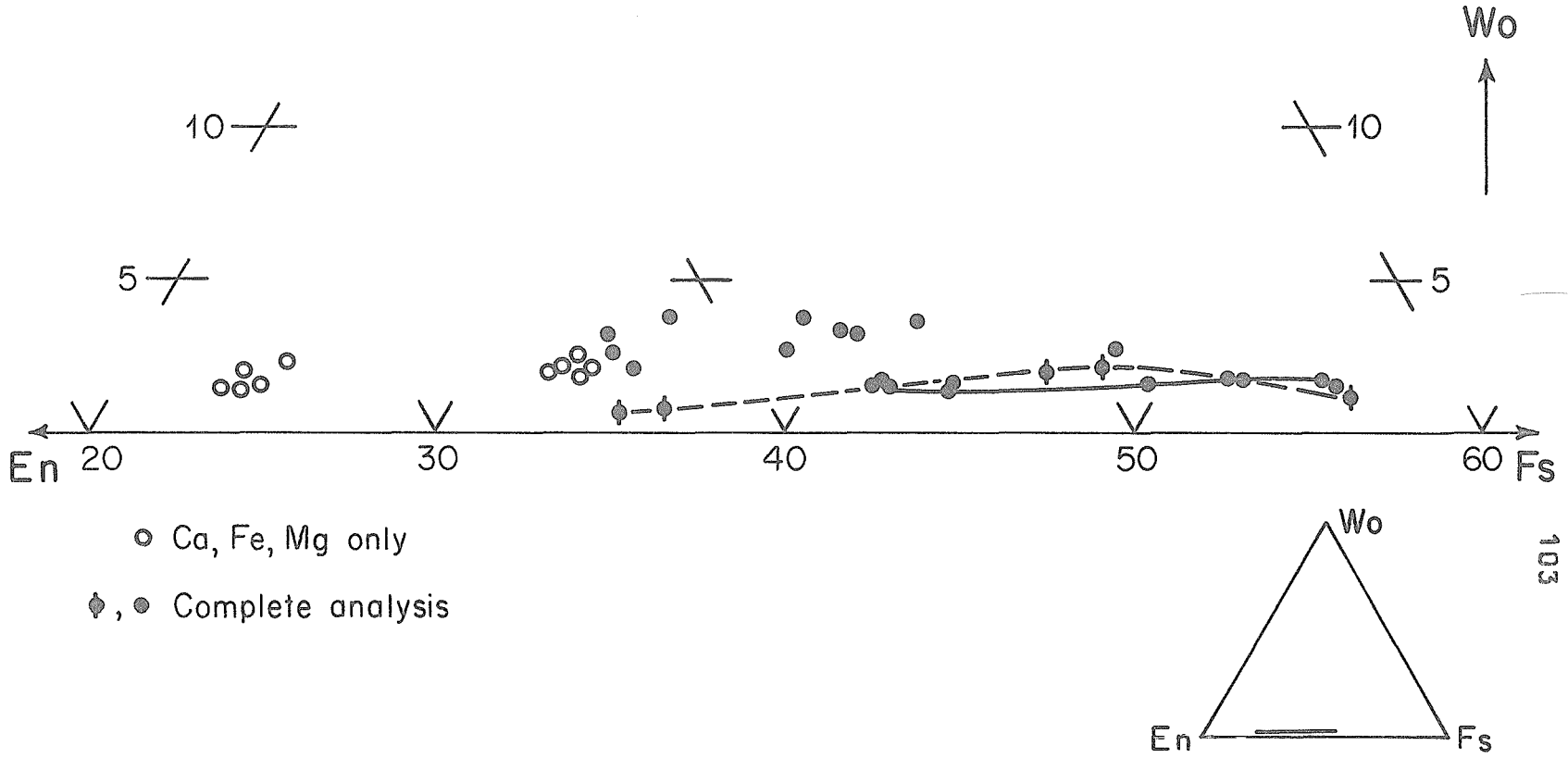

Figure 9. Orthopyroxene analyses plotted in part of the pyroxene quadrilateral. Each of the two lines joins a set of points representing analyses from a single zoned crystal.

small crystals marginal to olivine crystals, orthopyroxene is zoned from relatively Mg-rich compositions adjacent to and touching olivine to relatively Fe-rich compositions in the crystal extremities furthest from the adjacent olivine. An extreme case of this type of zoning is shown by the difference between analyses 2 and 3 in Table 11. In independent orthopyroxene crystals, grain centers are more Mg-rich than grain margins; an extreme case of this type of zoning is shown by analyses 5, 6, and 7 (Table 11) of points in an equant crystal 0.6 mm in diameter. Much of the range of Fe-Mg zoning observed in orthopyroxene in one rock can be found in a single crystal in the rock, as can be verified by comparing Figures 9 and 11. The extent of zoning in small hypersthene crystals is surprising in view of the relatively slight zoning in the much larger, more intricately shaped augite crystals.

The calcium, aluminum, and titanium contents of orthopyroxene seem to be controlled as much by growth kinetics or extremely local equilibria as by any set of equilibrium conditions pervasive through a volume of rock as large as the size of a thin section blank. Aluminum and titanium generally decline erratically with respect to iron enrichment in orthopyroxene; the trends are very poorly defined. No trend is discernible for calcium. Under the conditions of analysis, microprobe results for elements present at the 0.5 weight percent level are precise within at least ± 10 percent of the amount present. Minor element variations within a single crystal in some cases considerably exceed this 10 percent variation and are not systematically related to major element zoning. One example is the Al_2O_3 variation between analyses 2 and 3 and analyses 5, 6, and 7 in Table 11. The variation in Ca content with respect to Fe enrichment can be seen in Figure 9. The variation is present in

a single thin section; in analyzed rock Ad163a an independent hypersthene crystal (Analysis 4, Table 11) has roughly three times the calcium content of a hypersthene crystal marginal to olivine (Analyses 2 and 3, Table 11). Manganese variations in orthopyroxene are somewhat more systematic. Manganese generally increases with iron, and the Mn/Fe ratios of almost all analyzed points fall in the range 0.02 to 0.03, a similar range to that observed in augite.

Textural and compositional evidence suggest that the orthopyroxene formed late in the crystallization history of the sill. The typical occurrence of hypersthene at the margins of olivine grains suggests that these grains nucleated when olivine crystals locally reacted with a residual magma. The suggestion is confirmed by the fact that hypersthene grains adjacent to olivine are zoned outwards from more Mg-rich compositions near the olivine to more Fe-rich compositions away from it. Olivine must have crystallized until late in the cooling history of the magma, as it occurs in crystals interstitial to plagioclase laths. Since hypersthene formed in part where olivine reacted with the magma, the orthopyroxene must have formed at an even later stage in the cooling history. Late formation of orthopyroxene is also suggested by its common occurrence near biotite, presumably a late-forming phase. The large range of Fe-Mg zoning and the erratic minor element variations are consistent with the hypothesis that the small quantities of orthopyroxene formed later and at a relatively lower temperature than the bulk of the augite and olivine. During most of the cooling history of the diabase magma, it is probable that only one pyroxene, augite, crystallized.

Pyroxene trends in relation to those in other intrusions

The compositions of pyroxenes crystallizing from a magma depend on the compositions of the magma and on its temperature and pressure. Pyroxene compositional trends in a rock sequence depend on the manner in which these three variables -- composition, temperature, and pressure -- change in the magma during differentiation. The pyroxene trends in the Sierra Ancha sill complex have been plotted in the pyroxene quadrilateral (Figure 10) together with a typical trend for tholeiitic basalt magmas (Skaergaard intrusion, Brown and Vincent, 1963) and a typical trend for alkalic basalt magmas (Black Jack teschenite sill, Wilkinson, 1956).

The calcium-poor pyroxene trend in the Sierra Ancha sill complex is quite different from the trends previously described in intrusives of basaltic composition. In the Sierra Ancha complex iron-enriched orthopyroxene crystallized instead of pigeonite. In the Skaergaard, Bushveldt, and similar intrusives pigeonite crystallized instead of hypersthene and ferrohypersthene (see Figure 10). Primary iron-enriched hypersthene has been described previously from only one other intrusive of basaltic composition (Guadalupe complex , Best and Mercy, 1967). However, similar primary pyroxenes have been described in salic volcanic rocks (Carmichael, 1967) and in metamorphic rocks.

The extended field of orthopyroxene composition indicates that calcium-poor pyroxene crystallized at lower temperatures from the Sierra Ancha magma than from the magma in the Skaergaard and other similar basaltic intrusives. In these intrusives the crystallization temperatures of calcium-poor pyroxenes became higher than the temperature interval of pigeonite-orthopyroxene inversion at an

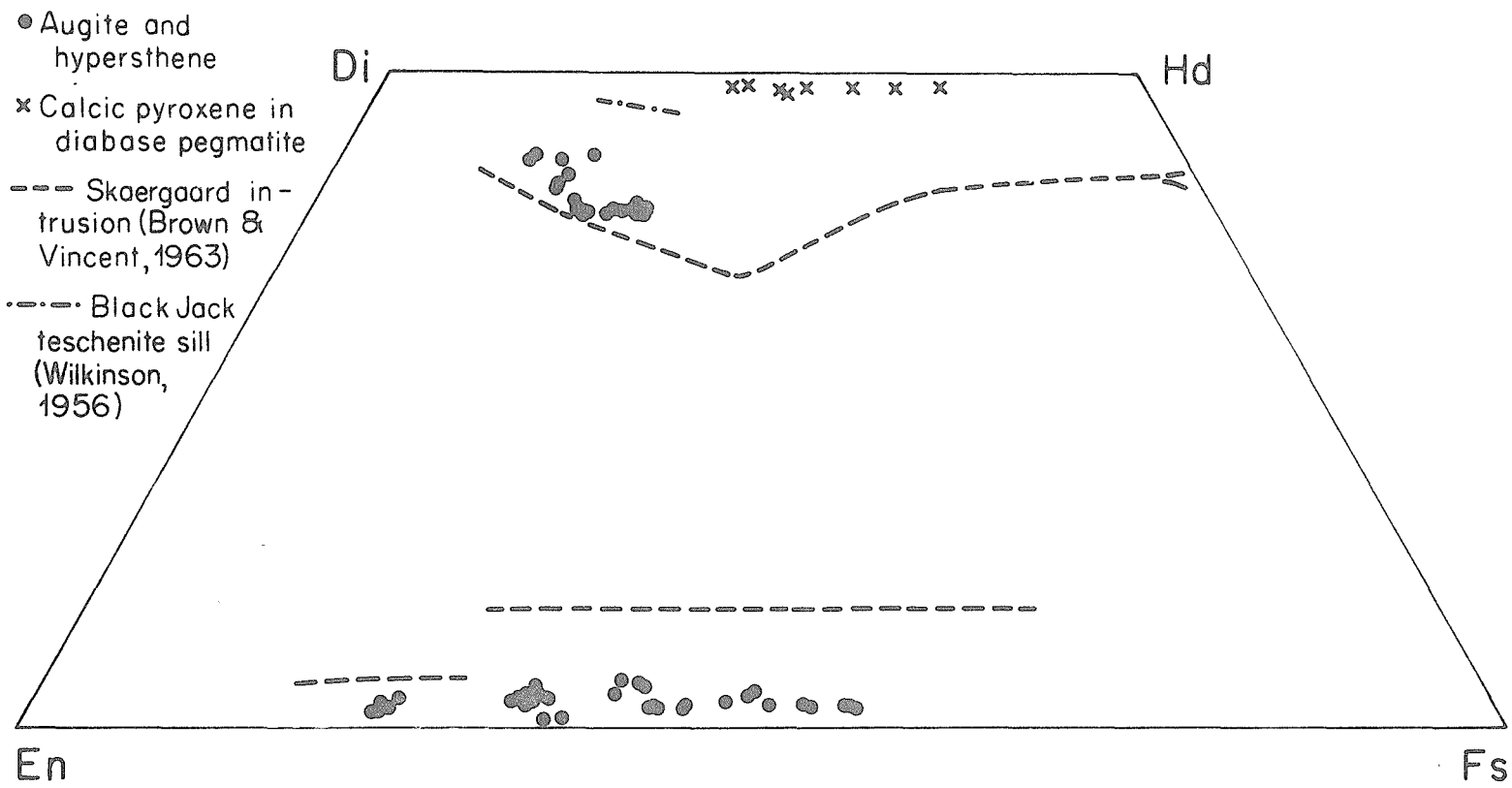

Figure 10. Compositions of primary pyroxenes in diabasic rocks plotted in the pyroxene quadrilateral.

orthopyroxene composition of about $En_{70}Fs_{30}$ (see Brown and Vincent, 1963, p. 193, and Brown, 1968, p. 348). In the Sierra Ancha magma all observed orthopyroxene (Fs 23-56) crystallized below the inversion curve. Experiments reported by Brown (1968) indicate that inversion takes place slightly below 1000°C for pigeonite with an Fe/(Fe + Mg) ratio of about 1/2. The 1000°C temperature may be considered an upper limit for crystallization of the iron-rich hypersthene in olivine diabase in the Sierra Ancha complex. The generally lower calcium contents of Sierra Ancha orthopyroxenes compared to Skaergaard orthopyroxenes probably reflect a range of solid solution more restricted by lower crystallization temperatures.

The calcium-rich pyroxene trend in the Sierra Ancha sill can be best considered in its two parts, the augite trend and the late calcic pyroxene trend. The augite trend is similar to but slightly more calcic than the Skaergaard trend. The clinopyroxene trend in the Kap Edward Holm complex described by Deer and Abbott (1965) is very similar to the Sierra Ancha trend, as is the early part of the trend in salic volcanic rocks described by Carmichael (1967). The clinopyroxene suites from alkalic intrusives appear considerably more calcic. Since the influences of Al and Ti on major element concentrations are not understood, perhaps only trends of pyroxenes with similar minor element compositions should be compared closely. The Al and Ti contents of the Skaergaard and Sierra Ancha pyroxenes are very similar but are considerably less than the contents of the pyroxenes in the

Black Jack sill.*

If augite in the Sierra Ancha sill crystallized in equilibrium with a calcium-poor pyroxene, an unlikely possibility in view of the apparent late nature of the orthopyroxene, then the augite trend might be considered to define an intersection of the solvus with the solidus in the pyroxene system. The fact that the Sierra Ancha augite trend is more calcic than the Skaergaard augite trend would then indicate a generally lower crystallization temperature for calcic pyroxene in the Sierra Ancha magma. However, the slightly more calcic trend might simply reflect a relatively higher chemical potential of calcium in the magma.

The compositional trend of the late, primary calcic pyroxene in the diabase pegmatites is unique. No similar, highly calcic iron-enriched pyroxene trend has been described elsewhere. Though pyroxene trends in alkalic rocks are in some cases highly calcic, they show only limited iron enrichment (Wilkinson, 1956). The few iron-enriched pyroxenes described previously from alkalic rocks are enriched in the acmite molecule ($NaFe^{3}Si_2O_6$) rather than the hedenburgite molecule ($CaFeSi_2O_6$) (Brown and Vincent, 1963, p. 194). As noted earlier, the late calcic pyroxenes in the Sierra Ancha diabase

*In plotting points in the quadrilateral it is commonly assumed that the Al and Ti contents of the pyroxenes can be disregarded. One analyzed pyroxene from the Black Jack sill contains 6.6% Al_2O_3 and 3.0% TiO_2 (Wilkinson, 1957, Table 2). If 2/3 of the Al and Ti are arbitrarily assigned to a Ca-Tschermak's molecule ($Ca(Ti^{+3}, Al)_2O_6$) to reduce the Al and Ti to amounts comparable to those in the Sierra Ancha and Skaergaard augites, then the pyroxene position in the quadrilateral changes from $Wo_{49}En_{37}Fs_{14}$ to $Wo_{45}En_{40}Fs_{15}$, a value closer to but still more calcic than the Sierra Ancha trend.

pegmatites contain little Na. Pyroxenes of similar compositions have been described previously only from metamorphic rocks. The limited solid solution of the (Mg, Fe)Si_2O_6 molecule and of Al and Ti in the later highly calcic pyroxene is believed to reflect a low crystallization temperature.

The assemblage apparently stable with the late calcic pyroxene -- iron-rich chlorite, apatite, sphene, alkalic feldspar, prehnite, and minor minerals -- has been described at length earlier as have the reactions the early, primary minerals underwent while the late assemblage was being formed. The calcic pyroxene in this assemblage is apparently a product of the fractional crystallization of a basaltic magma just as the iron-enriched augite in the Skaergaard intrusion is. The Sierra Ancha augite trend closely parallels the early Skaergaard trend. The break between the augite trend and the calcic pyroxene trend of this sill complex emphasizes the different nature of the residual differentiates in this system and in the Skaergaard intrusion. The iron-rich residual differentiates from which these Sierra Ancha calcic pyroxenes crystallized may have been aqueous fluids rather than silicate melts.

Olivine

Olivine is a major mineral in feldspathic olivine-rich diabase and normal diabase. It is readily altered and is not found in diabase subject to intense deuteric alteration. Olivine does not occur in diabase pegmatite, quartz diabase, or granophyre. Compositions in the sill range from $Forsterite_{74}Fayalite_{26}$ to $Forsterite_{54}Fayalite_{46}$. The ranges of olivine composition in typical rocks in the sill are shown in Figure 11. Representative analyses of points on olivine grains are in Table 12.

TABLE 12

Representative Olivine Analyses

	1	2	3	4	5
SiO_2	36.6	35.8	36.0	34.9	35.4
TiO_2	0.05	0.05	0.06	0.07	0.04
Al_2O_3	n.d.	n.d.	n.d.	0.01	0.01
Fe as FeO	26.0	28.3	32.2	36.1	37.4
MnO	0.39	0.46	0.56	0.63	0.62
MgO	35.6	34.6	30.9	28.2	27.1
CaO	0.07	0.09	0.08	0.06	0.13
Na_2O	n.a.	n.a.	n.a.	n.a.	n.d.
K_2O	n.a.	n.a.	n.a.	n.a.	n.a.
Cr_2O_3	n.d.	0.01	n.a.	n.a.	n.a.
NiO	0.11	n.a.	n.a.	n.a.	0.05
	98.8	99.3	99.8	100.0	100.7

1. $For_{71}Fay_{29}$ From an analyzed specimen of feldspathic olivine-rich diabase Ad36d(B4)

2. $For_{68}Fay_{32}$ From an analyzed specimen of olivine diabase Ad36s(C4)

3. $For_{63}Fay_{37}$ From olivine diabase Ad163g(B5)

4. $For_{58}Fay_{42}$ From olivine diabase Ad163c(C6)

5. $For_{56}Fay_{44}$ From an analyzed specimen of olivine diabase Ad163e(B4)

n.a. not analyzed
n.d. not detected

Most olivine crystals have no detectable major element zoning. Their compositions are constant within a range of one-half a scale unit, i.e. within a range such as from $Fo_{70}Fa_{30}$ to $Fo_{70.5}Fa_{29.5}$. No crystals examined had zoning significantly greater than one scale unit, i.e. greater than from $Fo_{70}Fa_{30}$ to $Fo_{71}Fa_{29}$. In several instances the slight zoning present was reverse zoning, from more iron-rich centers to more Mg-rich rims. The lack of zoning is remarkable, particularly in view of the strong zoning locally present in hypersthene grains bordering olivine crystals. The difference in zoning between olivine and hypersthene adds additional weight to the hypothesis that hypersthene crystallized at lower temperatures than olivine. Diffusion processes which would eliminate zoning depend exponentially on temperature.

The range of olivine composition present within single rock specimens is commonly as great as 4 percent fayalite molecule (Figure 11). Most of the range is due to compositional variations between different crystals. No systematic compositional differences were noted between smaller equant crystals and larger interstitial crystals in the same thin section.

Olivines are essentially "pure" minerals. No minor element except manganese is present in the analyzed olivines in concentrations in excess of 0.11 weight percent, as can be seen in the analyses in Table 12. Manganese in olivine increases with total iron; the ratio Mn/Fe is fairly constant, varying between 0.015 and 0.018 in the crystals studied. The ratio is notably lower than in the pyroxenes, indicating a preference for manganese in the "looser" pyroxene structure. Calcium and titanium are present in olivine in small but detectable amounts. Particular care was taken for the determination

of nickel in the two analyses in Table 12; Ni is lower in the more iron-rich olivine. Essentially no aluminum was found,in conformity with the finding of J. V. Smith (1966) and with his suggestion that aluminum shown in wet chemical analyses of olivine is due to contamination.

Application of Partition Data Between Pyroxenes and Olivine

If two phases such as augite and orthopyroxene equilibrate, then the partitions of Fe, Mg, and minor elements between the two phases depend on the temperature and pressure of equilibration and on the compositions of the phases. Under suitable conditions measurements of the partitions permit the determination of relative temperatures of equilibration between mineral pairs in different rocks, and, if a scale for calibration exists, the determination of absolute temperatures is possible. It would seem, then, that at least potentially the study of partition factors may provide quantitative answers to classical petrologic questions. Of course, application of partition data depends critically on whether equilibration ever took place, and, if it did, what significance the temperature of equilibration has. Since it is possible with the electron microprobe to determine zoning and compositions of phases actually in contact, microprobe studies enhance the possibilities of realistically applying partition studies.

Because only solid phases are involved in the reactions determining the partitions of Fe and Mg between olivine and pyroxene, moderate changes in pressure do not have much effect on distribution coefficients. Ramberg and deVore (1951, p. 200) calculated that the olivine-orthopyroxene distribution coefficient would be changed only

about ten percent by a 10 kilobar pressure change. Kretz (1961, p. 377) calculated a similar ten percent effect for a 5 kilobar pressure change for the pair orthopyroxene-calcic pyroxene. Pressure will therefore be ignored in subsequent discussions of partition data.

Microprobe determination of the relative amounts of ferrous and ferric iron in pyroxenes is not practical at present, and all iron has been calculated as ferrous iron. Since olivine and orthopyroxene contain relatively little ferric iron, meaningful distribution coefficients for Fe^{+2} and Mg^{+2} can be calculated between the two phases from microprobe data. Augite may contain a significantly higher proportion of ferric iron. Skaergaard augites with compositions like the Sierra Ancha augites have ferric/ferrous iron ratios in the range 0.1 to 0.2 (Brown, 1957, Table 11). Because of the uncertain amounts of ferric iron in the Sierra Ancha augites, it is impossible to accurately calculate distribution coefficients for Fe^{+2} and Mg between augite and other phases, though the coefficients can be determined approximately.

Disequilibrium is a characteristic feature of igneous rocks. One of the important principles of igneous petrology, Bowen's reaction principle, was partly based on the exceedingly common evidence of disequilibrium in igneous rocks. Zoning is characteristic of some igneous minerals. Partition data calculated from bulk chemical analyses of mineral separates from a rock must always be regarded as only a rough approximation to true partition data, unless positive evidence of phase homogeneity is available. The extent of zoning in augite, olivine, and orthopyroxene in the Sierra Ancha sill complex has been noted previously. The ranges of the Fe/(Fe + Mg) ratios in the three phases in selected thin sections are summarized in Figure 11. Certain gross features of the partitions

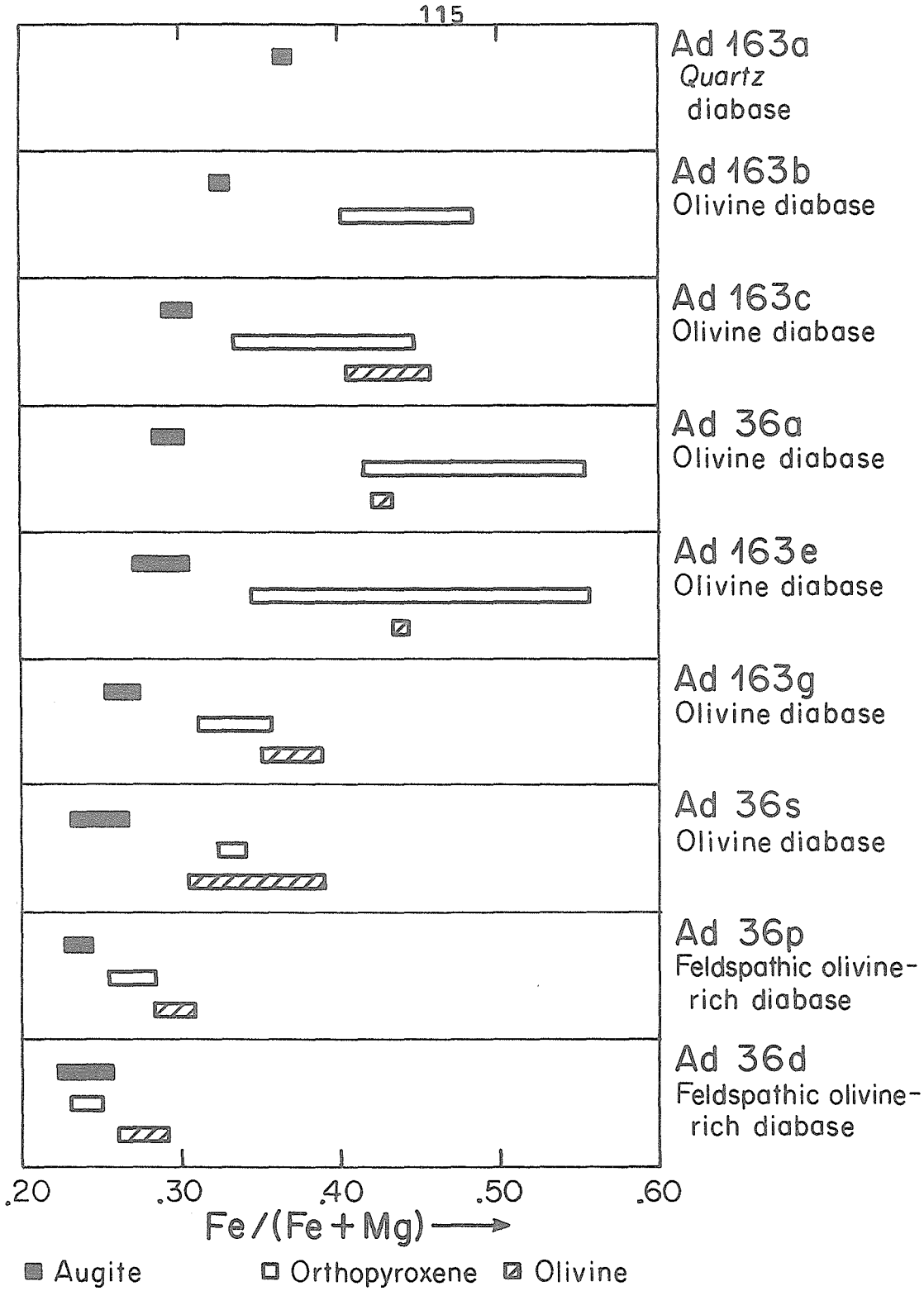

Figure 11. Ranges of values of the Fe/(Fe+Mg) ratio in pyroxene and olivine in selected rocks. The ranges are guides to the ranges a more extensive sampling would reveal. More points were sampled in some rocks than others.

between phases can be noted in the figure. However, partitions will be discussed whenever possible in terms of the available data for compositions of phases in contact determined on points only tens of microns apart. These partitions should be more meaningful than those calculated from average compositions of the phases in a hand specimen.

Should it ever be possible to accurately calculate absolute temperatures from the partition data presented here, the exact significance of the temperatures will still be unknown. Some calculated temperatures will probably lie in a 25°C or 50°C interval above the temperature of crystallization of the last melt in the rock. Other calculated temperatures may fall at intermediate points in the crystallization ranges of the phases. A body the size of the Sierra Ancha sill would cool fairly rapidly once it had solidified. Moreover, diffusion and reaction take place much more rapidly through the medium of a disordered melt phase than in the solid state. Still, reactions do occur even after solidification. Data on the iron-titanium oxides to be discussed later indicate reactions in magnetite-ulvospinel solid solutions took place down to a temperature of about 600°C, probably at least 300°C below the temperature of final crystallization of most primary minerals in olivine diabase.

Fe-Mg partition between olivine and orthopyroxene

Since orthopyroxene grains commonly occur at the margins of olivine grains, partition data between adjacent olivine and orthopyroxene were gathered easily despite the low abundance of orthopyroxene in most rocks in the sill. As noted previously, orthopyroxene apparently nucleated where olivine reacted with the melt. Data for nine olivine-orthopyroxene pairs are listed in Table 13.

TABLE 13

Fe/(Fe+Mg) in Contacting Olivine and Orthopyroxene

Rock	$K=(Fe/Mg)_{ol} \times (Mg/Fe)_{opx}$	Fe/(Fe+Mg) olivine	Fe/(Fe+Mg) orthopyroxene
Ad36d	1.23	0.28	0.24
Ad36p	1.21	0.31	0.27
	1.21	0.31	0.27
Ad36s	1.30	0.39	0.33
Ad163a	1.42	0.39	0.31
	1.36	0.38	0.31
Ad163e	1.46	0.44	0.35
Ad163c	1.45	0.45	0.36
	1.41	0.42	0.34

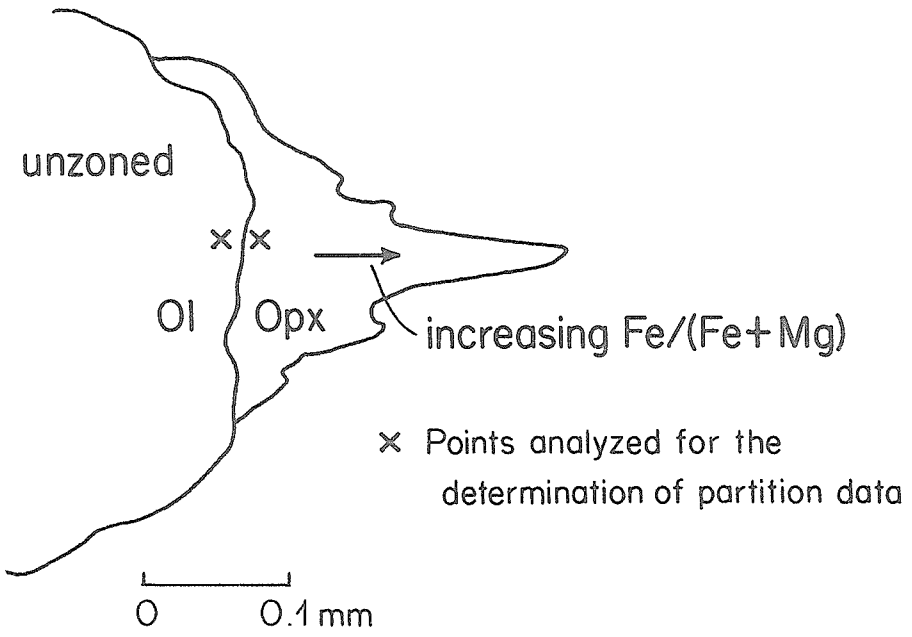

Figure 12. Schematic drawing of olivine-orthopyroxene relationships.

These data were taken with the smallest possible microprobe beam spots (1 to 2 microns diameter) from near contacts between almost unzoned olivine grains and zoned orthopyroxene grains. A schematic drawing of a typical olivine-orthopyroxene relationship is shown in Figure 12.

Though some orthopyroxene grains are zoned outwards to Fe/(Fe + Mg) ratios greater than those of the associated olivine crystals, orthopyroxene adjacent to olivine invariably is less iron-rich than the olivine. The compositions of adjacent points in the two phases may be the compositions in equilibrium with residual magma at the olivine-orthopyroxene reaction boundary in the complex natural system represented by the rock. The compositional relationship between the two adjacent phases is similar to that in most other natural occurrences. Data on occurrences summarized by Ramberg and deVore (1951, Figure 2) show that, at an Fe/(Fe + Mg) ratio of about 0.3, olivine characteristically has a ratio about 0.03 higher than associated orthopyroxene; the ratio increases faster in olivine than in associated orthopyroxene.

Both olivine and orthopyroxene have simple compositions that can be expressed approximately by components in the system FeO-MgO-SiO_2, and some experimental work done on the system can be used to interpret the partition data. Initial work on the system by Bowen and Schairer (1935) showed that olivine is more iron-rich than coexisting orthopyroxene at magmatic temperatures, but their work was not sufficiently detailed for use in interpreting temperatures of formation of coexisting natural minerals. Nafziger and Muan (1967) studied coexisting olivine and calcium-free pyroxene solid solutions at 1200°C. They found that pyroxene solid solutions

were practically ideal in activity-composition relations, while olivine solid solutions displayed moderate deviations from ideality. They presented compositional data for olivine-pyroxene pairs equilibrated at 1200°C. Medaris (1968) stated in a brief abstract that he studied the partitioning of Mg and Fe^{+2} between the two phases at 900°C and 800°C and found the partitioning to be "very similar" to that found by Nafziger and Muan at 1200°C. He concluded that the partitioning did not vary sufficiently for use as a geothermometer. Larimer (in press) found that the distribution of Fe and Mg was independent of temperature between 1100° and 1300°C. He calculated limits for the maximum possible variation of the distribution coefficient with temperature, but he did not conclude whether or not any temperature variation actually occurred. He did conclude that the variation with temperature would be small enough so that the distribution of Fe and Mg between the phases could not be used for "precise geothermometry" (Larimer, p. 15).

Compositions of coexisting olivine and pyroxene solid solutions equilibrated at 1200°C by Nafziger and Muan (1967, Table 5) are plotted together with the data from the Sierra Ancha rocks in Figure 13. Because olivine is not an ideal solid solution, quantitative calculations of the variation of the distribution coefficient with temperature cannot be made. The data comparison does allow certain qualitative deductions. The partitions between olivine and contacting orthopyroxene in specimens of feldspathic olivine-rich diabase are of the same magnitude or less that the partitions determined by Nafziger and Muan for silicates of essentially the same compositions equilibrated at 1200°C. For the more iron-rich silicates in normal olivine diabase, the partitions are substantially greater than the experimental values at 1200°C. Data of Larimer

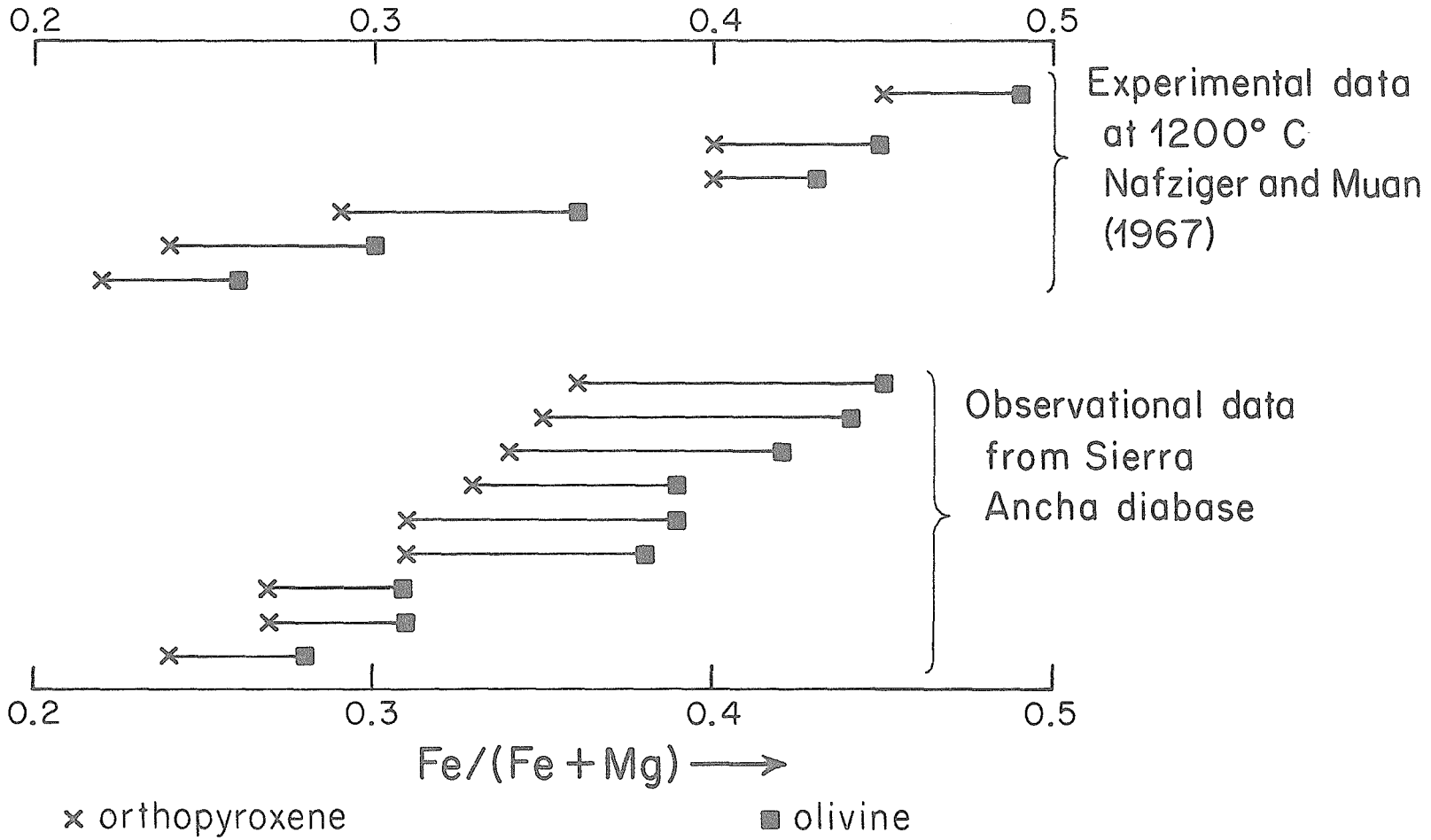

Figure 13. Fe/(Fe+Mg) ratios of points a few tens of microns apart across the boundaries of contacting olivine and orthopyroxene grains compared with ratios determined experimentally.

are not shown, as all but one of his runs were made with olivine compositions more magnesian than Fo_{80}. Partition coefficients $((Fe/Mg)_{ol}/(Fe/Mg)_{opx})$ calculated from his data fall in the range 1.1 to 1.2, while the Sierra Ancha values lie between 1.2 and 1.5 (Table 13).

The data comparison in Figure 13 suggests that Fe and Mg in olivine and touching orthopyroxene in feldspathic olivine-rich diabase equilibrated at temperatures in the neighborhood of 1200°C. However, the work of Larimer (in press) indicates that the equilibration anywhere in the temperature range 1100°-1300° would give essentially the same results. Partitions generally increase with decreasing temperature because of the entropy effect. Crystallization temperatures of olivine and pyroxene decreased with increasing iron enrichment. Since the Fe-Mg partitions in olivine diabase samples are distinctly greater than the experimental values, the data suggest that the observed partitions reflect the influence of temperature on the distribution coefficient, and that Fe and Mg in olivine and contacting orthopyroxene in olivine diabase equilibrated below 1100°C. This last conclusion would be expected in view of the apparent late nature of the orthopyroxene. Experimental data on solidus temperatures of basalts discussed later indicate that both olivine and orthopyroxene probably crystallized above 900°C. Therefore, the Sierra Ancha data suggest that the Fe-Mg distribution coefficient between olivine and orthopyroxene increases a measurable amount as temperature decreases from 1100°C to 900°C. Whether or not the change can be used as a precise geothermometer, it may still provide a meaningful one. For instance, a comparison of the partition coefficients in Table

13 with the meteorite values tabulated by Larimer (in press, Figure 4) suggests that olivine and orthopyroxene in most chondrites equilibrated at temperatures greater than 900°C.

If the results of Medaris (1968) for the partitioning at 900°C and 800°C are conclusive, then some explanation other than a temperature effect must be sought for the differences between the experimental and natural data. It is possible that the partitioning differs between the natural and experimental pairs because of the influence of minor elements in the natural minerals, particularly in orthopyroxene. The ranges of minor elements observed are summarized in Table 14. Though it is not probable, it is possible that the minor amounts of other elements present might noticeably influence the observed partitions. Since Al and Ti generally decrease and Mn generally increases with iron enrichment (and decreasing crystallization temperature) in orthopyroxenes, systematic effects on partitions due to the varying abundance of trace elements will be difficult to distinguish from effects due to varying equilibration temperatures. As noted earlier, all iron was determined as ferrous iron, and it is possible that changes in the relative ferric/ferrous iron ratio in orthopyroxene might cause systematic changes in the apparent Fe-Mg partition. However, the apparent partitions would be greater if ferric iron had been determined, as olivine would contain less ferric iron than orthopyroxene. Of course, it is possible that the observed partitions differ from the ones determined experimentally because olivine and touching orthopyroxene did not equilibrate in the rocks studied.

TABLE 14

Ranges of Minor Elements in Completely Analyzed Olivine and Orthopyroxene Grains in Sierra Ancha Diabasic Rocks

Olivine	Weight Percent Oxides	Orthopyroxene
0.15-0.06	CaO	1.9-0.2
0.64-0.39	MnO[1]	0.9-0.55
0.01-0.0	Al_2O_3[1]	0.7-0.04
0.07-0.04	TiO_2[1]	0.4-0.02
0.11-0.04	NiO	not analyzed

[1] Complete analyses are not available for the most Mg-rich orthopyroxenes. These might contain more Al and Ti and less Mn than the more iron-rich specimens analyzed completely.

Fe-Mg partition between augite and olivine

The ranges of Fe/(Fe + Mg) in augite and olivine in any one rock are relatively small. The relative proportions of iron and magnesium in the two minerals in a series of rocks are shown in Figure 11. Olivine is more iron-rich than associated augite, and the partition of Fe and Mg between the two phases increases as they become more iron-rich. Compositions of points a few tens of microns apart in touching augite and olivine crystals from a variety of rocks in the sill complex are listed in Table 15.

The Fe-Mg partitions between augite and olivine in the Sierra Ancha rocks are similar to those in other mafic intrusives. Both in intrusives of alkalic basalt composition (Wilkinson, 1956, p. 726) and in the Skaergaard intrusion (Brown and Vincent, 1963, Figure 1) olivine is more iron-rich than associated augite, and the partition between the two phases generally increases with increasing iron-enrichment in olivine. Experimental data with which to interpret the observed partitions are lacking.

Fe-Mg partition between augite and orthopyroxene

General relationships between associated augite and orthopyroxene in the Sierra Ancha sill can be seen in Figure 11. The partition of iron between the two phases favors orthopyroxene, and the partition increases with increasing iron content of the pyroxene. Of course, pyroxene crystallization temperatures in the rocks decrease as the pyroxenes become more iron-rich. Orthopyroxene is a minor mineral in most rocks in the sill, and it is commonly associated with olivine rather than augite. Orthopyroxene and

TABLE 15

Compositions of Augite and Olivine Measured with the Microprobe on Spots near the Contacts of Adjoining Grains

Rock	Augite				Olivine
	Ca	Mg	Fe	Fe/(Fe+Mg)	Fe/(Fe+Mg)
Ad36d	43.5	44.1	12.4	0.219	0.294
Ad36p	43.8	42.7	13.4	0.239	0.284
Ad36s	42.5	43.2	14.3	0.248	0.355
Ad36s	42.8	42.7	14.5	0.254	0.362
Ad163g	41.3	43.7	15.0	0.256	0.357
Ad163c	39.6	42.0	18.4	0.304	0.415

TABLE 16

Microprobe Analyses of Points less than 0.1 mm. Apart in Contacting Augite and Orthopyroxene Grains

	1	2
SiO_2	50.7	51.9
TiO_2	1.0	0.33
Al_2O_3	1.7	0.47
Fe as FeO	11.7	22.2
MnO	0.34	0.62
MgO	15.1	22.5
CaO	19.8	1.9
Na_2O	0.41	0.02
K_2O	n.d.	n.d.
	100.5	99.9

1. $Wo_{39.4}En_{42.0}Fs_{18.7}$ Augite. Ad163c(C11). Fe/(Fe+Mg) = 0.30

2. $Wo_{3.7}En_{61.4}Fs_{34.9}$ Orthopyroxene. Ad163c(C4) Fe/(Fe+Mg) = 0.36

n.d. not detected

augite in contact were sampled in only one rock, Ad163c. Complete analyses of two points less than 0.1 mm apart in the two phases are presented in Table 16.

The partition of ferrous iron and magnesium between augite and orthopyroxene is of particular interest because many studies have indicated that both phases may behave as ideal solid solutions for the two elements (i.e. Mueller, 1961; Kretz, 1963; and Schmus and Koffman, 1967). Kretz (1963, Figure 3) even established a tentative relationship between the distribution coefficients and temperature. Because of the uncertainty in the ferric/ferrous iron ratios in the Sierra Ancha augites, Kretz's relationship cannot be applied to the partitions in the Sierra Ancha rocks. Distribution coefficients calculated from average mineral compositions in rocks Ad36d and Ad36p and from the compositions of the pair of points in rock Ad163c are 1.0, 0.83, and 0.76, respectively. If the ferric/ferrous iron ratio is arbitrarily assumed to be 0.2 in augite and 0 in orthopyroxene, the distribution coefficients become 0.79, 0.67, and 0.61, respectively. The absolute values of the coefficients mean little; they are values characteristic of igneous rather than metamorphic rocks. The relative values suggest that equilibration takes place at lower temperatures for more iron-rich pyroxene pairs, as the coefficient should approach 1 with increasing temperature. However, as in the olivine-orthopyroxene case, other elements in the two phases may influence the Mg-Fe partition and mask any temperature dependence present.

It was noted earlier that the Mn/Fe ratio is fairly constant in the analyzed orthopyroxenes, clinopyroxenes, and olivines. Manganese is undoubtedly present almost entirely in one valence

state in the minerals. With further work the partition of manganese between the phases may prove to be of more value as a temperature indicator than the partition of iron when only microprobe analyses are available.

Partition of Ni between olivine and augite

The fractionation of nickel between coexisting olivine and augite has potential as a geothermometer. In a recent paper, Häkli and Wright (1967) determined the fractionation of Ni between augite and olivine in a series of samples of volcanic rocks from a cooling Hawaiian lava lake. The fractionation changed rapidly and systematically with the measured temperature of the samples at collection, as shown in Figure 14 (modified from Häkli and Wright, 1967, Figure 2).

Microprobe determinations* were made of nickel in olivine and augite in a specimen of feldspathic olivine-rich diabase, Ad36d. The weight percents of NiO in olivine and augite were determined as 0.11 and 0.013, respectively. The ratio (counts Ni in olivine/ counts Ni in augite) equals 8.5. When compared with the data of Häkli and Wright (Figure 14), the observed fractionation suggests that the nickel contents of olivine and augite in the feldspathic

*Determinations were made at 30 kilovolts and 0.4 microamps on brass with a moderately broad spot. Olivine and augite were stable under these conditions for times in excess of several minutes. Computed counting statistics were better than 2% on olivine and 4% on augite. Background determinations were carefully made, as background near the Ni wavelength changes rapidly with wavelength and sample. Absolute values are with reference to an olivine (174.1) with 0.40% NiO (separate determination by Lois Jones, U. S. G. S.).

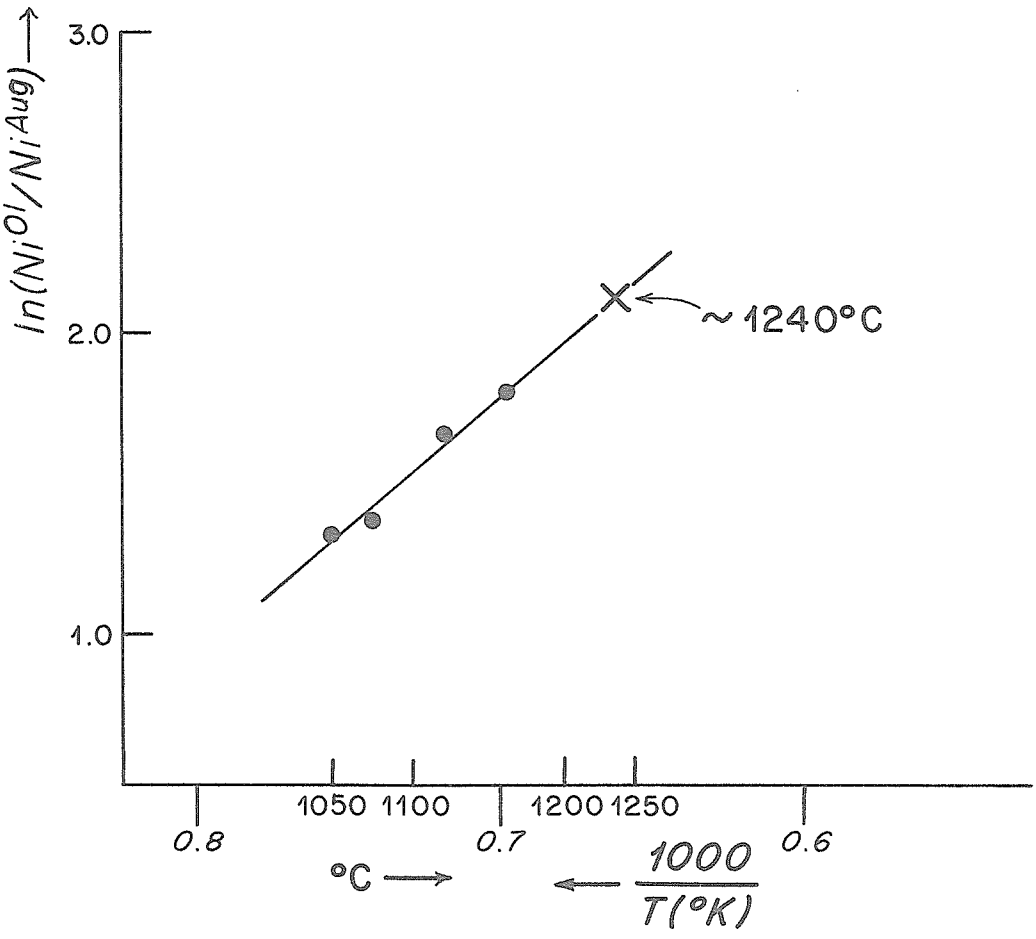

Figure 14. Ni fractionation between olivine and augite in feldspathic olivine-rich diabase compared with the observed fractionations in mineral pairs from a Hawaiian lava lake reported by Hakli and Wright (1967). Figure adapted from Hakli and Wright (1967, Figure 2).

olivine-rich diabase sample equilibrated at temperatures distinctly higher than those in the Hawaiian lava lake and perhaps near 1240°C.

As Häkli and Wright point out, their data cannot be applied indiscriminately to other rocks. However, a pressure difference of a kilobar is unlikely to make much difference in the nickel partition between two solid phases. The olivine and augite compositions in Ad36d are similar to though somewhat more magnesian than those of the Hawaiian phenocrysts. If nickel equilibration between augite and olivine occurred in the Sierra Ancha feldspathic olivine diabase, it may have done so near 1240°C. However, more data are needed for olivine-augite pairs of different compositions in a variety of rock types before the temperature-fractionation relationship in Figure 14 can be used with confidence. Because olivine and augite in olivine diabase contain considerably less nickel than in feldspathic olivine-rich diabase, the fractionation was not determined in other rocks in the sill.

Summary of Principal Observations and Conclusions on Pyroxenes and Olivine

Calcium-rich pyroxene occurs in all diabasic rock types in the sill complex. The varieties of calcium-rich pyroxene found and the rock types in which they occur can be summarized as follows.

(1) Primary augite is preserved in all the diabasic rock types except albite diabase. The compositional range found is from $Wo_{43}En_{44}Fs_{13}$ to $Wo_{40}En_{38}Fs_{22}$.

(2) Apparently primary iron-enriched calcic pyroxene crystallized in diabase pegmatite. The compositional range found is from $Wo_{49}En_{28}Fs_{23}$ to $Wo_{49}En_{19}Fs_{32}$.

(3) Calcic pyroxene, less iron-enriched than the primary variety, formed as a deuteric alteration product of augite in various diabasic rocks. In intensely-altered rocks, the deuteric calcic pyroxene occurs with chlorite in aggregates replacing augite.

Orthopyroxene is present in trace amounts in olivine-rich diabase and in amounts up to a few modal percent in olivine diabase. Important features of its occurrence are listed below.

(1) Orthopyroxene in many instances nucleated at the margins of olivine crystals, suggesting that it crystallized when olivine reacted with the magma in a late stage of melt crystallization.

(2) The compositional range present is from $En_{77}Fs_{23}$ to $En_{44}Fs_{56}$.

(3) The orthopyroxene appears primary, and there is no evidence that any of it formed by inversion from pigeonite.

(4) Orthopyroxene in olivine diabase has strong Fe-Mg zoning.

The augite, primary calcic pyroxene, and orthopyroxene compositions define trends in the pyroxene quadrilateral. Important features are listed below.

(1) The augite compositions define a trend similar to but slightly more calcic than the early part of the trend defined by augite from the Skaergaard intrusion.

(2) There is a sharp break between the augite trend and the primary calcic pyroxene trend.

(3) The primary calcic pyroxenes in diabase pegmatite define an iron-enriched trend more calcic than any trend previously described for igneous pyroxenes.

(4) The primary orthopyroxene compositions define a trend which continues to values unusually iron-rich for primary orthopyroxenes in mafic igneous rocks.

Olivine is present only in feldspathic olivine-rich diabase and olivine diabase. Olivine compositions lie between $Fo_{74}Fa_{26}$ and $Fo_{54}Fa_{46}$. Crystals in olivine diabase typically have interstitial shapes, suggesting that olivine crystallized until late in the cooling history of the melt. The crystals are almost unzoned.

The fractionations of Fe and Mg between the mineral pairs olivine and augite, orthopyroxene and augite, and contacting olivine and orthopyroxene increase with increasing iron enrichment in the phases. Al and Ti decrease in calcic pyroxene with increasing iron enrichment. Mn increases with iron enrichment in all three of the minerals.

The following relationships provide information on crystallization temperatures of the diabasic rocks.

(1) Comparison of Fe-Mg partitions between olivine and contacting orthopyroxene with experimental results suggests the pairs equilibrated at temperatures greater than 1100^{o} in feldspathic olivine-rich diabase and less than 1100^{o} in olivine diabase.

(2) The observed partition of Ni between olivine and augite in feldspathic olivine-rich diabase, when compared to the partitions between mineral pairs from a Hawaiian lava lake, suggests olivine-augite equilibration temperatures of greater than $1200^{o}C$ in the olivine-rich rocks. More data are needed before confidence can be placed in this result.

(3) Because primary orthopyroxene must have crystallized below the pigeonite-orthopyroxene inversion curve, the iron-rich orthopyroxene in olivine diabase probably crystallized below $1000^{o}C$.

Feldspars

Feldspars are present in all rocks in the sill complex, and compositional trends in them can be related to trends in other minerals and to the general differentiation history of the diabase magma. Feldspars stable under deuteric alteration and in the late stages of crystallization of diabase pegmatite are distinctly different from those formed in olivine and olivine-rich diabase in the early part of the magmatic history of the sill. The feldspars in quartz diabase form still a different group. The feldspars in each of these three groups will be discussed separately.

Plagioclase is the only feldspar present in feldspathic olivine-rich diabase and in all but one specimen of normal olivine diabase; in one otherwise undistinguished specimen, a grain of potassic feldspar was found intergrown with plagioclase. Diabase pegmatite and some deuterically-altered diabase contain Na feldspar and K feldspar end-members. In quartz diabase, partly unmixed alkali feldspar forms rims on altered plagioclase. Since feldspars have been discussed in the section on the petrography of the diabasic rocks, textural relationships will only be mentioned briefly in the following sections, which deal with feldspar compositions in the diabasic rocks.

Plagioclase in olivine-rich and olivine diabase

Plagioclase in feldspathic olivine-rich diabase and olivine diabase varies in composition from $An_{72}Ab_{27}Or_1$ to $An_{16}Ab_{78}Or_5$. Most crystals are normally zoned, but a few crystals in almost every rock show one or more slight reversals in zoning. Zoning

TABLE 17

Feldspar Compositions in Feldspathic Olivine-rich Diabase and Olivine Diabase[1]

Rock Number	Most Calcic Plagioclase Analyzed	Most Sodic Plagioclase Analyzed	Rock Type
Ad36d	$An_{70}Ab_{29}Or_1$	$An_{58}Ab_{41}Or_1$	Feldspathic olivine-rich diabase
Ad36s	$An_{67}Ab_{32}Or_1$	$An_{52}Ab_{46}Or_2$	Olivine diabase
Ad163g	$An_{72}Ab_{27}Or_1$	$An_{39}Ab_{59}Or_2$	Olivine diabase
Ad163e	$An_{63}Ab_{35}Or_1$	$An_{18}Ab_{78}Or_4$	Olivine diabase
Ad163c	$An_{56}Ab_{43}Or_1$	$An_{18}Ab_{79}Or_3$	Olivine diabase
Ad163b	altered	$An_{16}Ab_{78}Or_5$	Olivine diabase with extensive alteration

[1]For sample locations see Figures 3 and 28 .

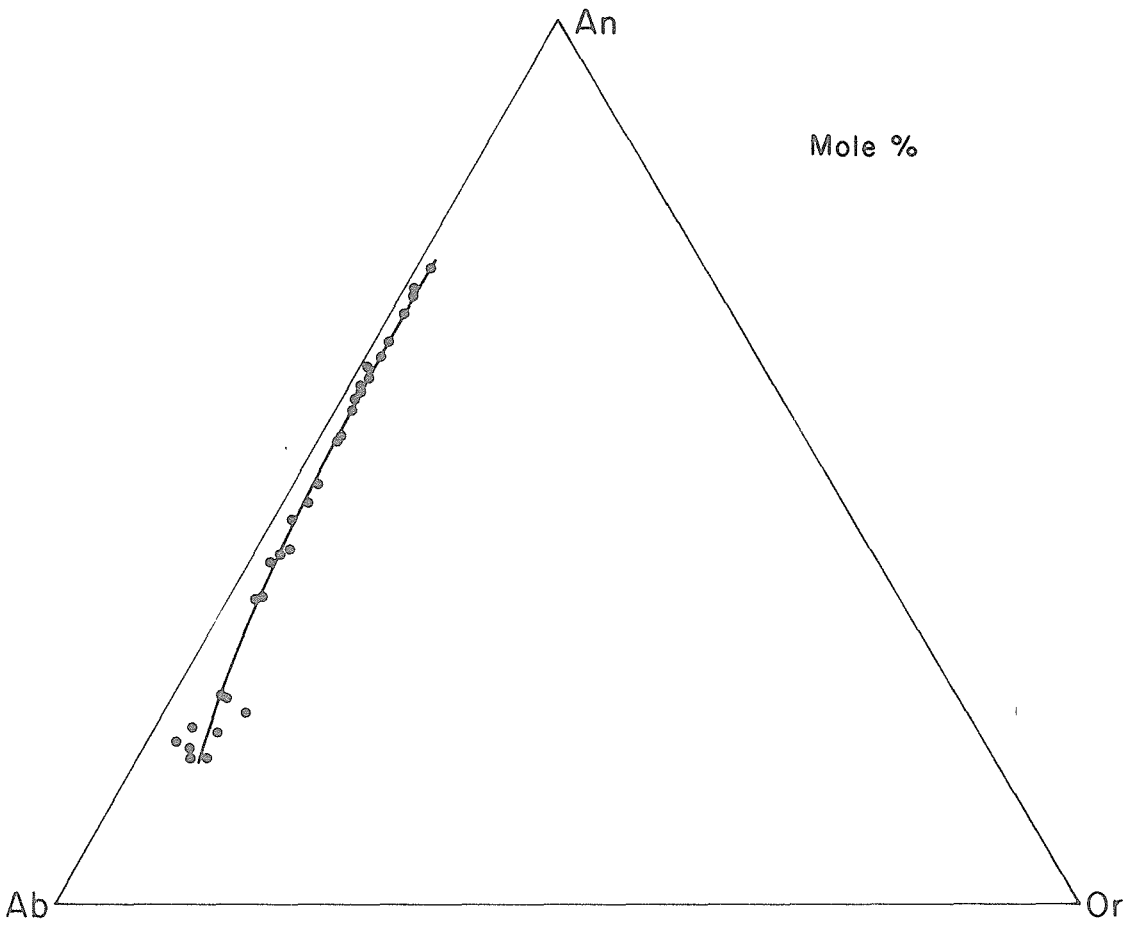

Figure 15. Plagioclase compositions in olivine diabase and feldspathic olivine-rich diabase. The compositions were determined by microprobe analyses for Ca, K, and Na.

is more intense in the more differentiated rocks in the sill. Though the most calcic feldspar found in nearly every rock studied was calcic labradorite or very sodic bytownite, the average feldspar in the more differentiated rocks is considerably more sodic. Plagioclase compositions in typical rocks in the sill determined from microprobe analyses for Ca, Na, and K are listed in Table 17 and plotted in Figure 15. Compositions for many rocks in the sill were determined by measuring extinction angles in albite-Carlsbad twins; the results found are in accord with the microprobe results in Table 17. It should be noted that the microprobe results represent compositions of volumes of plagioclase a few microns in diameter; the bulk compositions in any one rock lie between the sodic and calcic compositions given for the rock.

Plagioclase compositions in the rocks listed in Table 17 show a clear trend when compared with iron enrichments in mafic minerals in the same rocks shown in Figure 11. More sodic plagioclase is found in rocks with silicates more enriched in iron, as can be seen from the data in Table 25.

Alkali feldspar-plagioclase relationship in rock Ad163c.

Primary potassium-rich feldspar was found in only one sample of olivine diabase, rock Ad163c. The rock contains unaltered olivine, augite, hypersthene, and plagioclase; it does not contain quartz nor does it have the alkalic rims on plagioclase characteristic of quartz diabase. Only one small, clear, anhedral grain of alkali feldspar was found; though its 2V appeared small, the optic axis of the grain was too far off center for a quantitative estimate of 2V to be made. Microprobe traverses showed the grain to have a sharp contact with adjoining sodic plagioclase.

Whether or not the alkalic feldspar crystallized as a result of contamination of diabase magma, from textural relationships there seems no reason to doubt that the alkalic feldspar and adjoining sodic plagioclase crystallized together from a residual melt. A plagioclase grain adjoining the potassic grain is asymmetrically zoned from a composition of $An_{56}Ab_{43}Or_2$ away from the alkalic grain to a composition $An_{24}Ab_{72}Or_5$ near it. The potassic feldspar grain is zoned from central values as potassic as $An_{0.5}Ab_{21}Or_{79}$ to marginal values as sodic as $An_2Ab_{30}Or_{68}$. The compositions $An_{24}Ab_{72}Or_5$ and $An_2Ab_{30}Or_{68}$ represent points about 10 microns apart in contacting feldspar grains.* These compositions probably coexisted together with the last stages of the melt, inasmuch as there are no signs of post-solidification reactions between the two phases.

It is theoretically possible to use the feldspar compositions as a geothermometer and accurately determine a hypothetical equilibration temperature of the adjacent feldspar rims. Using existing experimental data, Perchuk and Ryabchikov (1968, Figure 15) have derived a relationship between the albite contents of coexisting plagioclase and alkali feldspar, ignoring the presence of K in plagioclase and Ca in orthoclase. Using their curves, a temperature between 600°C and 700°C is indicated for equilibration (crystallization ?) of the adjoining feldspar rims. More experimental data and data on natural occurrences are needed before their scheme can be applied with confidence. If post-crystallization reactions have

*Values of a 10 micron step traverse across the boundary indicate that problems of fluorescence across the phase boundary were minimal; the compositions given were not affected by it.

not occurred, a temperature of 600° to 700°C might be the temperature of crystallization of the last fraction of melt in rock Ad163c.

Feldspars in diabase pegmatite and deuterically-altered rocks

Na and K feldspar end-members were stable in the late assemblages in diabase pegmatite and deuterically altered rock. Calcic plagioclase was not stable and was altered to clays and prehnite. The similarities between the mineral assemblages in diabase pegmatite, deuterically-altered diabase, and albite diabase were emphasized in the discussion of the petrography of the diabasic rocks. The feldspars stable in these rocks were probably not precipitated from any melt phase but rather were formed when primary feldspar reacted in the presence of late liquids or melts. The pure compositions of the end-member feldspars present are guides to the low temperatures which must have prevailed during the final stages of feldspar reaction.

The most calcic plagioclase composition determined in the two analyzed specimens of diabase pegmatite (Ad28 and Ad98b) was $An_2Ab_{97.5}Or_{0.3}$; albite compositions as pure as $An_{0.3}Ab_{99.5}Or_{0.2}$ were found. Most K feldspar compositions determined were at least as potassic as $An_0Ab_2Or_{98}$. The analyzed specimen, Ad163f, a coarse-grained rock of a type intermediate between diabase pegmatite and the coarse-grained segregations, contained intensely-altered, relict grains of calcic andesine ($An_{45}Ab_{52}Or_3$) as well as almost pure Na and K feldspar. Plagioclase present in albite diabase, Ad141d, was found to have compositions near $An_{0.5}Ab_{99.3}Or_{0.1}$. Feldspar in diabase subjected to intense deuteric alterations seems similar to that in albite diabase.

The compositions of the intimately intermixed K feldspar (near $An_0Ab_2Or_{98}$) and Na feldspar (more sodic than $An_2Ab_{97.5}Or_{0.3}$) in the diabase pegmatite can be used as a rough geothermometer to indicate the temperature at which cation exchange between the two phases essentially ceased. Because reliable experimental data for low temperatures do not exist, and because the structural states of the feldspars in diabase pegmatite are unknown, the temperature can be determined only approximately. Extrapolation of the data of Orville (1963, p. 221) indicates Na-K exchange must have occurred at temperatures at least as low as about 400°C.

Feldspars, like pyroxenes, were formed in both the early magmatic stage of crystallization and the late deuteric stage. Oligoclase, andesine, and labradorite were stable with augite. Nearly pure Na and K feldspar were stable with the late calcic pyroxene. The sharp compositional distinction between the early and late pyroxenes is mirrored by the equally sharp distinction between the early plagioclase and the late end-member alkali feldspars.

Feldspar in quartz diabase

In quartz diabase, altered plagioclase laths are rimmed by alkali feldspar. Compositions of the original plagioclase could not be obtained because of its extensive alteration. Most alkali feldspar rims have almost completely unmixed to patchy intergrowths of nearly pure Na and K feldspar heavily dusted with tiny inclusions of clays(?). Some rims have only partly unmixed. Compositions varying from $An_5Ab_{46}Or_{49}$ to $An_{11}Ab_{77}Or_{12}$ were obtained with the microprobe on spots in an optically homogeneous, clear feldspar rim

around an altered plagioclase grain in the analyzed specimen, Ad286c. The compositions might represent actual alkali feldspar compositions in the rims. However, it is also possible that the optically homogeneous rims may consist of submicroscopic two phase intergrowths.

Iron-titanium Oxides

Introduction

Iron-titanium oxides can be valuable guides to the temperatures and oxygen fugacities in crystallizing magmas. Compositions of minerals in the system Fe-Ti-O depend on the bulk composition of the system in which they form and upon the temperature, pressure and oxygen fugacity of equilibration. Four important phases in the system are the spinel-structure minerals magnetite (Fe_3O_4) and ulvospinel (Fe_2TiO_4) and the rhombohedral-structure minerals hematite (Fe_2O_3) and ilmenite ($FeTiO_3$). Solid solutions between magnetite and ulvospinel and between hematite and ilmenite are found in many igneous rocks. Lindsley (1963) experimentally determined the compositional dependence of coexisting rhombohedral and spinel oxide phases on the temperatures and oxygen fugacities at which they were in equilibrium; he determined that total pressure had little effect upon the coexisting solid solutions. Lindsley (1962, 1963) and Buddington and Lindsley (1964) have shown that minor element partitions between the coexisting oxides vary with temperature. Because they are commonly intimately intergrown and because their opaqueness makes the purity of separates difficult to establish, reliable oxide compositional data, particularly for minor elements, have been scarce until very recently. Few thorough studies of iron-

titanium oxide variations in differentiated rock suites have been published. Because of their petrologic importance, the opaque minerals in the Sierra Ancha sill have been examined petrographically and with the electron microprobe to study temperature and oxygen fugacity variations in the sill.

The occurrences of the oxide minerals have been treated in detail in the discussions of the petrography of the diabasic rocks. Both ilmenite-hematite solid solutions and magnetite-ulvospinel solid solutions (henceforth called ilmenite$_{ss}$ and magnetite$_{ss}$, respectively) occur in olivine diabase and feldspathic olivine-rich diabase. Ilmenite$_{ss}$ was the only oxide recognized in diabase pegmatite. However, textural evidence suggests that magnetite$_{ss}$ crystallized in the pegmatites but was later destroyed by reaction. In some samples of intensely-altered diabase, magnetite$_{ss}$ grains partly reacted to form unidentified compounds lower in iron, in some cases sheet-structure silicates. Ilmenite$_{ss}$ was the only oxide identified in albite diabase, quartz diabase, and granophyre. In these three rock types and in diabase pegmatite, some ilmenite$_{ss}$ grains have reacted to and are rimmed by sphene.

Analytical procedures for Fe-Ti oxides

More analytical problems were encountered for the iron-titanium oxides than for other mineral groups. Oxygen, an important and variable element in the phases, was not determined directly with the microprobe but was calculated assuming stochiometry. Mineral formulas had to be recalculated after exclusion of minor elements for comparison with experimental data. Because of these considerations, analytical procedures for the oxides are discussed here rather than in an appendix.

Oxide analyses were made with an Applied Research Laboratories EMX microprobe on grains in polished thin sections. Analytical conditions were 15 kv with currents from 0.05 to 0.1 microamps. At all analyzed points Fe, Ti, Al, Cr, Mn, and Mg were determined. Standards used were: Fe, hematite; Ti, rutile; Al, kyanite; Cr, chromite; Mn, rhodonite; Mg, pyrope. Less than 0.1 weight percent CaO was present in typical ilmenite and magnetite grains examined. Vanadium analysis is difficult in Fe-Ti oxides because of the near coincidence of the $V_{k\alpha}$ and $Ti_{k\beta}$ x-ray emission peaks; in ilmenite accurate probe analysis for small quantities of V is almost impossible. The Cr-rich magnetite in Ad36d was found to contain 0.8-1.0 weight percent V_2O_3 and the coexistent ilmenite 0.1-0.2 weight percent.

After corrections for background and deadtime, microprobe x-ray counts were reduced to weight percent oxides with a CITRAN program incorporating the method of Bence and Albee (1968). Alpha factors for the interactions of FeO and TiO_2 were redetermined for this work; the values found were $\alpha(Fe) = 1.04$ and $\alpha(Ti) = 0.89$. The factors are considered to have an uncertainty of $\pm 2\%$ because

of microprobe variations and multiplication of errors in the process of alpha determination. No attempt was made to determine valence states of the analyzed elements with the microprobe. All the analyzed magnetite$_{ss}$ grains were assumed to lie on the join Fe_2TiO_4-Fe_3O_4 and all the analyzed ilmenite$_{ss}$ grains on the join $FeTiO_3$-Fe_2O_3 after correction for minor elements. The amount of ferric iron in each analysis was determined by appropriate calculations after calculating the excess of iron over available titanium. The excess oxygen determined by the presence of Fe_2O_3 instead of FeO was automatically entered into a CITRAN program for final determination of weight percent oxides.

Calculated weight percents of the major elements, Fe and Ti, are probably accurate to within ±2%. Counting statistics impose a limit of precision of about ±0.5% or less for the counting levels commonly attained for Fe and Ti. Microprobe stability problems and possible error in the data reduction system are responsible for the wider limits of error assigned. The precision for minor elements decreases as their amounts in the analyzed samples decrease. For elements present at a level of 1 weight percent oxide, the accuracy is probably ±5 to 10 percent. For elements present at a level of 0.1 weight percent oxide, the accuracy is probably no better than ±50%.

The sums of the analyses give one measure of the accuracy attained, though the assumptions involving ferric and ferrous iron obscure their usefulness. All but 6 of the 59 ilmenite analyses calculated sum between 99 and 101 percent. Seven of the fourteen magnetite analyses calculated sum between 98 and 100 percent and seven between 97.4 and 98 percent. Certainly one reason the magnetite analyses sum low is because V_2O_3, ZnO, SiO_2 and other elements were not analyzed. Carmichael's (1967) analyses of magnetites and

ilmenites demonstrate that magnetite contains considerably more of the three elements mentioned above than does coexisting ilmenite. Magnetite in rock Ad36d was analyzed for V_2O_3 and contained about 1 weight percent. The magnetites may also sum low because: (1) the data reduction system gives too low a value for iron, perhaps because of the uncertain relations between hematite and pure FeO; or (2) the magnetites may be more oxidized than compositions on the Fe_2TiO_4-Fe_3O_4 join -- such oxidized magnetites exist in igneous rocks and are probably formed by subsolidus oxidation of magnetite$_{ss}$ (Buddington and Lindsley, 1964, p. 317-318).

Ilmenite-hematite solid solution standards were analyzed with the unknowns. Standard compositions derived from microprobe analyses on different days are compared with the stated compositions in Table 18. The agreement of the analyses with the stated compositions is good. However, the agreement is a better check of consistency than of absolute accuracy, since the alpha factors used for data reduction were derived from these standards. Fe and Ti were always determined simultaneously for the oxide analyses. When the analyses are converted to mineral formulas such as $Ilm_{90}Hem_{10}$, the formula is probably accurate to within plus or minus one mole percent. The variations in Table 18 are within this one percent deviation.

The element proportions of the analyzed minerals have been calculated by CITRAN program into formulas in the systems magnetite-ulvospinel and hematite-ilmenite. The minor elements were combined and discarded by the same methods as used by Buddington and Lindsley (1964, pp. 327-329) for oxides with complete analyses. For magnetite$_{ss}$, iron was then combined with titanium

TABLE 18

Analyses of Standards

Stated Composition	Ilm_{100}	$Ilm_{70}Hem_{30}$	$Ilm_{30}Hem_{70}$
	$Ilm_{99.6}Hem_{.4}$	$Ilm_{71.0}Hem_{29.0}$	$Ilm_{30.9}Hem_{69.1}$
Compositions calculated from microprobe data	$Ilm_{99.7}Hem_{.3}$	$Ilm_{71.0}Hem_{29.0}$	
	$Ilm_{99.3}Hem_{.7}$	$Ilm_{70.7}Hem_{29.3}$	
	$Ilm_{99.4}Hem_{.6}$		
	$Ilm_{99.7}Hem_{.3}$		
	$Ilm_{100.0}Hem_{.0}$		

in the Fe_2TiO_4 molecule and the excess iron cast into the Fe_3O_4 molecule; then Fe_2TiO_4 and Fe_3O_4 were recalculated to 100 mole percent. A similar procedure was followed for ilmenite$_{ss}$. The way in which minor elements are treated is critical in interpretation of the relationships between magnetite and ilmenite. For instance, some ilmenite$_{ss}$ analyses with a molecular excess of Ti over Fe calculate to formulas with 5 or more mole percent hematite; combination of Mg and Mn with Ti into the molecules $MgTiO_3$ and $MnTiO_3$ decreases Ti so that Fe is present in excess of that needed to form $FeTiO_3$. The treatment of minor elements of Buddington and Lindsley (1964) was followed closely to permit comparison with their results. They justified it on the grounds that the effects of the minor elements on the activities of the major molecules is probably small.

Petrography of coexisting ilmenite$_{ss}$ and magnetite$_{ss}$

Both magnetite$_{ss}$ and ilmenite$_{ss}$ occur in olivine diabase and feldspathic olivine-rich diabase. These rock types contain from 3 to 8 modal percent oxides. Ilmenite$_{ss}$ generally predominates over magnetite$_{ss}$ by at least 3 to 1. The two minerals appear somewhat alike in polished section, and precise estimates of relative abundances were difficult to make. In reflected light magnetite$_{ss}$ appears dark gray and isotropic, while ilmenite$_{ss}$ appears lighter gray and anisotropic.

Magnetite$_{ss}$ occurs in more-or-less equidimensional, euhedral to anhedral grains 0.1 to 1 mm in maximum diameter. Most magnetite$_{ss}$ grains contain lamellae or grains of ilmenite$_{ss}$

or are bordered by grains of ilmenite$_{ss}$. Ilmenite$_{ss}$ also occurs in independent anhedral and subhedral grains. Some of these grains are highly irregular in form and appear to be interstitial to the silicates; some are crystallographically but not physically continuous in thin section for 3 to 4 mm.

Analytical data

Analyses of magnetite$_{ss}$ and ilmenite$_{ss}$ from a wide variety of rocks in the sill are listed in Tables 19, 20, and 21. The rocks in Tables 19 and 20 are listed in order of iron enrichment in pyroxenes and olivine, based mainly on the results shown in Figure 11. The rocks with the least iron-enriched silicates are at the top of each table. Therefore, the rocks are listed in approximate order of decreasing average silicate crystallization temperatures from the top to the bottom of both Tables 19 and 20. The rock sequences in the two tables overlap. Comparison of mafic silicate compositions (Figure 11) indicates that rock Ad163g (Table 20) had a lower average pyroxene crystallization temperature than rock Ad36s (Table 19); rock Ad28 (Table 19) had a lower average temperature than all specimens in Table 20 except rock Ad163a (see Figure 5). Ilmenite compositions in the granophyric rocks (Table 21) are included here for comparative purposes. Because of the salic compositions of these rocks, ilmenite in them probably formed at lower temperatures than primary ilmenite$_{ss}$ in the diabasic rocks.

TABLE 19
Ilmenite and Magnetite Compositions

Rock	Magnetite$_{ss}$						Derived Ilmenite$_{ss}$						Independent Ilmenite$_{ss}$					
	Al_2O_3	Cr_2O_3	R_2O_3	MgO	MnO	RO	Al_2O_3	Cr_2O_3	R_2O_3	MgO	MnO	RO	Al_2O_3	Cr_2O_3	R_2O_3	MgO	MnO	RO
Ad36d feldspathic olivine-rich diabase	$Mgt_{81}Usp_{19}$						$Ilm_{94}Hem_6$						$Ilm_{86}Hem_{14}$					
	2.78	2.97	5.74	1.57	0.32	1.89	0.08	0.38	0.46	4.88	0.61	5.49	0.07	0.37	0.44	3.37	0.40	3.77
	$Mgt_{83}Usp_{17}$						$Ilm_{93}Hem_7$											
	2.80	3.16	5.96	1.43	0.28	1.71	0.05	0.26	0.31	4.59	0.56	5.15						
	$Mgt_{89}Usp_{11}$						$Ilm_{92}Hem_8$											
	2.98	3.64	6.62	1.20	0.22	1.42	0.08	0.34	0.42	4.80	0.56	5.36						
Ad36p feldspathic olivine-rich diabase	$Mgt_{80}Usp_{20}$						$Ilm_{90}Hem_{10}$						$Ilm_{86}Hem_{14}$					
	3.12	3.24	6.36	1.30	0.33	1.63	0.08	0.31	0.39	4.08	0.45	4.53	0.13	0.40	0.53	3.72	0.43	4.15
	$Mgt_{85}Usp_{15}$						$Ilm_{94}Hem_6$											
	3.28	5.26	8.54	1.43	0.25	1.68	0.03	0.44	0.47	4.29	0.53	4.82						
Ad36s olivine diabase	$Mgt_{82}Usp_{18}$						$Ilm_{96}Hem_4$						$Ilm_{93}Hem_7$					
	2.66	0.37	3.03	0.65	0.28	0.93	0.04	0.15	0.19	2.16	0.83	2.99	0.10	0.09	0.19	2.68	0.53	3.21
	$Mgt_{86}Usp_{14}$												$Ilm_{94}Hem_6$					
	2.42	0.37	2.79	0.67	0.29	0.96							0.10	0.10	0.20	2.62	0.51	3.13
Ad36a olivine diabase	$Mgt_{66}Usp_{34}$						$Ilm_{98}Hem_2$						$Ilm_{94}Hem_6$					
	1.79	0.39	2.18	0.17	0.55	0.72	0.0	0.13	0.13	0.92	0.96	1.88	0.08	0.06	0.14	1.10	0.78	1.88
													$Ilm_{96}Hem_4$					
													0.06	0.07	0.13	1.21	0.73	1.94
Ad6a olivine diabase with heavy deuteric alteration	$Mgt_{67}Usp_{33}$						$Ilm_{95}Hem_5$						$Ilm_{96}Hem_4$			grain center		
	1.52	0.42	1.94	0.25	0.78	1.03	0.03	0.04	0.07	0.06	2.92	2.98	0.05	0.04	0.09	1.70	0.66	2.33
	$Mgt_{78}Usp_{22}$												$Ilm_{96}Hem_4$			grain rim		
	1.48	0.19	1.67	0.07	0.64	0.71							0.02	0.05	0.07	0.37	2.38	2.75
													$Ilm_{93}Hem_7$			grain center		
													0.05	0.04	0.09	1.13	0.63	1.76
													$Ilm_{94}Hem_6$			grain rim		
													0.07	0.04	0.11	0.92	1.02	1.94
Ad28 diabase pegmatite	not present												$Ilm_{95}Hem_5$					
													0.02	0.02	0.04	0.12	0.84	0.96

All specimens from Reynolds Creek drainage; locations are shown in Figure 3.

TABLE 20
Ilmenite and Magnetite Compositions

Rock	Magnetite$_{ss}$						Derived Ilmenite$_{ss}$						Independent Ilmenite$_{ss}$					
	Al_2O_3	Cr_2O_3	R_2O_3	MgO	MnO	RO	Al_2O_3	Cr_2O_3	R_2O_3	MgO	MnO	RO	Al_2O_3	Cr_2O_3	R_2O_3	MgO	MnO	RO
Ad163g olivine diabase (-150)	$Mgt_{78}Usp_{22}$						$Ilm_{95}Hem_5$						$Ilm_{90}Hem_{10}$					
	3.30	0.75	4.05	0.65	0.27	0.92	0.05	0.06	0.11	3.65	0.71	4.36	0.13	0.08	0.21	2.85	0.45	3.30
	$Mgt_{80}Usp_{20}$						$Ilm_{95}Hem_5$						$Ilm_{91}Hem_9$					
	3.37	0.83	4.20	0.82	0.28	1.10	0.06	0.06	0.12	2.78	0.75	3.53	0.09	0.06	0.15	2.18	0.46	2.64
													$Ilm_{91}Hem_9$					
													0.07	0.07	0.14	1.90	0.63	2.53
Ad163e olivine diabase (-80)	$Mgt_{72}Usp_{28}$						$Ilm_{96}Hem_4$						$Ilm_{93}Hem_7$					
	2.74	0.18	2.92	0.69	0.38	1.07	0.06	0.04	0.10	2.25	0.80	3.05	0.04	0.04	0.08	1.06	0.81	1.87
	$Mgt_{72}Usp_{28}$						$Ilm_{96}Hem_4$						$Ilm_{93}Hem_7$					
	2.18	0.20	2.38	0.48	0.43	0.91	0.05	0.06	0.11	1.47	1.12	2.59	0.06	0.04	0.10	1.75	0.85	2.60
	$Mgt_{80}Usp_{20}$												$Ilm_{92}Hem_8$					
	2.74	0.28	3.02	0.49	0.33	0.82							0.06	0.05	0.11	1.90	0.50	2.40
Ad163f coarse-grained segregation (-80)	not present												$Ilm_{92}Hem_8$		blade center			
													0.05	0.0	0.05	0.74	0.56	1.30
													$Ilm_{94}Hem_6$		blade edge			
													0.03	0.01	0.04	0.17	2.43	2.60
													$Ilm_{96}Hem_4$		blade edge			
													0.03	0.0	0.03	0.11	3.59	3.70
Ad163b olivine diabase extensively altered (-32)	$Mgt_{74}Usp_{26}$						$Ilm_{96}Hem_4$						$Ilm_{94}Hem_6$					
	0.77	0.34	1.11	0.07	0.50	0.57	0.03	0.06	0.09	0.07	2.54	2.61	0.07	0.05	0.12	1.18	0.77	1.95
							$Ilm_{95}Hem_5$						$Ilm_{94}Hem_6$					
							0.04	0.06	0.10	0.19	2.12	2.31	0.07	0.07	0.14	0.54	1.11	1.65
													$Ilm_{94}Hem_6$					
													0.04	0.06	0.10	0.28	1.00	1.28
Ad163a quartz diabase (-20)	not present												$Ilm_{96}Hem_4$					
													0.01	0.04	0.05	0.06	1.26	1.32
													$Ilm_{97}Hem_3$					
													0.0	0.02	0.02	0.05	2.23	2.38
													$Ilm_{97}Hem_3$					
													0.0	0.01	0.01	0.11	1.03	1.14

All specimens from a section 140 feet thick at the roof of the sill in the Workman Creek drainage. Numbers in parentheses are distances below roof of sill complex. See Figure 28.

TABLE 21

Compositions of $Ilmenite_{ss}$ in Granophyre

Rock	Al_2O_3	Cr_2O_3	R_2O_3	MgO	MnO	RO
Ad91c pyroxene granophyre	$Ilm_{97}Hem_3$					
	0.0	0.03	0.03	0.07	0.98	1.05
	$Ilm_{98}Hem_2$					
	0.0	0.04	0.04	0.06	1.28	1.34
Ar-Gi-Rcgphr 1-6 hornblende granophyre	$Ilm_{98}Hem_2$					
	0.0	0.03	0.03	0.06	0.93	0.99
	$Ilm_{98}Hem_2$					
	0.0	0.02	0.02	0.05	1.02	1.07
Ad23h aplitic pyroxene granophyre	Ilm_{100}(0.5 wt.% excess TiO_2)					
	0.01	0.06	0.07	0.14	0.86	1.00
	Ilm_{100}(1.1 wt.% excess TiO_2)					
	0.0	0.05	0.05	0.09	1.22	1.31
Ad163 pyroxene-biotite granophyre	Ilm_{100}(0.8 wt.% excess TiO_2)					
	0.02	0.06	0.08	0.15	0.95	1.10
	Ilm_{100}(1.2 wt.% excess TiO_2)					
	0.0	0.04	0.04	0.08	3.59	3.67
	Ilm_{100}(0.8 wt.% excess TiO_2)					
	0.0	0.04	0.04	0.13	2.26	2.39

Compositions of magnetite$_{ss}$

Calculated magnetite$_{ss}$ formulas range from $Mgt_{66}Usp_{34}$ to $Mgt_{89}Usp_{11}$. The range of values is close to that indicated by Buddington and Lindsley (1964, Figure 7) for gabbros in which external granule solution occurred.

None of the magnetite analyses in Tables 19 and 20 represent average grain compositions. Since microprobe analyses represent the compositions of volumes only a few cubic microns in size, they will not be representative of the bulk compositions of analyzed minerals unless the minerals are homogeneous. Magnetite$_{ss}$ grains in rocks of the Sierra Ancha sill are almost all inhomogeneous. Some grains contain microscopically visible lamellae of ilmenite$_{ss}$. Some areas of grains contain no visible lamellae, but nonetheless microprobe traverses show them to be markedly inhomogeneous on a scale of a few microns. Graphs of 1 and 10 micron step traverses analyzing Ti, Fe, and Al in magnetite$_{ss}$ in rock Ad36a are in Figures 16 and 17. In each graph can be seen an inverse relationship between Ti and Al; when Al increases, Ti decreases. A rough inverse relationship can also be seen between Ti and Fe; when Ti increases, Fe decreases in many instances. The variation may be due to the formation of sub-microscopic domains or lamellae rich in ulvospinel or hercynite ($FeAl_2O_4$). Exsolution of ulvospinel from magnetite$_{ss}$ has been described by Vincent (1960). Exsolution of hercynite from magnetite and phase relations in the system Fe_3O_4-$FeAl_2O_4$ have been discussed by Turnock and Eugster (1962). Some areas in magnetite grains are fairly homogeneous, despite the inhomogeneity of other

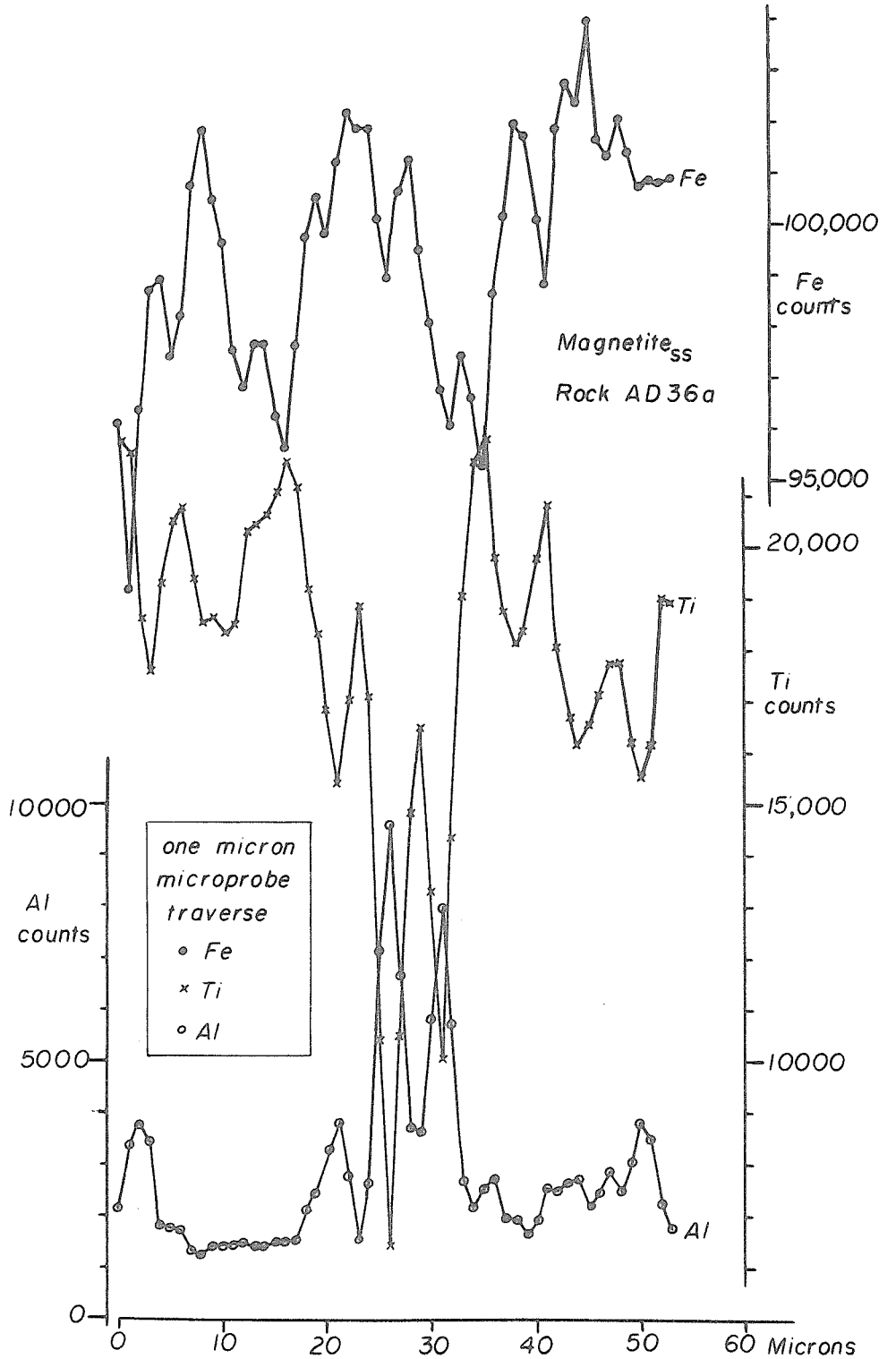

Figure 16. One micron microprobe traverse for Fe, Ti, and Al in an inhomogeneous magnetite$_{ss}$ grain. Counts corrected for background.

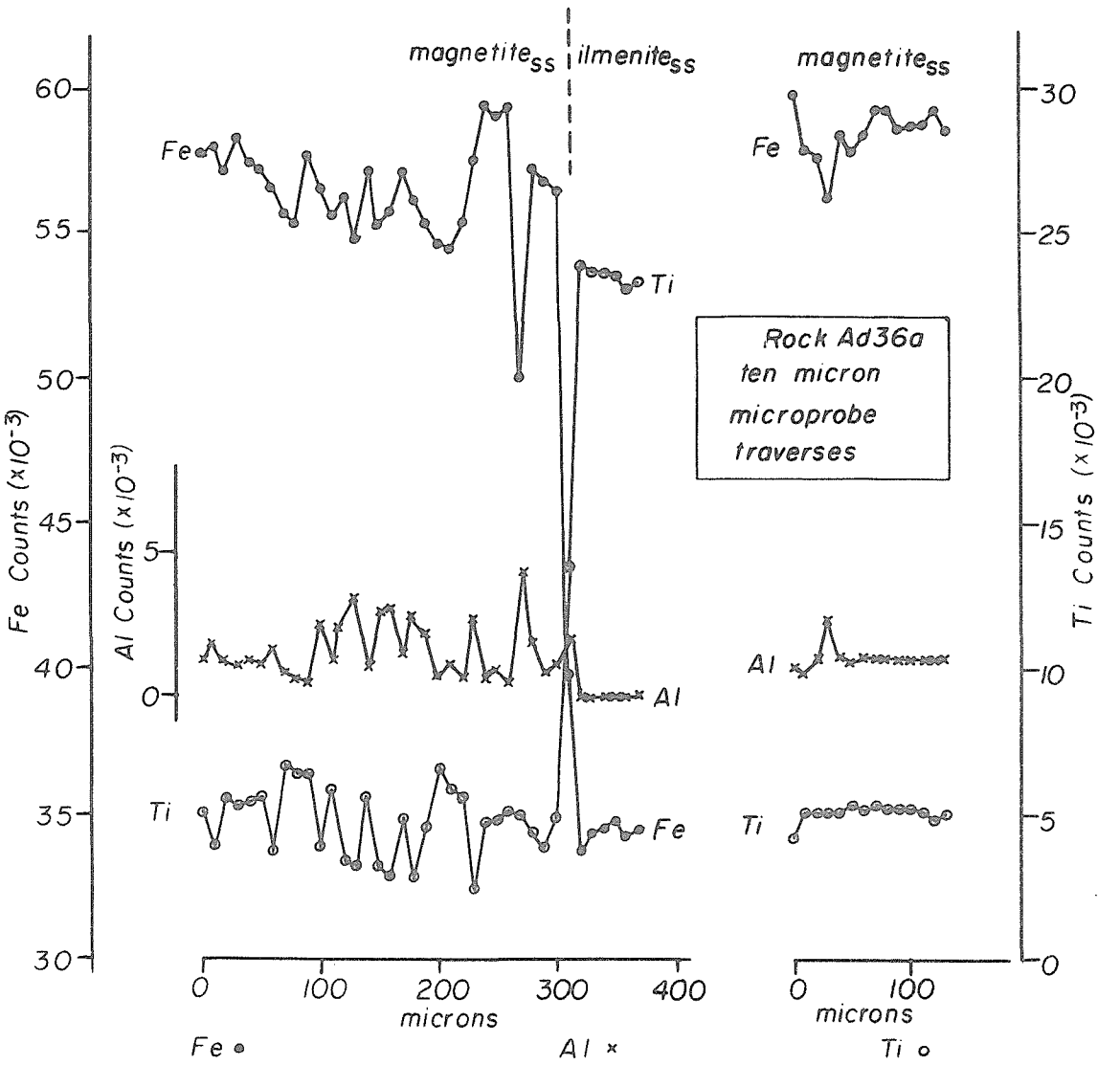

Figure 17. Microprobe traverses for Fe, Al, and Ti across parts of magnetite grains. Rock Ad36a. Counts corrected for background.

areas in the same grains. A 10 micron step traverse across a relatively homogeneous area in a magnetite$_{ss}$ grain is shown on the right side of Figure 17. Analyses of magnetite$_{ss}$ grains reported in Tables 19 and 20 were made in such homogeneous areas when possible. Even areas homogeneous on a small scale differ in composition from one another throughout a single grain. Magnetite$_{ss}$ close to or immediately adjacent to ilmenite$_{ss}$ lamellae generally is poorer in ulvospinel than magnetite$_{ss}$ in areas apparently free from ilmenite$_{ss}$ lamellae. For each rock an analysis for the most Ti-rich, reasonably homogeneous magnetite$_{ss}$ is reported, as well as, in many cases, analyses for magnetite$_{ss}$ poorer in ulvospinel.

Compositions of ilmenite$_{ss}$

Two distinct compositional groups of ilmenite$_{ss}$ grains can be recognized in rocks which also contain magnetite$_{ss}$. The two groups, which can be defined texturally equally as well as compositionally, are: (1) those ilmenite$_{ss}$ grains which crystallized independently from magnetite$_{ss}$ and which are called independent ilmenite$_{ss}$; and (2) those ilmenite$_{ss}$ lamellae and grains in composite grains with magnetite$_{ss}$ which are called derived ilmenite$_{ss}$.

The derived ilmenite$_{ss}$ formed by an exsolution-reaction process from the magnetite$_{ss}$, whether it occurs completely within magnetite$_{ss}$ grains or as bordering grains. It presumably formed by reaction of exsolved ulvospinel with oxygen, the reaction perhaps occurring contemporaneously with exsolution of the titanium-rich phase (Buddington and Lindsley, 1964, p. 322). Four steps in the "exsolution" process are illustrated with photomicrographs in Plates 17 and 18. Microprobe analyses in each case shown support

PLATE 17

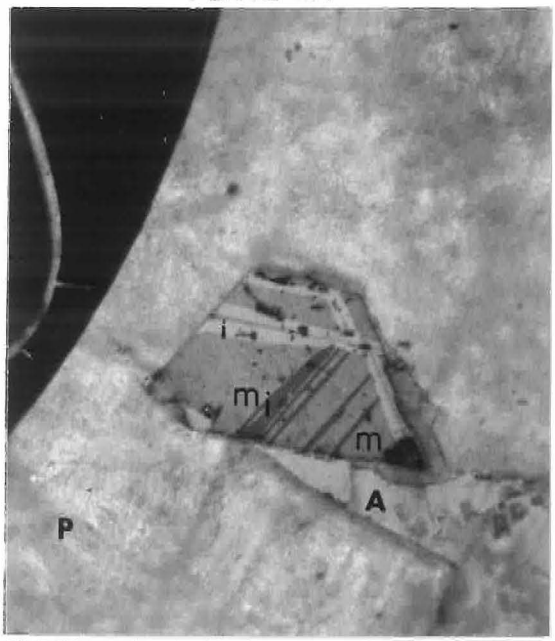

Rock Ad163b. 0.4x0.4 mm. Reflected light. Crossed nicols. Magnetite (m) with many small lamellae of anisotropic ilmenite (i) surrounded by augite (A) and plagioclase (P).

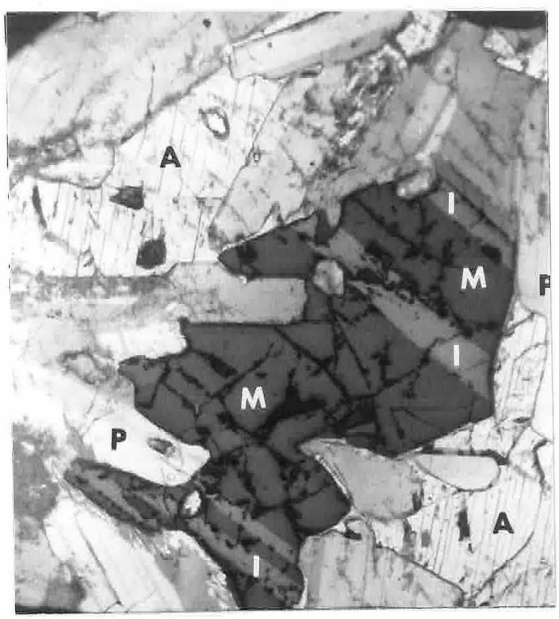

Rock Ad163g. 0.9x1.0 mm. Reflected light. Crossed nicols. Magnetite (M) with a few broad lamellae of ilmenite (I). Plagioclase (P) and augite (A) are also present.

PLATE 18

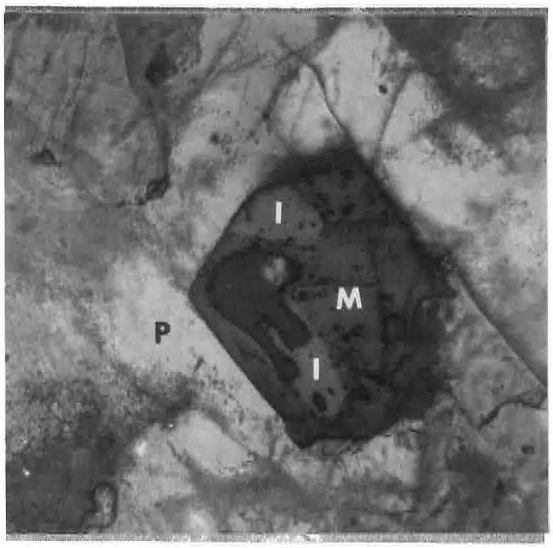

Rock Ad163g. 0.4x0.4 mm. Reflected light. Crossed nicols. Magnetite (M) including several granules of "exsolved" ilmenite (I). Partly altered plagioclase (P) is also present.

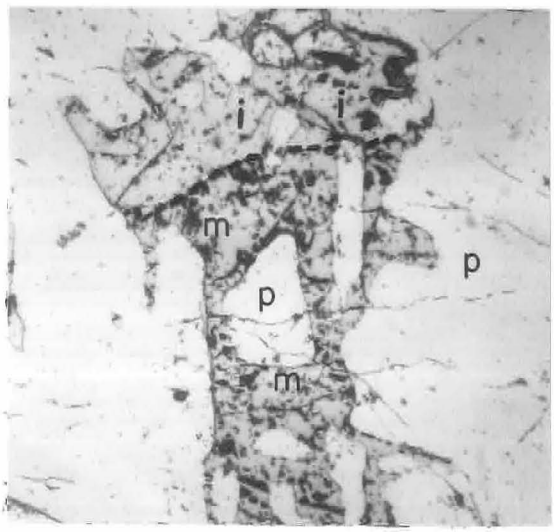

Rock Ad36p. 0.8x0.8 mm. Reflected light. An extreme case of granule "exsolution". Magnetite (m) with adjoining ilmenite (i) which formed by an exsolution-reaction process from the magnetite. The oxide grain is in a matrix of plagioclase (p).

the contention that the ilmenite$_{ss}$ formed by "exsolution" from magnetite$_{ss}$ rather than by direct crystallization from a melt.

No exsolution phenomena were observed within any ilmenite$_{ss}$ grain. Independent ilmenite$_{ss}$ in the rocks with more Mg-rich pyroxenes (Ad36d, Ad36p, Ad36s) is remarkably homogeneous. Independent ilmenite$_{ss}$ in other rocks is fairly homogeneous with respect to the major elements, Fe and Ti: however, grains are zoned in Mn and Mg, the rims being both enriched in Mn and depleted in Mg with respect to grain cores. Analyses for cores and rims are given for zoned ilmenites. Derived ilmenite$_{ss}$ is more variable in composition than independent ilmenite$_{ss}$. That which is immediately adjacent to magnetite is commonly poorer in hematite than that further from magnetite. Where a range in composition of derived ilmenite$_{ss}$ was found, analyses are given for typical values in the range.

Ilmenite$_{ss}$ compositions range from $Ilm_{86}Hem_{14}$ to Ilm_{100}. Ilmenites in the Fe-rich portion of the range are common (Buddington and Lindsley, 1964; Carmichael, 1967), but the ilmenites very low in hematite are unusual. Ilmenite analyses in two of the rocks in Table 21 calculate to formulas with no hematite in solid solution; actually all five formulas listed as Ilm_{100} have an excess of Ti over divalent elements. The excess ranges from 0.5 to 1.2 weight percent TiO_2 for the five analyses. It is probably the result of analytic error, as Taylor (1964, p. 1028) found no excess TiO_2 in hematite-ilmenite solid solutions at 1300°C; at temperatures below 1300°C, excess TiO_2 is probably negligible. Both rocks containing Ilm_{100} are granophyres and do not contain magnetite.

Compositional criteria for distinguishing primary and exsolved ilmenite$_{ss}$

The origin of ilmenite$_{ss}$ grains included within or immediately adjacent to magnetite$_{ss}$ grains in plutonic igneous rocks has been a problem in numerous petrologic studies. (Wright, 1961; Buddington and Lindsley, 1964). It is in many cases difficult to establish whether ilmenite$_{ss}$ grains crystallized from a melt or are a product of granule exsolution after reaction of magnetite-ulvospinel solid solution with oxygen. Microprobe analytical data from the Sierra Ancha sill allow a clear distinction to be made between independently crystallized ilmenite$_{ss}$ and derived ilmenite$_{ss}$ and suggest criteria for distinction of the two types of ilmenites in other sills. The data summarized in Tables 19 and 20 show that derived ilmenite$_{ss}$ consistently is lower in hematite and higher in manganese than independent ilmenite$_{ss}$, whether the derived ilmenite appears as obvious lamellae or as equant grains bordering magnetite. Microprobe step traverses across grain boundaries between magnetite$_{ss}$ and ilmenite$_{ss}$ can provide additional evidence as to the origin of the ilmenite$_{ss}$. Figure 18 shows a traverse across one of the lamellae boundaries in Plate 17. The buildup of Cr at the boundary is striking. Similar gradients of Al exist in magnetite$_{ss}$ at ilmenite$_{ss}$-magnetite$_{ss}$ boundaries. The gradients are observed whether the ilmenite occurs as lamellae or as included grains. The magnetite$_{ss}$ analysis from rock Ad36p (Table 19) showing 5.3 weight percent Cr_2O_3 was made near the ilmenite$_{ss}$-magnetite$_{ss}$ grain boundary shown in Plate 18. Both Cr and Al are strongly concentrated in magnetite$_{ss}$ as compared to ilmenite$_{ss}$. When ilmenite$_{ss}$ is formed at the expense of magnetite$_{ss}$, the expelled Cr and Al are

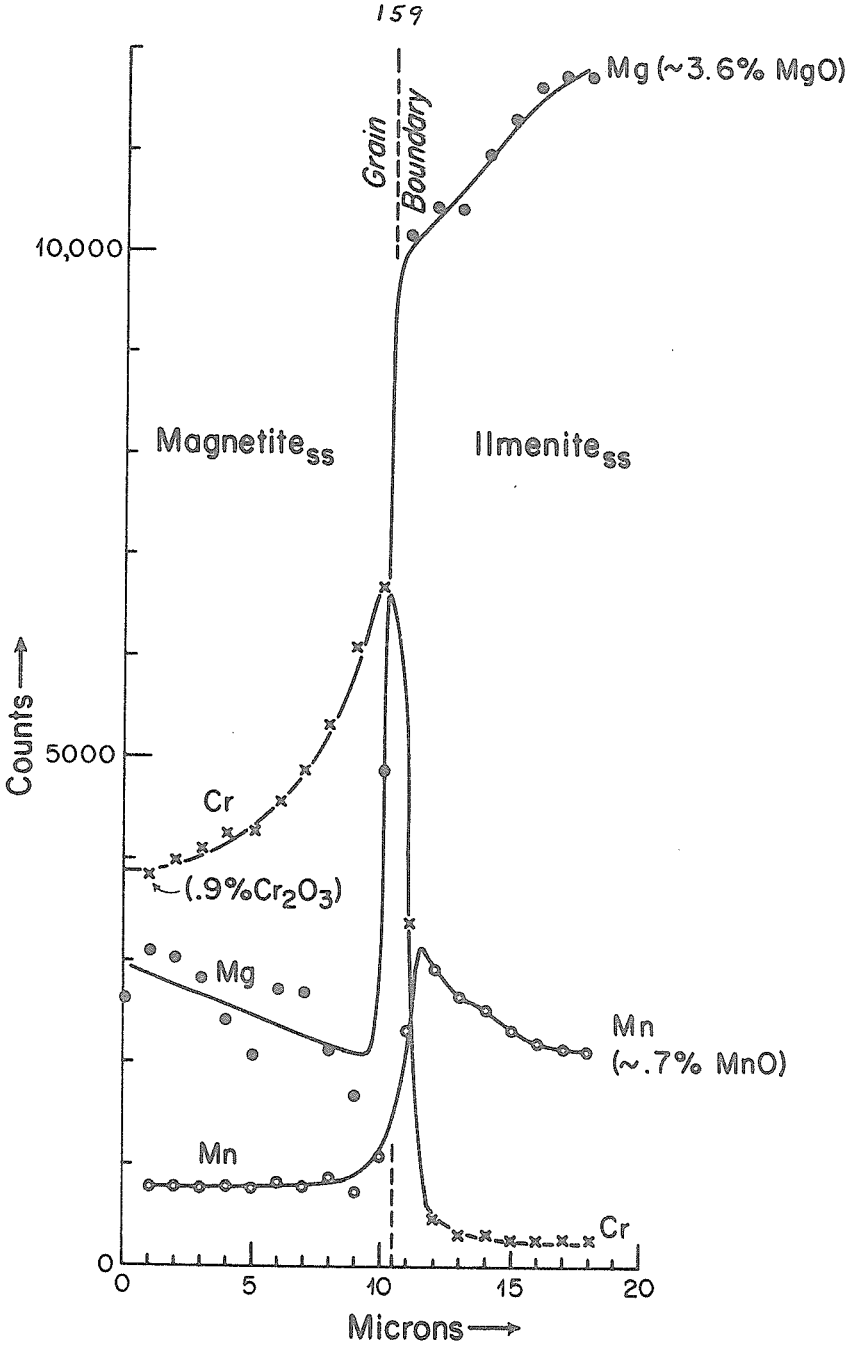

Figure 18. Results of a microprobe traverse across one boundary of an ilmenite$_{ss}$ lamella within a magnetite$_{ss}$ grain. Rock Ad163g. Counts corrected for background.

concentrated in magnetite at the boundary between the two phases; the resulting concentration gradients are "frozen in" at the mutual grain boundaries as temperature drops. Such concentration gradients would not be observed at ilmenite$_{ss}$-magnetite$_{ss}$ grain boundaries if the ilmenite$_{ss}$ crystallized independently from an igneous melt.

Temperatures and oxygen fugacities indicated by oxide pairs

Had the primary magnetite$_{ss}$ remained unaltered in the Sierra Ancha rocks, it would be possible to deduce temperatures and oxygen fugacities in the crystallization ranges of the diabasic rocks by using the experimental compositional relationships (Fig. 19) developed by Lindsley (1963, p. 64). Since some of the ulvospinel in all the magnetites has exsolved and reacted to form ilmenite$_{ss}$, it is possible to deduce only lower limits for the initial high temperatures of equilibration between the oxides. In addition, the temperatures and oxygen fugacities at which diffusion and reactions in the magnetite$_{ss}$ effectively ceased can be determined. Use of the composition of the independent ilmenite$_{ss}$ together with that of the most ulvospinel-rich magnetite$_{ss}$ in a sample provides a lower limit to temperatures of magmatic equilibration in the rock. Temperatures and oxygen fugacities derived using these compositions are given in Table 22. The average T and f_{O_2} are 720°C and 10^{-16} atm; the deviations from the average are random and not significant. The temperature is far too low to represent the crystallization temperature of the oxides; whether any significance can be attached to it is questionable. Consideration of Fe-Ti-O equilibria between

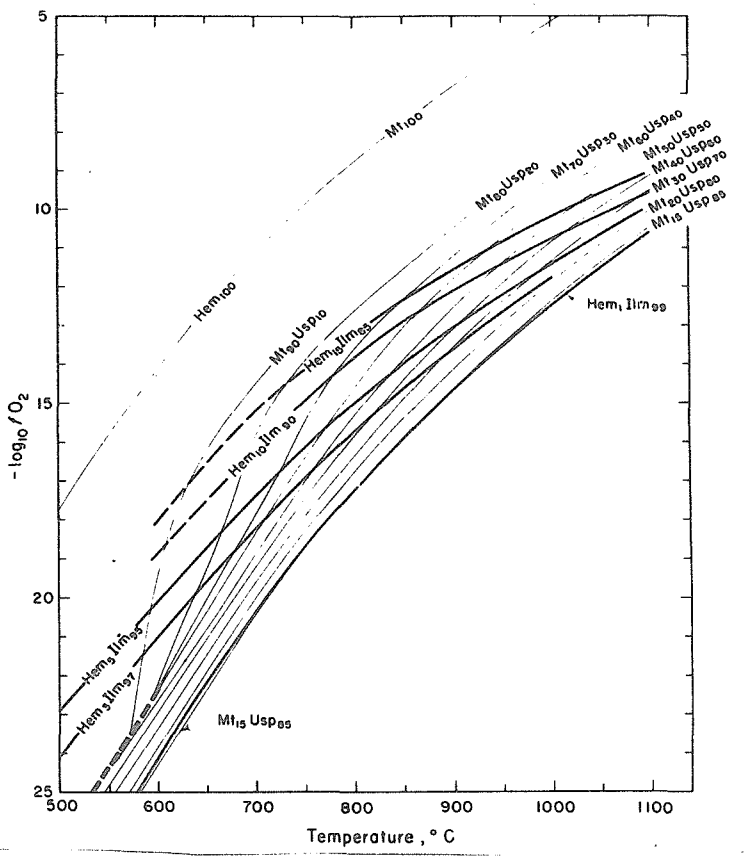

Figure 19. Experimental relationships determined by Lindsley (1963) relating the compositions of magnetite$_{ss}$ and ilmenite$_{ss}$ to the temperatures and oxygen fugacities at which they are in equilibrium. Figure reproduced from Buddington and Lindsley(1964, Figure 5).

TABLE 22

Temperatures and Oxygen Fugacities Derived from the Experimental Relationships Shown Above Using Data from Tables 19 and 20.

Independent Ilmenite and Ti-rich Magnetite					
Rock	T	Fo_2	Rock	T	Fo_2
Ad36d	720°C	10^{-15}	Ad6a	740°C	10^{-16}
Ad36p	720°C	10^{-15}	Ad163g	710°C	10^{-16}
Ad36s	670°C	10^{-18}	Ad163e	740°C	10^{-16}
Ad36a	740°C	10^{-16}	Ad163b	710°C	10^{-17}
Derived Ilmenite and Associated Magnetite					
Ad36p	630°C	10^{-19}	Ad163e	650°C	10^{-19}

magnetite$_{ss}$ and ilmenite$_{ss}$ fails to provide useful information on magmatic conditions in the sill.

By using the compositions of derived ilmenite$_{ss}$ and immediately adjacent magnetite$_{ss}$ in a composite grain, the lowest temperature and effective oxygen fugacity of solid state reaction can be obtained. Data from rocks Ad36p and Ad163e give temperatures and oxygen fugacities of about 640°C and 10^{-19} atm. These data suggest that diffusion and reaction in the magnetite$_{ss}$ effectively ceased at temperatures below 600°C.

The compositional trend shown by ilmenite$_{ss}$ which crystallized with magnetite$_{ss}$ provides information on oxygen fugacity changes in the diabase magma. The amount of hematite in solid solution in ilmenite$_{ss}$ decreases with decreasing silicate crystallization temperature. In the higher-temperature rocks with more magnesian silicates (Ad36d, Ad36p) in the sill complex, the ilmenite$_{ss}$ compositions are about $Ilm_{86}Hem_{14}$. In the lower-temperature rocks with more iron-rich silicates (Ad6a, Ad163b), ilmenite$_{ss}$ compositions are near $Ilm_{94}Hem_{6}$. Reference to Lindsley's data shows that the f_{O_2} must have decreased at least an order of magnitude between equilibration of the oxides in the earlier and later diabasic rocks; if the temperature of equilibration in the later rocks was 50°C lower than in the olivine-rich rocks, then the f_{O_2} must have been two orders of magnitude lower. If the oxides in the feldspathic olivine-rich rocks (Ad36d, Ad36p) are presumed to have equilibrated at 1050°C, then they did so at an f_{O_2} slightly greater than 10^{-10} atm and their initial magnetite$_{ss}$ had a composition of $Mgt_{45}Usp_{55}$. The amount of exsolution seen seems compatible with such an original

magnetite$_{ss}$ composition.* For comparison, Buddington and Lindsley (1964, Figure 8) inferred the Skaergaard gabbros to have had original magnetite$_{ss}$ compositions near $Mgt_{20}Usp_{80}$ at about 1075°C, corresponding to an f_{O_2} slightly less than 10^{-10} atm. In short, the compositions of ilmenite$_{ss}$ coexistent with magnetite$_{ss}$ suggest that the diabase magma had an oxygen fugacity similar to that in the Skaergaard intrusion and that the fugacity decreased as crystallization proceeded.

Minor element partitions between oxides

Minor element distribution in the oxides follows the patterns indicated by Carmichael (1967, p. 46) and others. Compared to ilmenite$_{ss}$, magnetite$_{ss}$ is enriched in Al_2O_3 and Cr_2O_3 and impoverished in MgO and MnO. The ranges of minor element weight percents in magnetite$_{ss}$ are: Al_2O_3, 3.4-0.8; Cr_2O_3, 5.3-0.2; MnO, 0.8-0.2; MgO, 1.6-0.1. Collectively, they total from 10.6 to 1.7 weight percent of the magnetites studied. The ranges of minor element weight percents in ilmenites$_{ss}$ are: Al_2O_3, 0.1-0.0; Cr_2O_3, 0.4-0.0; MnO, 3.6-0.4; MgO, 4.9-0.1. Collectively, they total from 6.0 to 1.0 weight percent of the ilmenites studied.

*If one mole Mgt_aUsp_{1-a} is oxidized to x moles Mgt_bUsp_{1-b} plus y moles Hem_cIlm_{1-c}, then $x = (1+2a-3c)/(1+2b-3c)$ and $y=3(b-a)/(1+2b-3c)$ and the ilmenite % of the result is $y/x+y=3(b-a)/(1-a+3b-3c)$. For rock Ad36d, if $Mgt_{45}Usp_{55}$ was oxidized to $Mgt_{80}Usp_{20}$ and $Hem_{14}Ilm_{86}$, then 40 mole percent or 33 volume percent of the resulting oxides would be ilmenite. Rough modal estimates of present proportions in composite grains make it seem unlikely that any magnetite in the sill was originally much richer in ulvospinel than $Mgt_{50}Usp_{50}$.

The equilibrium partition of an element between two phases depends on their compositions and on the temperature and pressure of equilibration. Thermodynamic equations for the chemical potential of a species 1 in phases A and B can be written:

$$(1.1) \quad \mu_{1,A}(P,T) = \mu^{o}_{1,A}(P,T) + RT\,\ell n a_{1,A}$$

$$(1.2) \quad \mu_{1,B}(P,T) = \mu^{o}_{1,B}(P,T) + RT\,\ell n a_{1,B} \quad .$$

If the two phases are in equilibrium, then $\mu_{1,A} = \mu_{1,B}$ and the following equation can be written:

$$(1.3) \quad a_{1,A}/a_{1,B} = e^{[(\mu^{o}_{1,B} - \mu^{o}_{1,A})/RT]} \quad .$$

If the solid solution for the range of compositions involved is ideal ($a = x$) or obeys Henry's law ($a = kx$), then the ratio of the activities can be expressed as constant times the ratio of the concentrations. For many condensed phase reactions, changes in pressure of the magnitudes encountered in the upper crust do not significantly affect differences in thermodynamic potentials such as $(\mu^{o}_{1,B} - \mu^{o}_{1,A})$; as a first approximation the difference can be assumed to be solely a function of temperature. With these approximations, equation 1.3 can be written:

$$x_{1,A}/x_{1,B} = k\,f(T) \quad .$$

If the equation holds true for the distribution of an element between two coexistent phases, then the distribution can be used as a geologic thermometer.

The fractionation of minor elements between coexistent rhombohedral and spinel oxide phases has some promise as a

geothermometer. Buddington (1964) and Buddington and Lindsley (1964, p. 352) found that the ratio of Mn in ilmenite$_{ss}$ to Mn in magnetite$_{ss}$ varied from low values (1.4-5) in basic igneous rocks through intermediate values (5-5.5) for quartz syenites and granites to high values (5-15 or greater) for high-grade metamorphic rocks and pegmatites. Carmichael (1967) analyzed coexistent, homogeneous oxide pairs from salic volcanic rocks with an electron microprobe and computed equilibration temperatures for the pairs using the data of Lindsley (1963). Distribution ratios (weight percent oxide in ilmenite/weight percent oxide in magnetite) for both magnesium and manganese computed from his data are plotted against his calculated equilibration temperatures for the pairs in Figure 20. The scatter of points about the arbitrarily drawn lines is large; excluding two samples the standard deviations about the two lines are $\pm$ 25°C and $\pm$ 32°C for Mn and Mg respectively. However, the data do indicate that the distribution ratios for both elements increase with decreasing temperature of Fe-Ti-O equilibration.

The study of minor element abundances in coexistent magnetite$_{ss}$ and ilmenite$_{ss}$ in the Sierra Ancha sill is made difficult by the subsolidus reactions which have affected the magnetite$_{ss}$ grains and by the Mn-Mg zoning in some ilmenite$_{ss}$ grains. The subsolidus reaction of magnetite-ulvospinel and oxygen to yield ilmenite$_{ss}$ and a magnetite$_{ss}$ poorer in ulvospinel results in an increase of Al and Cr and decrease in Mn and Mg in the magnetite$_{ss}$. The microprobe step traverse in Figure 18 illustrates some of the partitions which occur between the reacting and forming phases. Newly-formed ilmenite solid solution draws Mn and Mg from the surrounding magnetite$_{ss}$, depleting it in these elements. Al and Cr are expelled

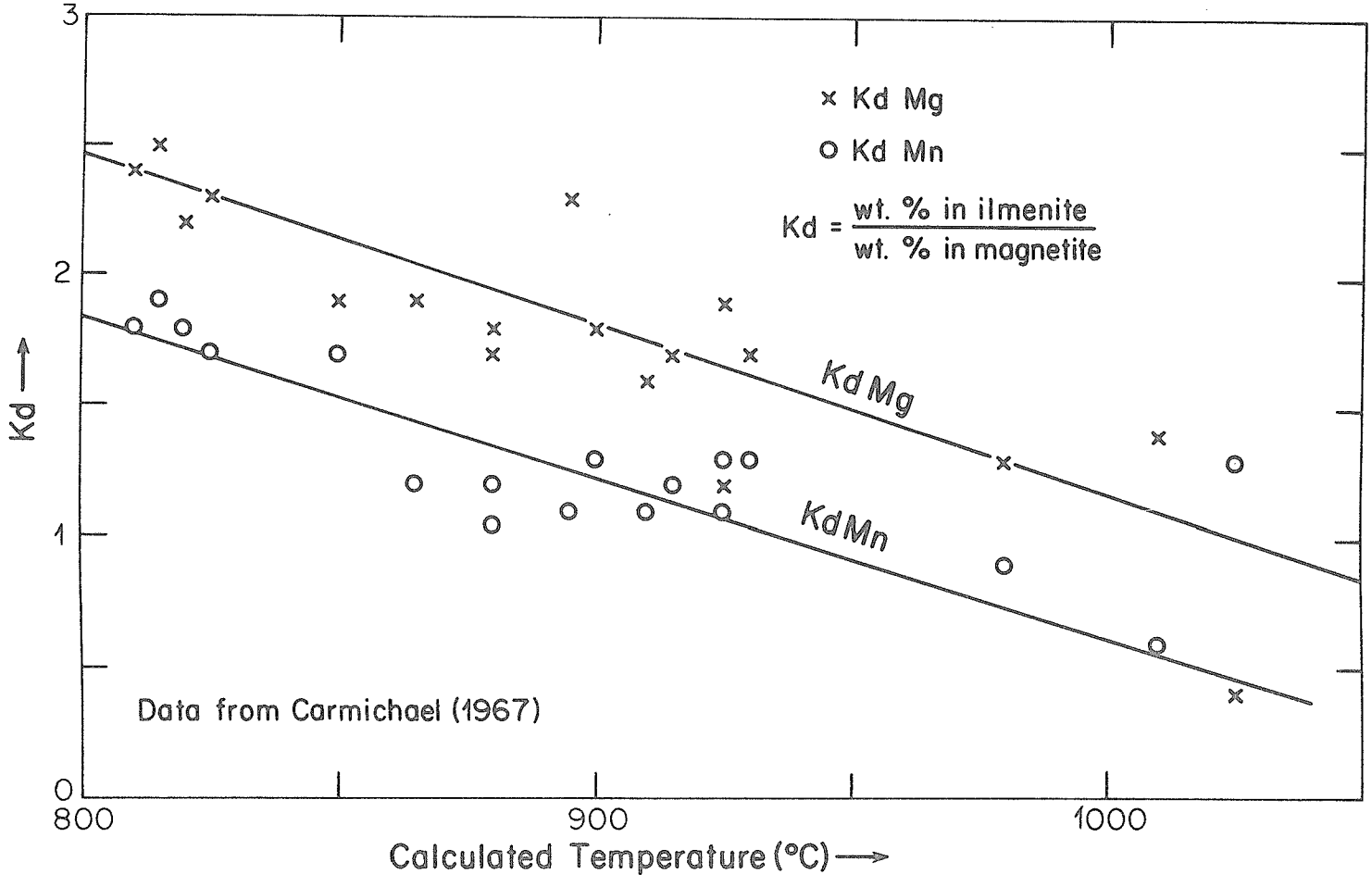

Figure 20. Distribution of Mn and Mg between coexisting ilmenite$_{ss}$ and magnetite$_{ss}$ grains in volcanic rocks, taken from data reported by Carmichael (1967). The temperatures were calculated by Carmichael using the experimental data of Lindsley (1963).

from the ilmenite$_{ss}$ as it is formed; eventually the expelled Al and Cr diffuse uniformly throughout the magnetite$_{ss}$ giving it higher concentrations of these elements. Rough calculations using the formulas in the footnote on page 163 and approximate partition values show that, in a typical reacted magnetite$_{ss}$, manganese concentrations might be 2/3 and magnesium 4/10 of their concentrations in primary magnetite$_{ss}$. In reacted magnetite$_{ss}$ in any one rock, the RO-group elements should decrease and the R_2O_3-group elements increase with decreasing ulvospinel in magnetite$_{ss}$; the analyses in Tables 19 and 20 do not all display these patterns. Evidently the minor elements are not redistributed in the magnetite$_{ss}$ on an equilibrium basis. Meaningful numerical values for element ratios between the two oxide phases cannot be obtained with any degree of confidence.

Approximate values of the distribution ratios between the two minerals for minor elements are: Al_2O_3, 1/30; Cr_2O_3, 1/10; MnO, 1.5/1 to 2/1; MgO, 3/1 to 5/1. If the concentrations of MnO and MgO are increased by 3/2 and 10/4 respectively to make them comparable to original concentrations in primary magnetite$_{ss}$, then the distribution ratios are: MnO, 1/1 to 1.5/1; MgO, 1/1 to 2.5/1. These values fall in the temperature range 800°C to 1000°C on the graph of distribution ratios compiled from Carmichael's data (Figure 20). Manganese is greater in derived ilmenite$_{ss}$ than in independent ilmenite$_{ss}$ in the same rock, as would be expected if the Mn distribution ratio increased with declining temperature. No such consistency is apparent in the data for Mg.

Compositional trends in primary ilmenite$_{ss}$

Clearly-defined compositional trends in independent ilmenite$_{ss}$ grains are defined by the analyses in Tables 19, 20, and 21. With decreasing pyroxene crystallization temperature, independent ilmenite$_{ss}$ becomes richer in manganese, poorer in magnesium, and poorer in solid solution hematite. Perhaps because the analytical error for elements present in amounts less than 0.1 weight percent may be ± 50%, trends cannot be clearly defined for aluminum and chromium; however, both elements show some decreases in ilmenite$_{ss}$ with declining crystallization temperatures. The general consistency of the compositional trends in the ilmenite$_{ss}$ is independent evidence supporting the ordering of the diabase samples according to the degree of iron enrichment in pyroxenes and olivine.

Individual independent ilmenite$_{ss}$ grains in the late-crystallizing rocks show the same trends as does the suite of analyzed grains. Grain cores are enriched in Mg and depleted in Mn with respect to grain rims. In some instances grain cores are enriched in hematite with respect to rims. Figure 21 depicts Mn and Mg zoning in an irregularly-shaped ilmenite$_{ss}$ crystal. In grains with more regular geometric shapes, the zoning is more regular and better-related to grain geometry. A striking feature of the zoning is the systematic variation of the two elements with respect to one another. Figure 22 depicts the zoning seen in a microprobe traverse across a blade of a skeletal ilmenite crystal in a pegmatitic diabase phase; Figure 23 shows the variations of Mn and Mg in the crystal. As Mn increases, Mg decreases.

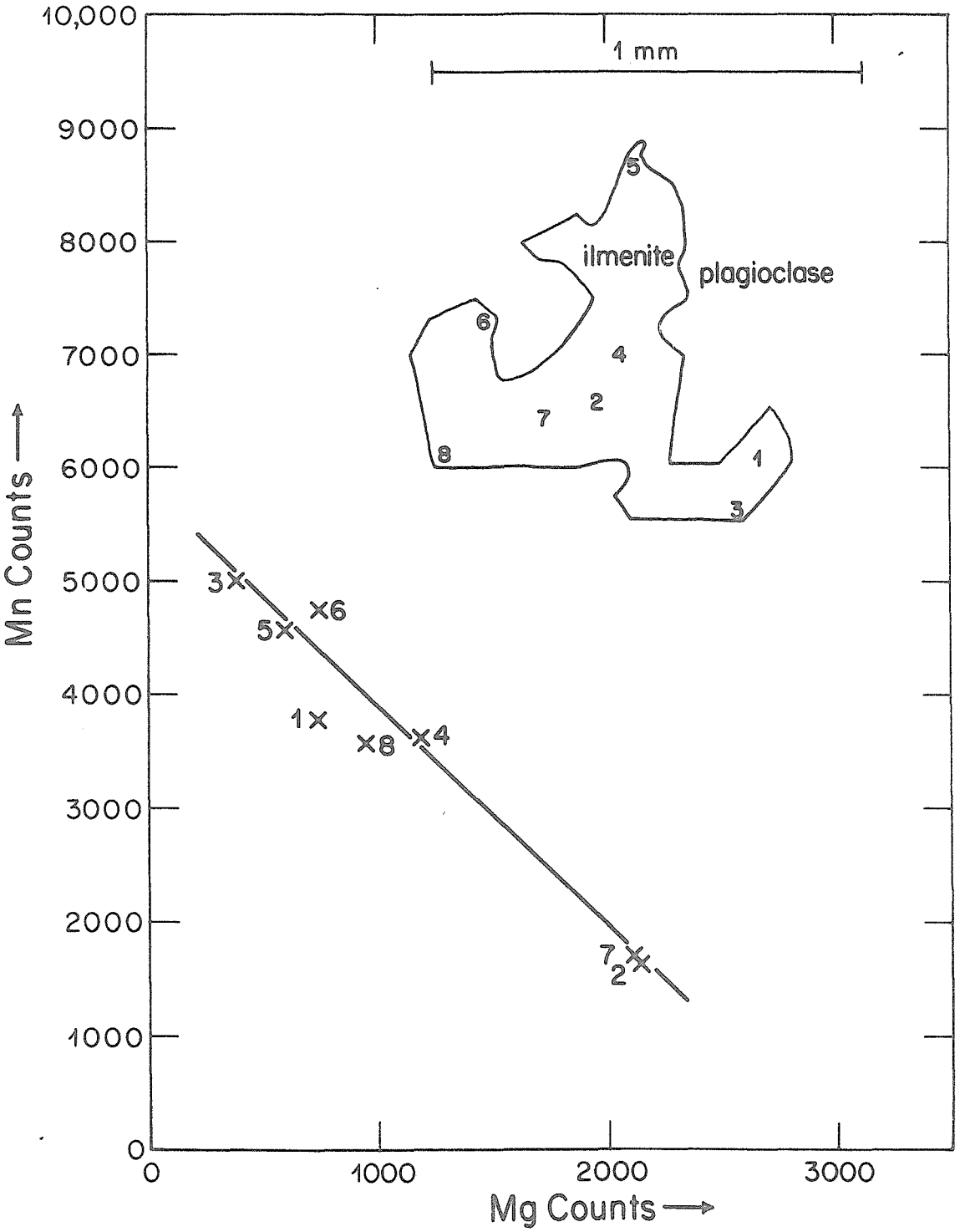

Figure 21. Mg and Mn variations in a zoned ilmenite crystal. Microprobe counts have been corrected for background.

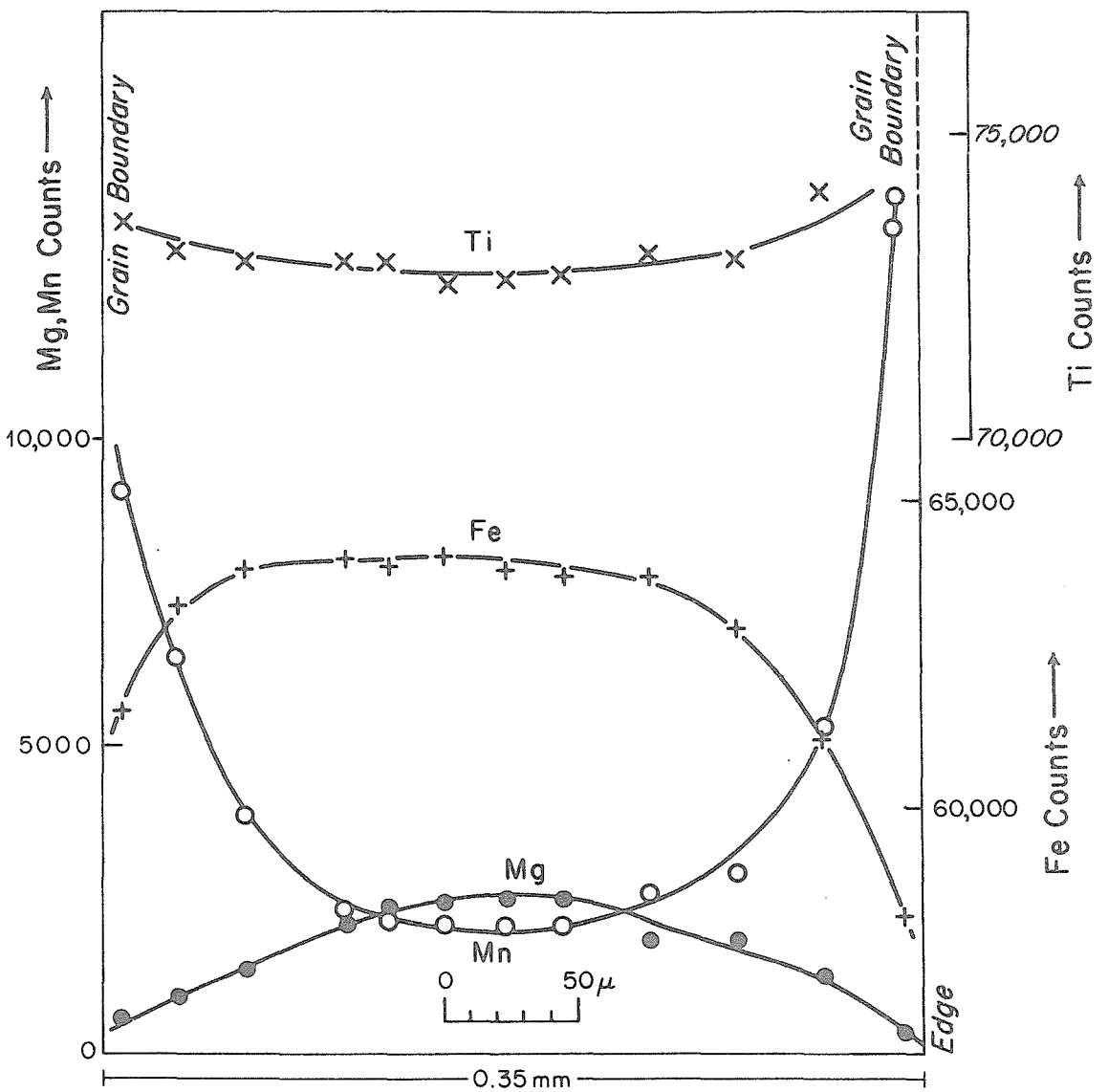

Figure 22. Variations in Ti, Fe, Mg, and Mn shown by a microprobe traverse across an ilmenite blade. Rock Ad163f. Counts corrected for background.

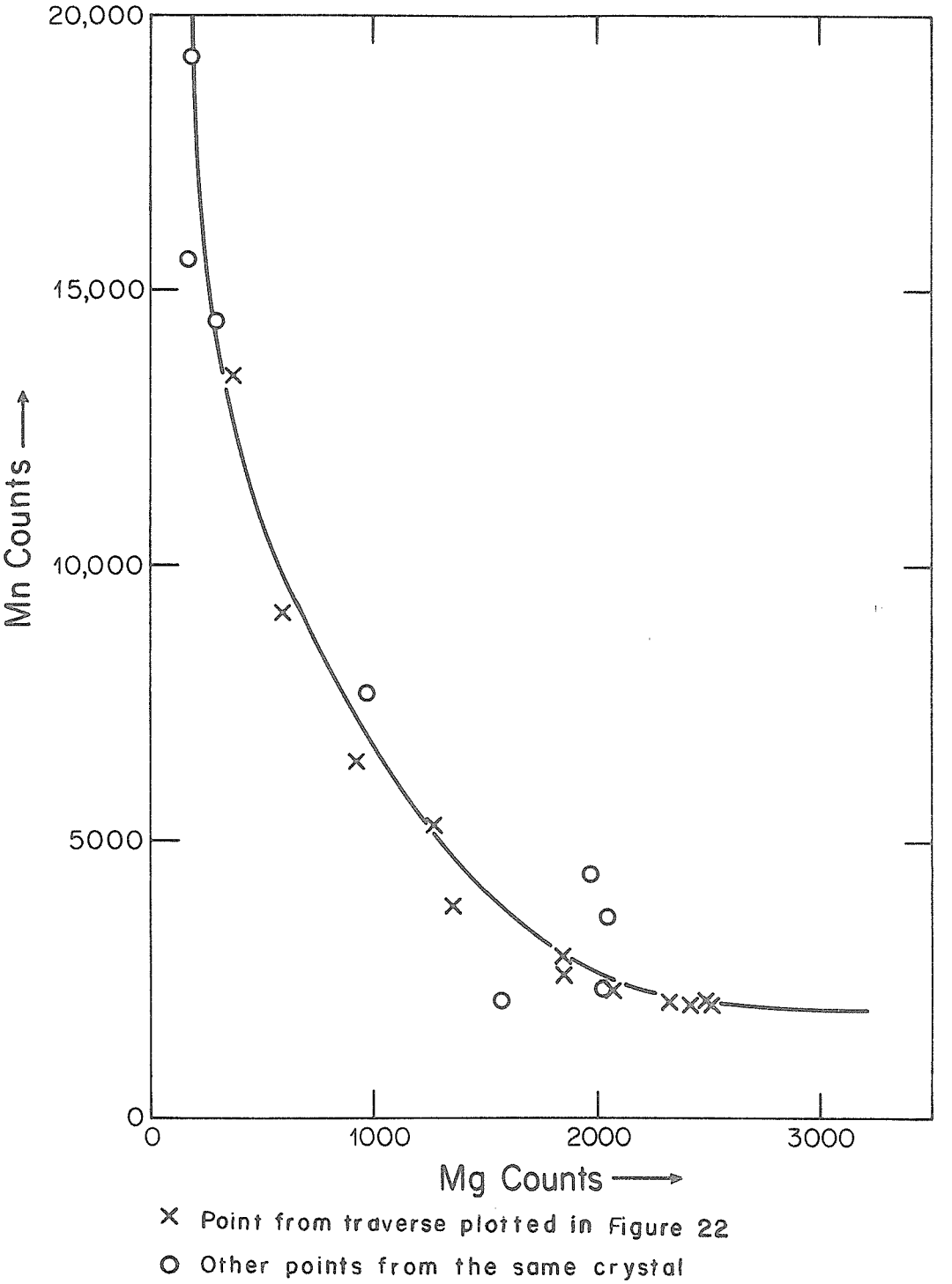

Figure 23. Relationship between Mg and Mn variations in a bladed crystal of ilmenite$_{ss}$ in rock Ad163f. Counts corrected for background.

There are two basic explanations for systematic changes in primary mineral compositions in a differentiated igneous rock suite. The first is that the melt from which the minerals crystallized varied systematically in composition. If the melt became richer in manganese as crystallization proceeded, oxides crystallizing from the melt might also become richer in manganese. The second explanation is that the partition of elements between the growing solid phases and the melt changed as some intensive variable such as temperature, pressure, or oxygen fugacity changed. Temperature is an especially important intensive variable. Because the contribution of the entropy of mixing to the free energy of a phase becomes less important as temperature decreases, typically phases become more "pure" and solid solutions become more restricted in composition with declining crystallization temperatures. This entropy-of-mixing effect alone might explain the decrease of some minor elements in ilmenite$_{ss}$ with decreasing crystallization temperatures.

Changes in the compositions of the melts from which the independent ilmenite$_{ss}$ crystallized may partially explain some of the compositional trends observed. The MgO, MnO, FeO, and Fe_2O_3 contents of chemically analyzed rocks are compared with the compositions of microprobe analyzed ilmenites in these rocks in Table 23. In the analyzed specimens of diabasic rocks, MgO decreases and the ratio MnO/FeO increases with decreasing average crystallization temperatures of pyroxenes (the index minerals).

The increase in the Mn/Fe ratio in the cores of ilmenite$_{ss}$ grains in the later differentiates is probably related to the similar increases in MnO/FeO in the rocks. Since the diabase melt was enriched in manganese with respect to iron during differentiation

TABLE 23

Comparison of Ilmenite and Rock Compositions

	Rock Values					Ilmenite$_{ss}$ Values	
Rock	MgO	MnO	FeO	MnO/FeO	Fe_2O_3	MgO	Mn/Fe^{+2} (calc)
				feldspathic olivine-rich diabase			
Ad36d	9.65	0.09	6.37	.014	1.61	3.37	0.011
				olivine diabase			
Ad36s	8.03	0.15	8.02	.019	2.34	2.62-2.68	.013-.014
Ad163e	6.72	0.15	7.46	.020	3.22	1.06-1.93	.013-.021
				coarse-grained segregation			
Ad163f	4.24	0.22	8.25	.027	3.80	0.11-0.74	.013-.088
				diabase pegmatite			
Ad28	3.26	0.18	5.48	.033	2.08	0.12	.019
				granophyres			
Ad91c	1.47	0.05	2.17	.023	1.82	0.06-0.07	.021-.029
Ar-Gi-Rcgphr 1-6	0.77	0.08	3.30	.024	2.29	0.05-0.06	.023
Ad23h	1.04	0.06	2.15	.028	1.69	0.09-0.14	.019-.027
Ad163	1.39	0.05	2.41	.021	3.68	0.08-0.15	.020-.083

processes in the sill, as shown by the trend of the whole rock MnO/FeO ratios, the last fluid to crystallize in any rock might have been relatively enriched in manganese. Perhaps the ilmenite$_{ss}$ rims in some rocks are so manganese-rich because they crystallized in equilibrium with such a residual melt-fraction. However, it is also possible that the fractionation of manganese between ilmenite$_{ss}$ and the melt increasingly favors the solid phase with declining temperature.

The ratio (MgO in rock/MgO in ilmenite) increases from 3/1 in feldspathic olivine-rich diabase (Ad36d) to 26/1 in diabase pegmatite (Ad28). Although depletion of the magma in Mg with differentiation may partly explain the MgO trend in ilmenites, the data also suggest that the fractionation of magnesium between ilmenite and melt increasingly favors the melt with decreasing temperature.

The systematic decrease of hematite in ilmenite$_{ss}$ with declining temperature does not seem explainable solely on a basis of decreasing oxygen fugacity, though such a trend is indicated for rocks with two oxide phases. The whole rock ferric to ferrous iron ratio is in general higher in the late-crystallizing rocks than in the early-crystallizing ones. The ilmenite-hematite solvus (Carmichael, 1961) occurs at temperatures too low to explain the decrease in hematite in solid solution. The decrease in hematite, like part of the decrease in magnesium, might be an example of the entropy-of-mixing effect.

Summary of Fe-Ti oxide data

Both magnetite-ulvospinel and ilmenite-hematite solid solutions occur in feldspathic olivine-rich diabase and olivine diabase. Diabase pegmatites and granophyric rocks overlying the sill contain only ilmenite-hematite. Lamellae and grains of ilmenite$_{ss}$ have formed from magnetite$_{ss}$ by an exsolution-reaction process. No unreacted magnetite$_{ss}$ was found.

Comparison of the analytical data with the experimental results of Lindsley (1963, p. 64) suggests that:

(1) compositions of ilmenite$_{ss}$ in feldspathic olivine-rich diabase are compatible with oxide equilibration at 1050°C and at 10^{-10} atm. oxygen fugacity, values similar to those proposed for the Skaergaard intrusion;

(2) ilmenite$_{ss}$ compositions in olivine diabase indicate oxide equilibration took place at oxygen fugacities less than 10^{-10} atm;

(3) exsolution-reaction in magnetite$_{ss}$ grains ceased at about 600°C and 10^{-19} atm. oxygen fugacity.

A clear distinction can be made between primary ilmenite$_{ss}$ and that derived by exsolution-reaction from magnetite$_{ss}$ on the basis of microprobe analytical data. The following points were observed:

(1) derived ilmenite$_{ss}$ is consistently lower in calculated hematite and higher in manganese than primary ilmenite$_{ss}$ in the same rock;

(2) distinctive minor element gradients occur at grain boundaries between magnetite$_{ss}$ and "exsolved" ilmenite$_{ss}$. The

gradients arise because minor elements are fractionated between the two phases during "exsolution". With respect to magnetite$_{ss}$, ilmenite$_{ss}$ is enriched in Mg and Mn and depleted in Al and Cr.

When rock samples are arranged in a differentiation sequence, primarily in order of increasing iron enrichment in pyroxenes and olivine, ilmenite$_{ss}$ compositions show the following trends:

(1) calculated hematite decreases;

(2) MgO decreases;

(3) MnO increases.

The trends can be observed in single zoned crystals. They can be explained by changes in melt composition during differentiation and by changes in crystal-melt fractionations. The consistency of the trends supports the differentiation sequence assumed.

WHOLE ROCK CHEMISTRY OF THE SIERRA ANCHA DIABASES

Composition of the Undifferentiated Magma

The uncontaminated diabasic rocks in the Sierra Ancha sill complex are related genetically, as shown by the systematic changes in mineralogy from one rock to another. However, the exact composition of the undifferentiated melt from which the rocks formed is not known. The composition cannot be taken as that of the chilled facies at the sill margins. As described earlier, the chilled facies is altered and commonly contains poikilitic biotite and other secondary minerals. Even if the chilled facies were unaltered, it need not represent a parent melt if differentiation took place before intrusion, as it probably did in the composite Sierra Ancha sill. In fact, studies suggest that the chilled facies of many basaltic intrusions do not represent parent melts (Tilley, Yoder, and Schairer, 1968, p. 457). The rock which may represent the closest approach to the undifferentiated magma of the Sierra Ancha sill complex is the analyzed specimen of olivine diabase, Ad36s (Table 5). It does not seem to be a cumulate rock like the feldspathic olivine-rich diabase, and it is less iron-enriched and less altered than the other normal diabasic rocks studied. However, the magma represented by rock Ad36s may be somewhat more differentiated than the magma which precipitated the cumulate crystals in the feldspathic olivine-rich diabase.

The composition of rock Ad36s is compared with some rock compositions from other sources in Table 24. The compositions of the diabasic rocks cannot be compared strictly to basaltic compositions because there is no certainty that the diabase compositions

TABLE 24

A Sierra Ancha Olivine Diabase Composition together with Representative Basalt Compositions

	1	2	3	4	5
SiO_2	45.47	48.08	48.27	49.36	46.46
TiO_2	3.24	1.17	.89	2.50	3.01
Al_2O_3	17.02	17.22	18.28	13.94	14.64
Fe_2O_3	2.34	1.32	1.04	3.03	3.27
Fe	8.02	8.44	8.31	8.53	9.11
MnO	0.15	0.16	0.17	0.16	0.14
MgO	8.03	8.62	8.96	8.44	8.19
CaO	10.25	11.38	11.32	10.30	10.33
Na_2O	2.66	2.37	2.80	2.13	2.92
K_2O	0.64	0.25	0.14	0.38	0.84
H_2O^+	1.64	1.01	0.15		
H_2O^-	0.49	0.05	0.07		
P_2O_5	0.24	0.10	0.07	0.26	0.37
S	0.12	0.01			
	100.31	100.17	100.47		

1. Olivine diabase, Ad36s, Sierra Ancha sill complex. Analyst, Asari.

2. Marginal chilled olivine gabbro, Skaergaard intrusion (Wager, 1960, Table 2).

3. High-alumina basalt, Medicine Lake Highlands (Yoder and Tilley, 1962, Table 2).

4. Average Hawaiian tholeiitic basalt (Macdonald and Katsura, 1964, Table 9).

5. Average Hawaiian alkali basalt (Macdonald and Katsura, 1964, Table 10).

correspond exactly to those of liquids; removal or addition of material may have taken place by movement either of early-formed crystals or of a residual fluid. However, the comparison of olivine diabase and basalt compositions still indicates the general nature of the Sierra Ancha diabase magma.

There is no indication that the olivine diabases have been contaminated significantly by any constituents from the sedimentary rocks in their immediate environment. Since these sedimentary rocks are high in K and contain little Na, contaminated diabase should have a high K_2O/Na_2O ratio. The ratio in olivine diabase is very similar to that of the average Hawaiian alkali basalt.

The normal olivine diabases have some of the chemical characteristics of alkali olivine basalts, but they are not strongly alkalic. When plotted on the familiar alkali-silica diagram (Figure 24), olivine diabase analyses fall into the alkali basalt field defined for Hawaiian lavas by Macdonald and Katsura (1964, p. 87). The low SiO_2 and high TiO_2 contents of the Sierra Ancha diabase also suggest an alkalic basalt affinity for the magma. The Al_2O_3 contents of olivine diabase analyses (Tables 5 and 6) suggest an affinity between the diabase and high-alumina basalt. Kuno (1960, p. 125) states that, "...except for the high Al_2O_3 content, the high-alumina basalt is chemically intermediate between the tholeiite and the alkali basalt." The aluminum and alkali contents of olivine diabase have been plotted in Figure 24 on a diagram designed by Kuno to illustrate compositional distinctions between tholeiitic, alkalic, and high-alumina basalts of similar silica contents. The points fall into the alkali olivine basalt field near the high-alumina basalt field outlined by Kuno.

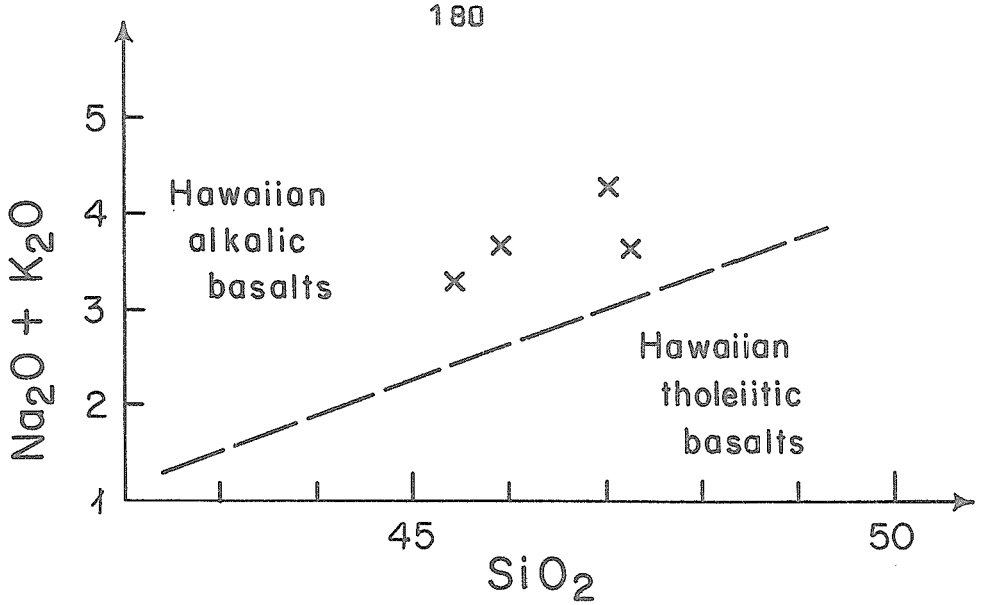

Boundary between Hawaiian basalt types taken from Macdonald and Katsura (1964, Figure 1).

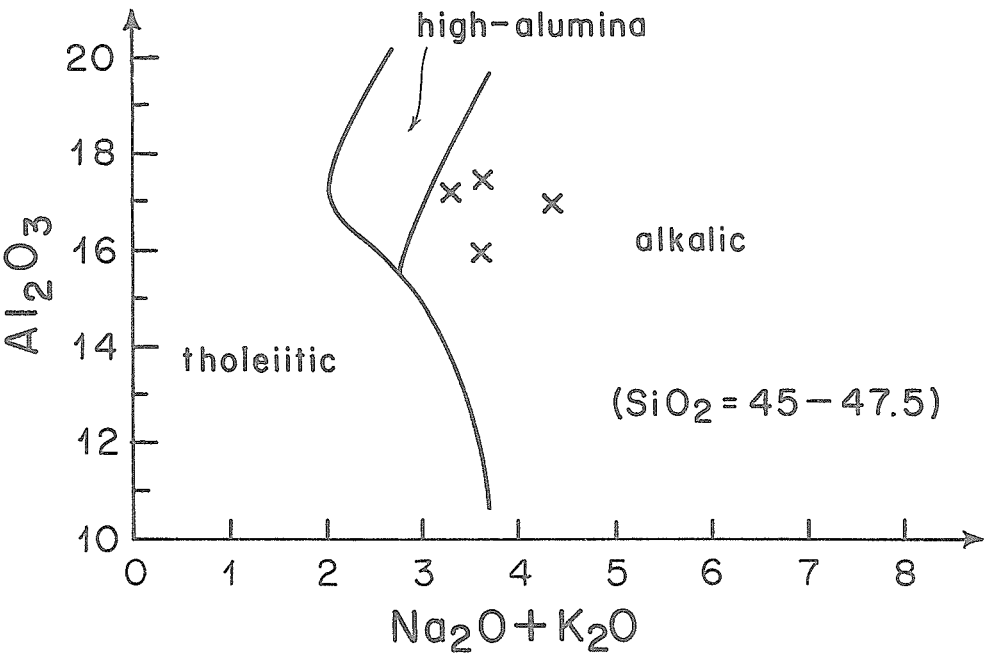

Boundary between basalt types taken from Kuno (1960, Figure 5).

Figure 24. Sierra Ancha olivine diabase compositions compared with compositions of different types of basalts (Analyses from Tables 5 and 6).

Mineralogically, the Sierra Ancha diabase has some tholeiitic characteristics. The important mineralogic distinction between tholeiite and alkali basalt, as emphasized by Tilley (1950), Kuno (1960), Macdonald and Katsura (1964), and others, is that in tholeiites olivine has a reaction relationship with calcium-poor pyroxene, while in alkali basalts olivine and calcic pyroxene crystallize together in equilibrium. In the Sierra Ancha diabases, olivine and augite crystallized together and in equilibrium through almost all the cooling history of the melt. However, in all rocks orthopyroxene was formed, in some cases only in trace quantities, in reaction relationship with olivine late in the crystallization of the melts. The augite is slightly more calcic than that in many tholeiitic rocks but is distinctly less calcic than that in alkalic rocks (Figure 10); the amounts of Al and Ti in the augites are similar to those in the Skaergaard augites. The mineralogy of the diabase is most compatible with that of high-alumina basalt, as Kuno (1960, p. 121) states: "Mineralogically, the high-alumina basalt is intermediate between the tholeiite and alkali basalt."

The preceding discussions indicate that the olivine diabase magma must have been generally intermediate in composition between classical alkali olivine basalt and olivine tholeiite magmas; relatively, it was somewhat high in Al_2O_3. Assigning a specific name to the olivine diabase magma is a rather arbitrary exercise. According to mineralogic criteria it might be called an olivine tholeiite magma. According to some chemical criteria it might be called an alkali olivine basalt magma. If a normative classification scheme like that of Yoder and Tilley (1962) is used, it would be called an olivine tholeiite magma. Since high-alumina basalt as

defined by Kuno (1960) is generally intermediate between alkali olivine basalt and olivine tholeiite, the olivine diabase magma might be called a high-alumina basalt magma.

Crystallization Temperatures Deduced from Experimental Melting Studies

Comparison of olivine diabase compositions with the compositions of basalts studied experimentally yields information on the approximate ranges of crystallization temperatures of major phases in the diabase. Crystallization and melting studies on a wide variety of basaltic rocks have been reported by Yoder and Tilley (1962) and by Tilley, Yoder, and Schairer in a series of articles in Carnegie Institute of Washington Year Books 62 through 66. Most of the experimental work has been done under anhydrous conditions at one atmosphere pressure, and therefore it is not exactly applicable to crystallization problems in the Sierra Ancha sill. The diabase crystallized under load pressures probably less than a kilobar and water pressures less than (or possibly equal to) load pressures. Effects due to the greater load pressure on the diabase magma are insignificant in comparison to the uncertainties introduced because of the unknown water content of the magma. Data reported by Yoder and Tilley (1962, Figures 27, 28, and 29) for basalts of three quite different compositions indicate liquidus temperatures are an average of 70°C lower at one kilobar of water pressure than at zero water pressure. Solidus temperatures are lowered by about 100°C at one kilobar water pressure, and basalt crystallization ranges are greater than in anhydrous experiments. Initial plagioclase crystallization temperatures are depressed more by increasing water pressure than

are temperatures of appearance of olivine or pyroxene. The small amounts of apparently primary biotite and the ubiquitous deuteric effects in the diabase indicate water was present in the magma, so experimental studies can only furnish approximate results for crystallization temperatures in the sill complex.

Experimental results of Tilley, Yoder and Schairer (1963, 1965) indicate that liquidus temperatures of a series of basaltic rocks decrease with bulk rock iron enrichment. For some rock series, plots of liquidus temperatures against the ratio $(FeO+Fe_2O_3)/(MgO+FeO+Fe_2O_3)$ are nearly linear. Their results show that for the same degree of iron enrichment, liquidus temperatures are generally 25°C to 50°C higher for alkali basalts than for tholeiitic basalts. Assuming the diabasic rocks have a character intermediate between alkalic the tholeiitic basalts, comparison of the Sierra Ancha diabases with basalts of similar iron enrichment studied experimentally (Tilley, Yoder, and Schairer, 1965, Figure 1) indicate the following anhydrous liquidus temperatures for analyzed diabases: rock Ad36d, about 1330°C; rock Ad36s, about 1230°C; and rock Ad163e, about 1200°C. Rock Ad36d, feldspathic olivine-rich diabase, is probably a cumulate rock, and its composition may not represent a liquid. The compositions of olivine diabase samples Ad36s and Ad163e probably approximate magmas; rock Ad36s is probably closer to the magma composition than rock Ad163e. The comparison with experimental results suggests that the diabase magma began crystallization near 1200°C.

Olivine and plagioclase begin crystallization within a narrow temperature interval in the high-alumina basalts studied by Tilley, Yoder, and Schairer (1963, Figure 12; 1965, Table 3; 1968, Table 16); either phase may appear on the liquidus. Calcic pyroxene begins

crystallization at a distinctly lower temperature. The crystallization order in the Sierra Ancha sill complex is in accord with the experimental observations. Plagioclase phenocrysts in chilled diabase suggest plagioclase was the earliest mineral to crystallize. Feldspathic olivine-rich diabase contains cumulate plagioclase and olivine crystals and clearly late-forming augite crystals, showing that both plagioclase and olivine began crystallization before augite.

The total range of crystallization temperatures of the Sierra Ancha diabase magma cannot be determined by reference to the experimental studies on basalts because differentiation by fractional crystallization and perhaps by contamination took place in the sill complex; the residual products were rich in alkalis, phosphorus, titanium, and other constituents and were not basaltic in composition. The experimental data do indicate the temperature at which most of the magma must have been solidified. Yoder and Tilley (1962, p. 383) found that the maximum crystallization range in any of the diverse basaltic rocks studied experimentally was 195°C. Field observations on a Hawaiian lava lake (Peck, Wright, and Moore, 1966, p. 637) suggest that the solidus for Hawaiian tholeiitic basalt is about 980°C. The experimental and field observations suggest that the early, primary minerals -- augite, hypersthene, olivine, calcic plagioclase, and Fe-Ti oxides -- in olivine diabase must have chiefly crystallized above 1000°C if the magma was anhydrous. The water content of the diabase melt probably increased as crystallization proceded and vapor pressure might have reached the load pressure near the solidus; some textural features in diabase pegmatite might be interpreted as once having been vugs. Under a kilobar of water pressure, an appreciable percentage of magma might have been present until temperatures as low as 900°C were approached during cooling. The late primary

minerals in apparent equilibrium with chlorite must have crystallized at temperatures considerably below 900°C; however, these minerals constitute only a small fraction of the quantity of diabasic rock in the sill complex.

Whole Rock Differentiation Trends

The whole rock differentiation trend in the Sierra Ancha sill complex shows characteristics seen in other mafic igneous rock suites -- first, enrichment in iron followed by enrichment in alkalis. The trend can be seen when rock compositions are plotted on an A-M-F diagram (Figure 25). In olivine-rich and olivine diabasic rocks the trend is towards iron enrichment; in coarse-grained segregations and diabase pegmatite, the trend is toward alkali enrichment.

Iron enrichment in the Sierra Ancha rocks is relatively slight in comparison to the Skaergaard and many other tholeiitic rock suites. Osborn (1959) and others have shown that degree of iron enrichment during differentiation should depend upon the oxygen fugacity of the melt; melts with higher oxygen fugacities should differentiate to less iron-enriched residual products, because of the earlier and more abundant precipitation of iron oxides. The crystallization of late biotite and chlorite and the ubiquitous deuteric alteration in the Sierra Ancha rocks suggest that the diabase magma was wetter than the relatively dry Skaergaard magma. However, data from $ilmenite_{ss}$ nevertheless indicate similar oxygen fugacities in the two magmas during crystallization. Perhaps the diabase magma became relatively more enriched in alkalis at a lower iron enrichment than the Skaergaard magma simply because initially the diabase magma was more alkalic. The Sierra Ancha A-M-F trend

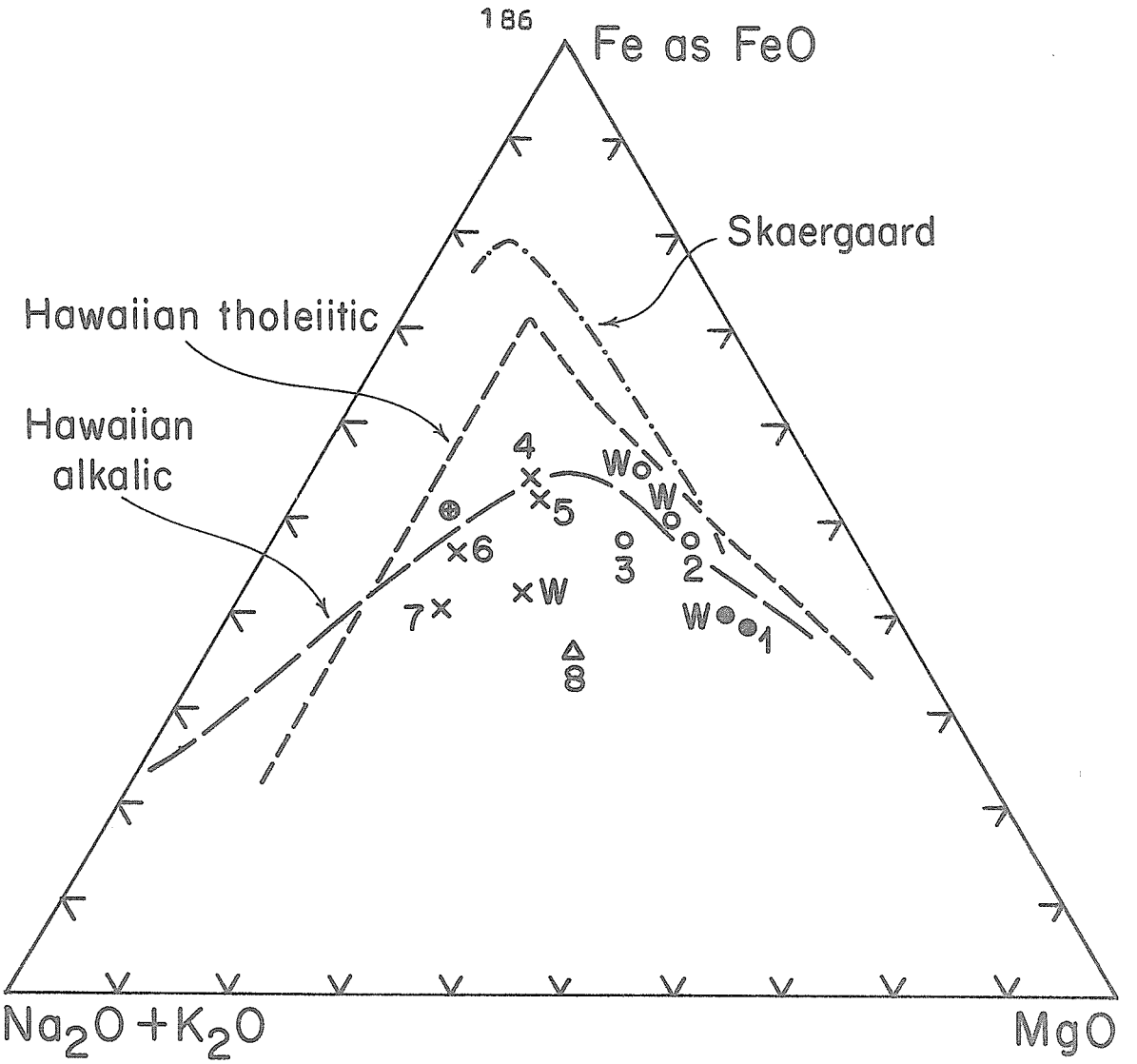

- ● Feldspathic olivine-rich diabase (1, Ad 36d)
- ○ Olivine diabase (2, Ad 36s; 3, Ad 163e)
- × Coarse-grained segregations and diabase pegmatite (4, Ad 163f; 5, Ad 98b1; 6, Ad 98b2; 7, Ad 28)
- △ Albite diabase (8, Ad 141d)
- ⊕ Quartz diabase
- W Williams (see Table 6)

Figure 25. AFM diagram for Sierra Ancha diabasic rocks, together with Hawaiian trends (MacDonald and Katsura, 1964) and the Skaergaard trend (Wager, 1960).

is quite similar to the early portion of the A-M-F trend for Hawaiian alkalic rocks (Figure 25).

Though the Sierra Ancha whole rock compositions indicate only rather limited differentiation towards alkali-rich magnesium-poor end products, the residual fluids in the pegmatites were considerably more differentiated. As emphasized in the discussions of petrography and mineralogy, the pegmatites contain a late assemblage of iron-enriched calcic pyroxene and chlorite and alkali feldspar which crystallized in disequilibrium with early-formed augite and calcic plagioclase. The bulk rock pegmatite compositions reflect both the early and late assemblages. If the residual fluids in the pegmatites had separated and crystallized apart from the early-formed minerals, rocks might have formed with compositions as alkalic and magnesium-poor as the more differentiated Hawaiian alkalic rocks indicated in Figure 25.

Major element variations in diabasic rock types are shown in Figure 26, a silica variation diagram. SiO_2 is about the same in feldspathic olivine-rich diabase and olivine diabase, but it is slightly greater in diabase pegmatite. The high aluminum in feldspathic olivine-rich diabase may reflect the accumulation of early-crystallizing calcic plagioclase in these rocks. CaO is about the same in all the normal diabasic rocks in the sill. The MgO and FeO trends evident from the A-F-M diagram (Figure 25) are masked in the silica variation diagram, because SiO_2 did not vary significantly in the early stages of differentiation.

The composition of the analyzed sample of quartz diabase, Ad286c, is similar in many respects to the compositions of the diabase pegmatites. On the silica variation diagram most of the oxides in the sample plot on trends defined by the other diabasic

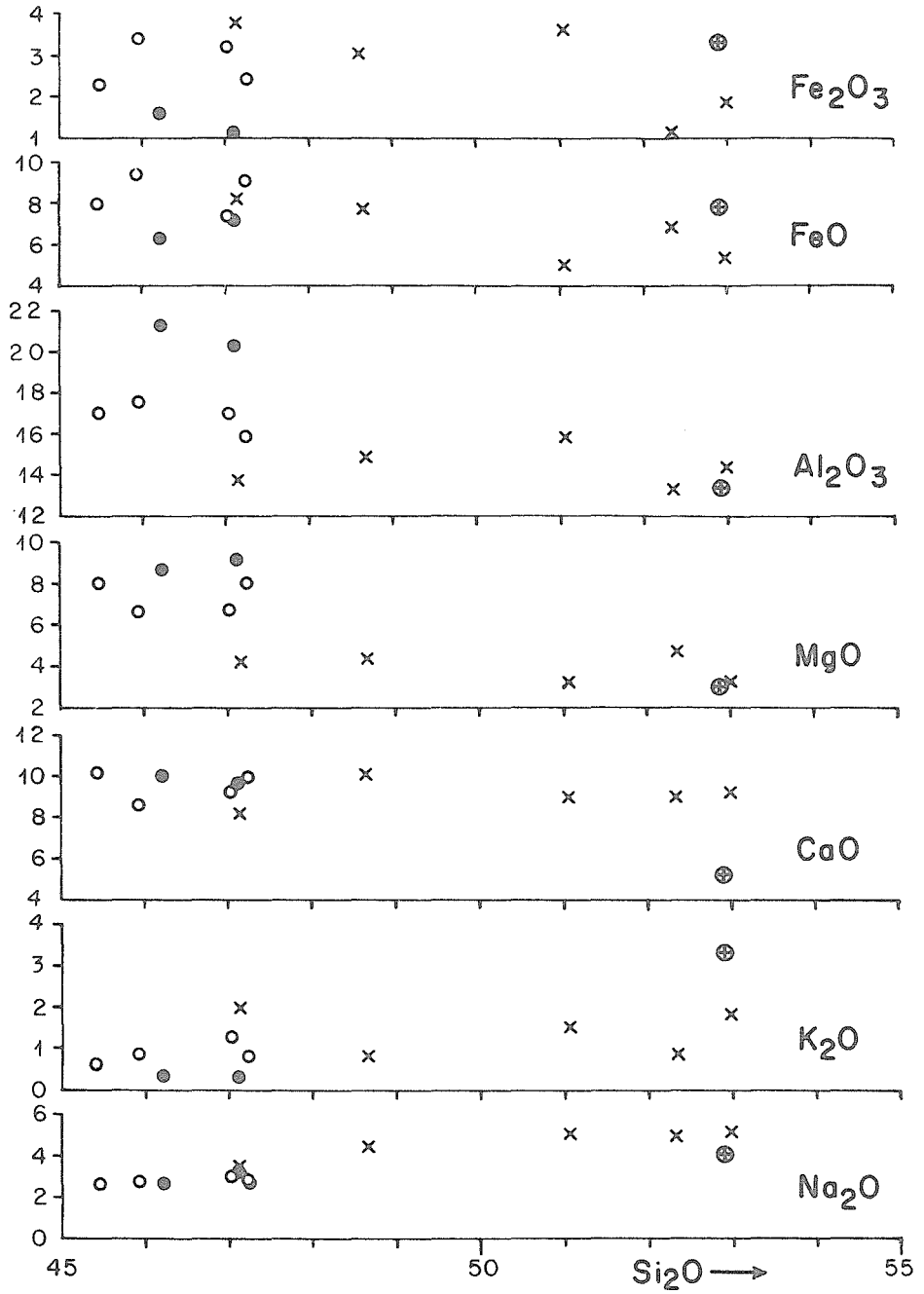

Figure 26. Silica variation diagram for diabasic rocks. Analyses in Tables 5 and 6 .

rocks. If more specimens of quartz diabase had been analyzed, it is likely that a range of compositions approaching those of the normal diabase rocks would have been found. For these reasons the quartz diabase in part appears to be a differentiation product of the diabase magma. However, there are significant compositional differences between the analyzed sample of quartz diabase and the diabase pegmatites. It is lower in Ca, higher in K, and has a much higher K/Na ratio. The K concentration in the quartz diabase sample can reasonably be ascribed to contamination by the K-rich sedimentary rocks in the Dripping Spring Quartzite. The compositional data, like the field evidence, suggest that the quartz diabase may be a hybrid rock, a contaminated diabase differentiate.

Trace element concentrations (Table 5) show systematic variations with the degree of differentiation of rocks in the sill complex. Concentrations of Co, Ni, Sr, and Cu follow the trends noted by Cherukupalli (1959, pp. 45-47). The concentrations of Co, Ni, and Sr are highest in the most magnesian rock type in the sill, feldspathic olivine-rich diabase, and decrease systematically in the more differentiated rocks. Presumably the Co and Ni trends are caused by the fractionation of these elements into olivine. The Sr trend could be explained if the element were preferentially incorporated into calcic plagioclase, as suggested by Brooks (1968). Copper shows no enrichment trend; it must not be strongly fractionated either into the melt or into any major phase. As mentioned by Williams (1957, p. 69), Cr is fractionated into augite. It is also concentrated in magnetite. The high Cr abundance in the least-differentiated rock analyzed with abundant magnetite and augite, sample Ad36s, is explained by the fractionation of Cr into these two minerals. Zr, Yb, Ga, and Y apparently are not incorporated into

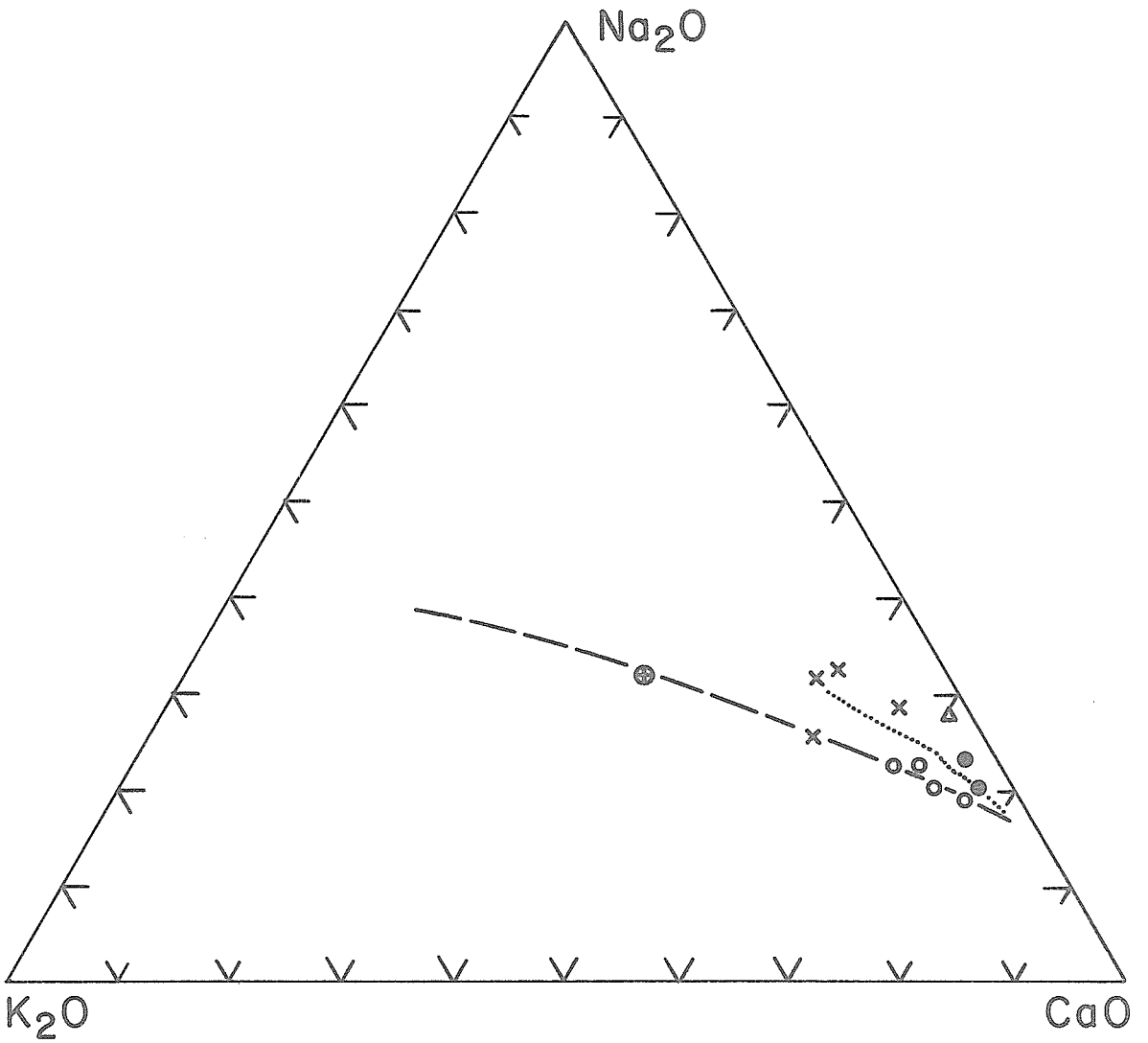

—— Trend for Keweenawan intrusive bodies (unpublished compilation)

····· Trend for estimated Skaergaard liquids (Wager, 1960)

- ● Feldspathic olivine-rich diabase
- ○ Olivine diabase
- × Coarse grained segregations and diabase pegmatite
- △ Albite diabase
- ⊛ Quartz diabase

Figure 27. Na_2O-K_2O-CaO diagram for Sierra Ancha diabasic rocks. (Analyses from Tables 5 and 6.)

any of the early-crystallizing phases, and they are enriched in the pegmatites, the residual products of the crystallizing magma.

Some of the whole rock compositions in the Sierra Ancha sill complex may have been affected by processes other than those occurring in normal magmatic igneous differentiation. These processes are reflected by the anomalous position of the albite diabase composition plotted on the A-M-F diagram (Figure 25); it is unlikely that albite diabase was formed by the same processes giving rise to the igneous trends plotted on the diagram. The unusual compositions of the albite diabase and some of the analyzed diabase pegmatites are particularly noticeable when the Sierra Ancha rock analyses are plotted in an Na_2O-K_2O-CaO diagram (Figure 27). Trends for several normal igneous rock suites are plotted for comparison. The albite diabase is very low in potassium and does not plot near the igneous rock trends. Several of the diabase pegmatite samples have higher Na_2O/K_2O ratios than would be expected from the trends.

Potassium loss from diabase rocks may have taken place during crystallization and alteration under deuteric conditions. The similarity of late-stage mineral assemblages in albite diabase, deuterically-altered diabase, and diabase pegmatite was noted in the discussions of the petrography and mineralogy of the diabasic rocks. Late primary minerals in diabase pegmatite and secondary minerals in altered diabase probably formed under the same deuteric conditions. Deuteric conditions favoring potassium loss may be part of the normal sequence of magmatic events in the crystallization of diabases. In describing the albitic "ultimate magmatic residues" of tholeiitic sills in a discussion of diabase differentiation, Walker (1957, p. 11) states: "...these veins are almost potash-free...

elimination of potash must have taken place previously and evidence of this is found in the poikilitic biotite in the basaltic chilled phases of sills in the Palisadan and Karroo provinces." In a discussion of the mineralogy of spilites, Battey (1956, p. 101) remarks: "There certainly seems to be a range of conditions under which chlorite is stable, rather than biotite, in the presence of potash, and where the potash possesses a migratory tendency..." Some of the diabasic rocks in the Sierra Ancha sill complex may have lost potassium as a part of the sequence of events occurring during deuteric recrystallization.

Relation of Bulk Rock Trends to Mineral Trends

Bulk rock chemical trends can be correlated with mineralogical changes for a more complete understanding of the differentiation of the diabase magma. Some bulk rock chemical parameters and mineral data for selected rocks are summarized in Table 25. These data can be compared with the calcic pyroxene data summarized in Figure 10 and the bulk rock data plotted on the A-M-F diagram (Figure 26). The information can be used both to characterize the differentiation trend and to establish the differentiation sequence of rocks within the sill.

The feldspathic olivine-rich and olivine diabase which make up the bulk of the sill display a differentiation trend characterized by only moderate iron enrichment. The experimental studies of melting relations of basaltic rocks discussed earlier show that the major minerals in these rocks must have crystallized almost completely within the temperature interval 1250°C to 900°C. The minerals present show definite compositional trends that can be correlated

TABLE 25

Summary of Selected Parameters Related to Differentiation of the Diabase

Sample	(FeO+Fe2O3) ÷ (FeO + Fe2O3+ MgO) in rock	Normative Plagioclase	Plagioclase Present	Fe/(Fe+Mg) in augite	Fe/(Fe+Mg) in orthopyroxene	Fe/(Fe+Mg) in olivine	Fe/(Fe+Mg) in calcic pyroxene	Fe/(Fe+Mg) in chlorite	MgO/MnO in primary ilmenite	R2O3in primary ilmenite
				Feldspathic olivine-rich diabase						
Ad36d	0.45	An_{67}	An_{70-58}	.22-.26	.23-.25	.26-.30	n.p.	n.p.	8.4	.44
Ad36p	n.a.	n.a.	n.a.	.22-.25	.25-.29	.28-.31	n.p.	n.p.	8.7	.53
				Olivine diabase						
Ad36s	0.56	An_{58}	An_{67-52}	.23-.27	.32-.34	.30-.39	n.p.	n.p.	5.1	.19-.20
Ad163g	n.a.	n.a.	An_{72-39}	.25-.28	.31-.36	.35-.39	n.p.	n.p.	3.0-6.3	.14-.21
Ad36a	n.a.	n.a.	n.a.	.28-.31	.41-.56	.42-.44	n.p.	n.p.	.55-1.7	.10-.14
Ad163e	0.62	An_{51}	An_{63-18}	.27-.31	.34-.56	.43-.45	n.p.	n.p.	1.3-3.8	.08-.12
Ad163c	n.a.	n.a.	An_{56-18}	.29-.31	.33-.45	.40-.46	n.p.	n.p.	n.a.	n.a.
Ad163b	n.a.	n.a.	$An_{?-16}$	.32-.33	.40-.49	a.	n.p.	n.p.	.28-1.5	.10-.14
				Quartz diabase						
Ad163a	n.a.	n.a.	a.	.36-.37	n.p.	n.p.	n.p.	n.p.	.02-.11	.01-.05
Ad286c	0.79	An_{19}	a.	n.a.	n.p.	n.p.	n.p.	n.p.	n.a.	n.a.
				Coarse-grained segregation						
Ad163f	0.74	An_{33}	An_{46-An_2}	.28	n.p.	n.p.	n.p.	n.p.	.03-1.3	.03-.05
				Diabase pegmatite						
Ad98b1	0.76	An_{37}	An_{1-0}	n.a.	n.p.	n.p.	.46-.55	.78-.82	n.a.	n.a.
Ad98b2	0.74	An_{29}								
Ad28	0.70	An_{20}	An_{1-0}	.35	n.p.	n.p.	.62-.73	n.a.	.16	.04
				Albite diabase						
Ad141d	0.54	An_{24}	An_{1-0}	n.p.	n.p.	n.p.	.24-.37	n.a.	n.a.	n.a.

a. altered
n.p. not present
n.a. not analyzed

both with increasing iron enrichment of the melt from which they formed and with decreasing crystallization temperatures. Ferromagnesian silicates become more iron-rich. Partitions between phases generally increase and minor element concentrations in them generally decrease in the more differentiated rocks, as would be expected with decreasing crystallization temperatures; manganese, because of its similarity to iron, is the only minor element which notably increases in the major silicate phases with decreasing temperature. Mineral zoning is generally greater in more-differentiated diabase, again a characteristic of lower temperature crystallization.

The coarse-grained segregations and pegmatites, comprising only a few percent of the diabasic rocks, display a differentiation trend characterized by alkali enrichment. The late ferromagnesian minerals in them are also iron-enriched. These rocks contain two generations of minerals -- early minerals typical of the primary phases in olivine diabase, and late relatively low-temperature minerals. These late minerals, such as calcic pyroxene, chlorite, sphene, prehnite, and albite, must have formed at temperatures lower than 650°C. Apatite is the only mineral present apparently stable both in the early and late diabase assemblage. The rocks relatively enriched in alkalis contain a strikingly different, much lower-temperature assemblage than is present in unaltered olivine diabase.

Conclusions as to the diabase differentiation sequence within the sill complex can be drawn from the mutually consistent bulk rock and mineral trends. The earliest and highest-temperature differentiate of the parent diabase magma is the feldspathic olivine-rich diabase forming the layer just below the center of the complex. The sample of olivine diabase, Ad36a, from below the olivine-rich zone in

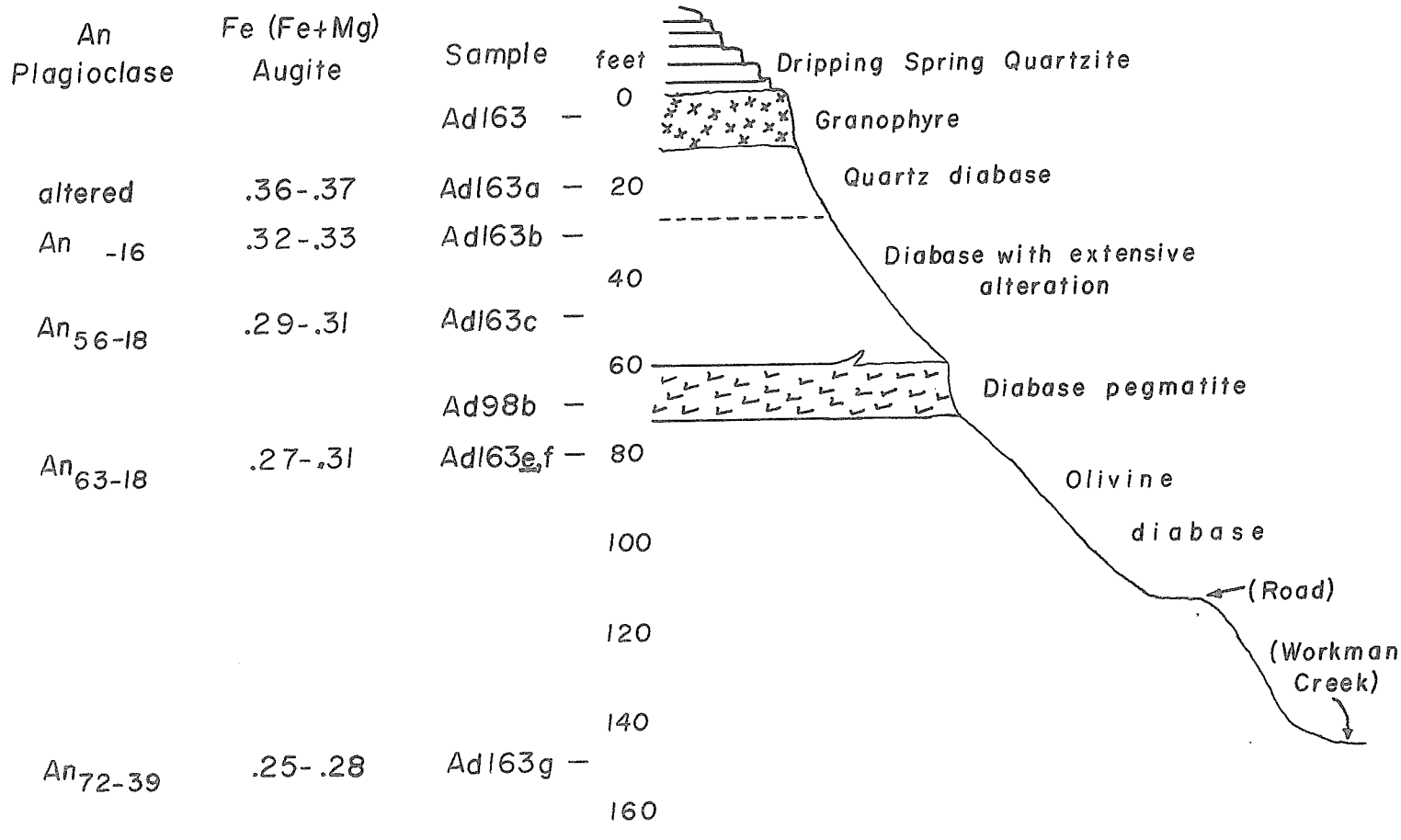

Figure 28. Sample locations in a section through the upper part of the sill complex near Workman Creek, together with mineral compositional data for some of the diabase samples. Other mineral and bulk rock compositional trends for the samples are summarized in Table 25.

Reynolds Creek is more differentiated than much of the olivine diabase above the zone. Whole rock diabase analyses reported by Williams (1957) indicate that the same situation occurs in Pocket Creek. These facts are consistent with the hypothesis of multiple intrusion suggested earlier. The Ad163 series comes from the best-exposed section of the upper part of the diabase sill (Figure 28). Mineral compositional trends within this section indicate that in the upper part of the sill crystallization generally progressed upwards; the olivine diabase at the top of the sill crystallized later than the olivine diabase below it.

The quartz diabase is probably a hybrid rock, a diabase differentiate contaminated by material from the Dripping Spring Quartzite. The composition of augite in one sample, Ad163a, falls at the iron-enriched end of the trend defined in the pyroxene quadrilateral by augites in olivine and olivine-rich diabase. Some of the bulk rock chemical characteristics of the quartz diabase also suggest it is a diabase differentiate enriched in alkalis and in Fe with respect to Mg. However, the K/Na ratio of the analyzed sample, Ad286c, suggests that contamination has occurred. The field relations of the rock make contamination suspect. Contamination could account for the mineralogical differences between the quartz diabase and the diabase pegmatites; no quartz is found in pegmatites which are removed from obvious sedimentary rock sources of contamination.

PROCESSES OF DIABASE DIFFERENTIATION

The feldspathic olivine-rich diabase, the olivine diabases with different degrees of iron enrichment, the coarse-grained segregations, and the diabase pegmatites are probably all differentiation products of one magma. Differentiation may have taken place by several mechanisms.

Differentiation may have begun by crystal settling in an unexposed magma chamber below the Sierra Ancha. The feldspathic olivine-rich diabase may represent magma enriched in early-formed olivine and plagioclase crystals which settled towards the bottom of the chamber, while the olivine diabase may have formed from magma from the upper part of the chamber and may have been partly depleted in the two minerals. The arguments that the feldspathic olivine-rich diabase was intruded into the sill complex as a separate magma pulse have been summarized previously.

Some differentiation of olivine diabase took place after the magma had been intruded into position in the sill complex. This differentiation is reflected by parts of the bulk chemical and mineral trends. The best-exposed olivine diabase section studied which displays a systematic differentiation trend is the section at the sill roof shown in Figure 28. The mineral trends demonstrate that in this section diabase nearer the sill roof is more differentiated than that lower down.

The processes producing differentiation within the Sierra Ancha sill are somewhat obscure. The differentiation processes advocated for other diabase sills include crystal settling (Walker, 1957, pp. 6-9), diffusion of volatiles, alkalis, and some associated elements independently of crystallization (Wilshire, 1967, pp. 149-

151; Hamilton, 1965, pp. 63-68), and diffusion and liquid circulation at a crystallization front (Hess, 1960, pp. 187-190). As in most diabase sills, evidence of long-range crystal settling within the sill complex is lacking; no igneous layering was observed. "Diffusion in response to pressure and temperature gradients" ('liquid fractionation' - Hamilton, 1965, p. 65) seems unlikely to have caused appreciable differentiation. The Sierra Ancha sill is too thin to have had large pressure differences within it and also must have crystallized within a few hundred years (see later discussion of cooling times). In addition, there is no reason to believe that, before the sill had substantially crystallized, the magma coexisted with a separate vapor phase which might have transferred alkalis. The most reasonable explanation remaining is that of Hess (1960, p. 187). He suggested that in diabase sills crystallization at a roughly-defined front might deplete the magma in components of the early-forming phases and enrich it in Na, K, Fe, and other "late" elements. Diffusion caused by the resulting concentration gradients in the magma might then act to enrich the melt away from the front in alkalis, iron and associated elements and to deplete it in Mg and other elements fixed in the crystallizing phases. Magma convection might aid the process by removing both the heat of crystallization and the alkalis and associated elements away from the front. This process apparently acts efficiently enough to produce the almost monomineralic layers in layered gabbroic intrusives (Hess, 1960, p. 113; Wager and Brown, 1967, p. 554). The differentiation sequence in the Sierra Ancha diabase section shown in Figure 28 is evidence that, at least locally, crystallization proceeded upwards towards the sill roof. The fractionation process suggested by Hess may have been largely

responsible for producing the observed differentiation trends here and elsewhere in the sill. Short-range crystal settling above the upward-moving crystallization front might also have been an effective fractionation agent.

The coarse-grained segregations and diabase pegmatites may contain the latest apparently uncontaminated differentiates in the sill complex. They have counterparts in many other diabase sills throughout the world. Like their counterparts, they probably formed in the manner suggested by Walker (1953). When the sill had almost crystallized, rifts and low pressure areas locally formed, probably in part by contraction fracturing. The residual liquids moved into these zones and crystallized to form the segregations and pegmatites.

DEUTERIC ALTERATION, ALBITE DIABASE, DIABASE PEGMATITE AND THE SPILITE PROBLEM

The origin of spilites is one of the classic problems of igneous petrology. Spilites are volcanic rocks of basaltic composition which are characterized by "the very high anorthite content of the normative feldspar relative to the modal feldspar, the apparent stable coexistence of chlorite and clinopyroxene, and the unusual compatibility of albite and clinopyroxene " (Yoder, 1967, p. 269). Theories for the origin of spilites include hypotheses that they are crystallization products of uncontaminated, hydrous basaltic magmas, that they were formed by basaltic magmas contaminated with sea water, and that they were formed by autometamorphism of basaltic rocks. These and other hypotheses are summarized by Amstutz (1967) and by Turner and Verhoogen (1960, pp. 258-272). In the Sierra Ancha sill complex there is a complete transition between rocks of basaltic composition and a basaltic mineralogy to those with a spilitic mineralogy. The sill rocks provide an unusual opportunity to study problems of the genesis of spilitic mineral assemblages.

Spilitic Assemblages Formed by Deuteric Alteration

Deuteric alteration is ubiquitous in the diabasic rocks. The petrography and mineralogy of the altered rocks have been discussed in previous sections. The mineral assemblage formed by the most intense deuteric alteration includes calcic pyroxene, chlorite, albite, prehnite, sphene, apatite, clays, and white mica, and minor amphibole and calcite. Albite diabase, apparently formed by complete deuteric recrystallization of normal diabase, is locally

present near the sill roof; it consists primarily of albite, calcic pyroxene, sphene, chlorite and apatite. Albite in albite diabase is more sodic than Ab_{99}. Calcic pyroxene compositions in altered and albite diabase range from $Ca_{49}Mg_{46}Fs_4$ to $Ca_{47}Mg_{33}Fs_{20}$. Deuteric chlorite in a sample of altered diabase had an Fe/Mg ratio of about 2/3. These minerals formed by recrystallization and replacement of calcic plagioclase, augite, olivine, magnetite, and other primary minerals. Deuteric reactions, or autometamorphism, produced spilitic mineral assemblages.

Chemical changes may have occurred locally when rocks were recrystallized under deuteric conditions. The albite diabase has the lowest K_2O value and the lowest K/Na ratio of any analyzed rock in the sill complex. It also has the highest CaO content and lowest Al_2O_3 content of the diabasic rock suite.

The sequence of deuteric reactions observed in the diabase may have taken place over a wide temperature range. In rocks with only moderate deuteric alteration, hornblende is a common alteration product of augite. In intensely altered rocks, hornblende is rare and augite is replaced by aggregates of chlorite and calcic pyroxene. In a series of experiments designed to determine the pressure-temperature range of formation of spilitic rocks, Yoder (1967, pp. 277-279) observed that amphibole-bearing assemblages formed at higher temperatures than chlorite-clinopyroxene assemblages. He suggested that a rock of appropriate basaltic composition would be represented by a gabbroic mineral assemblage at high temperatures, an amphibole-bearing assemblage at intermediate temperatures, and a spilitic assemblage at lower temperatures. The deuteric reaction sequence in the Sierra Ancha diabase may be analogous to the experimental sequence observed by Yoder. With

decreasing temperature, hornblende may have been the first deuteric reaction product of augite. Under favorable conditions, further deuteric reactions may have occurred at lower temperatures and led to the local development of chlorite-calcic pyroxene from hornblende.

Spilitic Assemblages in Diabase Pegmatites

The late-stage minerals common in diabase pegmatites include calcic pyroxene, chlorite, albite K feldspar, prehnite, sphene, and apatite. These minerals form a spilitic assemblage identical to that in intensely altered diabase and albite diabase with the addition of K feldspar. In diabase pegmatite, however, much of the chlorite and calcic pyroxene seems primary, not deuteric; textural evidence indicates that the two phases in part crystallized from a late-stage liquid and did not form by replacement of other minerals. The iron-rich compositions of both minerals are consistent with the theory that they formed from a residual liquid and not by recrystallization of other solid phases. Textural evidence indicates that the albite at least in part formed as a reaction product of more calcic plagioclase and by exsolution from alkali feldspar; there is no good evidence for the crystallization of primary albite. However, in diabase pegmatite two of the important spilite minerals, calcic pyroxene and chlorite, appear to have crystallized from a residual liquid. The iron-enriched liquid from which the two minerals crystallized may have been a hydrothermal fluid; however, the possibility that it was a silicate melt cannot be excluded.

Temperatures of Formation of the Spilitic Minerals

The spilitic mineral assemblages formed at much lower temperatures than the early primary minerals in the diabase. The assemblage common to the deuterically-altered diabase, albite diabase, and diabase pegmatite includes chlorite, calcic pyroxene, albite, sphene, apatite, and prehnite. The stability ranges of chlorite and prehnite provide the most useful information on the temperatures involved.

Chlorite must have formed at temperatures below about 650°C. Turnock (1960) determined that Fe-chlorite was stable only to about 600°C at one kilobar water pressure. Yoder (1952) found the upper stability limit of Mg-chlorite to be about 700°C at one kilobar water pressure. The field of chlorite stability is not restricted significantly by the presence of either albite or calcic pyroxene. The experimental investigations of Yoder (1967) on spilites are of great relevance to the assemblages studied here. He found that the stability of albite plus chlorite was limited by the breakdown of chlorite. In the presence of diopside, and at one kilobar water pressure, Mg-chlorite was found to be stable up to about 650°C, almost as high as its decomposition temperature.

The stability range of prehnite ($Ca_2Al(AlSi_3O_{10})(OH)_2$) seems more restricted than that of chlorite, and therefore it is potentially a more useful temperature indicator. Fyfe, Turner, and Verhoogen (1958, p. 168) could synthesize prehnite only between 300°C and 400°C at three kilobars water pressure; they theorized that its temperature stability range decreased markedly at lower pressures. If the experiments are conclusive, they imply that the formation of albite and prehnite in the diabasic rocks took place below 400°C. This temper-

ature is compatible with the temperature range indicated for cation exchange between K feldspar and albite in diabase pegmatite.

Implications of the Spilitic Mineral Assemblages Developed in the Diabase

The sequence of deuteric reactions in the Sierra Ancha diabase shows how a spilitic mineral assemblage can be produced by autometamorphism of a basaltic assemblage. The deuteric reactions probably took place so readily in the diabasic rocks because of water in the magma. As discussed later, the magma may have absorbed water from the surrounding sedimentary rocks. If the water came at least in part from the country rock, the deuteric minerals might be said to have formed because of the interaction of the magma with its intrusive environment. However, there is no good evidence that the external contribution of any substances besides H_2O was necessary for formation of the spilitic assemblages.

GRANOPHYRES

Introduction

Igneous-appearing crystalline rocks of syenitic and granitic composition locally occur in impressively thick lenses near and at the roof of the Sierra Ancha sill complex. In places along the ridge north of Reynolds Creek and on the slopes of Grantham Peak, these lenses reach a maximum thickness of 150 to 200 feet. Texturally, the crystalline rocks forming them appear to be igneous. They are composed chiefly of alkali feldspar with subordinate quartz and mafic minerals. Micrographic intergrowths of quartz and feldspar are well-developed in some of the rocks and are present in almost all of them, so these rocks can be loosely termed "granophyres." They are generally massive and show no relict sedimentary structures; some have flow textures. Locally, the crystalline masses have discordant, intrusive contacts with overlying sedimentary strata, and they commonly contain rotated and displaced sedimentary rock xenoliths.

These apparently igneous rocks are believed to be products of the interaction of diabase magma with sedimentary rocks from the Dripping Spring Quartzite. The compositions of some of the granophyres are nearly identical to those of adjacent, distinctively potassium-rich sedimentary rocks, while the compositions of others bear witness to a chemical interaction between diabase and the sedimentary rocks. Texturally and mineralogically, some of the massive crystalline rocks are identical to recrystallized rocks of obvious sedimentary heritage which occur as thin lamellae parallel to bedding planes interlayered with only slightly recrystallized sedimentary

rocks and as concordant layers a few feet thick at contacts between diabase and overlying sedimentary rocks.

Previous studies of the granophyric rocks

Most previous workers in the Sierra Ancha were aware only of the relatively small thicknesses of K feldspar-rich crystalline rocks formed at the roof of the sill in the immediate vicinity of uranium deposits. These occurrences were first discussed by Williams (1957, pp. 73-74), who noted that the sedimentary rocks immediately above the diabase are "...locally altered to coarse-grained, igneous-looking rocks" displaying features indicating small-scale mobilization. The same observations were made by Neuerburg and Granger (1960) and Granger and Raup (1959; 1964); these authors refer to the igneous-appearing leucocratic rock as "hornfels." Both Williams (1957) and Granger and Raup (1959) discuss briefly the problems of chemical exchange between the diabase and the overlying strata. Their observations were chiefly confined to the Workman Creek drainage, where the diabase is in contact with the gray unit of the upper member of the Dripping Spring Quartzite. The lenses of igneous-looking K feldspar-rich rocks here are commonly less than 5 feet thick and have a maximum thickness of about 30 feet.

The occurrence of large masses of granophyre north of Reynolds Creek was first noted by Silver (1960); he reported U-Pb isotopic data on zircons from several granophyre samples. Shride (1967) briefly described part of the granophyre mass north of Reynolds Creek. He suggested (pp. 60-61) that parts of the granophyre mass represent contaminated differentiates of the diabase and

that other parts "...formed in place by the soaking of feldspathic rocks with magmatic fluids."

The association of diabase with igneous-looking rocks of granitic composition and questionable origin is not unique to the Sierra Ancha. Similar associations are common in the Karroo diabase province of South Africa, where, according to Walker and Poldervaart (1949, p. 682), "...small intrusions of basalt magma without superheat have produced significant bodies of igneous-looking rocks of granitic composition by transfusion and sometimes mobilization of the adjacent sediments." The Karroo studies of Walker and Poldervaart (1942; 1949) and Mountain (1944; 1960) are particularly relevant to problems in the Sierra Ancha and will be cited later. There are many associations of granophyre and diabase in other basaltic provinces in which the granophyres are apparently of igneous origin.

Outline of the discussion of the granophyres

An understanding of the origin of the granophyric rocks must be based not only on their petrography and chemistry but also on their field relations to the diabase and sedimentary rocks. These topics will be discussed separately but will be related to one another throughout the text and in the conclusions. First, the textures and mineralogy of the recrystallized but layered and obviously metasedimentary rocks will be described. Next, the main types of granophyric rocks, their distribution, and their field relations will be discussed. Their mineralogy and chemistry will be treated in subsequent sections. Finally, the origin of the granophyres and the processes which formed them will be considered.

Mineralogy and Textures of Layered Metasedimentary Rocks

Rocks of the potassic upper member of the Dripping Spring Quartzite overlying the diabase display all gradations from apparently unmetamorphosed sedimentary rocks to recrystallized, laminated rocks which texturally and mineralogically resemble some of the massive granophyres. These rocks are of interest not only because of their relevance to the problem of the origin of the granophyres but also because of the unusual nature of the recrystallization. Rather than leading to an equigranular texture, metamorphic recrystallization in these rocks led to the development of intricate quartz and feldspar intergrowths.

Recrystallization of rocks in the upper member of the Dripping Spring Quartzite

Recrystallization phenomena in the sedimentary rocks overlying the sill are particularly well-developed at the contact between diabase and the upper member of the Dripping Spring Quartzite between Reynolds and Workman Creeks. Recrystallization textures are more evident in rocks of the black facies than in other rocks in the formation. In the first stages of recrystallization of these rocks, the average grain size did not change but tiny spots of biotite appeared scattered throughout the sedimentary matrix. The next stage of recrystallization occurred within distances varying from a few feet to about twenty feet from the sill roof. Some lamellae are recrystallized to intricate quartz-feldspar intergrowths (Plates 19 and 20) while adjacent lamellae appear unrecrystallized. In extreme cases some lamellae recrystallized to quartz-feldspar intergrowths with

PLATE 19

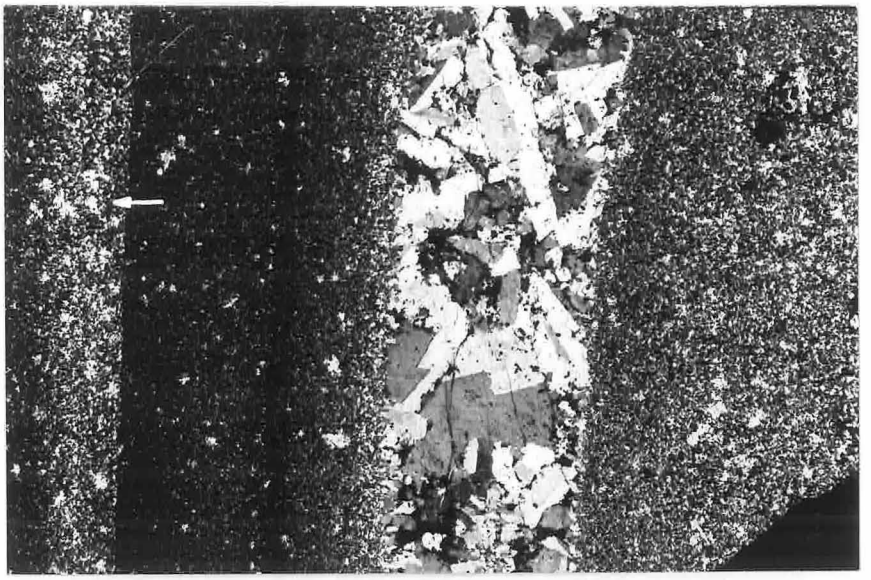

Rock Ad152d. 18x27 mm. Crossed nicols. Laminated, recrystallized metasedimentary rock from the black facies near Workman Creek. Note that the selective recrystallization leads to an apparent lit-par-lit texture.

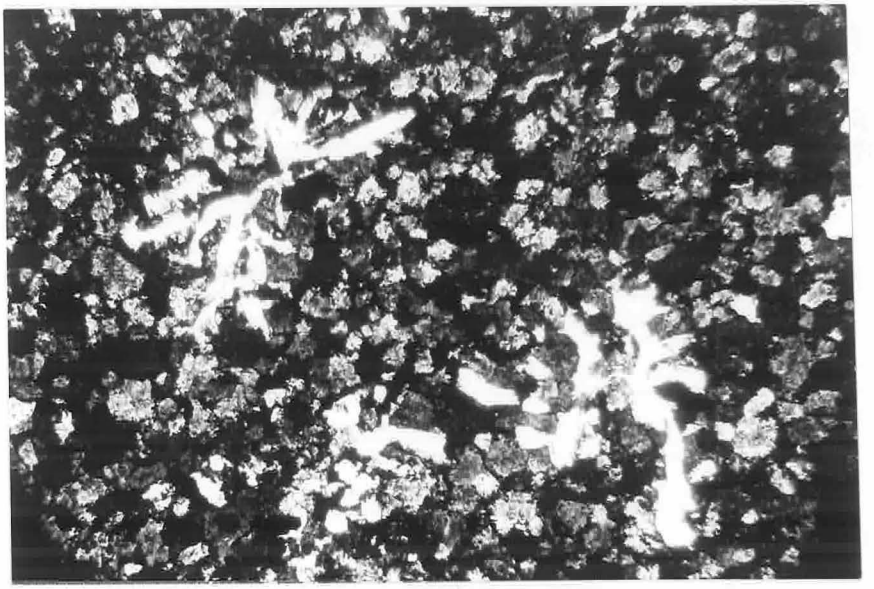

Rock Ad152d. 2x3 mm. Crossed nicols. Close-up of area (see arrow) in far left of photo above. Note the irregular shapes of the two large, optically-continuous quartz grains in a groundmass of finer-grained alkali feldspar.

PLATE 20

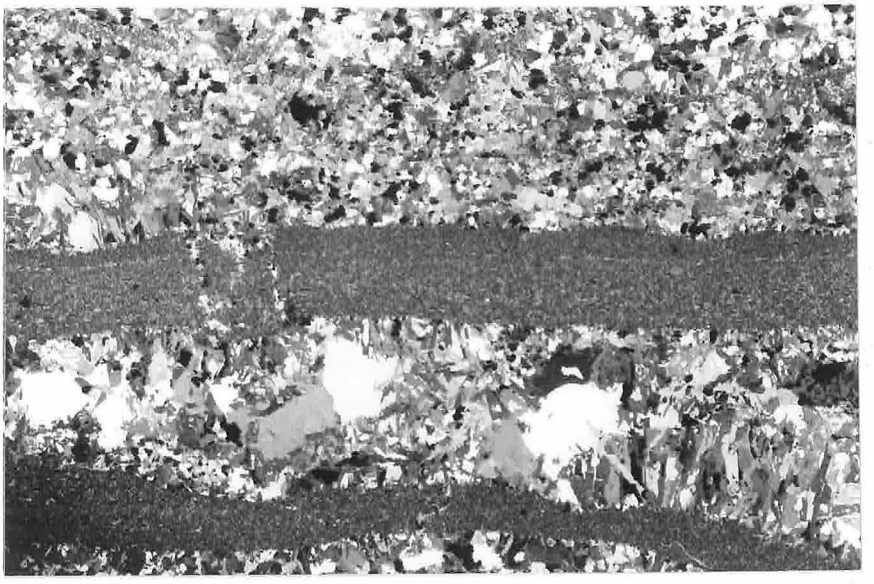

Rock Ad61. 18x27 mm. Crossed nicols. A layered metasedimentary rock with coarsely recrystallized lamellae.

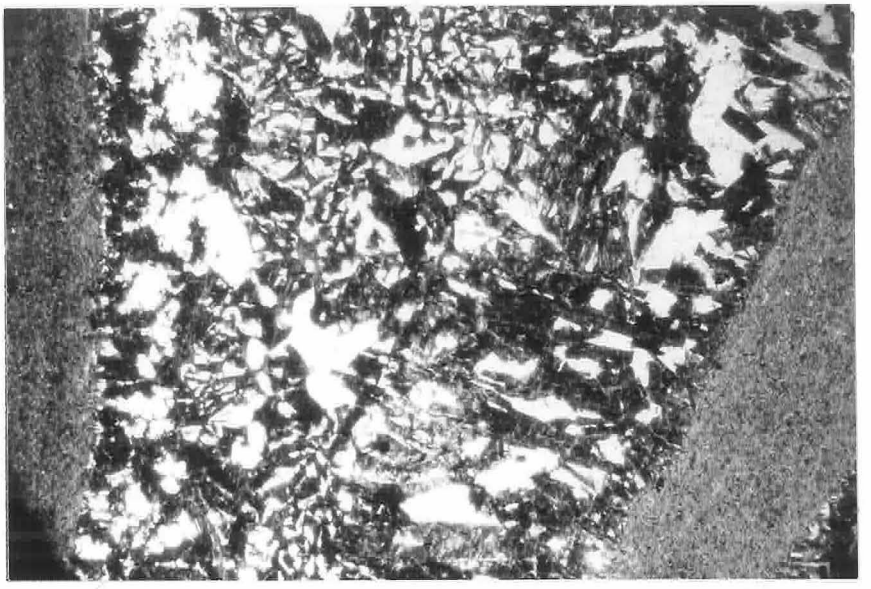

Rock Ad61. 6x9 mm. Close-up of coarse-grained, recrystallized lamella shown above. Clear grains are quartz, dark grains are turbid ("dusty") K feldspar. Note micrographic intergrowths.

an average grain size of 1 to 2 mm; they contrast sharply with adjacent lamellae with an average grain size of a few hundredths of a millimeter. Rocks with lamellae of such contrasting grain size appear to have the lit-par-lit texture commented on by Granger and Raup (1964, p. 54) and others. Recrystallization begins in some of the finer layers about scattered nuclei; in these layers small ovoids of coarse-grained feldspar crystals are scattered through a fine-grained matrix. In a few places near the contact the recrystallized material forms small, transgressive "dikes" a few inches in maximum thickness. At the contact in many places is a layer a few feet in thickness of completely recrystallized rock with an average grain size of a few millimeters.

The most abundant mineral in both the recrystallized and unrecrystallized rocks is K feldspar. It displays certain alteration features which characteristically occur in all the potassium-rich rocks near the sill roof. Most K feldspar grains are so heavily clouded with fine inclusions that they appear dusty brown and nearly opaque in thin section. Some grains contain clear areas. The negative 2V of the clear feldspar is highly variable, ranging from about 10^{o} to 70^{o}; this feldspar is unaltered, though commonly it is partly unmixed. The low 2V's indicate much of it is still sanidine. The negative 2V of the clouded feldspar is always large; this feldspar was apparently clouded during a period of pervasive, low temperature alteration which resulted in inversion to a low temperature form. Microprobe analyses discussed later indicate that clear feldspar is invariably richer in sodium than dusty feldspar in the same grains.

Other minerals in the recrystallized rocks include quartz, biotite, calcic pyroxene, opaques (mostly sulfides?), sphene, apatite, and allanite. The quartz occurs in intricately shaped grains interstitial to and in micrographic intergrowths with K feldspar. Biotite occurs in flakes pleochroic from light yellow-brown to deep red-brown. Calcic pyroxene is less abundant than biotite in recrystallized rocks of the black facies; it characteristically occurs in grains clear in thin section and with maximum diameters of a tenth of a millimeter or less. Sphene occurs in anhedral, irregularly-shaped grains several tenths of a millimeter in maximum diameter. Albite occurs in quantities of a percent or two in small, interstitial grains. Only traces of allanite were observed. An analysis and approximate mode of one recrystallized rock from the black facies, specimen Ad125r, are given in Table 26.

Other units of the upper member recrystallize to essentially the same assemblages as the black facies of the gray unit. The most noticeable difference is that they commonly contain more calcic pyroxene than biotite. Recrystallized quartz grains have the same, intricate shapes in these rocks. Though selective recrystallization of certain lamellae is not as striking a feature in these rocks as in the darker metasedimentary rocks, some excellent examples have been observed. These coarse lamellae are very similar to some of the fine-grained, pyroxene-bearing granophyric rocks in the large crystalline masses.

The unusual nature of the recrystallization of the metasedimentary rocks in the Dripping Spring Quartzite near the sill roof may be related to several contributing factors. First, the rocks

were probably wet; a separate vapor phase, probably chiefly H_2O, was present near the sill roof, as indicated by the occurrence of miarolitic cavities in massive granophyric rocks. Second, the average grain size of the layers was very small (a few hundredths of a millimeter). Third, many of the sedimentary rocks have compositions close to those in the simple system $KAlSi_3O_8$-SiO_2. Finally, thermal calculations and field evidence (discussed later) suggest that temperatures in some of the rocks were near minimum melting temperatures.

There are several possible reasons why some lamellae recrystallized more readily than adjacent ones. Lamellae containing fair amounts of both quartz and K feldspar seemingly recrystallized more readily than those consisting predominately of either mineral, though this conclusion is difficult to document quantitatively because of the very small grain size of the unrecrystallized lamellae. The compositions of such layers would be closer to minimum melting compositions. Differences in initial grain size, permeability, or porosity might also be responsible for the differences in recrystallized fabrics.

Metamorphism of the Mescal Limestone

Visible metamorphic effects are more widespread in the Mescal Limestone than in the Dripping Spring Quartzite. While metamorphic effects are generally almost undetectable in the Dripping Spring rocks some tens of feet away from the sill complex, Mescal Limestone several hundred feet above the diabase is recrystallized to new mineral assemblages. Locally, metamorphism by the diabase created asbestos deposits which have

been extensively prospected. Shride (1967, pp. 63-64) discussed the serpentine and other metamorphic minerals in the carbonate rocks.

The most common metamorphic assemblage observed in the Mescal is diopside-calcite. Layers of tremolite were formed in the plate of sedimentary rock included in the sill between Parker and Pocket Creeks. About one mile southeast of McFadden Peak at the upper contact of the sill where diabase is intruded directly against the Mescal, the assemblage garnet-calcite is found. Thin veins of asbestos are present in the Mescal Limestone in many localities; the occurrences of asbestos are of some significance, as they indicate the presence of water during the metamorphism of the sedimentary rocks by the diabase.

Summary of metamorphic effects in the obviously metasedimentary rocks

The most important observations on the crystalline rocks of obviously metasedimentary character are:

(1) large-scale recrystallization of layered sedimentary rocks in the Dripping Spring Quartzite occurs only within ten to twenty feet of the roof of the sill complex;

(2) recrystallized rocks contain an identical mineral assemblage to that in many of the massive granophyric rocks -- K-rich feldspar, quartz, biotite, calcic pyroxene, sphene, albite, and opaques (chiefly sulfides ?);

(3) some of these rocks have igneous-looking textures;

(4) an important feature of these textures is that intricately-shaped quartz grains are intergrown with K-rich feldspar, in some cases forming a true micrographic texture;

(5) certain thin layers recrystallized much more readily than others.

Some of these observations constitute important evidence leading to the conclusion that the massive granophyric rocks were in part derived from the overlying sedimentary rocks of the Dripping Spring Quartzite.

Igneous-looking Crystalline Rocks

The thickest lenses of massive crystalline rocks of granitic and syenitic composition crop out on the ridge north of Reynolds Creek and on the slopes of Grantham Peak. Two much smaller lenses crop out in the Workman Creek drainage. The sizes and shapes of the large lenses are shown in detail in Plates 4 and 5. The granophyric rocks in the lenses are light-colored and can be readily distinguished in field from the darker-colored diabasic rocks. These light-colored crystalline rocks are massive and more resistant than the sedimentary rocks and much more resistant than the diabase; they form cliffs and large, bouldery outcrops on steep slopes. North of Reynolds Creek the thick lenses of granophyric rocks form projecting points, while the thinner sections are dissected by drainage gullies.

All the granophyric rocks consist primarily of alkali feldspar. Like the obviously metasedimentary rocks, many of them also contain quartz, biotite, calcic pyroxene, sphene, albite, and sulfide minerals. In addition, some contain hornblende, ilmenite, and minor calcic plagioclase. Analyses, modes, and norms of typical examples of the granophyric rocks are presented in Table 26.

TABLE 26

Analyses of the Granophyric Rocks

	10	11	12	13	14[2]	15	16	17	18	19
	Ad241 aplite dike in diabase	Ad91c pyroxene granophyre	Ad91b aplitic pyroxene granophyre	Ad163 pyroxene-biotite granophyre	Ad285 biotite granophyre	Ar-Ci-Rcghr 1-6 hornblende granophyre	Ad23h aplitic pyroxene granophyre	Ad230 aplite	Ad125r metasedimentary rock Dripping Spring Q.	Ad125h sedimentary rock Dripping Spring Q.
Wet Chemical Analyses[1]										
SiO_2	64.03	61.80	63.76	59.90	62.59	62.71	66.57	69.40	66.73	74.75
TiO_2	0.82	1.32	1.10	1.12	1.26	0.87	0.87	0.70	1.31	0.52
Al_2O_3	15.29	15.03	14.67	14.96	14.44	15.03	13.64	12.28	12.78	11.56
Fe_2O_3	0.49	1.82	1.83	3.68	1.17	2.29	1.69	0.70	2.92	0.46
FeO	1.55	2.17	0.71	2.41	4.48	3.30	2.15	1.30	1.26	0.14
MnO	0.06	0.05	0.01	0.05	0.06	0.08	0.06	0.03	0.07	0.01
MgO	1.22	1.47	0.98	1.39	1.42	0.77	1.04	1.08	0.54	0.53
CaO	2.79	3.23	1.89	1.44	1.58	1.50	2.13	2.75	0.61	0.50
Na_2O	2.63	4.24	1.33	2.14	2.01	3.06	1.37	0.47	0.43	0.13
K_2O	9.50	7.11	11.07	9.83	8.21	8.06	9.31	9.65	10.54	9.60
H_2O^+	0.77	1.03	0.97	1.38	1.32	1.16	0.88	0.63	1.13	0.72
H_2O^-	0.59	0.49	0.46	0.64	0.56	0.70	0.60	0.45	0.59	0.65
P_2O_5	0.17	0.28	0.07	0.13	0.18	0.16	0.10	0.08	0.10	0.07
S	0.06	0.09	1.09	1.60	0.76	0.02	0.27	0.16	0.93	0.00
Total	99.97	100.12	99.94	100.67	100.04	99.71	100.78	99.68	99.94	99.64
Approximate Modes										
Quartz	12	7	15	9	15	15	20	35	20(?)	20(?)
Alkali Feldspar	70	70	75	70	60	60	65	55	70(?)	65(?)
Calcic Plagioclase	–	–	–	–	4	10	trace	–	–	–
Calcic Pyroxene	14	15	2	6	1	–	8	7	–	–
Hornblende	–	(?)	–	–	–	7	–	–	–	–
Biotite	–	3(?)	–	7	15	4	trace	–	4	–
Sphene	3	1	3	2	–	–	–	1	2	trace
Opaques	½	3	2	5	4	2	4	trace	5	6
Apatite	trace	trace	–	–	trace	trace	–	–	–	–
Zircon	1	trace	–	trace	–	trace	trace	–	–	–
Chlorite	–	(?)	–	1	–	trace	2	–	–	6
Weight % Norm[3]										
Quartz	7.01	4.42	(10.12)	6.01	12.95	9.70	18.43	24.84	22.56	36.21
Albite	22.57	36.38	(11.42)	18.36	17.32	26.50	11.68	4.03	3.70	1.19
Anorthite	1.88	0.99	(1.38)	2.21	6.24	3.55	3.60	2.94	1.85	2.06
Orthoclase	56.93	42.61	(66.41)	58.89	49.41	48.68	55.41	57.84	63.42	57.73
Diopside	8.70	8.41	–	2.21	0.59	2.50	5.09	6.61	–	–
Hypersthene	–	–	–	2.48	7.39	3.60	0.86	–	1.37	1.34
Magnetite	0.72	2.68	–	–	1.64	3.39	2.47	1.03	–	–
Ilmenite	1.58	2.54	–	1.43	2.44	1.70	1.66	1.35	0.62	0.32
Hematite	–	–	–	3.73	–	–	–	–	2.97	0.47
Pyrite	0.11	0.17	–	3.04	1.43	0.04	0.51	0.30	1.77	–
Wollastonite	0.08	1.11	–	–	–	–	–	0.83	–	–
Apatite	0.41	0.67	(0.17)	0.31	0.41	0.34	0.24	0.19	0.24	0.17
Corundum	–	–	–	–	–	–	–	–	–	0.22
Sphene	–	–	–	0.94	–	–	–	–	0.40	–
Rutile	–	–	–	–	–	–	–	–	0.84	0.36
Total	99.99	99.99		99.60	99.82	100.00	99.94	99.96	99.77	100.00
Fe/(Fe+Mg) in normative silicates	0.21	0.04	–	0	0.46	0.53	0.16	0.10	0	0

[1] Analyst: T. Asari.
[2] Average of two duplicate analyses; see appendix.
[3] Calculation procedures in appendix. Norm for sample Ad91b cannot be calculated because of too much sulfur.

TABLE 26(continued)

Spectographic Analyses* (ppm)

	10 Ad241	11 Ad91c	12 Ad91b	13 Ad163	14 Ad285	15 Ar-Gi-Rcgphr 1-6	16 Ad23h	17 Ad230	18 Ad125r	19 Ad125h
Ba	1500	500	530	470	550	250	530	580	610	1600
Co	44	20	70	36	52	11	28	52	120	150
Cr	n.d.	7	65	61	60	n.d.	49	31	68	48
Cu	4	13	73	56	25	7	30	110	40	63
Ga	25	22	19	17	21	20	17	17	17	13
Mn	480	500	87	390	450	690	530	230	380	n.d.
Ni	19	n.d.	60	40	17	n.d.	11	120	45	5
Sc	21	20	24	20	36	<20	22	38	22	n.d.
Sr	39	58	13	60	83	92	110	220	10	10
V	45	40	110	98	110	27	81	210	93	42
Y	240	97	110	66	160	110	93	50	140	98
Yb	15	8	7	6	9	7	6	3	6	5
Zr	1300	390	380	320	420	280	450	86	260	200
Pb	n.d.	n.d.	n.d.	n.d.	n.d.	n.d.	n.d.	n.d.	n.d.	50
Nb	31	n.a.	n.a.	n.a.	27	n.a.	n.a.	20	22	30

n.a. not analyzed
n.d. not detected
* analyst: E. Bingham

10. Ad241. Granophyric dike in diabase near sill roof. Roadcut on Workman Creek road. SW¼S29, T6N, R14E.

11. Ad91c. Granophyre, lower part of lens. North side of ridge north of Reynolds Creek.

12. Ad91b. Granophyre, upper part of lens. Same location as Ad91c.

13. Ad163. Granophyre, typical of lens. North side Workman Creek.

14. Ad285. Granophyre, typical of lens, on north slope of Grantham Peak. NW¼S7, T5N, R14E.

15. Ar-Gi-Rcgphr 1-6. Granophyre, lower part of lens. NE¼S18, T6N, R14E.

16. Ad23h. Granophyre, upper part of lens. Same location as Ar-Gi-Rcgphr 1-6.

17. Ad230. Dike in sedimentary rocks above Ad23h and Ar-Gi-Rcgphr 1-6.

18. Ad125r. Metasiltstone. Black facies, gray unit, upper Dripping Spring Quartzite.

19. Ad125h. Almost unmetamorphosed, altered tuff(?). Buff unit, upper Dripping Spring Quartzite.

Sample locations shown on Plate 4.

Types of granophyric rocks

The rocks can be classified as pyroxene, biotite, or hornblende granophyres depending on the predominate ferromagnesian silicate present. No granophyric rocks contain all three of the mafic phases in textural equilibrium. Rocks containing both calcic pyroxene and biotite are common, but many rocks contain predominately or solely one of the two; in some rocks textural evidence is preserved of calcic pyroxene reacting to form biotite. Rocks containing both calcic pyroxene and hornblende are not uncommon, but in most of these, textural evidence indicates that the pyroxene was unstable and partly reacted to form hornblende. Rocks containing the pair hornblende-biotite are less common; textural evidence suggests that the two minerals were not in equilibrium in many of the cases where they both occur. Examples of analyses of pyroxene, biotite, and hornblende granophyre are given in Table 26 by rocks Ad91c, Ad285, and Ar-Gi-Rcgphr 1-6, respectively; rock Ad163 in Table 26 is an example of a rock with major amounts of both pyroxene and biotite.

The grain sizes of the leucocratic, crystalline rocks are variable and provide another basis for classification. The granophyres typically have an average grain size of 2 to 3 mm. Coarser facies present locally in small quantity have average grain sizes of up to 10 mm. At many places near overlying sedimentary rocks the granophyric rocks are more leucocratic and distinctly finer-grained, with an average grain size of less than 0.5 mm. These finer-grained rocks are characterized by subhedral feldspar laths with interstitial quartz; granophyric intergrowths are only poorly developed in them. These rocks are here called "aplites", though

PLATE 21

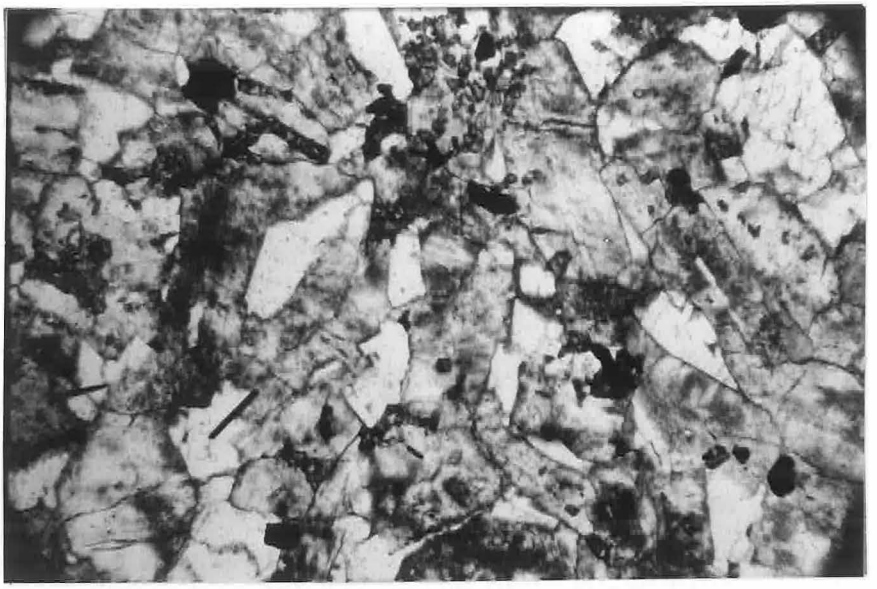

Rock Ad32h. 2x3 mm. Analyzed specimen of aplitic pyroxene granophyre. Subhedral alkali feldspar grains are slightly "dusty" especially near margins. Quartz is interstitial. Pyroxene and ilmenite are also present.

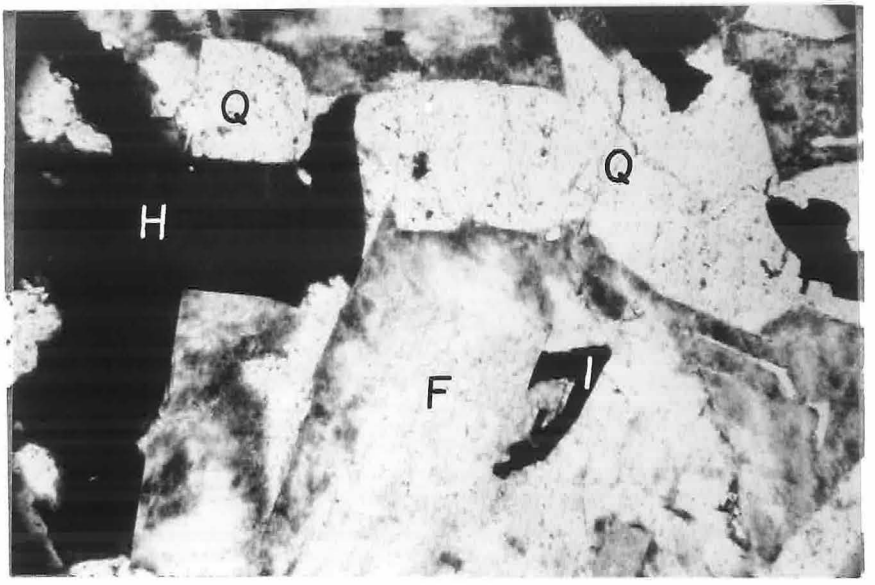

Rock Ar-Gi-Rcgphr 1-6. 2x3 mm. An analyzed specimen of hornblende granophyre. Hornblende (H), alkali feldspar (F), quartz (Q), and ilmenite (I).

a true "sugary" texture is rarely developed in them. Most of these aplites contain only pyroxene or pyroxene and minor biotite and would fall into the pyroxene-granophyre classification; rock Ad230 in Table 26 is a good example of an aplite.

Structural Settings of the Granophyres

All the larger granophyre masses are at local structural highs in the roof of the sill complex. The distribution of the thicker lenses north of Reynolds Creek is shown in the map and cross sections in Plate 4. The granophyre lenses pinch out both on the northwest and southeast where the diabase-sedimentary rock contact exposed on the ridge slopes drops below about 5900 feet elevation. The prominent bulges of granophyre are intruded against the buff and white units of the Dripping Spring Quartzite. Where the granophyre is thick, the gray unit of the upper member is missing.

The structural position of the contact of diabase with the overlying sedimentary rocks is obviously not the only factor controlling the occurrence of masses of granophyre. No granophyre masses are present on the ridge face south of Reynolds Creek, although the upper contact of the sill complex is exposed at the same 6000 foot elevation as it is north of the creek where thick granophyres crop out.

The two large lenses of granophyre on the slopes of Grantham Peak are below the most conspicuous high point in the sill roof in the area studied. The upper contact of the diabase sill climbs from an elevation of 5200 feet in Pocket Creek south of the peak to an elevation of 6000 feet on the north side above Parker Creek, transgressing the upper part of the Dripping Spring Quartzite

and cutting into the Mescal Limestone (Plate 5). Just north of Grantham Peak, the diabase abuts against sedimentary rock along a high-angle fault zone. Vertical displacement along the fault zone is relatively small, and the basic diabase-sedimentary rock juxtaposition would not have been changed even in the unlikely event that the vertical movement was post-intrusion.

Distribution of the Granophyric Rock Types

The distribution of the major types of leucocratic crystalline rocks -- pyroxene, biotite, and hornblende granophyre and aplite -- follow certain patterns. The distribution patterns are important as an aid in understanding the origins of the rocks.

The granophyric rocks studied in greatest detail form the lenses north of Reynolds Creek. Pyroxene and hornblende granophyres and aplite are present. The shapes of the lenses are shown in the map and cross sections in Plate 4. The general distribution of pyroxene and hornblende granophyres is indicated in the cross sections; aplite contains pyroxene as the major ferromagnesian silicate and has been included with pyroxene granophyre in the sections.

In the rocks north of Reynolds Creek, aplite occurs only at the upper parts of granophyre lenses in contact with the overlying sedimentary rocks and as dikes cutting the overlying rocks. Aplite commonly grades downwards into pyroxene granophyre, and, in some instances, into hornblende granophyre. Where granophyre lenses are thin, they consist entirely of pyroxene granophyre or pyroxene granophyre and aplite. Hornblende granophyre occurs only in the thicker lenses. Locally it underlies pyroxene granophyre,

and locally it forms thick sections which are directly in contact both with the overlying sedimentary rocks and with the underlying diabase. Two sections through granophyre lenses north of Reynolds Creek are shown in Figures 32 and 33.

Two small lenses of granophyre -- one about twelve feet thick and one about thirty feet thick -- are exposed in the Workman Creek drainage. Both these lenses contain only pyroxene-biotite granophyre.

The two thick lenses of granophyre exposed on the slopes of Grantham Peak (Plate 5) contain contrasting types of granophyre. The lens on the north and northwest slopes reaches a maximum thickness of about 200 feet. It consists of uniform biotite granophyre containing minor pyroxene. This lens is overlain and underlain by quartz diabase.

The distribution of rock types in the lens on the south and southwest slopes of Grantham Peak displays the same compositional pattern found in some of the lenses north of Reynolds Creek. Aplite is exposed in contact with overlying Dripping Spring Quartzite. Hornblende granophyre locally crops out beneath the aplite, and diabase crops out beneath it. This lens has a maximum thickness of about 160 feet.

The area on the west slope of Grantham Peak between the two lenses is covered by talus from cliffs of Troy Quartzite above.

Internal Features of the Granophyre Lenses

The leucocratic crystalline rocks forming the thick lenses appear igneous; they completely lack features suggesting a sedimentary heritage. No relict bedding is visible in the lenses. In some rocks, elongate crystals of pyroxene, hornblende, and apatite show strong parallel orientation, suggesting a flow alignment. In other rocks such crystals are randomly oriented. Miarolitic cavities up to several centimeters in diameter occur sparsely throughout the lenses and are particularly abundant in aplite in the upper parts. Euhedral quartz and feldspar crystals project into many of the cavities. Locally, the pyroxene and hornblende granophyres are notably inhomogeneous and contain patches of coarser rock with crystals of mafic minerals and feldspar greater than two centimeters long (Plate 22).

Angular inclusions of metasedimentary rock occur in all the large granophyre bodies. Most of the inclusions are very fine-grained; in thin section they can be seen to be recrystallized to fine-grained intergrowths of alkali feldspar and quartz with minor mafic minerals. The inclusions characteristically have sharp boundaries with the enclosing granophyres. They are typically rotated with respect to one another and show no distribution patterns which were interpreted as reflecting relict bedding. The distribution of inclusions is different in the thick, uniform lens of biotite granophyre and in the inhomogeneous lenses of pyroxene and hornblende granophyre and aplite.

Inclusions are distributed randomly throughout the lens of biotite granophyre on the north and northwest slopes of Grantham Peak. They comprise perhaps two percent of the lens. The inclusions

PLATE 22

Sharp upper contact of aplite with laminated rock of the Dripping Spring Quartzite. Southwest slope of Grantham Peak.

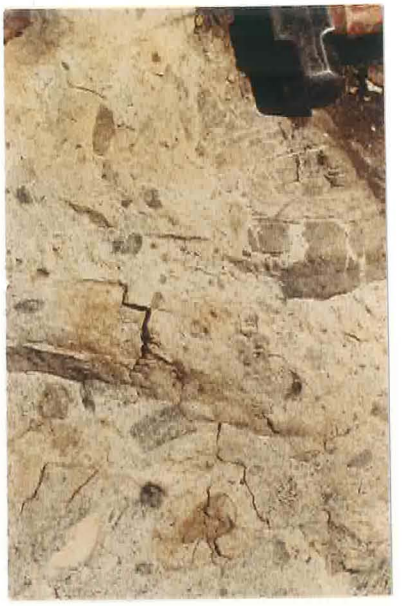

Aplite with numerous sedimentary rock inclusions near discordant contact. North of Reynolds Creek.

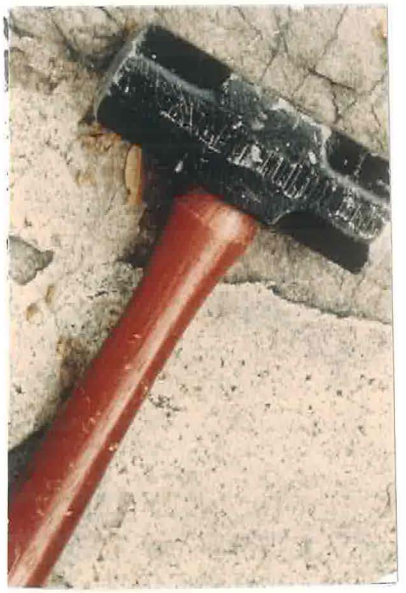

Typical hornblende granophyre with angular inclusion of quartz-rich metasediment (top). North of Reynolds Creek.

Coarse-grained patch of hornblende granophyre. North of Reynolds Creek.

vary in size from fragments several centimeters in diameter to thick, tabular blocks up to ten feet long and six feet thick. Two types of inclusions are present. The first type is black and very fine-grained and resembles lithologies present in the gray unit of the upper member of the Dripping Spring Quartzite. The second type consists of ovoid quartzite inclusions, a few centimeters in maximum diameter. These quartzite "eggs" appear to be relict quartzite pebbles because of their smooth, rounded outlines. However, it is conceivable that they might represent fragments of an orthoquartzite layer rounded by reaction. No layers with quartzite pebbles were recognized in the upper member of the Dripping Spring Quartzite, although orthoquartzite layers a few feet thick are present in it locally.

The distribution of inclusions is not random in the inhomogeneous granophyre lenses north of Reynolds Creek. Inclusions are most numerous in aplite (Plate 22) and less abundant in hornblende and pyroxene granophyre. Most inclusions are angular and less than two feet in maximum diameter. All of these sedimentary rock inclusions have lithologies like those present in the overlying buff and white units of the upper member of the Dripping Spring Quartzite.

In the superb exposures of granophyre in the thick bulge shown in Plate 1 and Figure 32, a particularly interesting distribution of inclusions is present. Inclusions are sparsely distributed throughout the upper part of the hornblende granophyre. The granophyre has a sharp, horizontal contact with the underlying quartz diabase. A few feet above this contact, numerous tabular and largely flat-lying inclusions are present. These inclusions are exceptionally large, some being as much as fifteen feet long and several feet thick. The most probable explanation for their presence is that they settled

through a liquid granophyre mass and came to rest above the already solidified diabase. None of the inclusions show signs of any substantial amount of assimilation by or reaction with the granophyre. A few quartz-rich inclusions have reaction rims of hornblende or pyroxene a few millimeters thick.

Inclusions of diabasic or basaltic rock in granophyre are rare. The absence of any fine-grained diabasic rock in the vicinity of the thick granophyre lenses is remarkable. Any chilled facies of the diabase magma must have been stripped from the sill roof by the granophyres or altered beyond recognition. Two inclusions about two feet in maximum dimension of fine-grained diabasic rock are preserved in the aplite near the top of the bluff north of Reynolds Creek seen in Plate 1. Though most rock in the inclusions is altered, some fresh patches remain. The fresh rock consists of labradorite (40%), anorthoclase (about Or_{80})(20%), olivine (10%), augite (15%), and minor opaques and biotite. The abundance of clear anorthoclase in apparent equilibrium with primary plagioclase suggests that the rock crystallized from contaminated diabase magma and does not represent a chilled facies of the primary diabase magma. No other basaltic or diabasic inclusions were observed in the granophyres.

Contacts of the Granophyre Lenses

The contacts of the granophyric rocks with overlying sedimentary rocks are sharp and well-defined. One such contact can be seen in the photograph in the frontispiece (Plate 1). The distribution of rock types in the thick granophyre lenses north of Reynolds Creek and on the southwest slope of Grantham Peak has already been noted.

Aplite, essentially a fine-grained pyroxene granophyre, occurs in the upper parts of granophyre lenses in contact with the overlying sedimentary rocks; it grades downwards into pyroxene granophyre in some localities and into hornblende granophyre in others. Pyroxene granophyre locally grades downwards into hornblende granophyre. In a few localities pyroxene and hornblende granophyre are in direct contact with overlying sedimentary rocks. The contacts of these two crystalline rock types with the country rock are sharp and can be seen from a distance in outcrop. The aplites are more leucocratic and finer-grained than pyroxene and hornblende granophyre, and they more closely resemble the overlying metasedimentary rocks. The resemblance is particularly strong where aplite is in contact with rocks from the buff and white units of the upper member of the Dripping Spring Quartzite, as is the case north of Reynolds Creek. From a short distance contacts between aplite and metasedimentary rock locally seem gradational, and Shride (1967, p. 60) states: "Everywhere the contact between aplite and hornfelsed sedimentary rock is vague." However, on close inspection the contact can everywhere be exactly defined. Important contrasts between the aplite and overlying metasedimentary rocks are:

(1) aplite is massive and commonly contains rotated inclusions while the metasediments are laminated and layered;

(2) aplite is obviously crystalline to the naked eye, while the layered metasedimentary rocks of the buff and tan units generally are very fine-grained. Laminated, partly coarsely crystalline rocks like the ones shown in Plates 19 and 20 are rare except in the black facies of the upper member. Contacts between aplite and sedimentary rocks are shown in thin section in Plate 24 and in outcrop in Plate 23.

Aplite is commonly finer-grained, by at least a factor of two, within an inch or less of sedimentary rock contacts; such fine-grained contact zones appear to be chill zones and constitute one argument that the aplite was mostly molten.

Contacts between the granophyric and sedimentary rocks are roughly concordant in some places but markedly discordant in others. Some of the most spectacular exposures of granophyric rocks are found in the thick lens north of Reynolds Creek shown in Plates 1 and 23 and Figure 32. Here a mass of aplite and underlying hornblende granophyre bulges up into the overlying buff and white units of the upper member of the Dripping Spring Quartzite; one contact of the bulge transgresses about sixty feet of section in a distance of several hundred feet (Plate 23). The descriptions of Shride (1967, p. 60) apparently are based mainly on relationships in this bulge. The aplite typically has somewhat discordant contacts with the metasedimentary rocks, and several dikes of aplite were observed in the overlying strata. One well-exposed dike crops out for about one hundred feet and extends twenty to thirty feet over the main granophyre mass at the eastern margin of the bulge described above. The dike is approximately vertical and about three feet thick; it cuts sharply through nearly horizontal, unrecrystallized sedimentary strata and contains numerous, small sedimentary rock xenoliths. The contact between the dike and sedimentary rock is sharp and can be precisely defined in thin section. The aplite is finer-grained at the contact than in the center of the dike; locally, the finer-grained aplite appears to contain a few percent alkali feldspar phenocrysts. An analysis, mode, and norm of a sample of aplite from the dike (Ad230) are in Table 26.

PLATE 23

View looking east from near point H in Plate 4. Flat-lying strata of the upper member of the Dripping Spring Quartzite are truncated by massive aplite and hornblende granophyre at the roof of the sill complex north of Reynolds Creek. A section through the granophyre is shown in Figure 32.

Aplite dike cutting thin-bedded strata of Dripping Spring Quartzite above granophyre north of Reynolds Creek (Photograph - L.T. Silver).

PLATE 24

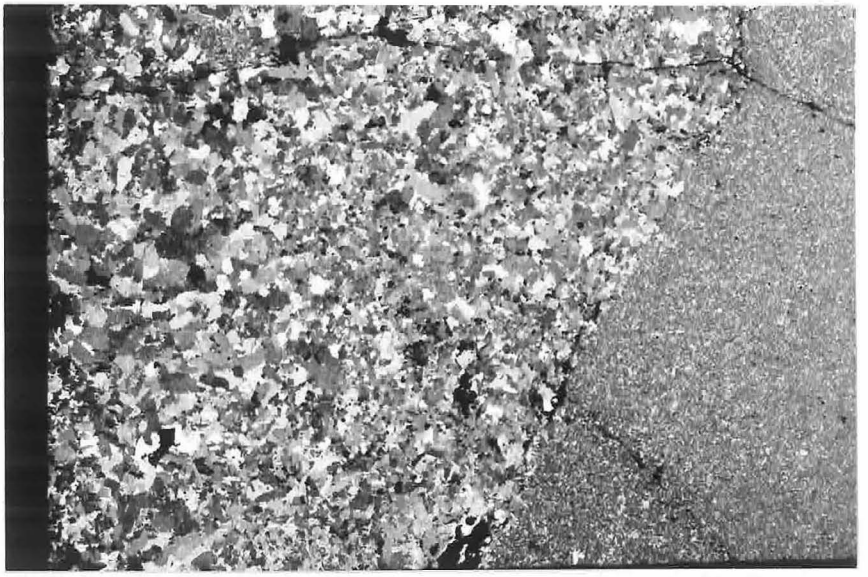

Rock Ad66. 16x24 mm. Crossed nicols. Sharp contact between aplite (left) and metasedimentary rock at top of sill complex. Note that the aplite is finer-grained near the contact.

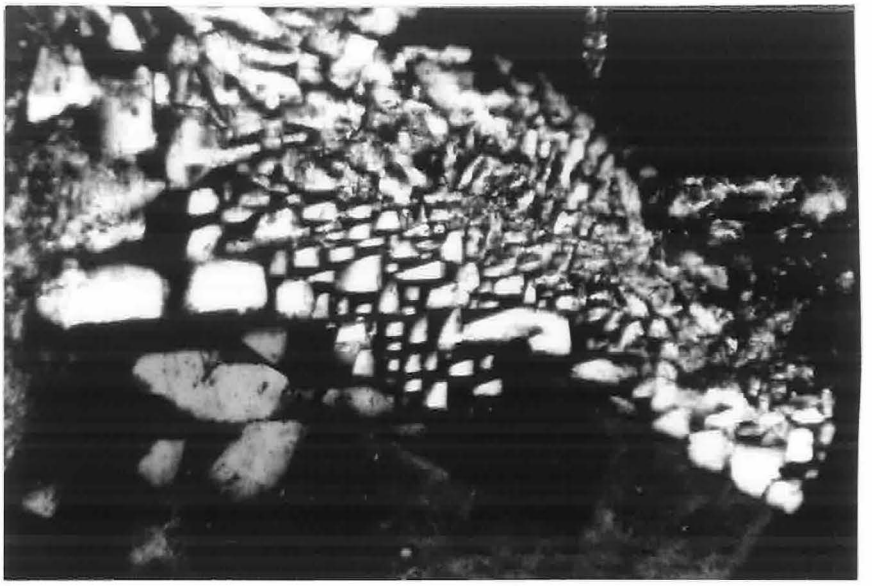

Rock Ad285. 0.5x0.75 mm. Crossed nicols. Analyzed biotite granophyre. Micrographic intergrowth between quartz and feldspar interstitial to larger feldspar laths.

The granophyric rocks are more resistant to weathering than diabase, and contacts between the two rock types are not exposed in many places. However, the contact between hornblende granophyre and diabase is well-exposed at the base of the granophyre bulge described above, and contacts between pyroxene granophyre and diabase are exposed at several places on the ridge north of Reynolds Creek. The contact between biotite granophyre and diabase was found at one locality on the northwest slope of Grantham Peak. All these contacts are approximately horizontal. All the granophyric rocks are considerably lighter in color than the diabasic rocks. Very few rocks were found which by hand specimen appearance could not be definitely categorized as granophyre or diabase, and contacts between the two types can generally be defined within an inch in outcrop and in hand specimen. The darker diabasic rock at the contact in some places seems broken, and irregular veinlets a few inches thick of lighter-colored granophyric rock extend into the diabase a maximum of several feet from the contact. The diabase at the contact is coarser-grained than normal diabase; locally it contains patches a few inches in maximum diameter rich in red alkali feldspar. These patches might either be remnants of inclusions of sedimentary rock or segregations. The coarser-grained diabase is in many places quartz diabase, containing alkali feldspar and quartz. The granophyric rocks in general show no systematic variations in grain size at contacts with the diabase. However, at the only contact observed between the biotite granophyre and quartz diabase north of Grantham Peak, both rock types are distinctly finer-grained within several feet of their mutual contact.

Inclusions and Dikes in the Diabase

Inclusions in diabase

Undoubted inclusions are extremely rare in diabase except near Grantham Peak. Two inclusions a few inches in maximum diameter were found by L. T. Silver north of Reynolds Creek below the large mass of granophyre shown in Plate 1. One of the two inclusions, consisting largely of altered feldspar and pale green calcic pyroxene, might have been derived from the Dripping Spring Quartzite. The other, consisting almost entirely of calcic pyroxene, was probably derived from the Mescal Limestone. The granophyre mass above the diabase here was intruded only to within about twenty feet of the Mescal, and the diabase is not in contact with the formation in any of the exposures. If the inclusion is from the Mescal Limestone, it must have been transported laterally to its present position.

Numerous angular inclusions of leucocratic rock mineralogically and texturally similar to aplite and fine-grained granophyre occur in the large mass of quartz diabase on the north and northwest slopes of Grantham Peak. The inclusions were found in quartz diabase above the biotite granophyre lens and below the overlying Mescal Limestone. They vary in size from fragments several inches across to tabular blocks at least four feet thick and fifty feet long. Many of the inclusions are uniform in texture, but others have irregular rims several centimeters thick with an average grain size of a few millimeters which surround finer-grained rock. The inclusions show no relict bedding. They consist primarily of alkali feldspar with intergrown quartz and minor hornblende and pyroxene. Micrographic quartz-feldspar intergrowths are common. The pyroxene is clear in

thin section, and the hornblende is less intensely pleochroic than the iron-rich varieties which have been analyzed. Some of the inclusions themselves contain ovoid inclusions of quartzite up to about five centimeters in maximum diameter; many of these quartzite "eggs" are surrounded by thin reaction rims of hornblende. The "eggs" are very similar to the ones found in the biotite granophyre lens cropping out below.

Dikes of granophyre within diabase

Dikes of granophyric rock in diabase are relatively rare but were observed in several localities. Dikes of aplite a few centimeters wide cut some of the outcrops of quartz diabase on the northwest slope of Grantham Peak. These dikes occur in localities with abundant inclusions, and they may represent fused or mobilized sedimentary rock. A vertical aplite dike, ten inches wide, was observed in diabase twenty to thirty feet below the sill roof in a roadcut along Workman Creek. An analysis, mode, and norm of a sample (Ad241) from this dike are reported in Table 26.

Mineralogy of the Granophyric Rocks

Feldspars

Alkali feldspar forms 60 to 80 percent of all the granophyric rocks in the sill complex. Description of the feldspars is complicated by the fact that after their initial crystallization they reacted readily with a later fluid. The reacted feldspars recrystallized, unmixed, and in many rocks became turbid to the point of seeming

opaque in thin section. Because of their reactivity the initial character of the feldspars in many rocks cannot be determined. Similar turbid feldspars are characteristic of many other granophyre bodies described in the literature.

Clear, unreacted alkali feldspar is present in many granophyric rocks and makes up the bulk of some specimens. Most of the alkali feldspar occurs in stout, subhedral laths, some as long as a centimeter. Negative 2V's for clear feldspar range from 10 to 70 degrees, values of about 40 degrees being most common; the entire range is present for feldspars in a single thin section. The variation presumably reflects varying degrees of inversion of primary potassium-rich sanidine. Many of the feldspar laths are simple Carlsbad twins. A few clear laths have developed stringers of hair perthite.

Feldspar compositions in representative rocks have been determined by partial microprobe analyses (K, Na, and Ca only). Only four of the analyzed granophyric rocks contained clear alkali feldspar. The ranges of clear feldspar compositions found in these rocks are in Table 27. The range of feldspar compositions in any one rock probably reflects processes of post-crystallization diffusion and alteration rather than initial zoning. No systematic zoning was detected either optically or with the microprobe, and analyses showed no systematic compositional differences between feldspar graphically intergrown with quartz and feldspar in the interior of lath-shaped crystals. The most sodic alkali feldspar analyzed in each rock probably reflects the primary feldspar compositions in the rock most closely.

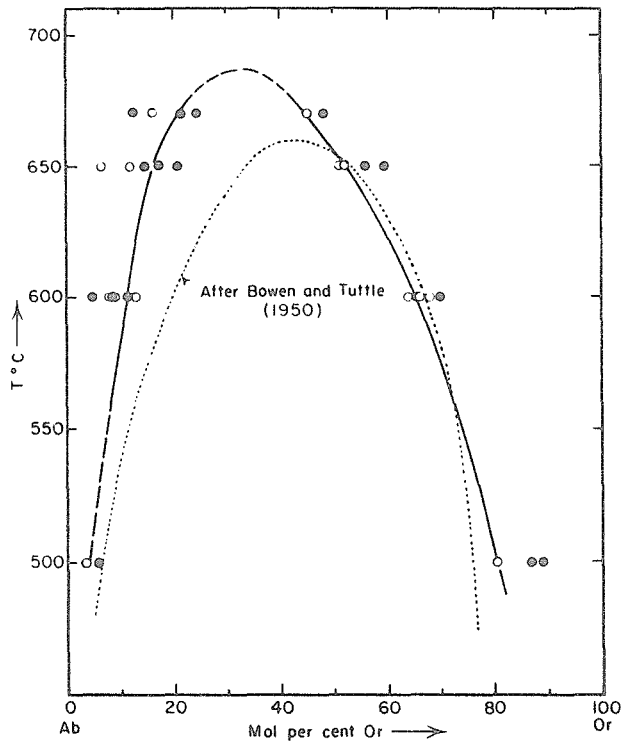

Figure 29. Alkali feldspar solvus determined by Orville (1963). The figure is reproduced from Orville (1963, Figure 9).

TABLE 27

Ranges of Clear Alkali Feldspar Compositions in Analyzed Rocks

Sample	Rock type	Alkali feldspar
Ar-Gi-Rcgphr 1-6	hornblende granophyre	Or 60-65
Ad163	pyroxene-biotite granophyre	Or 71-85
Ad285	biotite granophyre	Or 77-86
Ad23h	aplitic pyroxene granophyre	Or 79-90

In all the granophyric rocks, at least a fraction of the alkali feldspar is turbid and appears dusty brown in thin section; in many rocks no clear feldspar remains. Turbid areas in feldspar grains are invariably closer to end-member feldspar compositions than are associated clear areas. Highly turbid K feldspar is generally at least as potassic as $Or_{97}Ab_3$. Turbid Na feldspar is generally at least as sodic as Or_3Ab_{97} and in many cases is more sodic than Or_1Ab_{99}. Some rocks with no clear feldspar commonly contain lath-shaped composite crystals of small, intimately mixed, irregularly shaped volumes of K feldspar and albite. Both feldspars are turbid, but the albite is invariably clearer than the K feldspar. Such laths may represent unmixed, recrystallized sanidine grains; a photomicrograph of such a patch perthite lath is shown in Plate 25.

Some rocks with completely turbid K-rich feldspar contain several modal percent of only slightly turbid albite in small anhedral crystals interstitial to the larger feldspar laths. In some of these rocks, small euhedral albite crystals, only slightly turbid in thin section, project into miarolitic cavities together with quartz and diopside. The albite might have formed from sodium released during the recrystallization and alteration of original alkali feldspar.

Some granophyric rocks still containing clear alkali feldspar contain a few percent identifiable plagioclase feldspar in small subhedral laths. The plagioclase crystals alter to fine-grained clays which can be readily distinguished from the finer-grained, "dustier" alteration products characteristic of alkali feldspar. In some rocks such as the analyzed specimens Ar-Gi-Rcgphr 1-6 and Ad285, small unaltered plagioclase laths are preserved. These laths most commonly occur as oriented inclusions within larger, clear alkali feldspar

PLATE 25

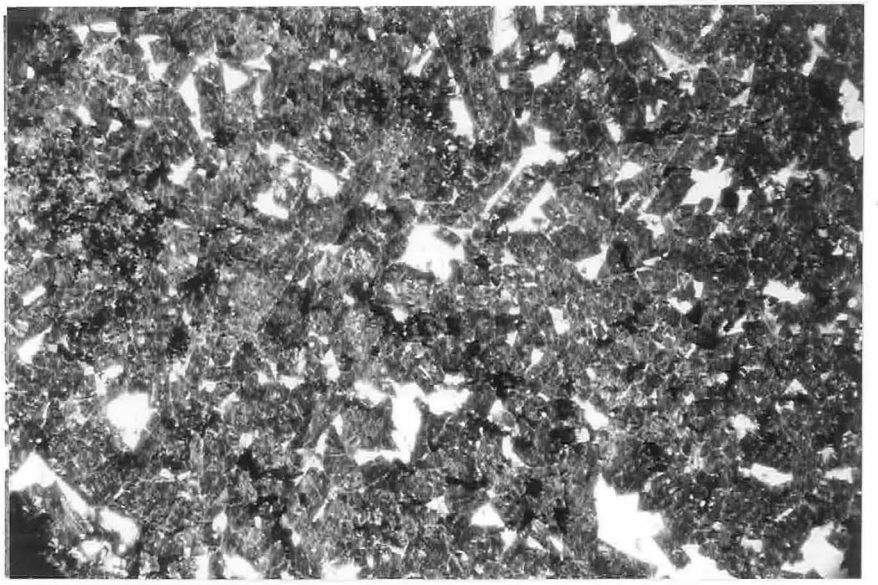

Rock Ad91b. 6x9 mm. Analyzed aplitic pyroxene granophyre. About 75% of this rock is turbid, recrystallized K feldspar. Clear interstitial grains are quartz.

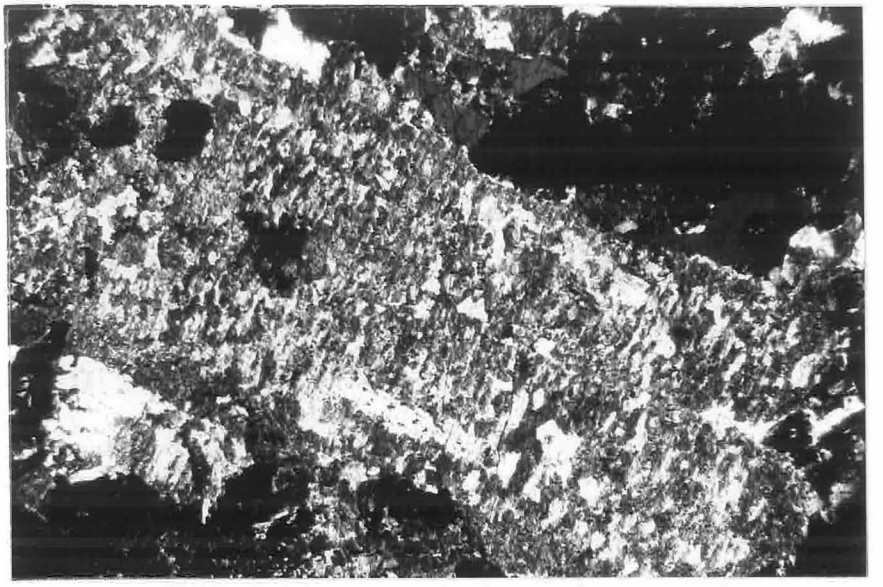

Rock Ad91c. 2x3 mm. Crossed nicols. Analyzed pyroxene granophyre. The single, large alkali feldspar lath in the center of the photo is composed of a patch intergrowth of K feldspar (dark) and albite (light).

grains, but in rock Ad285 some are in contact with interstitial micrographic quartz-alkali feldspar intergrowths. In rock Ad285 (biotite granophyre) the plagioclase shows little zoning and is near An_{56} in composition. In rock Ar-Gi-Rcgphr 1-6 (hornblende granophyre) most plagioclase grains are unzoned and near An_{40} in composition; one grain investigated is zoned to more sodic plagioclase (An_{30}). Representative compositions of clear alkali feldspar and coexisting unaltered plagioclase in the two rocks are plotted in a portion of the feldspar ternary diagram in Figure 30.

Feldspars in the different rock types

Petrographic and microprobe evidence indicate that primary alkali feldspar in aplite is less sodic than in the coarser-grained rocks. Aplites with turbid K feldspar contain less intermixed albite than do underlying, coarser-grained granophyres with turbid feldspar. Clear alkali feldspar in an investigated aplite was less sodic than clear feldspar in coarser-grained granophyres (Table 27). Differences in albite abundance are confirmed by differences in Na_2O/K_2O ratios of analyzed rocks (Table 26). Altered and fresh calcic plagioclase crystals are much less common in aplite than in the coarser rock types.

The feldspars as geothermometers

The composition of clear alkali feldspar and the compositions of coexisting alkali feldspar and plagioclase can be used as guides to the temperatures of primary feldspar crystallization in the granophyric rocks. The clear, unmixed alkali feldspars must have crystal-

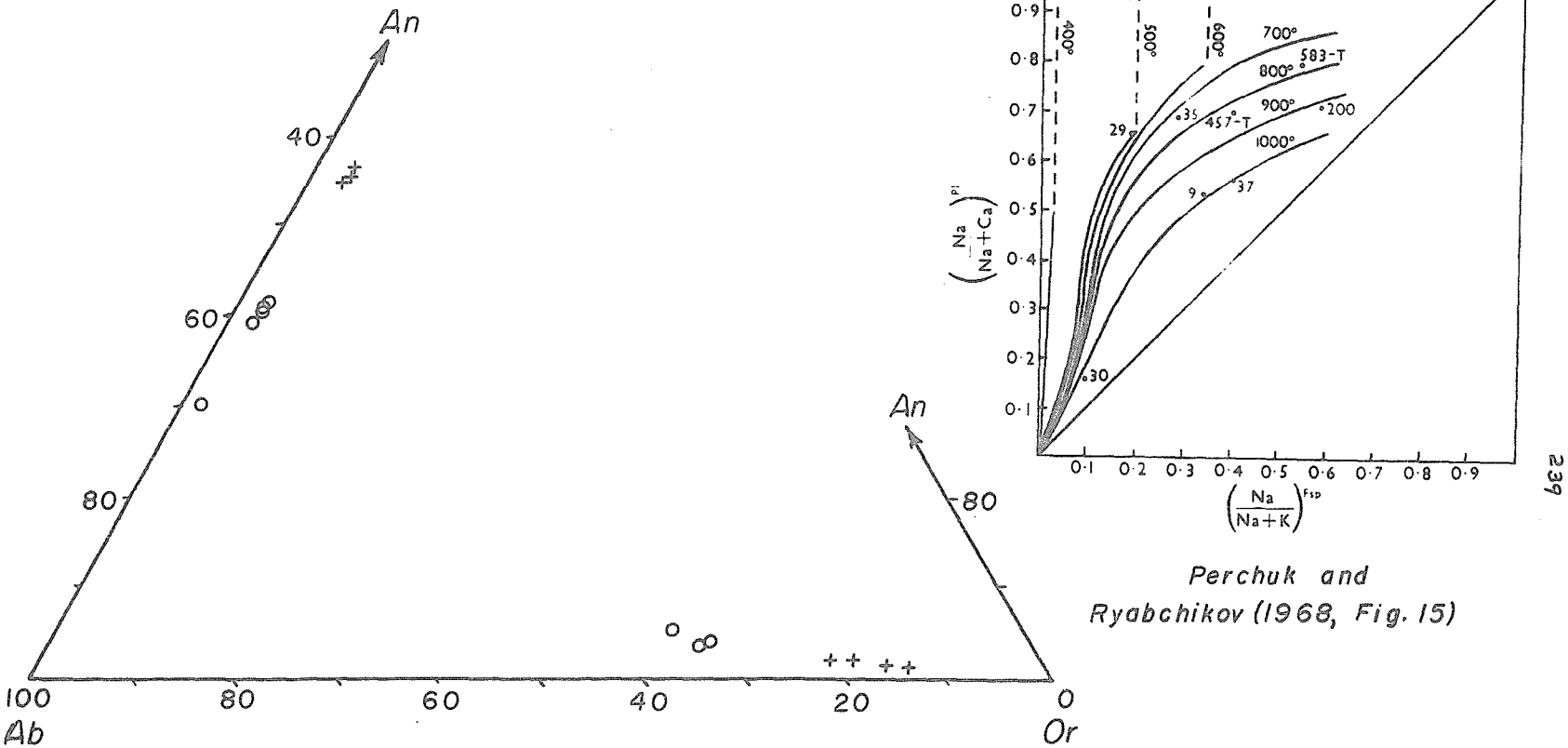

Figure 30. Compositions of coexisting clear alkali feldspar and plagioclase in two analyzed granophyre samples, together with a proposed two-feldspar geothermometer (Perchuk and Ryabchikov, 1968).

lized at temperatures above the alkali feldspar solvus. The data of Orville (1963, Figure 9) reproduced in Figure 29 indicate that solvus temperatures vary from about 625°C at a composition of $Or_{60}Ab_{40}$ to about 500°C at a composition of $Or_{80}Ab_{20}$. These data indicate that feldspar in the analyzed sample of hornblende granophyre must have crystallized at temperatures greater than 600°C. Feldspars in the other three rocks in Table 27 must have formed at temperatures greater than 500°C.

The distribution of sodium between coexisting alkali feldspar and plagioclase is a function of temperature, pressure, and feldspar composition. Because only solid phases are involved in the reaction, the pressure dependence of the reaction is probably relatively unimportant. Perchuk and Ryabchikov (1968) have derived relationships between temperature and coexisting feldspar compositions using experimental data and theoretical calculations and making certain simplifying assumptions. Application of their results (op. cit., p. 151) reproduced in chart form in Figure 30 suggests that feldspar equilibration temperatures were in the range 800°-950°C for hornblende granophyre Ar-Gi-Rcgphr 1-6 and in the range 900°-1000°C for biotite granophyre Ad285. These values indicate that the equilibration temperatures were high; the absolute values cannot be taken seriously without further work on the geothermometer.

The relatively pure nature of the turbid intergrown alkali feldspars suggests that cation exchange in the recrystallized feldspars took place at temperatures below 400°C.

Quartz

Quartz comprises from 3 to 35 modal percent of the granophyric rocks. More rocks are syenitic (less than 10% quartz) than granitic in composition. The aplitic rocks in the upper parts of the lenses tend to be richer in quartz than the coarser-grained rocks in the lower parts. Most quartz occurs in anhedral grains in the interstices of feldspar laths and in intricate intergrowths with feldspar at the margins of the laths. Micrographic intergrowths are less common in the finer-grained aplitic rocks than in the coarser-grained rocks. Such intergrowths are particularly well developed in the biotite granophyres (such as the analyzed specimen Ad285) from the slopes of Grantham Peak (Plate 24).

Pyroxene

Calcic pyroxene is the most common ferromagnesian silicate in the granophyric rocks. In any one rock its abundance never exceeds twenty modal percent and is less than 10 modal percent in most specimens. It most commonly occurs in anhedral grains less than a millimeter in maximum diameter. In a few of the coarser-grained rocks it also occurs in elongate, subhedral prisms up to a centimeter in length. In a few rocks, subophitic crystals are present. In several coarser-grained granophyric rocks, a few skeletal pyroxene crystals intergrown with alkali feldspar were observed. In some rocks pyroxene partly reacted to form biotite and in others it reacted to form hornblende. No exsolution lamellae are present in the pyroxene.

TABLE 28

Microprobe Analyses of Calcic Pyroxene and Chlorite in Analyzed Rock Ad23h

	1	2	3	4*	5*
SiO_2	52.7	51.4	52.0	33.1	29.5
TiO_2	0.05	0.07	0.06	0.53	0.23
Al_2O_3	0.18	0.25	0.32	18.0	19.8
Fe as FeO	12.3	15.0	17.2	27.7	30.0
MnO	0.32	0.37	0.47	0.23	0.27
MgO	11.7	9.8	9.4	9.5	9.3
CaO	23.4	23.4	21.3	0.60	0.23
Cr_2O_3	0.05	0.06	0.06	0.04	0.03
	100.7	100.4	100.8	(89.7)	(89.3)

1. $Wo_{47.2}En_{32.9}Fs_{19.9}$ Calcic pyroxene Ad23h(C1)

2. $Wo_{47.7}En_{27.8}Fs_{24.5}$ Calcic pyroxene Ad23h(B1)

3. $Wo_{44.3}En_{27.0}Fs_{28.7}$ Calcic pyroxene Ad23h(C2)

4. Primary(?) chlorite Ad23h(B2)

5. Primary(?) chlorite Ad23h(B3)

* Eleven weight percent H_2O assumed for calculation of analysis.

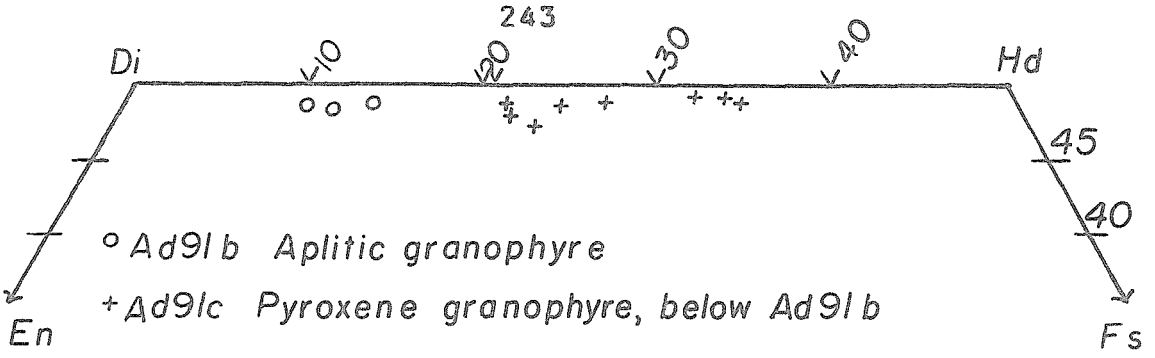

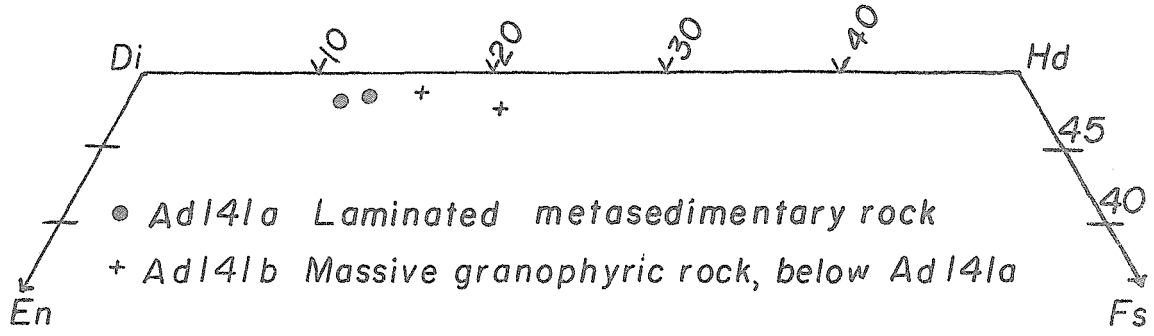

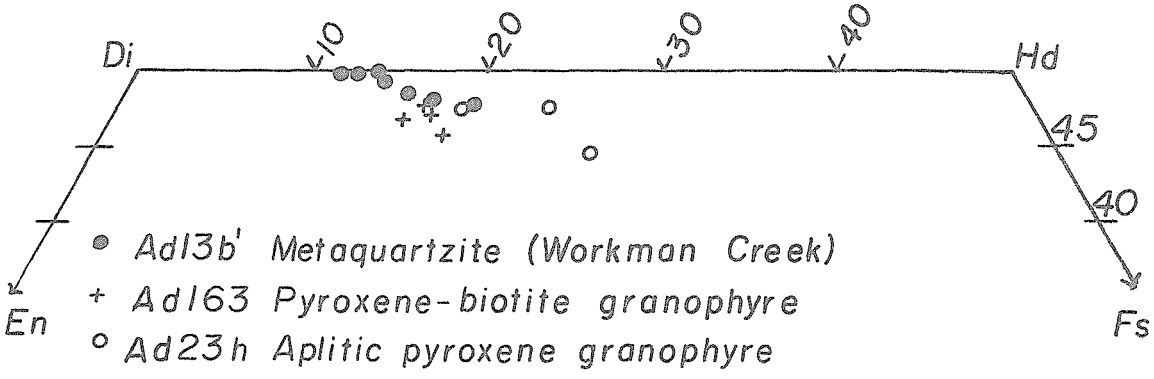

Figure 31. Representative compositions of pyroxenes in granophyres and metasedimentary rocks plotted in the pyroxene quadrilateral.

A range of calcic pyroxene compositions occur in the granophyric rocks. In the aplitic and fine-grained granophyric rocks in the upper parts of the lenses, pyroxene is colorless in thin section; in the coarser-grained rocks lower in the lenses, it is commonly pale green in thin section.

Complete microprobe analyses were made only of pyroxene in one rock, analyzed specimen Ad23h; these analyses are reported in Table 28. Partial microprobe analyses (Ca, Fe, and Mg only) were made of pyroxenes in a variety of other granophyric rocks and in a metamorphic quartzite from near Workman Creek and a laminated metasedimentary K-rich rock from above the sill in Reynolds Creek. These analyses are plotted in portions of the pyroxene quadrilateral in Figure 31. The granophyre pyroxenes are irregularly zoned; microprobe data were reduced for analyses showing the extremes of pyroxene compositions in the rocks as well as for some showing typical compositions.

The microprobe analyses show that:

(1) all pyroxenes in the granophyres are quite calcic and are technically salites;

(2) the colorless pyroxenes in massive granophyres are very similar in composition to pyroxenes in obviously metasedimentary rocks;

(3) the pale green pyroxenes are more iron-enriched;

(4) the pyroxenes contain very little Al and Ti.

The high calcium and low Al and Ti in the pyroxenes probably reflect relatively low crystallization temperatures compared to those of augite in the diabasic rocks. Their compositions are comparable to those of some deuteric pyroxenes in altered diabase and to those

of some of the less iron-enriched primary calcic pyroxenes in diabase pegmatite. The pyroxenes are distinctly less iron-rich than the hedenburgitic varieties described in most other granophyres (i.e., Hotz, 1953, p. 687; McDougall, 1962, p. 289; Wager and Brown, 1967, p. 48).

Hornblende

Hornblende forms up to fifteen modal percent of some of the rocks in the thick lenses of granophyre north of Reynolds Creek. Its abundant presence in granophyric rocks is of particular interest, because hornblende occurs only with extreme rarity in rocks of obvious metasedimentary origin. It is a common constituent of quartz diabase. Hornblende very similar in appearance to that found here occurs in granophyres associated with Tasmanian diabases (McDougall, 1962, p. 294).

Most hornblende in the granophyres forms anhedral grains a few millimeters in maximum dimension, but prismatic crystals over ten millimeters long are found in some coarser-grained rocks. Replacement and rimming of pyroxene by single crystals of hornblende was a common process in the granophyric rocks, but, texturally, most of the hornblende in these rocks appears primary. It is typically pleochroic in shades of brown and green, and asymmetrical color zoning of crystals is common.

A crystal about three millimeters in maximum dimension with particularly well-developed but not atypical color zoning in the analyzed rock Ar-Gi-Rcgphr 1-6 was selected for microprobe analysis. About half the crystal is pleochroic from light yellow-brown to very dark brown; analyses 1 and 2 in Table 29 represent

TABLE 29

Microprobe Analyses of Points in a Single Zoned Amphibole Crystal in Analyzed Rock Ar-Gi-Rcgphr 1-6

	1	2	3	4	5
SiO_2	41.8	42.1	42.7	43.1	53.3
TiO_2	2.1	1.3	0.28	0.21	0.01
Al_2O_3	8.1	8.0	5.8	6.2	0.32
Fe as FeO	29.8	29.0	33.5	32.1	14.2
MnO	0.44	0.39	0.41	0.36	10.3
MgO	3.8	4.4	2.2	2.9	9.7
CaO	10.5	10.8	10.5	10.4	12.3
Na_2O	1.9	1.9	1.5	1.5	0.04
K_2O	1.4	1.4	1.4	1.4	0.08
Cr_2O_3	0.03	0.03	0.05	0.03	0.02
	(99.9)*	(99.4)*	(98.2)*	(98.2)*	(100.5)*

1. $Na_{.57}K_{.28}Ca_{1.77}Mg_{.89}Mn_{.06}Fe_{3.93}Ti_{.25}Al_{1.51}Si_{6.58}$**
   Pleochroic light yellow-brown to very dark brown. (Ar 1-6, B2)

2. $Na_{.57}K_{.27}Ca_{1.83}Mg_{1.04}Mn_{.05}Fe_{3.83}Ti_{.16}Al_{1.49}Si_{6.63}$**
   Pleochroic light yellow-brown to very dark brown. (Ar 1-6, B4)

3. $Na_{.47}K_{.28}Ca_{1.84}Mg_{.53}Mn_{.06}Fe_{4.57}Ti_{.03}Al_{1.11}Si_{6.95}$**
   Pleochroic light yellow-green to deep blue green. (Ar 1-6, C2)

4. $Na_{.47}K_{.29}Ca_{1.80}Mg_{.69}Mn_{.05}Fe_{4.33}Ti_{.03}Al_{1.18}Si_{6.96}$**
   Pleochroic light yellow-green to deep blue-green. (Ar 1-6, C3)

5. $Na_{.01}K_{.02}Ca_{1.95}Mg_{2.12}Mn_{1.29}Fe_{1.75}Ti_{0}Al_{.06}Si_{7.90}$**
   Colorless. (Ar 1-6, C4)

* These analyses were calculated assuming the hornblende contained 2 weight percent H_2O. Addition of this water makes several of the summations unreasonably high.

** Formulas calculated for 23 oxygens, assuming all Fe as Fe^{+2}.

this material. About half the crystal is pleochroic from light yellow-green to dark blue-green and is represented by analyses 3 and 4 in Table 29. Both the brown and green hornblendes are optically typical of hornblende in the other granophyric rocks. Part of the crystal is fringed by a thin selvage of colorless amphibole in sharp contact with the green hornblende; the colorless amphibole, represented by analysis 5 in Table 29, is unusual and was observed only in one other rock. All three amphibole types in the crystal extinguish simultaneously under crossed nicols.

The microprobe analyses show the hornblende to be strikingly iron-rich with Fe/(Fe +Mg) ratios between 0.8 and 0.9. It is far more iron-rich than the granophyric pyroxenes. The color change between the brown and green varieties might reasonably be ascribed either to the difference in titanium or to a difference in iron valence states or both. No attempt was made to distinguish valence states with the microprobe. The colorless amphibole is extremely rich in manganese and might be called a manganactinolite. Because the colorless amphibole contains almost no Na, K, Ti, or Al and because it is enriched in manganese, it most likely crystallized at a relatively low temperature from a residual manganese-rich fluid. However, a solvus may exist between actinolite and hornblende (Ernst, 1968, p. 69), and it is possible that the colorless amphibole and intergrown green hornblende may have coexisted in equilibrium. Even if they did not form in equilibrium, the presence of a solvus might account for the sharp compositional break between the two varieties. Analyses 4 and 5 (Table 29) were made on points about 0.1 mm apart across the sharp boundary between the two amphiboles.

It is impossible to accurately determine the upper temperature of stability of the iron-rich hornblende with knowledge presently available, because of the complex composition and the undetermined ferric iron content of the mineral. Ernst (1968, p. 102) indicates that at one kilobar water pressure ferropargasite ($NaCa_2Fe_4AlSi_6Al_2O_{22}(OH)_2$) has a maximum temperature stability limit of 800°C and ferrotremolite ($Ca_2Fe_5Si_8O_{22}(OH)_2$) a limit of 465°C; the stability of these amphiboles is of course dependent on oxygen fugacity. Ernst also indicates that magnesian amphiboles are stable to much higher temperatures than their ferrous iron analogues, and that substitution of ferric iron for magnesium results in a further increase in stability. The most that can be said is that it is unlikely that the hornblende crystallized at temperatures greater than 800°C or 900°C.

Biotite

Biotite is less common than either pyroxene or hornblende in the granophyric rocks, and it is the major ferromagnesian silicate only in rocks in the northern Grantham Peak lense. Here it constitutes up to fifteen modal percent of a few specimens. Biotite commonly occurs with calcic pyroxene in rocks from the small Workman Creek lenses, but in these, its abundance is not greater than about seven modal percent. In most rocks where it is abundant, biotite is associated with pyrrhotite.

Most of the biotite is pleochroic from light yellow-brown to deep red-brown. Partial microprobe analyses of biotite in the analyzed rock Ad163 indicate that it contains about 4 weight percent TiO_2 and has a Fe/(Fe + Mg) ratio of about 0.4. The analyzed biotite grains

are intergrown with ilmenite and pyrrhotite. The high titanium content of the biotite is probably responsible for its deep red-brown pleochroism.

The stability limits of biotite do not contribute significant restrictions on the formation temperatures of the granophyric rocks. Data of Wones and Eugster (1965, p. 1241) indicate that biotite with a Fe/(Fe +Mg) ratio of 0.4 is stable to about 850°C at about one kilobar pressure and at an intermediate oxygen fugacity (Ni-NiO buffer).

Oxides and sulfides

Ilmenite, pyrrhotite, and pyrite are the only opaque minerals identified in the granophyric rocks. Only ilmenite and pyrrhotite are abundant. Pyrite appears secondary. It occurs only in small grains, most of which border larger pyrrhotite grains. The pyrite probably formed by granule exsolution and/or lower temperature alteration of primary pyrrhotite. Microprobe analytical results for ilmenite grains in granophyre were listed in Table 21.

The relative abundance of pyrrhotite and ilmenite in the granophyric rocks varies widely and may be a guide to the origin of the rocks. The black facies of the upper member of the Dripping Spring Quartzite owes its color to the presence both of fine-grained carbon and pyrite (Granger and Raup, 1964, pp. 38-39). The amount of pyrite in the black facies can be estimated from the sedimentary rock chemical analyses in Table 1, which show from 0.9 to 2.7 weight percent sulfur, corresponding to about 2 to 5 percent normative pyrite. In contrast, the diabasic rocks (Table 5) all contain less than 0.17 weight percent sulfur, present primarily in pyrrhotite.

Many of the finer-grained and aplitic rocks in the upper parts of the granophyre lenses north of Reynolds Creek contain two to five modal percent pyrrhotite as well as some ilmenite; the presence of the sulfide is reflected by the sulfur abundance in the analyses of rocks Ad23h and Ad91b in Table 26. As noted before, pyrrhotite occurs with biotite in the small granophyre lenses in Workman Creek and in the large lens on the north and northwest slopes of Grantham Peak. In most of these rocks pyrrhotite is in anhedral grains, a millimeter or two in maximum diameter, easily recognizable in hand specimens of fresh rock; ilmenite commonly occurs in smaller, subhedral grains with shapes of rods and thin plates. The coarser-grained pyroxene granophyres in the lower parts of granophyre lenses and the hornblende granophyres contain little or no pyrrhotite. Therefore, in some cross sections through the upper part of the sill complex there is a variation in sulfur content from high values in pyrite-containing sedimentary rocks to lower values in underlying pyrrhotite-containing aplitic granophyres to very low values in underlying coarser-grained granophyres.

Other minerals in granophyric rocks

Sphene makes up as much as three modal percent of some granophyric rocks and is completely absent in others. It characteristically occurs in anhedral or subhedral grains several tenths of a millimeter or less in maximum diameter. The sphene in many of the rocks is distinctly pleochroic from colorless to red-brown. Some crystals are irregularly zoned from pleochroic centers to colorless margins.

Chlorite is not a common mineral in the granophyric rocks, but it makes up as much as 4 percent of a few specimens. In most occurrences it seems to be a secondary alteration product of biotite, but in a few rocks it seems primary. Two microprobe analyses of apparently primary chlorite in analyzed rock Ad23h listed in Table 28 have Fe/(Fe +Mg) ratios near 0.6; as in the other cases examined, calcic pyroxene grains have lower Fe/(Fe +Mg) ratios than associated chlorite.

Apatite, allanite, and zircon are present in trace to minor quantities in many of the granophyric rocks. Apatite occurs in needle-like prisms up to a millimeter long. Allanite occurs in zoned, anhedral crystals pleochroic from light to dark brown. Zircon occurs in intricate skeletal crystals in some rocks and in simple euhedral prisms in others.

Compositions of the Granophyric Rocks

Compositions, modes, and norms of eight granophyric rocks from the Sierra Ancha sill complex are reported in Table 26. All the rocks are unusually high in potassium and have high K_2O/Na_2O ratios. The K_2O contents of the specimens fall in the range 7 to 11 weight percent; only one rock contains less than 8 weight percent K_2O. Only two rocks contain more than 3 weight percent Na_2O. All the analyzed rocks have from 59 to 70 weight percent SiO_2. Since all but two samples contain 15 percent or less modal and normative quartz, they might be called potassic syenites or potassic quartz syenites. The two samples with more quartz are both aplitic rocks.

The Na and K contents of the analyzed specimens of granophyre are probably in general representative of the alkali contents the rocks had at their initial high crystallization temperatures. In many of the granophyres, the feldspars are altered to turbid, low temperature forms with near end-member compositions. These feldspars apparently recrystallized in a hydrous environment at some period after initial granophyre crystallization. The possibility that some of the granophyric rocks were affected by late, lower temperature alkali metasomatism cannot be dismissed. However, three of the rocks analyzed (Ad23h, Ar-Gi-Rcgphr 1-6, and Ad285) have predominately clear feldspars with low optic angles and intermediate Na/K ratios; these clear feldspars show no indications of being affected by lower temperature processes. Since the compositions of these three rocks are similar to those of other granophyres, low temperature metasomatic processes apparently played little part in determining the alkali contents of most granophyres.

Compositional gradients in granophyre lenses

Compositional gradients are present in some of the inhomogeneous lenses of granophyre north of Reynolds Creek. Aplitic granophyre occurs at the tops of some of these lenses; where present, it grades downwards into coarser-grained pyroxene granophyre or into hornblende granophyre. Two samples from each of two vertical sections through granophyre lenses were chosen for complete chemical analyses. In addition, a sample from an aplite dike above one of the lenses was also analyzed. The two vertical sections marked with the locations of the analyzed rocks are shown in Figure 32. Analyzed rocks Ad91b and Ad91c come from pyroxene

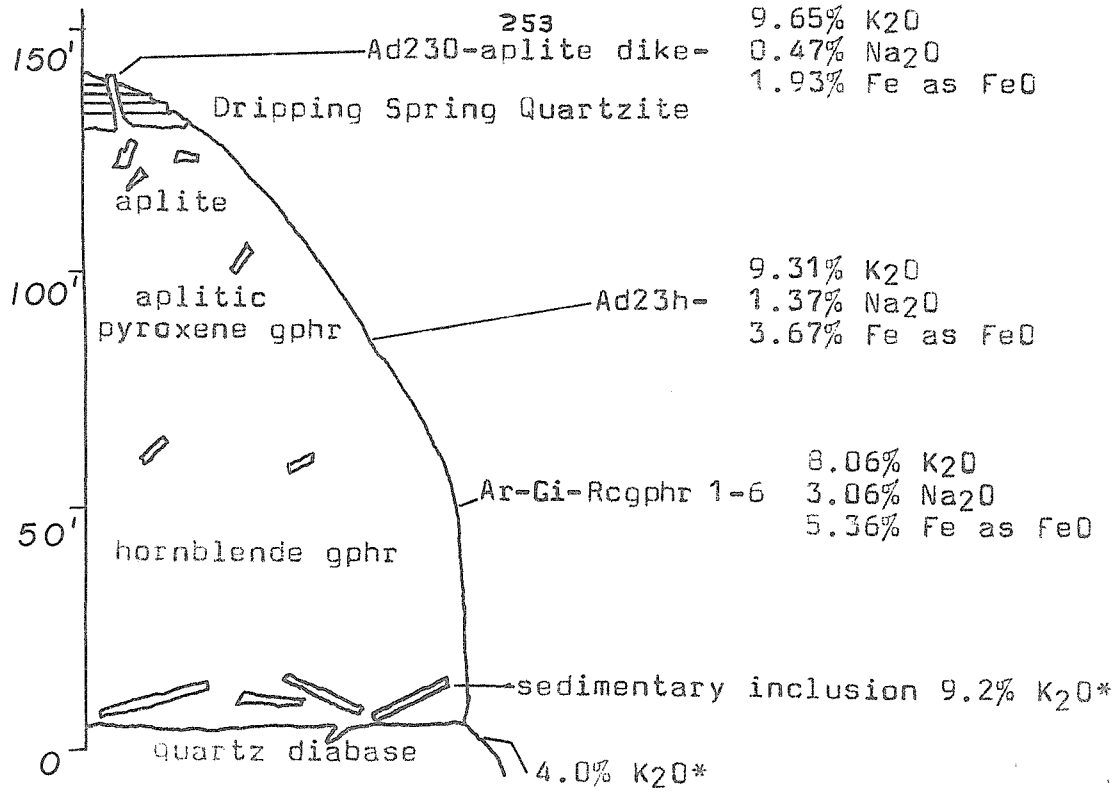

Section through granophyre lens north of Reynolds Creek, just west of Point I, Plate 4.

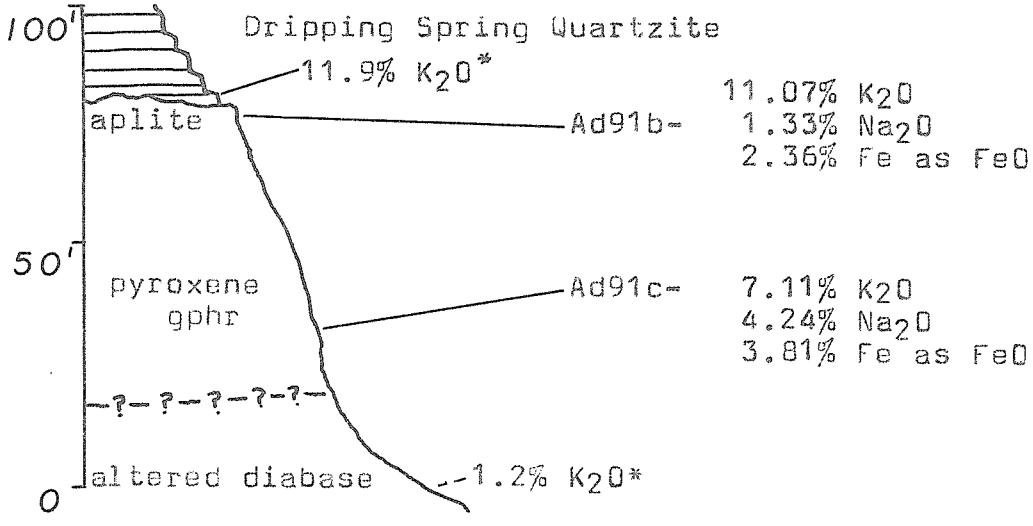

Section through granophyre lens on the north side of the ridge north of Reynolds Creek, east of Point F, Plate 4.

Figure 32. Sections through granophyre (* indicates x-ray fluorescence determination.)

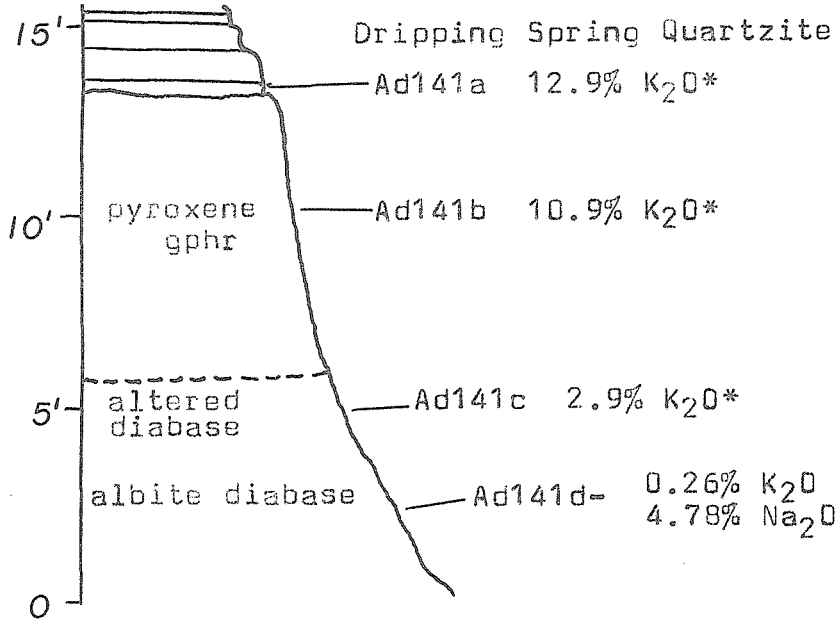

Section through massive granophyric layer on the south bank of Reynolds Creek.

Section through massive granophyric layer north of Workman Creek.

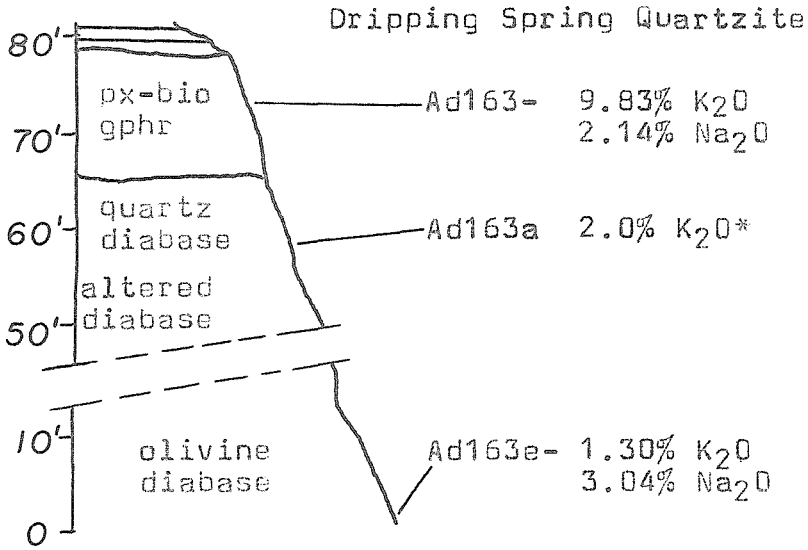

Figure 33. Sections through granophyre (* indicates x-ray fluorescence determination.)

aplite and underlying pyroxene granophyre, respectively. Analyzed rocks Ad230, Ad23h, and Ar-Gi-Rcgphr 1-6 come from an aplite dike, aplitic pyroxene granophyre, and underlying hornblende granophyre, respectively.

In each of the two sections the lower sample contains less potassium, more sodium, and more iron than the sample from higher in the lens. The lower samples also contain less silica, though the percentage difference is not as great as for the other three oxides mentioned above. Disregarding the analyzed dike sample, the two samples from the lower parts of the lenses contain less sulfur than the samples from above them.

The compositional differences shown by the analyses are consistent with mineralogical differences noted in these two sections and in other sections through the granophyre masses north of Reynolds Creek. In general, pyroxene in the lower parts of the lenses is pale green in thin section and is more iron-rich than colorless pyroxene from the upper parts of lenses. Hornblende, which commonly occurs in hornblende granophyre beneath pyroxene granophyre, is more iron-rich than any of the analyzed pyroxenes. Pyrrhotite is common in the upper parts of lenses but is almost absent in the lower parts. Alkali feldspar is more sodic in the rocks lower in the lenses.

Large compositional gradients occur between the granophyric rocks and underlying diabasic ones. The compositional gradients between granophyric rocks and overlying sedimentary rocks are much less severe. The variations of potassium between granophyres and underlying diabasic rocks are greater than the variations of the other elements. Potassium variations in sections through granophyre lenses are shown in both Figures 32 and 33.

Comparison of granophyre, sedimentary rock, and diabase compositions

The compositions of the leucocratic granophyric rocks are similar to those of sedimentary rocks in the upper member of the Dripping Spring Quartzite. However, there are definite compositional differences between the two groups of rocks. Analyses of two sedimentary rocks, one apparently unmetamorphosed (Ad125h) and one recrystallized but still fine-grained and laminated (Ad125r), are included with the granophyre analyses in Table 26. Averages and ranges of analyses of sedimentary rocks in the upper member are shown in Table 30. Approximate ranges of oxide percentages in granophyres, sedimentary rocks, and diabasic rocks are listed in Table 31. For comparative purposes, the granophyre compositions are shown together with sedimentary rock compositions on a silica variation diagram (Figure 34).

The sedimentary rocks have unusually high, distinctive potassium contents. The potassium contents of the granophyres are similar, though somewhat lower, and are also unusually high. The silica contents of rocks in the two groups are much the same, and only one granophyre (Ad230) has a silica content outside the range exhibited by analyses of sedimentary rocks from the gray unit of the upper member. The titanium and iron contents of the two sets of analyses are similar. The CaO and MgO contents of the two rock groups are slightly different, though there is a substantial area of overlap between them. The greatest compositional differences between the granophyres and sedimentary rocks are in Na, K, and S; the granophyres are generally lower in sulfur, higher in sodium, and lower in potassium than the sedimentary rocks.

TABLE 30

Average Sedimentary Rock Compositions[1]
Upper Member, Dripping Spring Quartzite

	Gray Unit (Seven Analyses)			Buff Unit (One Analysis)
	A	B	C	
SiO_2	61.93	66.73	57.9	74.75
TiO_2	0.94	1.31	0.63	0.52
Al_2O_3	14.47	15.64	12.78	11.56
Fe_2O_3	1.47	3.7	0	0.46
FeO	3.28	6.8	0.35	0.14
Fe as FeO	4.60	7.25	2.27	0.55
MnO	0.04	0.08	0	0.01
MgO	0.90	1.8	0.49	0.53
CaO	1.23	2.49	0.4	0.50
Na_2O	0.43	0.87	0.17	0.13
K_2O	12.12	13.40	10.54	9.60
P_2O_5	0.09	0.13	0.04	0.07
S	2.06[2]	2.7	0.93	0.01

A Average values.
B Maximum values.
C Minimum values.

[1] Based on analyses in Table 1 .

[2] Six analyses only.

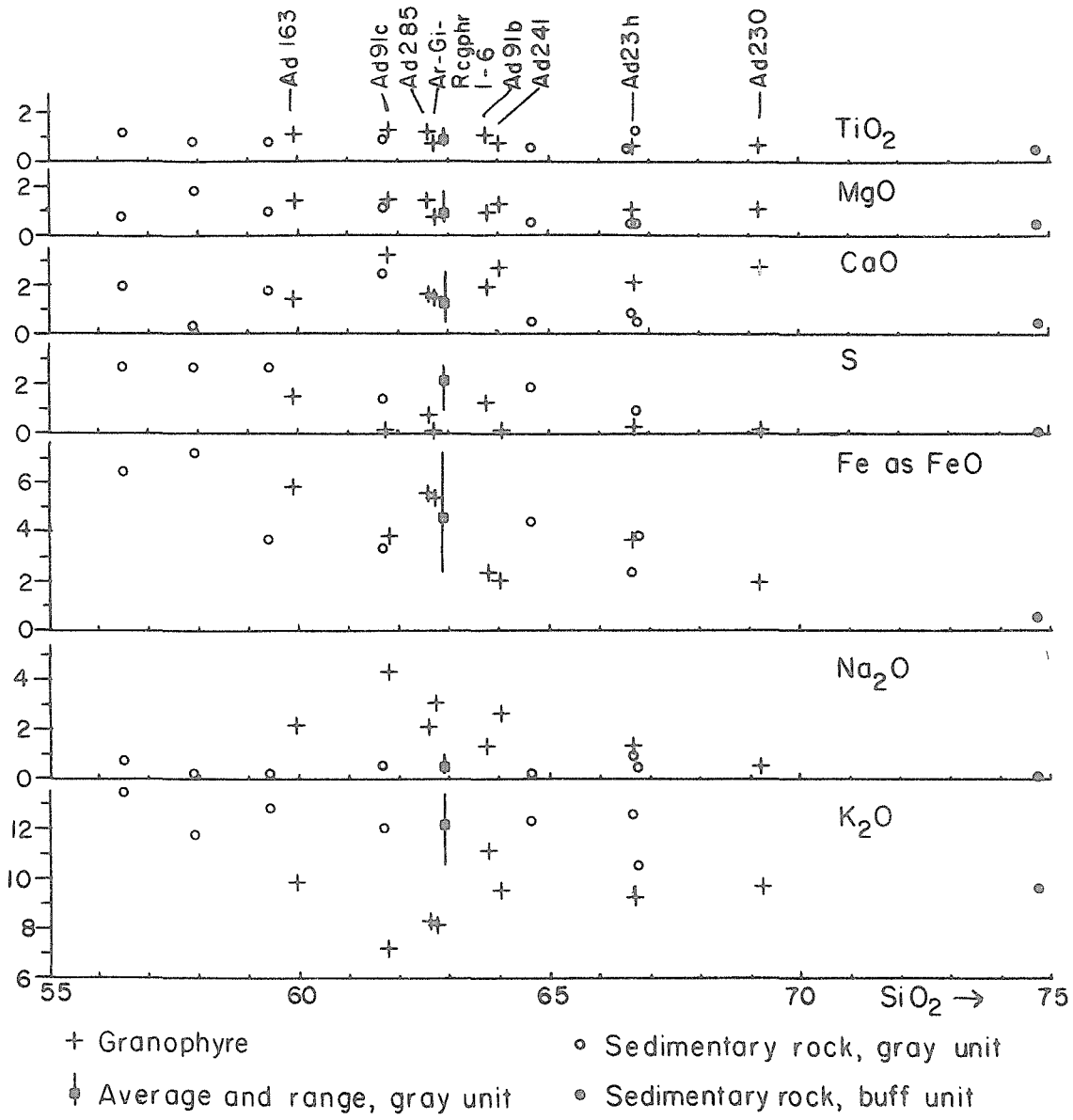

Figure 34. Comparison of granophyre and sedimentary rock compositions on a silica variation diagram.

TABLE 31

Comparison of Diabase, Granophyre, and Sedimentary Rock Compositions

	Approximate Compositional Ranges Weight Percent Oxides				
	1	2	3	4	5
SiO_2	45-48	47-53	53	60-70	57-75
TiO_2	0.6-3.2	2.7-5.6	2.9	0.7-1.3	0.5-1.3
Al_2O_3	16-21	13-16	14	12-15	11-16
Fe as FeO	8-13	7-12	11	2-6	0.1-7
MgO	6-10	3-5	3.1	0.8-1.5	0.5-1.8
CaO	8-10	8-10	5.1	1.4-3.2	0.4-2.5
Na_2O	2.6-3.1	3.6-5.2	4.1	1.3-4.2	0.1-0.9
K_2O	0.3-1.3	0.8-2	3.4	7-11	9-14
P_2O_5	0.1-0.4	0.2-1.2	0.8	0.1-0.3	0-0.2
S	0-0.1	0.1-0.2	0	0.1-1.6	0-2.7

1. Feldspathic olivine-rich diabase and olivine diabase.
2. Coarse-grained segregations and pegmatites.
3. Quartz diabase.
4. Granophyres.
5. Sedimentary rocks, upper member, Dripping Spring Quartzite.

Compiled from analyses in Tables 1, 5, 6, and 26.

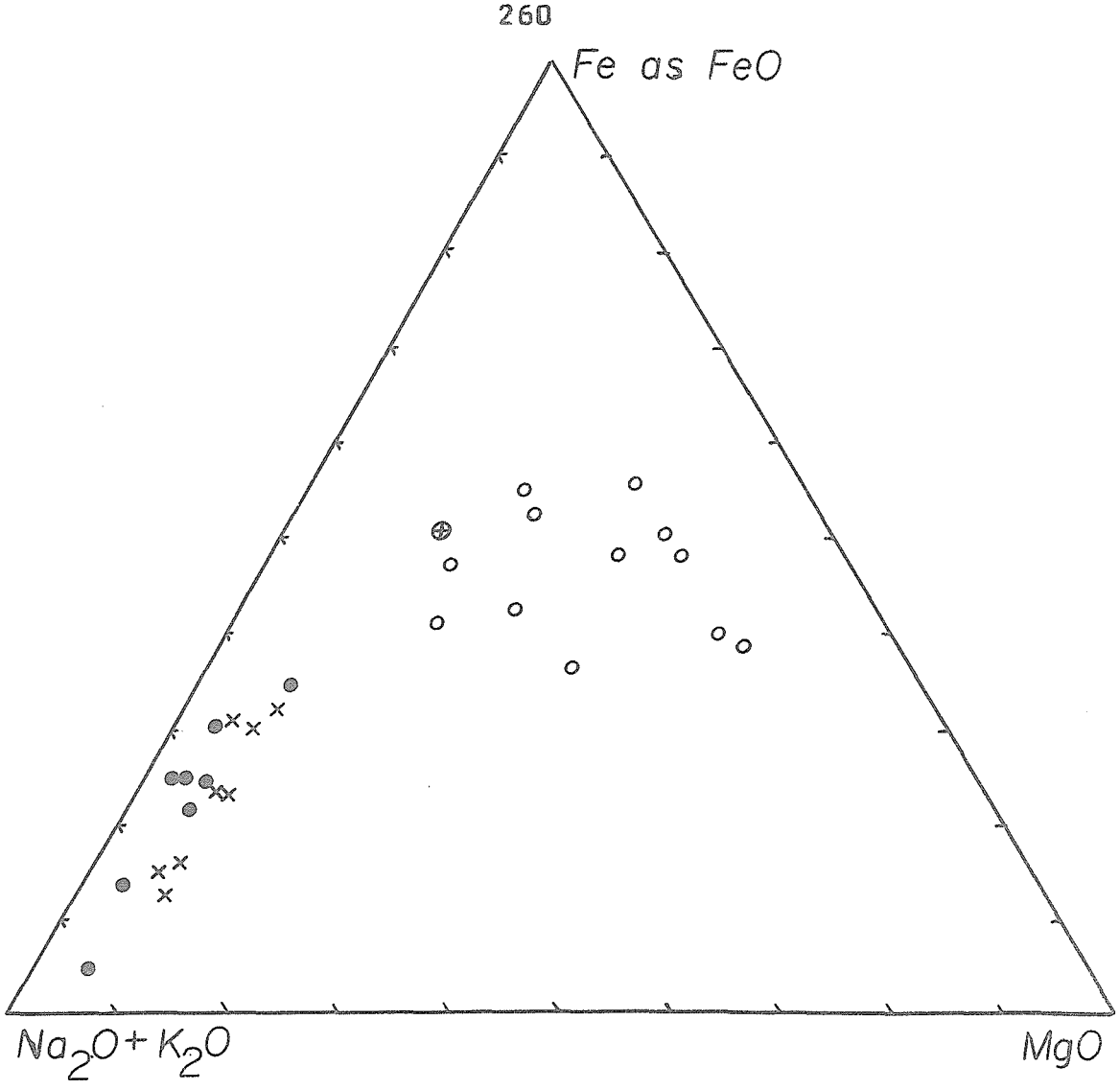

Figure 35. Compositions of sedimentary rocks, granophyres, and diabasic rocks plotted on an AFM diagram, based on analyses in Tables 1, 5, 6, and 26.

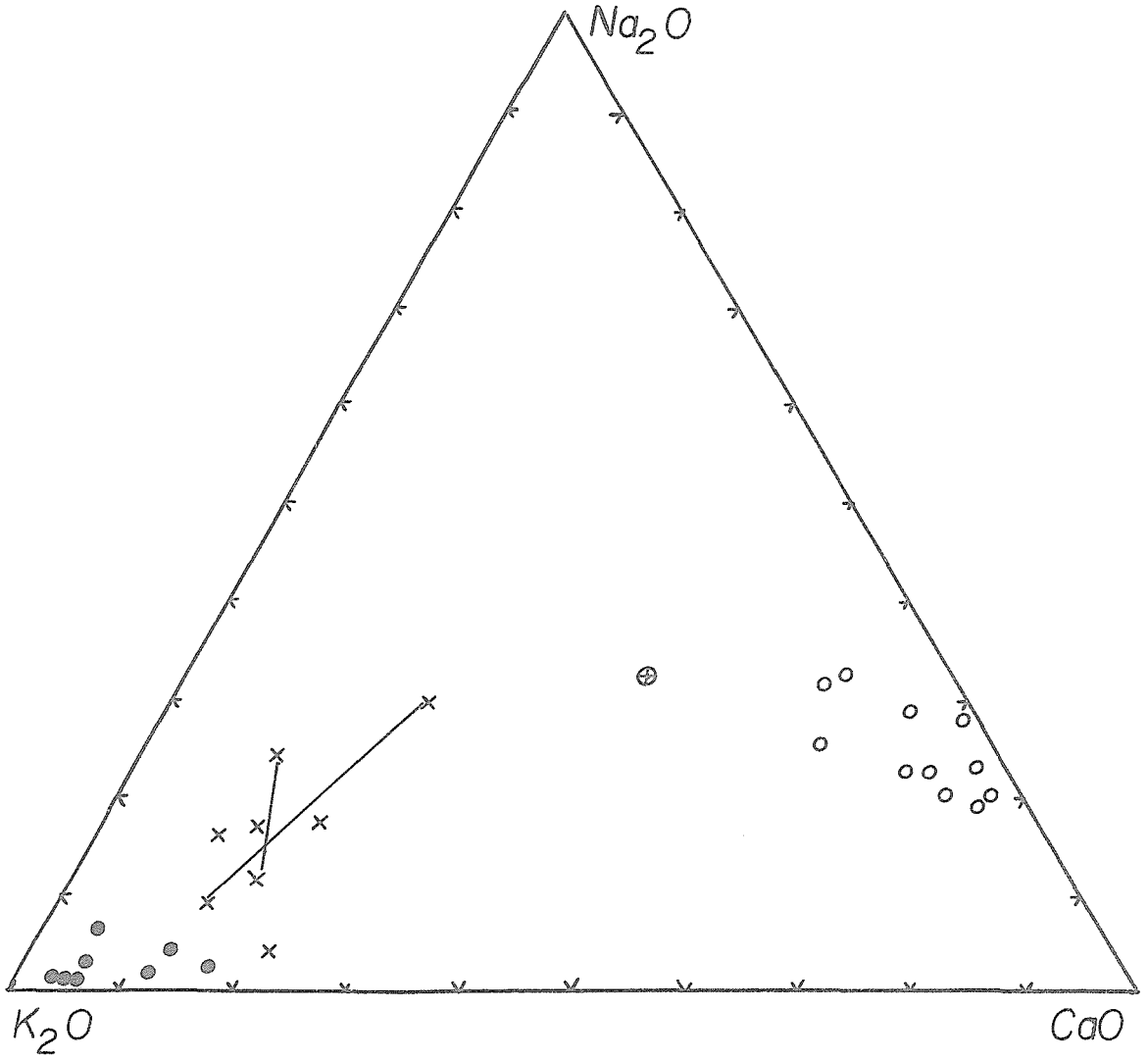

Figure 36. Compositions of sedimentary rocks, granophyres, and diabasic rocks plotted on an Na_2O-K_2O-CaO diagram, based on analyses in Tables 1, 5, 6, and 26. The two lines join points in the same vertical section. The more potassic points in both sections are nearer the sill roof.

The analyzed granophyres are distinctly different in composition from the analyzed diabasic rocks. The compositional ranges of the two groups of rocks are shown in Table 31. The greatest compositional differences are in potassium, calcium, and silica.

Some of the important compositional similarities and differences between the granophyres, sedimentary rocks, and diabasic rocks can be seen most readily on traditional AFM and Na_2O-K_2O-CaO diagrams (Figures 35 and 36). The diagrams illustrate that:

(1) the granophyres are quite different in composition from the diabasic rocks;

(2) they are quite similar in composition to the sedimentary rocks;

(3) there are, however, some distinct compositional differences between the granophyres and sedimentary rocks.

On both triangular diagrams there is a distinct gap between the compositions of the granophyres and the diabasic rocks. The break is most apparent on the Na_2O-K_2O-CaO diagram. Both Williams (1957) and Neuerburg and Granger (1960) present analyses of rocks which partially fill the gaps. These analyses are plotted on the triangular diagrams with the other analyses in Figure 37. Points 1, 2, and 3 in Figure 37 represent analyses of rocks from a drill core through the roof of the sill complex in Workman Creek. The analyses were reported by Williams (1957, Appendix I). Williams (1957, Appendix III) describes the samples as recrystallized Dripping Spring Quartzite (Point 1), coarse-grained diabase from about five feet below the first sample (Point 2), and diabase pegmatite from about thirty feet below the first sample (Point 3). Points 4 through 8 in Figure 37 represent "syenite" and "aplite" analyses reported by Neuerburg and Granger (1960, Table 5). No petrographic descriptions

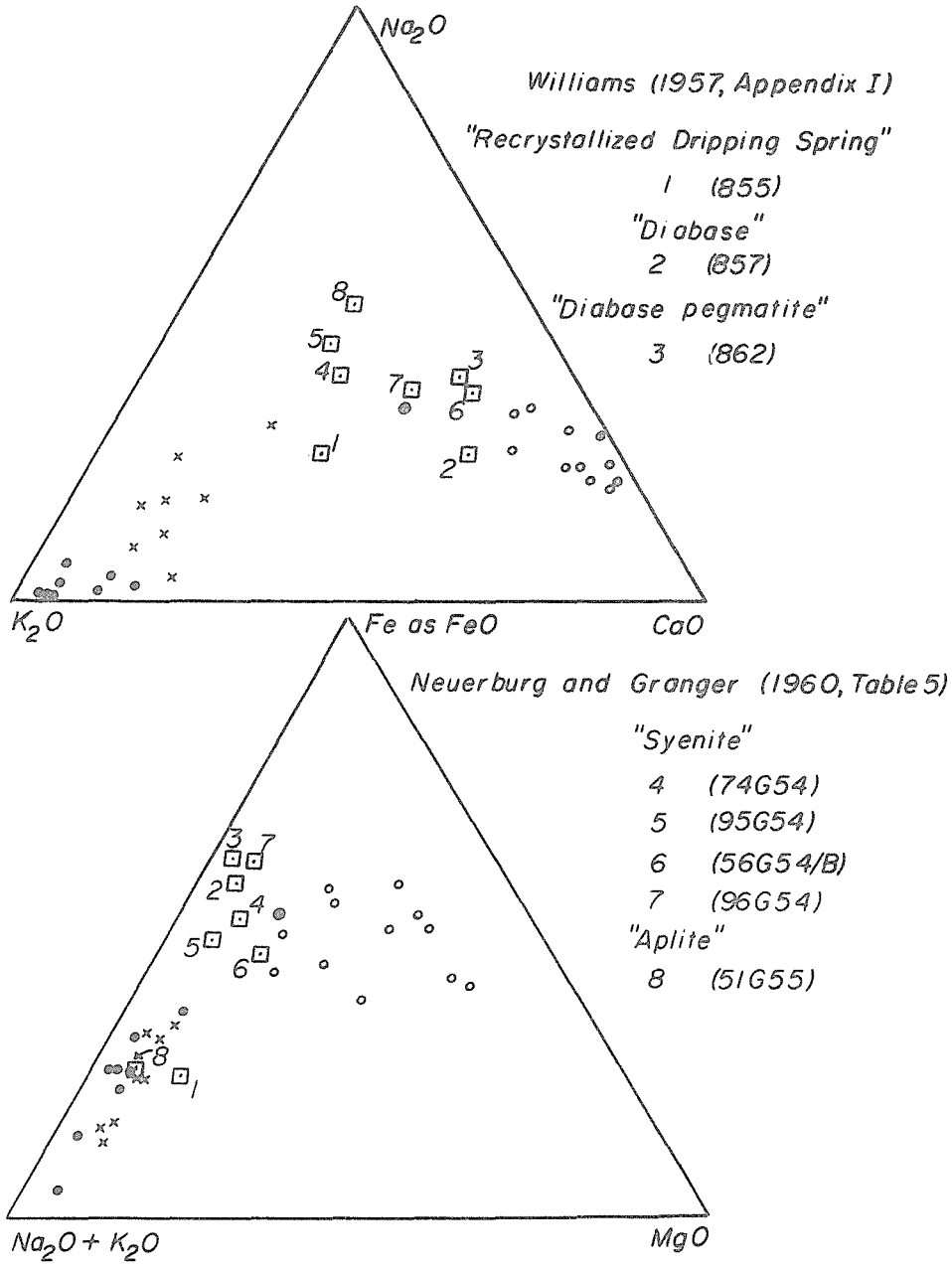

Figure 37. Compositions of rocks of uncertain nature and origin reported by Williams (1957) and Neuerburg and Granger (1960) plotted on AFM and Na_2O-K_2O-CaO diagrams. Compare with Figures 35 and 36.

of the analyzed samples are available and only a limited discussion of "syenite" and "aplite" is presented by Neuerburg and Granger (1960, pp. 768-769). They do indicate that the two rock types are most commonly found in lenses and dikes a maximum of several meters thick which occur near and at the roof of the sill complex. Three of their samples come from the Workman Creek area and two from near the southern boundary of the McFadden Peak quadrangle.

As is evident in Figure 37, it is possible that rocks having a continuous range of compositions from olivine diabase to granophyre may be present in the sill complex. However, the actual volume of intermediate rock must be very small, and any intermediate rocks present appear to be localized near the sill roof.

Source of the Granophyres

The leucocratic, granophyric rocks were apparently derived largely from sedimentary rocks from the Dripping Spring Quartzite. One powerful argument which leads to this conclusion is the compositional similarity between the sedimentary rocks in the upper member of the formation and the granophyres. The sedimentary rocks have almost unique, highly potassic compositions. The granophyres have similar K-rich compositions. The extraordinary potassium contents of rocks in the two groups are strong evidence in favor of the hypothesis that the granophyres are derived from the sedimentary rocks. The compositions of the granophyres are also similar to those of the sedimentary rocks in other respects, and they are quite different from those of the bulk of diabasic rocks in the sill complex. Highly potassic rocks like the granophyres would not be expected to form as

normal differentiates of a magma like that which crystallized to form the bulk of diabasic rocks in the sill complex; though the compositions of the typical diabasic rocks of the sill complex are not unusual, the compositions of the granophyres are almost unique.

There are strong textural and mineralogical similarities between the massive granophyres and recrystallized rocks of obvious metasedimentary origin. The similarities argue as powerfully for derivation of the granophyres from sedimentary rocks as do the compositional similarities.

Sedimentary rocks above the sill roof locally recrystallized to laminated rocks with intricate intergrowths of quartz and alkali feldspar; in some laminated rocks the intergrowths form true micrographic textures. Locally at the sill roof where the diabase is in contact with the black facies of the upper member of the Dripping Spring Quartzite, there is a continuous transition down towards the sill roof from apparently unrecrystallized sedimentary rocks above to rocks with coarsely recrystallized lamellae to completely recrystallized rocks forming concordant layers a few feet thick in contact with diabase. The completely recrystallized metasedimentary rocks are texturally similar to many of the massive granophyric rocks. The recrystallized, laminated rocks are developed best near Workman Creek, where they have also been described by Williams (1957, p. 74), Granger and Raup (1959, pp. 429-431), and others.

The mineralogy of many of the granophyric rocks is similar to that of many of the obviously metasedimentary rocks. Alkali feldspar, pyroxene, biotite, quartz, and sulfides are major phases common to both granophyres and metasediments. Pyroxene compositions in metasedimentary rocks and some granophyres are nearly

identical. The only major mineral occurring in the granophyres and not in the metasedimentary rocks is hornblende.

The types of granophyre may differ from one another in part because they may have formed from different units of the upper member of the Dripping Spring Quartzite. The gray unit of the upper member appears to have recrystallized more readily than the buff and white units. Both pyroxene and biotite formed in obviously metasedimentary rocks from the gray unit. Where granophyres are best-developed north of Reynolds Creek and on the southwest flank of Grantham Peak, they are intruded directly against the buff and white units and the gray unit is missing. The lens of pyroxene-biotite granophyre on the north and northwest slopes of Grantham Peak contains inclusions of rock resembling the black facies of the gray unit and also contains abundant pyrrhotite. The pyrrhotite may have formed from pyrite in the black facies. These observations suggest that the bulk of the granophyres may have been derived from the gray unit of the upper member of the Dripping Spring Quartzite.

Leucocratic aplite occurs in abundance only where the granophyre masses are intruded against overlying buff or white units of the upper member. Rocks from the buff and white units generally contain more visible quartz than those from the gray unit, and the only analyzed sample from the buff unit is distinctly more silica-rich than all the analyzed samples from the gray unit (Table 30). The analyzed aplites in the upper parts of granophyre masses (Ad23h, 91b, and 230) are more silica-rich than all but one of the other granophyre samples (Table 26). The leucocratic aplites in the upper parts of the inhomogeneous granophyre lenses may have been derived largely from rocks of the buff and white units with which they are in contact.

The hornblende granophyres cannot be so readily related to a specific unit in the upper member of the Dripping Spring Quartzite. They may have been derived largely from rocks from the gray unit. However, hornblende is rare in the obviously metasedimentary rocks.

Chemical Interactions between Diabase and Sedimentary Rocks

The systematic compositional differences between the granophyres and the sedimentary rocks from which they were derived must be due to an interaction between the sedimentary rocks and diabase magma. The interaction might have occurred either by a physical mixing of diabase magma with sedimentary rock material or by transfer of material in a vapor phase between diabase and granophyre.

Physical mixing between diabase and sedimentary rocks

Quartz diabase probably in part is the product of physical mixing and assimilation of sedimentary rock material in diabase magma. The quartz diabase mass on the north slope of Grantham Peak contains xenoliths which appear to be recrystallized fragments of sedimentary rocks. In other places recognizable xenoliths in diabase are very rare. However, the quantities of quartz diabase observed in other places are relatively small.

A physical mixing of diabasic magma with fused sedimentary rocks is one possible explanation to account for the compositional differences between sedimentary rocks and granophyres. Using the potassium contents of sedimentary rocks and diabasic ones

as a guide, even the least potassic granophyres are probably at least half sedimentary rock material. The hornblende granophyres are least like any of the obviously metasedimentary rocks and are the most likely granophyric rocks to have been affected by mixing. However, it seems unlikely that mixing was effective to a significant degree in determining the compositions of any of the leucocratic granophyric rocks. Both field relations and chemical data argue against it.

No field evidence is preserved of any significant amount of mixing of diabasic magma with sedimentary rock material in the granophyre masses. Recognizable inclusions of diabasic rock in granophyre are extremely rare. All contacts observed between the leucocratic granophyric masses and the darker-colored diabasic rocks are sharp, not gradational.

Chemical data indicate that compounding of sedimentary rock compositions with the compositions of any of the common diabasic rock types in the sill complex will not yield compositions like those of the granophyric rocks. These compositional relationships are particularly apparent on the ternary Na_2O-K_2O-CaO diagrams (Figures 36 and 37). There are very few "diabasic" rocks with compositions which, when compounded with sedimentary rock compositions, could yield rocks with alkali contents like those of the granophyres. The only ones with appropriate compositions are from several of the thin "syenite" and "aplite" dikes and lenses analyzed by Neuerburg and Granger (1960).

Metasomatic movement of material between diabase and granophyre

Vapor transfer of material between diabase and granophyre may be the explanation for the compositional differences between the granophyres and the sedimentary rocks from which they were largely derived. The physical and chemical conditions at the upper contacts of the diabasic rocks may well have been favorable for metasomatism to occur. Large temperature gradients must have existed at the contacts of the sill, as diabase magma with an initial temperature near 1200°C was intruded into sedimentary rocks which were initially probably below 100°C. The large compositional gradients existing between sedimentary rocks, granophyre, and diabasic rocks are illustrated by the analyses of samples shown in the sections in Figures 32 and 33. The diabasic rocks are not chilled but are rather coarser-grained at most of the diabase-granophyre contacts. A vapor phase was present in the granophyres, as shown by the occurrence of miarolitic cavities in them.

The most obvious compositional differences between the granophyres and sedimentary rocks involve sodium and potassium. The granophyres are more sodic and have higher Na/K ratios than the sedimentary rocks. In the lenses north of Reynolds Creek, granophyres closer to the diabase are more sodic than granophyres above them. Granophyres which are higher in sodium are lower in potassium, and metasomatism may have taken place by alkali exchange between feldspars and vapor. By comparison to the sedimentary rocks, one granophyre sample appears to have gained about 3 percent Na_2O, and gains of 1 to 2 percent appear to have been common. The sodium was presumably derived from the diabase, and potassium probably moved into it.

Most of the granophyres contain less sulfur than sedimentary rocks in the gray unit of the upper member of the Dripping Spring Quartzite. Sulfur may have been transported from the granophyres. The granophyres as a group are slightly higher in calcium and magnesium than the sedimentary rocks, and these elements may have moved to the granophyres from the diabase. The silica contents of the sedimentary rocks cover a wide range of values, and the data are insufficient to indicate whether or not silica was moved. It may have been added to the quartz diabase in contact with the granophyres. Titanium and aluminum apparently were unaffected by metasomatic processes.

Comparisons of granophyre and sedimentary rock compositions indicate that iron was not transported to the granophyres on a large scale. However, the variations in iron content in two vertical profiles through the granophyres (Figure 32) suggest some iron was contributed by the diabase. The occurrence of iron-rich amphibole in the lower parts of some lenses also suggests that iron was added from the diabase. Hornblende granophyre is generally closer to the diabase heat source than pyroxene granophyre in the lenses at the sill roof, and its presence is difficult to explain on a physical basis. Since hornblende has a considerably higher (Fe +Mg)/Ca ratio than calcic pyroxene, it is possible that the hornblende formed in response to metasomatic introduction of Fe into the lower parts of the granophyre masses. Thin veins and pods of magnetite are locally present in the Mescal Limestone. As noted by Shride (1967, p. 64), the magnetite veins may have formed from iron furnished by the diabase, but there is no positive evidence for this hypothesis.

The movement of K and Na between the granophyres and diabasic rocks can be partly interpreted in light of the experimental work of Orville (1963). He showed that alkali exchange occurs readily between feldspars and a vapor phase. He also demonstrated that the K/Na ratio in equilibrium with either a single potassic feldspar or with two coexisting feldspars decreases with decreasing temperature. Because of the decreasing ratio, K tends to diffuse down a temperature gradient in a vapor in equilibrium with two alkali feldspars. However, the initial K/Na ratio in the granophyres apparently was sufficiently great that Na moved into the granophyre. The quartz diabase below granophyre became enriched in K, perhaps by both assimilation of sedimentary rock inclusions and by vapor phase transport. However, as the diabase cooled, some K was probably removed from intensely altered diabase and albite diabase, perhaps into the sedimentary rocks. This later and less significant K movement may have taken place in response to a temperature gradient according to the mechanism outlined by Orville.

Possible low temperature alkali metasomatism of the granophyres

The chemical compositions of most of the granophyric rocks were probably fixed during the period of their initial high temperature crystallization. The granophyres with predominately clear, high-temperature feldspars are similar in bulk composition to granophyres with mostly turbid feldspars. However, it is possible that alkali exchange metasomatism may have affected the compositions of some of the granophyric rocks under lower temperature conditions after their initial crystallization. Taylor (1968, p. 66) has shown that turbid feldspars in many granophyric rocks have apparently undergone

oxygen isotope exchange with late-stage solutions, and he has suggested that cation exchange between solutions and feldspars may also have occurred in such rocks. O'Neil and Taylor (1967, p. 1433-1435) have suggested that cation exchange and oxygen exchange between feldspars and solutions proceed together.

Granger and Raup (1959, p. 429) and Neuerburg and Granger (1960, p. 769) describe several thin "aplite" dikes in the Workman Creek drainage which change composition as they cross the contact between the diabase and overlying sedimentary rocks. The dikes are rare, and they form an insignificant fraction of the rocks in the sill complex. Albite, the dominant feldspar in these dikes within the diabase, is apparently replaced by K feldspar near the point where they cross the contact (Neuerburg and Granger, 1960, p. 769). The rocks in these dikes may have been affected by alkali metasomatism occurring under deuteric conditions.

Sample Ad241 (Table 26) is from a ten-inch-wide dike in diabase exposed in a roadcut near the sill roof in Workman Creek; the dike was not observed to extend into the overlying sedimentary rocks. This dike may in part be similar to parts of some of the dikes described by Neuerburg and Granger. Some feldspar grains in the dike consist of almost pure albite rimmed by nearly pure K feldspar, and others consist of patchy intergrowths between the two phases. Both feldspar phases are somewhat turbid. Micrographic quartz-K feldspar intergrowths are common, as are skeletal calcic pyroxene and skeletal zircon crystals. The feldspar textures might indicate replacement of albite by K feldspar, but they might also be the result of exsolution from homogeneous alkali feldspar crystals. The composition of the analyzed sample is very similar to those of some of the normal granophyres. It is

possible that these dikes represent sedimentary rock material intruded into the diabase and Na metasomatized by it at high temperatures. Potassium may have been partly eliminated from some of the dikes during the same period of deuteric crystallization which affected the albite diabase.

Possible metasomatic effects in layered metasedimentary rocks

Possible major element metasomatism by the diabase was apparently limited almost completely to the thick lenses of igneous-looking, massive granophyric rocks. Recrystallized but laminated metasedimentary rocks a few feet above the roof of the sill complex are essentially identical in composition to apparently unrecrystallized rocks far removed from diabase, as shown by a comparison of analysis number 4 with the other analyses in Table 1. Possible major element metasomatic effects in the thin layers of granophyric "hornfels" created from the black facies at the sill roof in the Workman Creek area are extremely limited. Granger and Raup (1959, p. 434) and Williams (1957, p. 75) concluded that there was "very little" difference in composition between the "hornfels" and unrecrystallized sedimentary rocks. However, on the basis of semiquantitative spectographic analyses, Granger and Raup (1959, p. 431) also stated: "Metamorphism from siltstone to hornfels has apparently resulted in loss of potassium and magnesium and gain of sodium and calcium." On the basis of more numerous and more precise chemical analyses, Williams (1957, p. 75) could conclude only that CaO "may have moved" from diabase to recrystallized sedimentary rocks. All the data show that the differences in composition between unrecrystallized sedimentary rocks and laminated,

recrystallized rocks and thin layers of granophyre are very small. Metasomatic transfer of major elements from the diabase to country rock with recognizable sedimentary textural characteristics was negligible.

The evidence for minor element metasomatism by the diabase is controversial. Uranium deposits are systematically found in the gray unit of the Dripping Spring Quartzite near diabase intrusives. Neuerburg and Granger (1960) suggested that the uranium was derived from the diabase. Williams (1957) suggested the uranium was concentrated from the surrounding sedimentary rocks.

Possible metasomatism of recrystallized sedimentary rocks by diabase in the Karroo province

Granophyric, recrystallized sedimentary rocks associated with the Karroo dolerites may also show metasomatic changes. These changes have been summarized by Walker and Poldervaart (1949, pp. 679-683). They thought that, in general, Mg and Fe were added to the recrystallized sediments and Si was subtracted from them. In particular cases they thought that additions and losses of Na, K, Ca, and Ti occurred. They attributed the variability of the metasomatic effects to transfusion by various compositions of emanations from the diabase, the compositions depending on the stage of differentiation of the diabase. Evidence for series of emanations is poor, and it is more likely that metasomatic changes depend on the initial compositions of the sedimentary rocks and on the temperature gradients present. The Karroo studies do suggest that granophyric recrystallization of sedimentary rocks by diabase intrusives may be commonly accompanied by material transfer, presumably in a fluid phase.

The Granophyres as Melts

Rheomorphism, mobilization and fusion

Several lines of evidence indicate the granophyres were largely derived from sedimentary rocks. Yet, the granophyric rocks in the thick lenses have undoubtedly flowed. They have igneous textures and igneous mineral assemblages and have no recognizable relict sedimentary bedding or layering. The granophyres locally have abruptly discordant contacts with the overlying sedimentary rocks, and dikes of aplitic granophyre cut the strata. The granophyres contain rotated and displaced inclusions of sedimentary rocks.

Mountain (1944, 1960) and Walker and Poldervaart (1942, 1949) have suggested from their studies on the Karroo diabases that sedimentary rocks at the margins of diabase intrusives may be mobilized or flow with some small undefined degree of melting or even simply by plastic flow. Such processes of movement are variously called rheomorphism or mobilization. Rheomorphism has been defined (Walker and Poldervaart, 1949, p. 675) as covering "...all processes whereby sediments are fused sufficiently as to become capable of flow." Some other definitions are more restricted, such as one by Frankel (1967, p. 91) which defines rheomorphism as "...the transfer of country rock in a plastic state into the igneous body...accompanied by the addition of various amounts of migrating mineral." The term "mobilization" seems preferable to "rheomorphism", as the former simply implies movement. The cause of movement, whether fusion, plasticity, or disaggregation of the moved sedimentary rock, can be specified.

Most of the cases of mobilized sedimentary rocks described from the Karroo province are relatively small scale occurrences. Dikes of mobilized rock veining the diabases are rarely greater than two feet wide and are commonly made of only slightly recrystallized rock (Mountain, 1944, p. 107). Rather than being intruded by plastic flow, such dikes were probably intruded as masses of particles disaggregated by a vapor phase, as was the thin clastic dike in diabase described by Walton and O'Sullivan (1950). In some cases in the Karroo, tabular masses of sedimentary rock as great as seventy feet thick (Walker and Poldervaart, 1942, p. 288) have been converted to granophyric rock similar in many mineralogic respects to the Sierra Ancha granophyres. However, in these masses relict bedding or stratification is commonly preserved, and evidence of flow or rheomorphism is generally confined to small veins a few feet in width at diabase-granophyre contacts. In short, mobilization of sedimentary material as described at the borders of Karroo diabase masses does not approach in scale the mass movement of granophyre which locally occurred above the Sierra Ancha diabase sill.

Textural and field evidence combined make it seem probable that the massive granophyric rocks in the thick lenses in the Sierra Ancha complex were largely liquid. The intrusive nature of the aplite dikes and of some of the granophyre masses can most easily be accounted for by the assumption that a fluid magma was present. There is little textural evidence that the granophyric rocks deformed plastically; the rocks do not have the deformed fabrics commonly associated with plastic flow. The apparent chilled margins, an inch or so wide, at some aplite-metasedimentary rock contacts are positive evidence in favor of the hypothesis that some of the aplite was almost

entirely liquid. The concentration of large inclusions described at the base of one hornblende granophyre lens can be explained by the hypothesis that they settled through a liquid mass and came to rest above mostly-solidified diabase. Flow of a magma, not rheomorphism or plastic flow, seems the most likely explanation for the intrusive features of most of the Sierra Ancha granophyres.

Melting temperatures deduced from bulk rock compositions

Approximate melting temperatures for the granophyres can be deduced from their bulk chemistry. Orthoclase, albite, and quartz make up 80 to 87 percent of the norms of the eight analyzed specimens (Table 26), and so the rock compositions can be approximately expressed in the system Or-Ab-SiO_2. Experimental data on the system are available for various water pressures (Tuttle and Bowen, 1958; Shaw, 1963). One kilobar is a probable maximum for the load pressure on the granophyres during crystallization, and the presence of miarolitic cavities indicates vapor pressure attained load pressure during crystallization. The granophyre compositions, expressed in terms of their normative quartz, albite, and orthoclase have been plotted on a projection of the liquidus surface of the system Or-Ab-SiO_2-H_2O at one kilobar pressure (Figure 38). The average composition of sedimentary rocks of the gray unit of the upper member has also been plotted on the diagram.

The relationships in the ternary diagram in Figure 38 indicate that the granophyres would begin melting at temperatures in the neighborhood of 740°C. Melting would be completed in the vicinity of the temperature interval 900°-950°C. A rock of the average composition of the gray unit of the Dripping Spring Quartzite

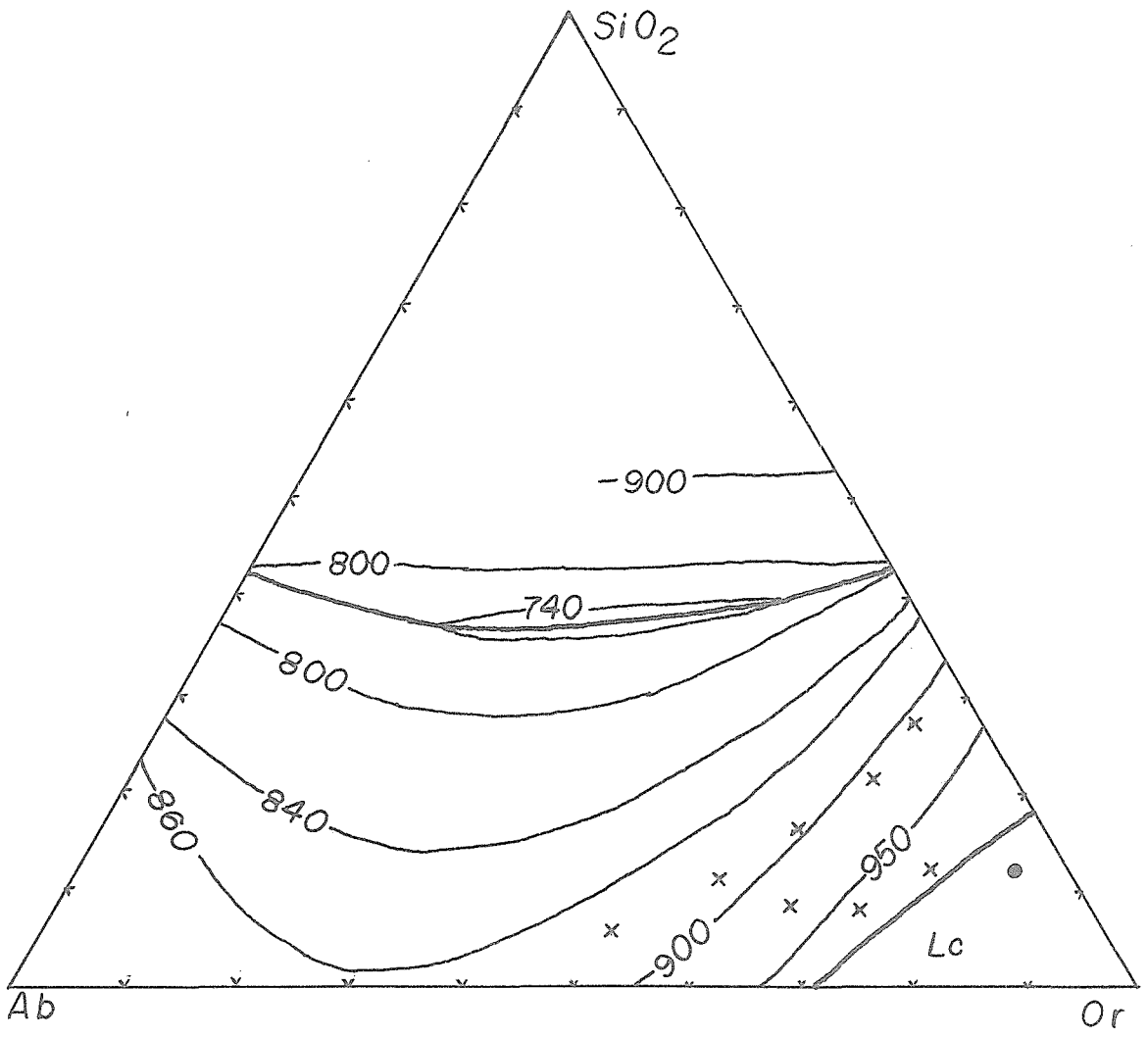

Figure 38. Normative compositions of granophyres plotted on a projection of the liquidus surface of the system Ab-Or-SiO_2-H_2O at one kilobar pressure. Liquidus data from Tuttle and Bowen (1958) modified according to work by Shaw (1963).

would have a similar solidus temperature and a slightly higher liquidus temperature. Uncertainties in the water pressure present do not affect these estimates by more than a few tens of degrees, as Tuttle and Bowen (1958, p. 56) indicate that the rate of change of melting temperatures in the system with water pressure is relatively small at water pressures greater than half a kilobar. The presence of other constituents probably would also only affect the temperatures a few tens of degrees.

The indicated temperatures of melting are so high that it may not seem reasonable that the granophyres were largely molten, though field evidence suggests that they were. However, it is perhaps more than a coincidence that the two-feldspar geothermometer discussed earlier suggests that feldspars in two of the granophyres crystallized at temperatures in the vicinity of 900°C. The problems of heat transfer associated with the hypothesis that the granophyres were largely molten are examined later.

The distribution of granophyre compositions plotted on the ternary diagram is consistent with the conclusion that the granophyres are not differentiates of the diabase. The compositions are near neither the ternary eutectic nor the low temperature trough, in contrast to what would be expected if the granophyres were simple magmatic differentiates.

Melting of Wall Rocks and the Cooling History of the Diabase Sill

The role of water

The Sierra Ancha sill complex has certain unusual features which can be attributed to interaction between the diabase magma and water from the sedimentary country rocks. Mineral composition trends in the best-exposed section through the upper part of the dia-

base indicate that crystallization proceeded towards the sill roof; rocks nearer to the top crystallized after rocks lower down (Figure 28). In some places no fine-grained, chilled facies caps the diabase; rather, the diabase at the roof contains quartz and is coarser-grained than the rock below it. The coarser-grained rock was probably contaminated by constituents from the overlying sedimentary rocks, but it is also in part a late-crystallizing, iron-enriched differentiate of the diabase. In these places, leucocratic granophyres were formed from the sedimentary rocks; these sedimentary rocks apparently were at least partially melted by the diabase. Diabase near the margins of the sill, particularly that near the sill roof, underwent extensive deuteric alteration. All these features can be explained by the hypothesis that the mafic magma absorbed water from the surrounding sedimentary rocks.

The possible importance of water on the cooling history of an intrusive was emphasized by Kennedy (1955). He suggested that if a relatively hot, dry magma were intruded into wet sedimentary rocks, the partial pressure of water in the rock bordering the intrusive would rise and water might diffuse into the outer parts of the magma body. Since crystallization temperatures of magma are lowered by the addition of water, crystallization might well begin in the hotter but dryer central portions and proceed towards the cooler but wetter margins. This process seems to have taken place locally in the upper part of the Sierra Ancha diabase. The presence of miarolitic cavities in the granophyres suggests that the sedimentary rocks were wet and proves that the vapor pressure in the granophyres rose till it exceeded load pressure. No chilled facies separates the diabase from most granophyric rocks, so there was no barrier to the diffusion of water into the magma. The observed

mineral composition trends indicate crystallization did take place towards the roof in at least one locality. The observed crystallization trends are compatible with Kennedy's theoretical hypothesis.

The hypothesis that the Sierra Ancha diabase magma absorbed water from the overlying sedimentary rocks is made more plausible by recent studies of basaltic rocks reported by Taylor (1968). He found that some mafic rocks in the Scottish Tertiary igneous province and in the Skaergaard intrusion have unusual oxygen isotope abundances in comparison to analogous rocks. He concluded that (op. cit., p. 66): "...many of the rocks in these localities have been contaminated or exchanged with meteoric water while they were still magmas." Taylor's work shows that the absorption of water from country rocks by mafic magmas may not be an uncommon process.

Cooling history of the sill and wall rock temperatures

Theoretical calculations provide some insight into the time it took the diabase to crystallize and into the temperatures reached in the granophyric rocks overlying the sill. The calculations provide only very general guidelines for the Sierra Ancha sill because of the following complications. First, the sill is probably a multiple intrusion; while the olivine diabase layers were probably intruded largely as liquids, the feldspathic olivine diabase layer may have been intruded as a crystal-liquid mush. Second, the effects of vapor movement and melting in the country rocks cannot be taken into account easily. Third, heat loss from the diabase depends on just how the sill crystallized, a process imperfectly known. Fourth, thermal constants for the sedimentary rocks can only be roughly

TABLE 32

Calculated Solidification Times for the Sierra Ancha Diabase Sill Complex

(Sill thickness = 250 meters)

I "Complete convection"- magma temperature uniform during solidification.
(Formula from Jaeger, 1964, pp.455-456.)

Crystallization Range (°C)	Solidification Time (years)
1200-900	320
1200-950	280
1150-950	240

II Fixed melting temperature, no convection.
(Formula from Jaeger, 1964, p.453.)

1200	410
1100	440

III No convection, no latent heat.
(Formula from Jaeger, 1967, p.508.)

1200-900	280

For all calculations, densities and thermal diffusivities of country rock and diabase were assumed equal. The following constants (cgs) were used:

thermal diffusivity	0.007
specific heat of country rock	0.25
specific heat of magma	0.3
latent heat of fusion of diabase	100

Values from Jaeger (1964).

estimated. Despite these complications, the calculations do indicate limits on wall-rock temperatures attained and place constraints on the amount of sedimentary rock melting and metamorphism possible.

The magma must have completely solidified by some time between about 300 and 800 years after intrusion. The minimum times are determined by the two cases where the magma is assumed to have no heat of crystallization (III, Table 32) and where the magma is assumed to convect perfectly so that the sill margins are always at the maximum possible temperature (I, Table 32). This last assumption of perfect convection approximates the case where a sill cools completely from the center outwards. A sill in which the magma has a fixed melting point and does not convect would solidify in about 400 years (II, Table 32). Jaeger (1967, p. 524) shows that a sill containing nonconvecting magma crystallizing over a reasonable temperature range would solidify in about twice the time of a sill with a fixed melting point, or in about 800 years. This time of 800 years must be high both because the Sierra Ancha sill in part did cool towards the roof and because the central zone in the sill was probably intruded as a liquid-crystal mixture. Though the exact solidification time cannot be determined, the range of times can be used as guides for calculations estimating possible temperatures in the sedimentary rocks near the sill roof.

Calculations of temperature profiles in the sedimentary rocks near the sill provide only very general guides to the temperatures actually attained. These temperatures depend on whether most of the sill cooled from the margins or from the center. They depend upon the rate at which it was emplaced. They also depend on the amount of water heated by the intrusion and on how the water moved. Heat absorbed by fusion and subsequently released by recrystallization

of sedimentary rock material would affect temperature profiles outside the sill. Because of these uncertainties, exact calculations of temperature gradients are meaningless. However, gradients calculated under extreme assumptions provide guides to the maximum temperatures which could have been reached in the wall rocks.

Two very different models were chosen for calculation of the temperature gradients. For both models the sedimentary rocks were assumed to be initially at $0^{o}C$. For the first model it was assumed that a diabase sill 250 meters thick was intruded instantaneously as a liquid at $1200^{o}C$. The liquid cooled in the normal manner from the contacts inwards and did not convect. For the calculations, the intrusion temperature was adjusted to $1500^{o}C$ to compensate for the heat of crystallization. Jaeger (1964, p. 454) indicates that this type of approximation gives accurate temperature gradients for distances not too close to the contact; calculations indicate that the model gives contact temperatures about thirty degrees too high at the contact. Graphs of the resulting temperature gradients are shown in Figure 39. The maximum wall rock temperature in the model is $750^{o}C$, and maximum temperatures fall below 700^{o} within several meters of the contact. This model shows that temperatures high enough to melt the sedimentary rocks could not have been attained if the sill did not convect, if it crystallized from the margins inwards, and if it was emplaced instantaneously.

This first model assumes that the sill was emplaced instantaneously. If magma flowed past the contacts, the temperature gradients would be higher close to the sill. For example, if diabase magma at $1200^{o}C$ flowed past the upper contact for one year without forming a chill zone, sedimentary rock within ten feet of the contact would be raised to above $750^{o}C$. This calculation ignores fusion

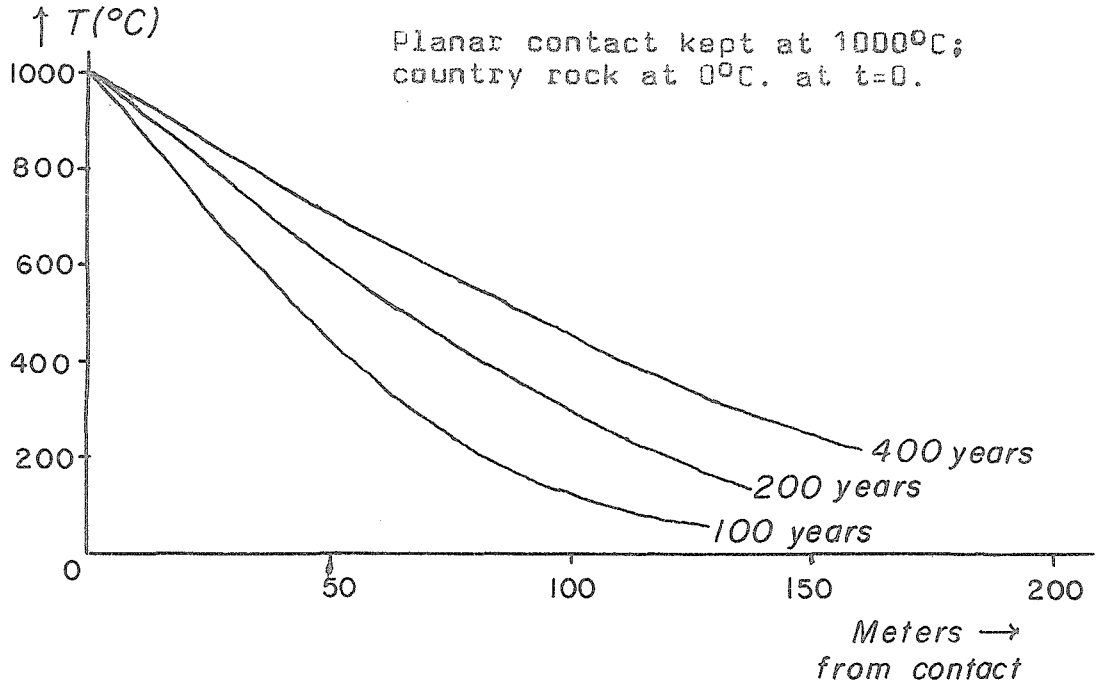

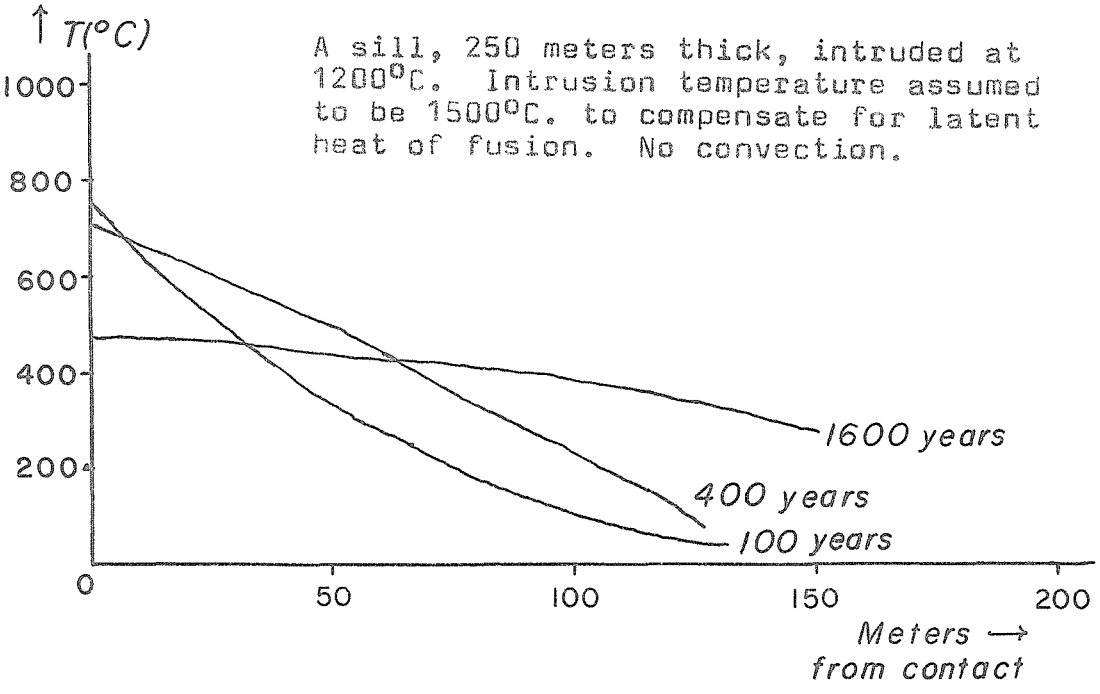

Figure 39. Temperature gradients in sedimentary rocks at the sill roof for two simple models.

processes, and the assumption that no chill zone would be formed is unrealistic. However, this calculation does show that magma flow past a contact might cause some fusion close to the contact. It also might "preheat" rock close to the contact.

Since locally a chilled facies is not present at the upper diabase contact and since observations indicate that in these places the diabase there now may have crystallized upwards, temperature gradients were calculated for a model assuming diabase magma remained at the upper contact for various periods of time. This model is consistent with the model of water diffusion into a sill presented by Kennedy (1955). For simplicity, the diabase magma was assumed to be at 1000°C, an estimate almost certainly correct for the quartz diabase within plus or minus 100°C. Temperature gradients for this model are shown in Figure 39. The gradients are not realistic because they ignore the problems of water heating, water movement, and wall rock fusion. However, they definitely show that if liquid magma remained at the sill roof for any substantial fraction of the solidification time of the magma, sedimentary rocks near the contact would have been at least partially melted. Fusion of sedimentary rocks at the sill roof is an inevitable consequence of adopting Kennedy's model for portions of the upper part of the sill. The heat for the fusion is provided by the heat from cooling and crystallization of the diabase magma.

Comparison of the two temperature models demonstrates that the size of an intrusion is not the factor which determines whether or not sedimentary rocks at the margins of the body are fused. Granitic liquid would not be produced by melting of initially cool sedimentary rocks at the contacts of a sill many times the size of the Sierra Ancha intrusive, if the sill cooled from the margins inwards

without convection and was instantaneously emplaced. Contact temperatures would never exceed about 700°C. The heat content and initial temperature of an intrusion are not critical. What is critical is how heat is transferred to the country rock.

The temperature gradients calculated for both models indicate temperatures about one hundred feet over the sill should have reached at least 400° or 500°C. Yet where granophyric rocks are absent, non-calcareous sedimentary rocks a few feet or tens of feet over the sill roof show little recrystallization. Non-calcareous sedimentary rocks a few feet over the large granophyre masses also show little recrystallization, and inclusions within the granophyres are characteristically fine-grained. Part of the explanation might be that the temperatures a few tens of feet over the intrusion were considerably lower than indicated by the thermal models because of heat transport by water; Turner (1968, pp. 19-22) has suggested that a lowering of contact temperatures because of movement of heated water might explain the negligible contact effects observed near many diabase sills. Another possible explanation is that temperatures near the sill must have exceeded 400-500°C for at most two thousand years. Rates of recrystallization of the quartz-feldspar rocks might be extremely slow at temperatures below minimum melting temperatures. Recrystallization would be much more rapid in the presence of a disordered melt phase. Extensive recrystallization in the non-calcareous rocks in the Dripping Spring Quartzite perhaps was essentially confined to those rocks in which a melt phase was formed. This explanation might account for the apparent lit-par-lit texture which locally formed in laminated rocks; those layers which coarsely recrystallized might have lower-melting compositions than those layers which did not.

Visible metamorphic effects are more widespread in calcareous rocks than in the quartz-feldspar rocks which make up most of the Dripping Spring Quartzite. No systematic study was made here either of the assemblages present in the Mescal Limestone or of the extent of metamorphic effects in the unit. However, samples of Mescal Limestone on the ridge north of Reynolds Creek from as much as 100 feet above the sill complex contain the assemblage diopside-calcite. The reactions by which diopside formed are not known. Experimental data of Metz and Winkler (1964) summarized by Winkler (1967, pp. 30-32) show that diopside forms from the assemblage tremolite-calcite-quartz at temperatures from about 350°C to 550°C at one kilobar fluid pressure, the exact temperature depending on the activities of water and carbon dioxide. These data suggest that temperatures one hundred feet over the sill complex may in fact have been greater than 400°C, as is also suggested by the calculated model temperature gradients.

Possible Reasons for Localization of the Granophyres

The thermal calculations suggest that sedimentary rocks at the sill roof should have been at least partly melted to form granophyres wherever diabase remained molten at the sill roof for any substantial length of time. However, the granophyres are not uniformly distributed. As noted earlier, the large masses were found in only two main areas at local high points in the sill roof, commonly near discordant diabase-sedimentary rocks contacts. Apparently then, in general the diabase did not crystallize upwards towards the sill roof. There is no obvious answer to the question of why the granophyres are localized. Perhaps the magma absorbed water

most readily near discordant contacts. Perhaps in these sites fresh magma was moved to the sill roof sometime after the initial intrusion; this later magma pulse may have stripped the chilled diabase from the roof, and, because it was intruded against pre-heated rock, cooled more slowly and had more time to absorb water than magma in the initial intrusive pulse. Perhaps the areas containing granophyric rocks are located above feeder dikes to the main body of diabase; if so, the sedimentary rocks in these areas might have been "preheated" by magma flowing to other parts of the sill complex. It is also possible that the large masses contain granophyre which flowed together from wide areas to concentrate at the local high points in the roof of the sill complex where the granophyres are now exposed. There are other speculative possibilities. Further detailed mapping in the Sierra Ancha may disclose other granophyre masses and provide clues leading to a more complete understanding of the origins of all the bodies.

PETROLOGIC IMPLICATIONS OF THE SIERRA ANCHA GRANOPHYRES

One of the classic questions of petrology is how silica-rich igneous rocks were formed. In the Sierra Ancha such rocks were formed locally at the top of a sill of basaltic magma. Many of these rocks appear igneous in every respect, and in places, they were intruded into overlying sedimentary rocks. Like many other igneous rocks, the granophyres consist largely of alkali feldspar with subordinate quartz, pyroxene, biotite, and iron-rich hornblende. Because of the unique K-rich compositions of the sedimentary rocks, the igneous-looking rocks can be unequivocally shown to have formed largely from sedimentary rock material. The leucocratic, crystalline rocks are not differentiates of basalt magma, though during their formation some constituents were added to them from the magma.

In the Karroo diabase province of South Africa, sedimentary rocks were also transformed into igneous-looking rocks (Walker and Poldervaart, 1949; Mountain, 1960). Though the occurrences are not as spectacular and mobilization was much more limited than in the Sierra Ancha, the Karroo granophyres also are evidence that igneous-appearing rocks can be formed from sedimentary ones. Relict sedimentary textures and structures provide the conclusive proof that these rocks are not diabase differentiates. Walker and Poldervaart (1949, p. 682) noted that the phenomena they observed might explain "...the associations of basic and acid rocks which are so widespread."

In both the Sierra Ancha and the Karroo, the processes producing granite-like rocks operated on limited scales at fairly shallow crustal depths, so the processes can be studied much more

readily than in regional metamorphic terrains. In both locations the processes had certain features in common:

(1) the ultimate products were granophyres, that is, rocks with micrographic quartz-feldspar intergrowths;

(2) many of the rocks contain turbid feldspars, indicating that late-stage reactions took place readily;

(3) a certain number of metasomatic changes may have occurred;

(4) the heat energy necessary for producing the igneous-looking rocks was provided by cooling and crystallization of a basaltic magma. Points 1, 2, and 3 suggest that the presence of a fluid phase may have been one of the requirements for production of the rocks.

Many of the occurrences of granophyres and associated mafic rocks described in the literature are similar to some of those in the Sierra Ancha in that granophyres are directly in contact with overlying roof rocks. No chilled facies of mafic rocks is present at the roofs. If mafic magma remained molten near sialic rocks at the roof of an intrusion for any substantial length of time, thermal calculations indicate melting would have taken place. Granophyres in such situations are particularly suspect of having formed from the country rocks. Complexes in which granophyre is at least locally directly against overlying country rocks and a chilled facies of basaltic rock is locally absent include the Muskox complex (Smith, 1962), the Bushveldt complex (Wager and Brown, 1967), several of the Keweenawan sills (Schwartz and Sandberg, 1940; Ernst, 1960) and possibly the Red Hill complex (McDougall, 1962).

The absence of a chilled facies of diabase above the granophyres of course does not prove that the granophyres were derived

from the country rock. They may have flowed and stripped away or altered beyond recognition any chilled facies originally present. Likewise, the presence of a chilled facies of mafic rock above them does not prove that granophyres represent uncontaminated basaltic differentiates. The thick K-rich biotite granophyre lens north of Grantham Peak is separated from the sill roof by diabase which is chilled against the overlying Mescal Limestone.

Chemical criteria to distinguish granophyres which are magmatic differentiates from those which formed from country rocks must be used with care. The Sierra Ancha granophyres appear to have largely formed from sedimentary rocks. However, there are distinct compositional differences between the granophyres and their parent material. Compositional changes, whether by mixing of basalt magma with country rock material or by metasomatism, may have taken place in many of the instances in which country rocks have been transformed to granophyric rocks by basaltic intrusives. Simply because the compositions of granophyres and possible parent country rocks are somewhat different does not necessarily imply that the granophyres are basaltic differentiates. For instance, granophyres in several Keweenawan sills are distinctly different in composition from overlying rhyolite flows; partially because of this difference, it has been said the granophyres are basaltic differentiates and were not chiefly derived from the rhyolites (Schwartz and Sandberg, 1940, p. 1163; Ernst, 1960, p. 299). The compositional arguments may not be valid reasons for believing that the granophyres are basaltic differentiates.

One possibly valid compositional test for the origin of salic granophyres depends on whether their normative compositions plot in the ternary minimum or low temperature trough in the plagioclase-

K feldspar-SiO_2 system. Granophyres with such normative compositions may or may not be basaltic differentiates. Those with compositions which plot elsewhere, like the Sierra Ancha granophyres, are unlikely to be basaltic differentiates.

Petrologists have for years suggested that many sialic magmas in the upper crust may be the partial or complete fusion products of rocks heated by basaltic magmas and subsequently intruded upwards. There are relatively few instances where the actual occurrence of this process has been demonstrated. Brown (1963) has presented compositional evidence suggesting that Tertiary granitic rocks in Skye and Rhum may have formed by country rock fusion. Moorbath and Bell (1965) and Hamilton (1966) have presented strontium and lead isotopic data which strengthen the interpretation that the Skye and Rhum granitic rocks are not basaltic differentiates. The aplite dikes above some of the main granophyre masses in the Sierra Ancha were injected into strata overlying the diabase sill. They probably crystallized from a silicate melt, and they undoubtedly formed largely from sedimentary rock material. The granophyre-diabase relationships at the roof of the Sierra Ancha sill may reproduce on a smaller scale the relationships at depth beneath Skye and Rhum and beneath many other localities with granitic intrusive rocks.

Some cross sections through the upper part of the Sierra Ancha sill complex are crudely similar to some cross sections through the continental crust; rocks of basaltic composition are overlain by more silica-rich crystalline rocks which in turn are overlain by sedimentary rocks. The processes which formed the leucocratic igneous-looking rocks in the Sierra Ancha may have operated on a much larger scale to produce many of the sialic igne-

ous rocks of the continents. These processes include metamorphic recrystallization, partial and perhaps complete fusion, and possibly metasomatism. In the Sierra Ancha, the processes took place in response to a rather simple event, the intrusion of a sheet of basaltic magma into a sedimentary rock series.

APPENDIX

Analytical Procedures and Accuracy of Results

Wet chemical analyses

All samples were crushed on a steel plate to fragments less than 1/4 inch in maximum diameter. Then they were reduced to minus one hundred mesh powders in a Shatterbox (Spex Industries, Inc.) lined with tungsten carbide. The samples were spectographically analyzed for tungsten by E. Bingham; it was not detected, implying less than 0.1% W was introduced into the samples. Clear quartz selected from a mineralogy collection was also reduced on the steel plate. It was ground three to six times longer in the Shatterbox than were the analyzed samples. Triplicate spectrographic analyses showed that the quartz powder contained 20-40 ppm Fe_2O_3, 100-200 ppm Co, and 3000-5000 ppm W. These results indicate that contamination of the analyzed samples was negligible.

Samples for wet chemical analyses were sent to the Japan Analytical Chemistry Research Institute, Tamiya Asari, Director, where they were analyzed by Tadashi Asari. The samples were sent in two batches, each of which contained a hidden duplicate. A sample of the U.S.G.S. standard basalt BCR-1 was also sent for analysis as an unknown. Analytical results for the duplicates and the standard are in Table 33. Evidently, some of the traditional analytical difficulties were encountered in determining SiO_2, Al_2O_3, FeO and Fe_2O_3. Since the powders were homogenized and split by hand, it is possible that the duplicate samples were not exactly alike. The analytical results are of acceptable quality in view of the range

TABLE 33

Wet Chemical Analyses of Duplicate Samples and of the U.S. Geological Survey Standard Basalt, BCR - 1

	Ad28	Ad28	Ad285	Ad285	BCR-1[1]	BCR-1[2]	BCR-1[2]
SiO_2	53.04	52.91	62.57	62.61	53.50	54.10	54.15
TiO_2	2.74	2.67	1.26	1.27	2.26	2.25	2.26
Al_2O_3	14.21	14.69	14.44	14.45	14.08	13.70	13.63
Fe_2O_3	2.08	1.80	1.11	1.23	4.04	3.24	3.17
FeO	5.48	5.52	4.58	4.28	8.55	9.07	9.09
MnO	0.18	0.18	0.06	0.05	0.17	0.19	0.19
MgO	3.26	3.21	1.43	1.41	3.62	3.47	3.50
CaO	9.33	9.28	1.60	1.56	7.17	6.91	6.92
Na_2O	5.27	5.08	2.01	2.01	3.39	3.26	3.32
K_2O	1.87	1.85	8.21	8.21	1.74	1.69	1.69
H_2O^+	1.38	1.75	1.39	1.26	0.84	0.50	0.62
H_2O^-	0.51	0.40	0.58	0.53	0.89	1.24	1.21
P_2O_5	1.23	1.26	0.17	0.18	0.37	0.35	0.35
S	0.18	0.14	0.75	0.78	0.06	0.04	0.04
Total	100.76	100.74	100.16	99.93	100.68	100.01	100.14
Analyst	T. Asari		T. Asari		Asari	Munson	Smith

Duplicates and the standard basalt were disguised under different numbers.

[1] From sample furnished to L.T. Silver. Split 27, Position 26.

[2] Analyses taken from Flanagan (1967).

of wet chemical results reported for standards in previous comparative tests (Fairbairn et al, 1951).

X-ray fluorescence analyses for potassium

X-ray fluorescence analyses for potassium were made by E. Bingham. The preparation of the rock powders is described in the discussion of the wet chemical analyses. One gram of rock powder was mixed with 0.1 grams of boric acid and compressed onto the top of a pellet with a pure boric acid base. The intensity measurements were made with a Norelco vacuum x-ray spectograph using a tungsten-target tube at 50 kv and 40 ma and an EDDT analyzing crystal. Intensities were measured for 50,000 counts and corrected for background. Pulse height analyses was used. Eleven of the wet-chemically analyzed samples were used as standards.

On a graph of x-ray intensity versus potassium content, all standards plot within five percent of a visually-estimated, best-fit straight line. Most standards fit well within the plus or minus five percent limit. Only background corrections were made, and the linear fit of the points is surprising in view of the variable compositions of the standards. Their K_2O contents range from about 1 to 11 weight percent. The K_2O contents determined for the unknowns are probably also precise within plus or minus five percent. Their accuracy depends on the accuracy of the wet chemical analyses.

Trace element emission spectrographic analyses

Analyses for trace elements were performed by E. Bingham on powdered samples. The preparation of the powders is described in the discussion of the wet chemical analyses. Analytical procedures were essentially the same as those reported by Schmitt, Bingham, and Chodos (1964, pp. 1973-1974).

Procedures for microprobe analyses

All electron microprobe analyses were made with the Caltech Applied Research Laboratories EMX microprobe on minerals in polished thin sections coated with carbon films. Analyses were made at 15 kv and at currents ranging from 0.03 to 0.15 microamps on brass. Most analyses were made with the smallest beam spots obtainable (one to two microns in diameter). All analyzed points were marked on Polaroid photomicrographs; this procedure enabled points to be relocated for further analyses and also provided a permanent record of where data were taken. All data were corrected for background and, when necessary, for deadtime; in general, counting rates were kept below levels requiring deadtime corrections.

Most data were converted to weight percent oxides and element proportions by procedures based on the method of Bence and Albee (1968). At first, calibration curves were constructed for the major elements in pyroxenes, olivines, and feldspars. The quality of curves for both pyroxenes and olivines was poorer than desired, in part because the curves had to be based upon somewhat unreliable chemical data. The construction of meaningful curves for calcic pyroxenes was particularly difficult because of their complex compo-

sitions. Only for feldspars could completely satisfactory calibration curves be prepared. The method of Bence and Albee (1968) was adopted for all minerals both because of its simplicity and because it largely avoids the problem of relying on possibly inaccurate wet chemical analyses.

The standards used for computation of analyses were: Na, albite (Amelia); Mg, synthetic pyrope; Al, kyanite; Si, quartz; K, microcline (Asbestos); Ca, wollastonite; Ti, rutile; Cr, chromite; Mn, rhodonite; Fe, synthetic ferrosilite (silicates) and hematite (oxides). All standards used have simple and well-known compositions and were reasonably homogeneous (rhodonite excepted). In addition to these standards, pyroxenes H35 and H39, sanidine (Leilenkopf), kyanite, and synthetic anorthite, ilmenite, and pyrope were often run as checks on the other standards. During microprobe runs, standards were run periodically to check for drift.

The three available microprobe channels permitted three elements to be determined simultaneously. Whenever possible, important groups of elements in any mineral were determined simultaneously. When this procedure is followed, any microprobe drift which affects all channels simultaneously does not affect ratios of the important elements. For instance, Ca, Fe and Mg were determined simultaneously for all pyroxene analyses, and Fe, Ti, and Al were determined together for oxide analyses.

The Caltech CITRAN system was invaluable for computation of microprobe analyses. Complete analyses were calculated using a CITRAN program modified from one written by A. E. Bence and R. Naylor. Other programs were written for calculation of partial analyses of pyroxenes, olivines, and feldspars. A few of the feldspar

analyses were computed from calibration curves; these were in agreement with those calculated with the CITRAN program.

Precision and accuracy of microprobe analyses

Precision in microprobe analysis basically depends upon the number of counts measured over background. Ignoring background, the standard deviation of a measurement made on N x-ray counts is the square root of N. For ten thousand counts, the standard deviation is plus or minus one percent. Most major element determinations were based on numbers of counts near or considerably greater than ten thousand, so the standard deviation for these determinations is of the order of one percent or less. For elements present at the level of about 1 weight percent oxide, the standard deviation was generally less than plus or minus five percent. At the 0.5 weight percent level, it was generally less than plus or minus ten percent, while for oxides present in amounts less than 0.1 weight percent, it was on the order of plus or minus fifty percent. Since they were run at fairly low sample currents to avoid vaporization problems, the statistics for feldspars are not quite as good as for other minerals.

It was found that no single element determination was reproducible to much better than plus or minus one percent, even though considerably better counting statistics were obtained. Ratios of counts corrected for background for two sets of standards are in Table 34. The standard sets were run at various dates over a time span of about two years. On most occasions at least 100,000 counts were accumulated for each standard. The ratios vary within about plus or minus one percent from their average values. The variation

TABLE 34

Count Ratios for Pairs of Microprobe Standards

Counts corrected only for background

A. Fe radiation, Ferrosilite/H39 (pyroxene)

3.159	3.165
3.181	3.190
3.177	3.136
3.160	3.148
3.191	3.166
3.197	3.181
3.190	3.176

Average, 3.172

B. Mg radiation, Pyrope/H35 (pyroxene)

1.857	1.859
1.851	1.852
1.856	1.831
1.867	1.862
1.890	1.898
1.862	

Average, 1.862

reflects counting statistics, microprobe drift, and possibly also standard inhomogeneities. The data show that no element determination can be considered to be accurate within much better than one percent. They also indicate that a precision of about plus or minus one percent is a realistic estimate for most major element determinations.

The accuracy of the microprobe analyses depends on the accuracy of the system used to convert x-ray intensities to element proportions. Bence and Albee (1968) discuss the accuracy of the system used here. The final set of correction factors published in their paper was modified slightly from the version of their factors used for analyses in this thesis.* Analyses of five standard pyroxenes computed with the factors used here are compared with analyses from the literature in Table 35. The comparison is not a completely reliable test, because of course, the grains analyzed here are different from those on which the reported analyses were made. Most of the major element determinations are within plus or minus several percent of one another. The microprobe analyses used here are certainly of sufficient accuracy to support all the petrologic conclusions reached in this thesis. For instance, a calculation showed that lowering the CaO content of a specific pyroxene by two percent (relative) changed its position in the pyroxene quadrilateral only from $Wo_{49.1}En_{13.5}Fs_{37.4}$ to $Wo_{48.5}En_{13.7}Fs_{37.8}$. Partial analyses computed for several standard feldspars in the Caltech reference collection are in Table 36. The accuracy of the

*Only the analyses in Tables 28 and 29 were calculated with the published factors.

TABLE 35

Comparison of Microprobe Analyses of Standard Clinopyroxenes with Analyses in the Literature

	SiO_2	TiO_2	Al_2O_3	Fe as FeO	MgO	CaO	Pyroxene
A	55.4	0	0	0.1	18.8	25.7	
B	55.6	0	0	0.1	18.7	25.9	Y6
C	55.0	0	0.03	0.03	19.2	25.9	
A	45.8	0.3	5.1	17.7	6.9	22.5	
B	46.4	0.3	4.5	17.5	6.6	22.5	H39
C	46.4	0.3	4.4	18.0	6.9	22.9	
A	54.5	0.04	0.4	2.7	17.2	24.9	
B	55.8	0.05	0.2	2.9	16.8	25.0	H35
C	53.8	0.05	0.2	2.8	17.5	25.2	
A	50.7	0.1	1.5	17.1	6.8	20.7	
B	50.9	0.04	0.9	18.1	6.6	21.1	R2395
C	49.5	0.04	0.3	18.5	6.7	21.6	
A	50.5	0.2	2.7	15.0	9.6	20.2	
B	51.6	0.2	1.6	15.2	9.7	20.3	R1133
C	49.8	0.2	2.2	15.5	10.0	20.9	

A Wet chemical data - Source: Smith (1966a).
B Probe determination by J.V. Smith (1966a).
C Probe determination by author using correction factors employed for analyses in this thesis.

Samples supplied to Caltech by J.V. Smith.

TABLE 36

Analyses of Homogeneous Feldspars in the Caltech Collection

	Weight Percent		
	CaO	K_2O	Na_2O
Leilenkopf Sanidine[1]	0.02	13.0	2.4
Kraeger Andesine[1]	4.7	0.58	8.7
Synthetic An_{60} (Calculated Values)	12.6 (12.38)	0.02 (0.00)	4.6[5] (4.56)

[1] Average of two determinations.

iron-titanium oxide analyses is discussed in the section on oxide compositions.

Calculation procedures for rock norms

All rock norms were calculated with a CITRAN program written for that purpose. The program uses modern molecular and atomic weights and rounds figures accurately. Before calculation, the program omits water and sums the other constituents to 100. With these exceptions, the program follows the CIPW conventions for norm calculation (Cross et al, 1902).

BIBLIOGRAPHY

Albee, A.L. (1962) Relationships between the mineral association, chemical composition and physical properties of the chlorite series. Am. Mineralogist 47, 851-870.

Amstutz, G.C. (1967) Spilites and spilitic rocks. Basalts: The Poldervaart Treatise on Rocks of Basaltic Composition. v2, 737-753.

Battey, M.H. (1956) The petrogenesis of a spilitic rock series from New Zealand. Geol. Mag. 93, 89-110.

Bence, A.E. and Albee, A.L. (1968) Empirical correction factors for the electron microanalysis of silicates and oxides. Jour. Geology 76, 382-403.

Best, Myron G. and Mercy, E.L.P. (1967) Composition and crystallization of mafic minerals in the Guadalupe igneous complex, California. Am. Mineralogist 52, 436-474.

Bhattacharji, S. (1967) Mechanics of flow differentiation in ultramafic and mafic sills. Jour. Geology 75, 101-112.

Bowen, N.L. (1933) The broader story of magmatic differentiation. Lindgren Volume, Am. Inst. Min. Met. Eng., 106-128.

Bowen, N.L. and Schairer, J.F. (1935) The system MgO-FeO-SiO_2. Am. Jour. Sci. 29, 151-217.

Brooks, C.K. (1968) On the interpretation of trends in element ratios in differentiated igneous rocks, with particular reference to strontium and calcium. Chemical Geology 3, 15-20.

Brown, G.M. (1957) Pyroxenes from the early and middle stages of fractionation of the Skaergaard intrusion, East Greenland. Min. Mag. 31, 511-543.

_____ (1963) Melting relations of Tertiary granitic rocks in Skye and Rhum. Min. Mag. 33, 533-562.

_____ (1968) Experimental studies on inversion relations in natural pigeonitic pyroxenes. Carnegie Inst. of Washington Yearbook 66, 347-353.

_____ and Vincent, E.A. (1963) Pyroxenes from the late stages of fractionation of the Skaergaard intrusion, East Greenland. Jour. Petrology 4, 175-197.

Buddington, A.F. (1964) Distribution of MnO between co-existing ilmenite and magnetite. Indian Geophysical Union Krishnan Volume, 233-248.

_____ and Lindsley, D.H. (1964) Iron titanium oxide minerals and synthetic equivalents. Jour. Petrology 5, 310-357.

Carmichael, C.M. (1961) The magnetic properties of ilmenite-hematite crystals. Proc. Roy. Soc. London, Ser. A, 263, 508-530.

Carmichael, I.S.E. (1967) The iron-titanium oxides of salic volcanic rocks and their associated ferromagnesian silicates. Contr. Mineral. and Petrol. 14, 36-64.

Cherukupalli, N.E. (1959?) Petrology of the olivine-dolerite sill, Sierra Ancha Mountains, Arizona. Masters dissertation, Columbia University.

Cornwall, H.R. (1951) Differentiation in lavas of the Keweenawan series and the origin of the copper deposits of Michigan. Geol. Soc. Am. Bull. 62, 159-202.

_____ (1951a) Ilmenite, magnetite, hematite, and copper in lavas of the Keweenawan series. Econ. Geol. 46, 51-67.

Cross, W., Iddings, J.P., Pirsson, L.V. and Washington, H.S. (1902) A quantitative chemico-mineralogical classification and nomenclature of igneous rocks. Jour. Geology 10, 555-690.

Deer, W.A. and Abbott, D. (1965) Clinopyroxenes of the gabbro cumulates of the Kap Edvard Holm complex, east Greenland. Mineral. Mag. 34, 177-193.

Deer, W.A., Howie, R.A. and Zussman, J. (1963) Rock-forming Minerals. vII. New York: John Wiley and Sons Inc., 379p.

Drever, H.I. and Johnston, R. (1967) The ultrabasic facies in some sills and sheets. Ultramafic and Related Rocks. New York: John Wiley and Sons, Inc., 51-63.

Ernst, W.G. (1960) Diabase-granophyre relations in the Endion Sill, Duluth, Minnesota. Jour. Petrology 1, 286-303.

_____ (1968) Amphiboles. New York: Springer-Verlag Inc., 125p.

Fairbairn, H.W. et al (1951) A cooperative investigation of precision and accuracy in chemical, spectrochemical,and modal analyses of silicate rocks. U.S. Geol. Surv. Bull. 980, 71p.

Flanagan, Francis J. (1967) U.S. Geological Survey silicate rock standards. Geochim. Cosmochim. Acta 31, 289-308.

Frankel, J.J. (1967) Forms and structures of intrusive basaltic rocks. Basalts: The Poldervaart Treatise on Rocks of Basaltic Composition. v1, 63-102.

Fyfe, W.S. Turner, F.J., and Verhoogen, J. (1958) Metamorphic reactions and metamorphic facies. Geol. Soc. America Mem. 73, 259p.

Gastil, R.G. (1950) Geology of the eastern half of the Diamond Butte quadrangle, Gila County, Arizona. Ph.D. dissertation, University of California.

_____ (1954) Late Precambrian volcanism in southeastern Arizona. Am. Jour. Sci. 252, 436-440.

Granger, H.C. and Raup, R.B. (1959) Uranium deposits in the Dripping Spring Quartzite, Gila County, Arizona. U.S. Geol. Survey Bull. 1046-P, 71p.

_____ (1964) Stratigraphy of the Dripping Spring Quartzite, southeastern Arizona. U.S. Geol. Survey Bull. 1168, 119p.

Gruner, J.W. and Thiel, G.A. (1937) The occurrence of fine grained authigenic feldspar in shales and silts. Am. Mineralogist 22, 842-846.

Haggerty, S.E. and Baker, I. (1967) The alteration of olivine in basaltic and associated lavas. Part I: High temperature alteration. Contr. Mineral. and Petrol. 16, 233-257.

Hakli, T.A. and Wright, T.L. (1967) The fractionation of nickel between olivine and augite as a geothermometer. Geochim. Cosmochim. Acta 31, 877-884.

Hamilton, E.I. (1966) The isotopic composition of lead in igneous rocks. I. The origin of some Tertiary granites. Earth and Planetary Science Letters 1, 30-37.

Hamilton, W. (1965) Diabase sheets of the Taylor Glacier region, Victoria Land, Antarctica. U.S. Geol. Survey Prof. Paper 456-B, 71p.

Hay, R.L. (1966) Zeolites and zeolitic reactions in sedimentary rocks. G.S.A. Special Paper 85, 130p.

_____ and Moila, R.J. (1963) Authigenic silicate minerals in Searles Lake, California. Sedimentology 2, 312-332.

Hess, H.H. (1960) Stillwater igneous complex, Montana. Geol. Soc. Am. Memoir 80, 230p.

Hotz, P.E. (1953) Petrology of granophyre in diabase near Dillsburg, Pennsylvania. Geol. Soc. Am. Bull. 64, 675-704.

Jaeger, J.C. (1957) The temperatures in the neighborhood of a cooling intrusive sheet. Am. Jour. Sci. 255, 306-318.

_____ (1964) Thermal effects of intrusions. Rev. Geophysics 2, 443-466.

_____ (1967) Cooling and solidification of igneous rocks. Basalts: The Poldervaart Treatise on Rocks of Basaltic Composition, v2, 503-536.

Kennedy, G.C. (1955) Some aspects of the role of water in rock melts. Geol. Soc. Am. Sp. Paper 62, 489-504.

Kretz, R. (1961) Some applications of thermodynamics to coexisting minerals of variable composition. Examples: orthopyroxene-clinopyroxene and orthopyroxene-garnet. Jour. Geology 69, 361-387.

_____ (1963) Distribution of magnesium and iron between orthopyroxene and calcic pyroxene in natural mineral assemblages. Jour. Geology 71, 773-785.

Kuno, H. (1960) High-alumina basalt. Jour. Petrology 1, 121-145.

Kushiro, I. (1960) Si-Al relations in clinopyroxenes from igneous rocks. Am. Jour. Sci. 258, 548-554.

Larimer, J.W. (in press) Experimental studies of the system Fe-MgO-SiO_2-O_2 and their bearing of the petrology of chondritic meteorites. Geochim. Cosmochim. Acta.

Lindsley, D.H. (1960) Geology of the Spray Quadrangle, Oregon. Ph.D. dissertation, Johns Hopkins University.

_____ (1962) Investigations in the system FeO-Fe_2O_3-TiO_2. Carnegie Inst. Wash. Yearb. 61, 100-106.

_____ (1963) Equilibrium relations of coexisting pairs of Fe-Ti oxides. Carnegie Inst. Wash. Yearb. 61, 60-66.

Macdonald, G.A. and Katsura, T. (1964) Chemical composition of Hawaiian lavas. Jour. Petrology 5, 82-133.

McDougall, I. (1962) Differentiation of the Tasmanian dolerites: Red Hill dolerite-granophyre association. Geol. Soc. Am. Bull. 73, 279-316.

Medaris, L.G. (1968) Partitioning of Mg^{++} and Fe^{++} between coexisting olivine and orthopyroxene. Am. Geophys. Union Trans. 49, 360-361 (abs.).

Metz, P. and Winkler, H.G.F. (1964) Experimental investigation of the formation of diopside from tremolite, calcite, and quartz. Natur. Wiss. 51, 160.

Moorbath, S. and Bell, J.D. (1965) Strontium isotope abundance studies and rubidium-strontium age determinations on Tertiary igneous rocks from the Isle of Skye, northwest Scotland. Jour. Petrology 6, 37-66.

Mountain, E.D. (1944) Further examples of syntexis by Karroo dolerite. Geol. Soc. S. Africa, Trans. 47, 107-121.

_____ (1960) Felsic material in Karroo dolerite. Geol. Soc. S. Africa, Trans. 63, 137-152.

Mueller, R.F. (1961) Analysis of relations among Mg, Fe, and Mn in certain metamorphic minerals. Geochim. Cosmochim. Acta 25, 267-296.

Nafziger, R.H. and Muan, A. (1967) Equilibrium phase compositions and thermodynamic properties of olivines and pyroxenes in the system MgO-"FeO"-SiO_2. Am. Mineralogist 52, 1364-1385.

Neuerburg, G.J. and Granger, H.C. (1960) A geochemical test of diabase as an ore source for the uranium deposits of the Dripping Spring district, Arizona. N. Jb. Miner., Abh. 94, 759-797.

Noble, J.A. (1948) High-potash dikes in the Homestake Mine, Lead, South Dakota. Geol. Soc. Am. Bull. 59, 927-939.

Nockolds, S.R. (1954) Average chemical compositions of some igneous rocks. Geol. Soc. Am. Bull. 65, 1007-1032.

O'Neil, J.R. and Taylor, H.P. (1967) The oxygen isotope and cation exchange chemistry of feldspars. Am. Mineralogist 52, 1414-1437.

Orville, P.M. (1963) Alkali ion exchange between vapor and feldspar phases. Am. Jour. Sci. 261, 201-237.

Osborn, E.F. (1959) Role of oxygen pressure in crystallization and differentiation of basaltic magma. Am. Jour. Sci. 257, 609-647.

Peck, D.L., Wright, T.L., and Moore, J.G. (1966) Crystallization of tholeiitic basalt in Alae Lava Lake, Hawaii. Bull. Volcanologique 29, 630-655.

Perchuk, L.L. and Ryabchikov, I.D. (1968) Mineral equilibria in the system nepheline-alkali feldspar-plagioclase and their petrological significance. Jour. Petrology 9, 123-167.

Pettijohn, F.J. (1957) Sedimentary Rocks. New York: Harper and Brothers, 718p.

Ramberg, H. and deVore, G. (1951) The distribution of Fe^{++} and Mg^{++} in coexisting olivines and pyroxene. Jour. Geology 59, 193-210.

Schairer, J.F. and Yoder, H.S. (1960) The nature of residual liquids from crystallization, with data of the system nepheline-diopside-silica. Am. Jour. Sci. 258-A, 273-283.

Schmitt, R.A., Bingham, E., and Chodos, A.A. (1964) Zirconium abundances in meteorites and implications to nucleosynthesis. Geochim. Cosmochim. Acta 28, 1961-1979.

Schmus, W.R. Van, Koffman, D.M. (1967) Equilibration temperatures of iron and magnesium in chondritic meteorites. Science 155, 1009-1011.

Schwartz, G.M. and Sandberg, A.E. (1940) Rock series in diabase sills at Duluth, Minnesota. Geol. Soc. Am. Bull. 51, 1135-1172.

Sederholm, J.J. (1929) The use of the term "deuteric". Econ. Geol. 24, 869-871.

Shaw, H.R. (1963) The four-phase curve sanidine-quartz-liquid-gas between 500 and 4000 bars. Am. Mineralogist 48, 883-896.

Shannon, E.V. (1926) The mineralogy and petrology of intrusive Triassic diabase at Goose Creek, Loudoun County, Virginia. Proc. U.S. National Museum 66, article 2, 86p.

Sheppard, R.A. and Gude, A.J. (1964) Reconnaissance of zeolite deposits in tuffaceous rocks of the western Mojave Desert and vicinity, California. U.S. Geol. Survey Prof. Paper 501-C, 114-116.

Shride, A.F. (1967) Younger Precambrian geology in southern Arizona. U.S. Geol. Survey Prof. Paper 566, 89p.

Silver, L.T. (1960) Age determinations on Precambrian diabase differentiates in the Sierra Ancha, Gila County, Arizona. Geol. Soc. Am. Bull. 71, 1973-1974, (abs.).

Smith, C.H. (1962) Notes on the Muskox intrusion, Coppermine River Area, District of Mackenzie. Geol. Survey of Canada Paper 61-25, 16p.

Smith, J.V. (1966) X-ray emission microanalysis of rock-forming minerals. II. Olivines. Jour. Geology 74, 1-16.

_____ (1966a) X-ray emission microanalyses of rock-forming minerals: VI. Clinopyroxenes near the diopside-hedenbergite join. Jour. Geology 74, 463-477.

Taylor, R.W. (1964) Phase equilibria in the system FeO-Fe_2O_3-TiO_2 at 1300°C. Am. Min. 49, 1016-1030.

Taylor, H.P. (1968) The oxygen isotope geochemistry of igneous rocks. Contr. Mineral. and Petrol. 19, 1-71.

Tilley, C.E. (1950) Some aspects of magmatic evolution. Quart. Jour. Geol. Soc. London 106, 37-61.

Tilley, C.E., Yoder, H.S., and Schairer, J.F. (1963) Melting relations of basalts. Carnegie Inst. of Wash. Yearb. 62, 77-84.

_____ (1965) Melting relations of volcanic tholeiite and alkali rock series. Ibid. 64, 69-82.

_____ (1968) Melting relations of igneous rock series. Ibid. 66, 450-457.

Turner, F.H. (1968) Metamorphic petrology: mineralogical and field aspects. New York: McGraw-Hill, Inc.,403p.

Turner, F.J. and Verhoogen, J. (1960) Igneous and Metamorphic Petrology. New York: McGraw-Hill Inc., 694p.

Turnock, A.C. (1960) The stability of iron chlorites. Carnegie Inst. of Wash. Yearb. 59, 98-103.

Turnock, A.C. and Eugster, H.P. (1962) Fe-Al Oxides: Phase relationships below 1000°C. Jour. Petrology 3, 533-565.

Tuttle, O.F. and Bowen, N.L. (1958) Origin of granite in the light of experimental studies in the system $NaAlSi_3O_8$-$KAlSi_3O_8$-SiO_2-H_2O. Geol. Soc. Am. Mem. 74, 153p.

Verhoogen, J. (1962) Distribution of titanium between silicates and oxides in igneous rocks. Am. Jour. Sci. 260, 211-220.

Vincent, E.A. (1960) Ulvospinel in the Skaergaard intrusion, Greenland. N. Jb. Miner. Abh. 94, 993-1016.

Wager, L.R. (1960) The major element variation of the layered series of the Skaergaard intrusion and a re-estimation of the average composition of the hidden layered series and of the successive residual magmas. Jour. Petrology 1, 364-398.

Wager, L.R. and Brown, G.M. (1967) Layered Igneous Rocks. San Francisco: W.H. Freeman and Co., 588p.

_____ and Wadsworth, W.J. (1960) Types of igneous cumulates. Jour. Petrology 1, 73-85.

Walker, F. (1953) The pegmatitic differentiates of basic sheets. Am. Jour. Sci. 251, 41-60.

_____ (1957) The causes of variation in dolerite intrusions. Dolerite symposium, University of Tasmania, 1-25.

_____ and Poldervaart, A. (1942) The metasomatism of Karroo sediments by dolerite. Roy. Soc. S. Africa Trans. 29, 285-307.

_____ (1949) Karroo dolerites of the Union of South Africa. Bull. Geol. Soc. Am. 60, 591-706.

Walton, M.S. Jr. and O'Sullivan, R.B. (1950) The intrusive mechanics of a clastic dike. Am. Jour. Sci. 248, 1-21.

Weiss, M.P. (1954) Feldspathized shales from Minnesota. Jour. Sed. Petrology 24, 270-274.

Wilkinson, J.F.G. (1956) Clinopyroxenes of alkali-basalt magma. Am. Mineralogist 41, 724-743.

_____ (1957) The clinopyroxenes of a differentiated teschenite sill near Gunnedah, New South Wales. Geol. Mag. 94, 123-134.

Williams, F.J. (1957) Structural control of uranium deposits, Sierra Ancha region, Gila County, Arizona. U.S. Atomic Energy Comm. Report RME-3152, 117p.

Wilshire, H.G. (1967) The Prospect alkaline diabase-picrite intrusion, New South Wales, Australia. Jour. Petrology 8, 97-163.

Wilson, E.D. (1962) A resume of the geology of Arizona. Arizona Bur. Mines Bull. 171, 140 p.

Winkler, H.G.F. (1967) Petrogenesis of Metamorphic Rocks. New York: Springer-Verlag Inc., 237p.

Wones, D.R. and Eugster, H.P. (1965) Stability of biotite: experiment, theory, and application. Am. Mineralogist 50, 1228-1272.

Wright, J.B. (1961) Solid-solution relationships in some titaniferous iron oxide ores of basic igneous rocks. Min. Mag. 32, 778-789.

Yoder, H.S. (1952) The MgO-Al_2O_3-SiO_2-H_2O system and the related metamorphic facies. Am. Jour. Sci. Bowen Volume, 569-627.

_____ (1967) Spilites and serpentinites. Carnegie Inst. Wash. Yearb. 65, 269-279.

_____ and Tilley, C.E. (1962) Origin of basalt magmas. Jour. Petrology 3, 342-532.